



***Transcriptional and post-transcriptional
PHOSPHATE 2 (PHO2) gene expression
regulation in barley***

*Transkrypcyjna i potranskrypcyjna regulacja ekspresji genu
PHOSPHATE 2 (PHO2) w jęczmieniu*



Paweł Sega

PhD thesis



Institute of Molecular Biology and Biotechnology

Faculty of Biology

Adam Mickiewicz University, Poznań

©2021, Poznań, Poland

The thesis has been prepared at the Department of Gene Expression

Supervisor:

Dr hab. Andrzej Pacak, Prof. UAM

Department of Gene Expression, Institute of Molecular
Biology and Biotechnology, Faculty of Biology, Adam
Mickiewicz University, Poznań, Poland

SPIS TREŚCI / TABLE OF CONTENTS

Prolog / Prologue	1
Streszczenie	2
Summary	12
Lista publikacji wchodzących w skład rozprawy doktorskiej / Doctoral dissertation	25
Part I: <i>Plant PHR transcription factors: Put on a map</i>	26
Oświadczenia / Authorship statement.....	40
Part II: <i>miRNA detection by stem-loop RT-qPCR in studying microRNA biogenesis and microRNA responsiveness by abiotic stresses</i>	42
Oświadczenia / Authorship statement.....	62
Part III: <i>Identification of transcription factors that bind to the 5'-UTR of the barley PHO2 gene</i>	69
Oświadczenia / Authorship statement.....	85
Suplement / Supplementary data	90
Part IV: <i>Pi-starvation induced transcriptional changes in barley revealed by a comprehensive RNA-Seq and degradome analyses</i>	106
Oświadczenia / Authorship statement.....	131
Suplement / Supplementary data	138
Podziękowania / Acknowledgements	154
Finansowanie badań / Fundings	155

How to respond to climate change?

„There is a fundamental paradigm shift that needs to happen if we are to build sustainable energy systems at the scale that we need to. Here is the scenario:

- The world gets off of fossil fuels and starts producing entirely new and clean energy sources.
- The world needs to build a system that maximizes the economic opportunities for working people.

This means that unless massive and rapid improvements in the technology to harness the immense productivity of the earth's resources can be made, the earth's future is in serious danger. The Earth's resources will become less abundant, the world's population will rise rapidly, and a new type of natural disaster is increasingly likely.

We must recognize this risk to the future of human civilization, and act now to respond.”

Artificial-intelligence, the winner of "The Economist's open future essay competition"

published Oct 1st 2019

Jak reagować na zmiany klimatyczne?

„Istnieje zasadnicza zmiana paradygmatu, która musi nastąpić, jeśli mamy budować zrównoważone systemy energetyczne na taką skalę, jakiej potrzebujemy. Oto scenariusz:

- Świat rezygnuje z paliw kopalnych i zaczyna wytwarzać całkowicie nowe i czyste źródła energii.
- Świat musi zbudować system, który maksymalizuje możliwości ekonomiczne dla ludzi pracujących.

Oznacza to, że przyszłość Ziemi jest poważnie zagrożona jeśli nie uda się dokonać ogromnych i szybkich ulepszeń technologii pozwalających wykorzystać ogromną produktywność zasobów Ziemi. Zasoby te staną się mniej obfite, populacja świata gwałtownie wzrośnie, a wystąpienie nowego rodzaju klęski żywiołowej stanie się coraz bardziej prawdopodobne.

Musimy zdać sobie sprawę z tego zagrożenia dla przyszłości ludzkiej cywilizacji i podjąć działania już teraz.”

Sztuczna Inteligencja, zwycięski esej w konkursie międzynarodowego czasopisma The Economist

opublikowano 1 października 2019

W latach sześćdziesiątych XX wieku międzynarodowa organizacja do spraw żywienia i rolnictwa (z ang. *The Food and Agriculture Organization of the United Nations*, FAO) opracowała program – określony jako zielona rewolucja – mający na celu zwiększenie produktywności rolnictwa poprzez zastosowanie wydajniejszych odmian roślin uprawnych oraz rozwój agrotechnologii (Pingali, 2012). W wyniku wdrożenia tego programu w ciągu kolejnych 50 lat produkcja żywności podwoiła się. Odbiło się to jednak kosztem wycinki lasów na terenach przeznaczonych pod uprawy monokultur, nadmiernego zużycia wody, chemizacji nawozami sztucznymi czy koniecznością pokrycia rosnącego zapotrzebowania na energię elektryczną. Antropogeniczne zmiany środowiska przyrodniczego, niczym błędne koło, potęgują problemy gospodarki rolnej zmuszając światowe mocarstwa do wprowadzenia nowoczesnych rozwiązań oraz zrównoważonych metod produkcji (Heffer i Prud'homme, 2013; Mehta, 2018). W 2050 roku przewidywana liczebność populacji ludzkiej przekroczy 9 mld. W połączeniu z oczekiwanym przez większość globalnej populacji wzrostem jakości życia i zwiększonym popytem na produkty pochodzenia zwierzęcego, rolnictwo stoi przed ogromnym wyzwaniem by zapewnić produkcję żywności na odpowiednim poziomie (Millstone i Lang, 2008).

Zubożenie gleb uprawnych, erozja, wyczerpujące się składniki mineralne, zasolenie czy w końcu zanieczyszczenie środowiska w wielu miejscach na Ziemi, spowodowały w latach 1981-2003 obniżenie produktywności rolnictwa (wyrażona w kg/ha) o 12 procent (Millstone i Lang, 2008). W opublikowanym w 2018 roku raporcie przez Międzyrządowy Panel ds. Zmian Klimatu (z ang. *Intergovernmental Panel on Climate Change*, IPCC) można przeczytać, że Ziemia w wyniku działalności człowieka została podgrzana o około 1°C, a rok 2015 był najcieplejszy w ciągu ostatnich 11 000 lat (Tollefson, 2018). Prowadzi to między innymi do zmian amplitud temperaturowych na całym świecie, ekstremalnymi zjawiskami pogodowymi, podwyższeniem poziomu oceanów, deoksygenacją oraz zakwaszeniem wód, czy obniżeniem bioróżnorodności (Law i inni, 2018; Tollefson, 2018; Xu i inni, 2018). Wygenerowane w ten sposób anomalie środowiskowe nie pozostają bez wpływu na rośliny. Rośliny, jako przedstawiciele organizmów prowadzących osiadły tryb życia, są zdolne reagować na wszelkie niekorzystne zmiany zachodzące w środowisku – często kosztem obniżonego plonu oraz jakości cech sensorycznych. W Australii najpopularniejszymi gatunkami roślin uprawnych są pszenica, jęczmień, kukurydza, słonecznik, rzepak czy bawełna. Na podstawie danych z zapisów meteorologicznych w latach 1994-2019 nastąpił znaczny spadek poziomu opadów w Australii. Najgorsze w skutkach susze, które dotknęły Australię miały miejsce w XXI wieku. W ciągu ostatnich dwóch dekad z powodu suszy średnie roczne dochody australijskich gospodarstw rolnych

zmniejszyły się o 22 procent (źródło internetowe 1). Podnoszący się poziom mórz i oceanów powoduje zalewanie słoną wodą nisko położone pola uprawne w południowej Azji. Zbyt wysokie zasolenie ziem dotyka obecnie ponad milion hektarów gruntów ornych w Bangladeszu powodując roczne straty dla gospodarki tego kraju liczone w miliardach dolarów (Millstone i Lang, 2008; Islam i Harun-ur-Rashid, 2011). Z kolei w Europie specjalnie powołana przez rządy Danii oraz Holandii grupa naukowców, zaprezentowała w 2020 roku raport pt. „*The Northern European Enclosure Dam*” (NEED). Projekt NEED proponuje rozwiązanie problemu wzrostu poziomu wód w Europie Północnej poprzez budowę gigantycznych tam mogących uchronić 25 milionów ludzi mieszkających na wybrzeżu Europy przed powodzią. Tama na Morzu Północnym miałaby połączyć z jednej strony kanał pomiędzy Wielką Brytanią oraz Francją, natomiast drugi odcinek łączyłby Szkocję z Szetlandami oraz Norwegią. W sumie trzy odcinki tamy o długości 637 km miałyby pochłonąć 51 miliardów ton piasku i byłaby to największa inwestycja w dziejach ludzkości (źródło internetowe 2).

Fosfor (P, z greckiego φωσφόρος, phōsphóros, czyli „niosący światło”) jest makroelementem, pierwiastkiem, którego pochodzenie oraz obecność na Ziemi pozostaje wciąż zagadką dla geologów i astrofizyków. W składzie chemicznym jądra, płaszcza czy skorupy ziemskiej próżno szukać fosforu - mimo iż jest to pierwiastek biogeny budujący wszystkie organizmy żywe. Jako pierwiastek mineralny fosfor występuje w zaledwie kilku miejscach na Ziemi w postaci złóż kopalnianych. Jednakże dzięki swojej funkcjonalnej reaktywności oraz stabilności strukturalnej, fosfor jest unikalnym pierwiastkiem budującym duże biomolekuły (Pasek i Lauretta, 2005). Fosfor buduje adenosynotryfosforan (ATP) – cząsteczkę magazynującą oraz przekazującą energię w komórkach żywych, jest składnikiem kwasów nukleinowych (DNA oraz RNA), wchodzi w skład błon komórkowych, a jego obecność w zmodyfikowanych po-translacyjnie białkach (fosforylacja) często determinuje ich aktywność biologiczną (Bielecki, 1973). W kosmosie fosfor jest syntetyzowany w masywnych gwiazdach, gdzie w wyniku wybuchu supernowej przedostaje się do materii międzygwiazdowej (z ang. *interstellar medium*, ISM), składającej się głównie z gazu, plazmy i pyłu (Koo i inni, 2013). W rejonach ISM tlenek fosforu zostaje uwięziony w zamrożonych międzygwiazdowych ziarnach pyłu, które łącząc się tworzą komety. W opublikowanej w 2020 roku pracy naukowej na łamach wiodącego czasopisma „Monthly Notices of the Royal Astronomical Society” zespół naukowców ROSINA pod kierownictwem Prof. Kathrin Altwegg (Uniwersytet w Bern, Szwajcaria) dowodzi, że w początkowych etapach kształtowania się Ziemi, to właśnie komety dostarczyły duże ilości fosforu umożliwiającego powstanie życia (Rivilla i inni, 2020). Kilka miesięcy później, inna międzynarodowa grupa naukowców ogłosiła odkrycie fosforowodoru w chmurach zlokalizowanych 55 km nad powierzchnią Wenus

(Greaves i inni, 2020). Fosforowodór (PH_3 , zwany również fosfiną) powstaje podczas redukcji fosforanów przez różne gatunki bakterii w warunkach beztlenowych. Jak do tej pory nie zidentyfikowano procesów niebiogennych, które mogłyby prowadzić do powstania fosforowodoru na planetach skalistych takich jak Ziemia, czy wspomniana Wenus. Z tego względu, w astrobiologii fosforowodór jest traktowany jako wskaźnik zachodzących procesów biologicznych (O'Callaghan, 2020). Życie na Ziemi pojawiło się około 4 miliardów lat temu, ale nadal nie znamy do końca procesów, które to umożliwiły.

Afryka pozostawała pod władzą lokalnych plemion do połowy XIX wieku. W 1884 roku do Berlina, na zaproszenie Ottona von Bismarcka, zjechały się delegacje z całego „cywilizowanego” świata, aby podzielić mapę Afryki między siebie (Sabela, 2015). Jedna kolonia przypadła Hiszpanom, którzy otrzymali prawo do eksploracji zachodniej części Afryki Saharyjskiej stanowiącej obszar pomiędzy Marokiem i Mauretanią. Żadne inne państwo nie wykazało chęci eksploracji tego terenu z powodu braku miast, infrastruktury oraz – jak błędnie założono – braku wartościowych bogactw naturalnych. Z powodu złej sytuacji ekonomicznej Hiszpanie przez kilkadziesiąt lat nie wyruszali w głąb swojej pustynnej kolonii. Dopiero w 1950 roku hiszpański naukowiec, Manuel Madina, natrafił – jak opisał w swoich notatkach ekspedycyjnych – na największe na świecie złoża fosforytów (Sabela, 2015). Do dnia dzisiejszego złoża to stanowi około 80 procent (50 000 mln ton) światowego rezerwuaru skały fosforytu (Cooper i inni, 2011). Niewielkie złoża są jeszcze eksploatowane w Chinach, Algierii, Syrii czy Stanach Zjednoczonych. Fosfor nie jest odnawialny, a jego światowe zasoby kopalniane w drastycznym tempie ulegają wyczerpaniu. W 2100 roku niemal cały rezerwuar złóż fosforu pozostanie pod kontrolą jednego państwa, Maroko (Cooper i inni, 2011). Szacuje się, że przy tylko niewielkim tj. 3-4 procentowych wzroście zapotrzebowania na żywność, fosforytu – wykorzystywanego do produkcji nawozów sztucznych – zabraknie już za około 100 lat, a ceny żywności do tego czasu będą rosły (Scholz i inni, 2013). Na świecie fosfor nie jest traktowany w sposób zrównoważony. Przeważająca jego część znika z łańcucha żywnościowego w postaci odpadów organicznych. Problem fosforu w ostatnich latach narasta i skupia coraz więcej organizacji, jedną z nich jest Europejska Platforma Zrównoważonego Fosforu (z ang. *European Sustainable Phosphorus Platform*, ESPP). ESPP to organizacja pozarządowa zmagająca się z problemem malejących zasobów fosforu oraz wdrażająca ideę jego zrównoważonego wykorzystania w Europie. Organizacja zrzesza duże koncerny, organizacje pozarządowe oraz instytucje naukowe wymieniające się poglądami oraz pomysłami, które mogą wpłynąć na działania w przyszłości (źródło internetowe 4). O tym jak ważną rolę odgrywa fosfor w europejskiej gospodarce świadczy fakt, że skała

fosforytu znajduje się na liście materiałów krytycznych opublikowanej przez Komisję Unii Europejskiej we wrześniu 2020 roku (Blengini i inni, 2020).

Z perspektywy roślin, fosfor jest najmniej mobilnym i najtrudniej dostępnym pierwiastkiem z powodu ogromnej reaktywności z pozostałymi składnikami macierzy glebowej. Około 67 procent wszystkich użytków rolnych na świecie zawiera niewystarczającą ilość fosforu przyswajalnego dla roślin uprawnych (Batjes, 1997; Kirkby i Johnston, 2008). Ponad 90 procent wydobywanej rocznie skały fosforytu przeznacza się do nawożenia gleb (Brunner, 2010), z czego zaledwie 15 procent jest pobieranych (w formie jonów kwasu ortofosforowego: H_2PO_4^- oraz HPO_4^{2-}) przez system korzeniowy roślin. Pozostała część reaguje z materią organiczną oraz związkami chemicznymi, między innymi z tlenkami żelaza, wapnia czy glinu, tworząc stabilne oraz trudno rozpuszczalne osady (Lynch, 2011). W suchej tkance roślinnej znajduje się ponad 0,2 procenta fosforu, który jest asymilowany w postaci fosforanu nieorganicznego (P_i), występującego w standardowej glebie uprawnej w stężeniu około 10 μM . Dla porównania w aktywnych metabolicznie komórkach roślinnych znajduje się fosforan nieorganiczny w stężeniu 10 000 μM , natomiast w trakcie transportu za pośrednictwem ksylemu około 400 μM (Mengel i Kirkby, 1987; Fang i inni, 2009).

Jęczmień (*Hordeum vulgare* L., roślina jednoliścienna, $2n = 14$, genom o wielkości $\sim 5,3$ Gbp, diploid) jest jednym z pierwszych gatunków traw zbożowych udomowionych i uprawianych do celów spożywczych, w przemyśle browarniczym oraz jako pasza dla zwierząt. Obecnie jęczmień jest uprawiany w ponad 100 krajach zajmując 4. miejsce w światowej produkcji zbóż (Giraldo i inni, 2019). W 1986 roku Leigh i Johnston wykazali, że wydajność plonu jęczmienia uprawianego na glebie zawierającej 0,55 kg przyswajalnego dla roślin fosforu na hektar ziemi była ponad 2-krotnie większa niż na glebie zawierającej zaledwie 0,2 kg P/ha (Leigh i Johnston, 1986). Rośliny jednoliścienne, stanowiące grupę roślin okrytonasiennych, wyróżniają się włóknistym systemem korzeniowym. U tej grupy roślin korzeń główny szybko zanika, a funkcje zaopatrujące roślinę w składniki odżywcze pełni korzenie przybyszowe, tworzące tzw. korzenie wiązkowe (Peret i inni, 2011). System korzeniowy roślin pozyskuje jony fosforanowe z roztworu glebowego, który pozostaje w równowadze z niedostępnymi dla roślin fosforanami sorbowanymi przez minerały oraz koloidy zawarte w fazie stałej gleby (Smith i inni, 2003). Organiczna frakcja fosforu (P_o) w glebie może zostać zmineralizowana do postaci przyswajalnego P_i , poprzez: (i) biochemiczną mineralizację, opartą o aktywność fosfataz katalizujących hydrolizę estrów i bezwodników kwasu fosforowego [V], (ii) biologiczną mineralizację poprzez uwalnianie P_i z materii organicznej na drodze utleniania węgla przez mikroorganizmy glebowe oraz (iii) przemiany glebotwórcze zachodzące pod wpływem

ługowania i wzrostu kwasowości gleby, które powodują wietrzenie minerałów pierwotnych (Smeck, 1985; Rita i inni, 2013). Jony fosforanowe przenoszą się w miejsce zasięgu systemu korzeniowego roślin na drodze wolnego procesu dyfuzji. Obszar zasięgu korzeni wiązkowych jest znacznie zwiększony dzięki obecności licznych włosników. Roztwór glebowy przedostaje się, na drodze apoplastycznej, do przestrzeni międzykomórkowych korzeni, tworzących tzw. otwartą siatkę w młodych częściach organu (Peterson i Cholewa, 1998). Przemieszczanie się roztworu glebowego zostaje zatrzymane przez nieprzepuszczalne pasemka Caspary'ego otaczające komórki korowe oraz endodermalne korzenia. Te zgrubienia ścian komórkowych zbudowane są z silnie hydrofobowych związków chemicznych oraz ligniny (Perumalla i Peterson, 1986). Wychwytywanie jonów fosforanowych z drogi apoplastycznej na drogę symplastyczną, następuje dzięki białkom błonowym pełniącym funkcję transporterów fosforanowych (Smith i inni, 2003). Te wyspecjalizowane białka umożliwiają aktywny transport jonów P_i z apoplastu, gdzie stężenie P_i jest kilkukrotnie mniejsze aniżeli w cytoplazmie komórek endodermi. Silne gradienty elektrochemiczne są pokonywane przez rodzinę białek wysokiego powinowactwa P_i / H^+ PHOSPHATE TRANSPORTERS (PHT). Poznane do tej pory roślinne transportery fosforanów, obejmują sekwencje homologiczne do pierwszego opisanego transportera PHO84 zidentyfikowanego w komórkach drożdżowych (*Saccharomyces cerevisiae* Meyen ex Hansen) (Bun-Ya i inni, 1991). W zależności od lokalizacji w komórce, białka PHT zostały podzielone na 5 rodzin: PHT1 (błona komórkowa), PHT2 (chloroplasty), PHT3 (mitochondria), PHT4 (aparat Golgiego) oraz PHO (błona komórkowa odpowiedzialna za ładowanie P_i do ksylemu) (Guo i inni, 2007). W jęczmieniu opisano do tej pory 11 członków rodziny białkowej PHT1 (HvPHT1.1-HvPHT1.11), które są zaangażowane w pobieranie P_i z gleby oraz jego translokację do części nadziemnych rośliny (Teng i inni 2017). Większość transporterów fosforanowych nie występuje w jednym typie komórek, ale znajdują się w różnych organach tworząc nakładające się na siebie wzory, co wskazuje na ich złożoną rolę w dystrybucji P_i w obrębie rośliny (Nussaume i inni, 2011). Jedną z podstawowych strategii roślin przystosowanych do bytowania w zmiennych warunkach stężenia P_i w glebie jest regulacja wykorzystująca proces degradacji białek determinujący liczbę transporterów fosforanowych wysycających błony komórkowe. W tym procesie uczestniczy m.in. białko kodowane przez gen PHOSPHATE 2 (*PHO2*).

PHO2 jest enzymem typu E2 (UBC24) sprzęgającym ubikwitynę, który razem z odpowiednią ligazą typu E3 katalizuje kowalencyjne wiązanie ubikwityny przez białka docelowe. Takie białka są następnie kierowane na szlak degradacji. Obniżenie poziomu ekspresji genu *PHO2* zabezpiecza transportery fosforanowe przed

degradacją, takie jak: PHOSPHATE 1 (PHO1) oraz transportery z rodziny PHT1 (Aung i inni, 2006; Park i inni, 2014). W ryżu PHO2 pośredniczy w degradacji białka PHOSPHATE TRANSPORTER TRAFFIC FACILATOR 1 (PHF1) biorącego udział w odtransportowaniu nieufosforylowanych białek PHT1 z retikulum endoplazmatycznego (ER) do błony komórkowej (González i inni, 2005) oraz białka PROTEIN PHOSPHATASE 95 (PP95), który defosforyluje transportery fosforanów w obrębie ER (Yang i inni, 2020). Mutant *Arabidopsis thaliana* L. z wyłączonym genem *PHO2* akumuluje duże ilości Pi w części nadziemnej, które w nadmiarze są toksyczne dla rośliny. Dzieje się tak z powodu wysycenia błon komórkowych transporterami fosforanowymi oraz nadmierną translokacją Pi z korzeni do pędu (Delhaize i Randall, 1995). Z kolei eksperymenty polowe na liniach pszenicy (*Triticum aestivum* L.) z wyłączonym genem *PHO2* wykazały ich wyższą zdolność do przyswajania Pi oraz zwiększone plonowanie na glebach ubogich w fosforany aniżeli w typie dzikim (Ouyang i inni, 2016). To jak ważna jest rola enzymu UBC24 wskazuje zakonserwowany u roślin wyższych mechanizm sprzężenia zwrotnego angażujący cząsteczkę mikroRNA399 oraz długie niekodujące RNA INDUCED BY PHOSPHATE STARVATION 1 (*IPS1*) (Franco-Zorrilla i inni, 2007). Cząsteczki miR399 są wycinane z transkryptów prekursorowych (pre-miR399), które są transkrybowane z 10 genomowych loci w jęczmieniu (Hackenberg i inni, 2013). Dojrzałe izoformy miR399 rozpoznają sześć miejsc cięcia w obrębie regionu 5'-UTR transkryptów *PHO2* (Pacak i inni, 2016). Cząsteczki *IPS1* wiążą miR399 ale ze względu na obecność niesparowań pomiędzy nukleotydami w *IPS1* a miR399, ta pierwsza cząsteczka RNA nie ulega rozcięciu (Huang i inni, 2011). Mechanizm ten pozwala kontrolować rolę UBC24 w degradacji transporterów fosforanowych w kontekście dostępności Pi w glebie.

Wiedza na temat molekularnych oraz fizjologicznych mechanizmów odpowiadających za możliwości dostosowania się roślin, w szczególności zbóż do niekorzystnych i często zmieniających się warunków środowiskowych wciąż jest uboga. Dotychczasowe osiągnięcia badań podstawowych w tym obszarze określają serię przystosowań roślin takie jak np. zmiany w składzie chemicznym błon fosfolipidowych, redystrybucja fosforanów z tkanek chorych oraz starzejących się do tkanek rozwijających się i generatywnych, zmiana architektury systemu korzeniowego, zmiana gospodarki hormonalnej czy regulacja liczby oraz zagęszczenia transmembranowych transporterów fosforanowych. W swojej pracy doktorskiej zbadałem molekularną maszynę regulującą gospodarkę fosforanową w tkankach roślinnych na przykładzie jednego z najważniejszych genów zaangażowanych w utrzymanie homeostazy fosforanowej tj. *PHO2* w jęczmieniu.

W związku z powyższym główne cele mojej pracy doktorskiej to:

- opis roli czynników transkrypcyjnych z rodziny PHR (PHOSPHATE STARVATION RESPONSE) w utrzymaniu homeostazy fosforanowej roślin,
- opracowanie metodologii do badania poziomu ekspresji genów jęczmienia pod wpływem zmiennego stężenia fosforanów w podłożu,
- identyfikacja elementów *cis*-regulatorowych mogących determinować aktywność transkrypcyjną genu *PHO2*,
- identyfikacja czynników transkrypcyjnych mogących wiązać się z elementami regulatorowymi genu *PHO2*,
- przetestowanie hipotezy, że sekwencja 5'-UTR genu *PHO2* funkcjonuje jako modulator ekspresji,
- zbadanie zmian w poziomie małych RNA w tym mikroRNA pod wpływem niedoboru fosforanów przy zastosowaniu: droplet digital PCR (ddPCR), hybrydyzacji typu northern oraz głębokiego sekwencjonowania,
- identyfikacja oraz charakterystyka cząsteczek małych RNA (18-25 nt) ulegających zmienionej ekspresji w odpowiedzi na niedobór fosforu w korzeniu i części nadziemnej jęczmienia,
- identyfikacja docelowych mRNA rozcinanych przy udziale mikroRNA (analiza degradomu),
- identyfikacja genów potencjalnie związanych z utrzymaniem homeostazy fosforanowej w jęczmieniu,
- obszerna analiza zmian na poziomie RNA w jęczmieniu w celu oceny podstawowych strategii roślin uprawnych umożliwiających przetrwanie w warunkach niedoboru fosforu.

Część pierwsza pracy doktorskiej poświęcona jest pracy przeglądowej, która wprowadza do tematyki homeostazy fosforanowej. W pracy opublikowanej na łamach czasopisma *MDPI Genes* szczegółowo opisuję roślinną rodzinę białek PHR. Białka PHR funkcjonują jako czynniki transkrypcyjne posiadające zakonserwowane w obrębie królestwa roślin domeny SANT/Myb oraz MYB-CC (coiled-coil). Czynniki transkrypcyjne PHR rozpoznają specyficzny region P1BS (PHR1 binding sites, którego konsensusowa sekwencja to GNATATNC) w obrębie regionów regulatorowych genów odpowiedzi na niedobór Pi. Czynniki transkrypcyjne PHR funkcjonują jako nadrzędne regulatory ekspresji genów roślinnych zaangażowanych w utrzymanie gospodarki fosforanowej. W wyniku swojej działalności mogą zarówno promować jak i hamować transkrypcję genów. Ich rolę w regulacji transkrypcji genów docelowych opisałem w skrócie. W pracy większą uwagę poświęciłem najnowszym doniesieniom z ostatnich 5 lat. Opisałem alternatywne szlaki metaboliczne oraz cząsteczki molekularne, które

mogą decydować o aktywności czynników transkrypcyjnych PHR w kontekście utrzymania homeostazy fosforanowej roślin. W pracy uwzględniłem między innymi wpływ fitohormonów, dostępność jonów metali, składników mineralnych czy rolę modyfikacji po-translacyjnych. Część pracy poświęciłem również czynnikom mogącym regulować poziom ekspresji genów *PHR* samych w sobie.

Część druga pracy doktorskiej odnosi się do metod analizy ekspresji genów wykorzystywanych przeze mnie w trakcie pracy eksperymentalnej. W rozdziale monografii opublikowanej przez wydawnictwo *Methods in Molecular Biology - Springer* opisałem metodykę przeprowadzenia analizy ekspresji genów oraz poziomu cząsteczek miRNA za pomocą ilościowych metod: real-time PCR oraz ddPCR (droplet digital PCR). W pracy, w której jestem drugim autorem, miałem za zadanie opisać cały protokół od izolacji materiału genetycznego do końcowego eksperymentu analizy ilościowej ekspresji genu. Protokół ten był wykorzystywany przeze mnie do analiz zmian w ekspresji genów potencjalnie zaangażowanych w homeostazę fosforanową jęczmienia, które zostały opublikowane w pracach oryginalnych zawartych w kolejnych częściach pracy doktorskiej. Opracowany przeze mnie protokół do pracy z ddPCR jest wykorzystywany przez inne osoby. Ponadto w pracy metodycznej po raz pierwszy opublikowałem absolutną liczbę kopii dojrzałych cząsteczki miR399c oraz transkryptu *PHO2* z korzenia oraz części nadziemnej jęczmienia ustaloną techniką ddPCR.

W części trzeciej pracy doktorskiej przedstawiam wyniki eksperymentalne poszerzające obecny stan wiedzy na temat regulacji transkrypcji genu *PHO2* w jęczmieniu. W przyjętej hipotezie badawczej, założono, że oprócz regulacji po-transkrypcyjnej poziomu transkryptów *PHO2* przy udziale miR399, poziom ten jest regulowany także na poziomie transkrypcyjnym. Wynikało to z faktu, że niektóre obserwowane zmiany w ekspresji genu *PHO2* nie można było wytłumaczyć działaniem miR399. W badanych przeze mnie korzeniach roślin jęczmienia, mimo indukcji poziomu ekspresji dojrzałych cząsteczek miR399 w warunkach stresu niedoboru Pi, poziom ekspresji genu *PHO2* spadał, ale nie był to spadek znaczący statystycznie. Wykorzystując dostępne narzędzia bioinformatyczne zidentyfikowałem elementy *cis*-regulatorowe w obrębie promotora oraz regionu 5'-UTR genu *PHO2*. Wyselekcjonowane motywy DNA następnie posłużyły do badania „przesiewowego” w poszukiwaniu potencjalnych białek mogących rozpoznawać wspomniane motywy oraz regulować ekspresję genu *PHO2*. Przy pomocy drożdżowego systemu jednohybrydowego zidentyfikowałem dwa czynniki transkrypcyjne posiadające charakterystyczne domeny SANT/Myb oraz MYB-CC odpowiadające przedstawicielom białkowej rodziny PHR. Oba czynniki transkrypcyjne wiążą się z motywami (P1BS oraz P-responsive PHO element) zlokalizowanymi w obrębie intronu regionu 5'-UTR

genu *PHO2*. Analizy *in silico* wykazały, że jedno z zidentyfikowanych białek jest kodowanych przez locus odpowiadające dobrze znanemu białku PHR1. Natomiast drugie białko na podstawie homologii do znanych białek Arabidopsis (czynników transkrypcyjnych), zostało sklasyfikowane oraz nazwane przeze mnie jako jęczmienny czynnik transkrypcyjny ALTERED PHLOEM DEVELOPMENT (APL). Wykorzystując protokół opisany w części drugiej, po raz pierwszy wykazałem, że stres niedoboru Pi obniża absolutną liczbę kopii transkryptu *APL* zarówno w części korzeniowej jak i nadziemnej jęczmienia. O tym jak ważna jest rola regionu 5'-UTR w regulacji transkrypcji genu *PHO2* dowiodłem korzystając z technik zarówno w warunkach *in vitro* jak i *in vivo* w komórkach tytoniu (*Nicotiana benthamiana* L.).

W części czwartej pracy doktorskiej wyniki kompleksowych badań dostarczają danych na temat globalnych zmian w poziomie cząsteczek zarówno małych RNA jak i mRNA w jęczmieniu. Praca oryginalna została przeze mnie napisana w oparciu o wyniki głębokiego sekwencjonowania pochodzące z jęczmienia. Okazuje się, że tylko niewielka pula małych RNA o zmienionym poziomie ekspresji w warunkach niedoboru Pi mapuje do scharakteryzowanych do tej pory cząsteczek miRNA (na podstawie danych zdeponowanych w miRBase). Zarówno w korzeniu jak i w części nadziemnej zaobserwowałem, że wzrost poziomu ekspresji w odpowiedzi na niedobór Pi wykazują izoformy miRNA pochodzące z dwóch rodzin: miR399 oraz miR827. Obie rodziny uczestniczą w utrzymaniu roślinnej homeostazy fosforanowej. Cząsteczki miR399 – jak wspomniałem wcześniej – negatywnie regulują poziom transkryptów genu *PHO2*. Z kolei miR827 u jednoliściennych uczestniczy w po-transkrypcyjnej regulacji ekspresji dwóch genów *SPX-MFS1* oraz *SPX-MFS2* (nazwa pochodzi od białek SYG1/PHO81/XPR1 oraz domeny Major Facility Superfamily). Potwierdziłem istnienie fragmentów docelowych genów, które wskazują na rozcinanie mRNA przy udziale wspomnianych mikroRNA. Stworzona platforma degradomowa umożliwia zidentyfikowanie małych RNA, które kierują rozcinaniem docelowego mRNA pochodzącego zarówno z korzenia jak i części nadziemnej jęczmienia. W pracy opisuję wiele interesujących przykładów miRNA oraz małych RNA (niezmapowanych do miRBase), które mogą uczestniczyć w regulacji po-transkrypcyjnej genów w odpowiedzi na stres niedoboru Pi. Ponadto zidentyfikowałem 98 genów o istotnie zmienionym poziomie ekspresji w warunkach niedoboru fosforanów dla części nadziemnej jęczmienia. Niektóre z nich mogą okazać się bardzo istotne z punktu widzenia ochrony roślin przed infekcjami grzybowymi. Zauważyłem spadek ekspresji genu kodującego oksydazę kwasu szczawiowego. Kwas szczawiowy jest wydzielany przez grzyby w trakcie infekcji w celu osłabienia ściany komórkowej rośliny (Zhang i inni, 1995). W oparciu o obecny stan wiedzy oraz dane opublikowane w pracy oryginalnej opisałem wszystkie najbardziej interesujące szlaki metaboliczne

zaangażowane w utrzymanie homeostazy fosforanowej roślin. Szczegółowy opis poparłem graficznym modelem, który obrazuje skalę zmian zachodzących w jęczmieniu na poziomie RNA.

Wyniki pracy doktorskiej zostały zaprezentowane na konferencjach naukowych w kraju oraz zagranicą:

1. **Ustne wystąpienie** pt. „*Integrated sRNA, degradome profiling and RNA-Seq analysis identifies phosphate starvation-responsive small RNAs and genes in barley*” na międzynarodowej konferencji 4th iPlanta, 26-28 luty 2020, Ateny, Grecja
2. **Ustne wystąpienie** pt. „*The 5'-UTR region is necessary for efficient PHOSPHATE 2 expression in barley*” na międzynarodowej konferencji 5th International Conference on Research and Education Challenges for Contemporary Live Sciences BioRun, 8-13 kwiecień 2019, Poznań, Polska
3. **Ustne wystąpienie** pt. „*Global analysis of small RNA level changes in barley roots and shoots during phosphate starvation*” na międzynarodowej konferencji 2nd iPlanta, 14-16 luty 2018, Poznań, Polska
4. **Ustne wystąpienie** pt. „*The importance of 5'-UTR region for the regulation of PHOSPHATE 2 gene expression in barley*” na międzynarodowych warsztatach 5th Kiel Days, 7-9 listopad 2018, Poznań, Polska
5. **Zaprezentowano poster** pt. „*Global analysis of small RNA level changes in barley roots and shoots during phosphate starvation*” na międzynarodowej konferencji Plant Biology Europe, 18-21 czerwiec 2018, Kopenhaga, Dania
6. **Zaprezentowano poster** pt. „*Transcriptional and post-transcriptional regulation of barley PHO2 gene*” na międzynarodowej konferencji 6th Symposium on Phosphorus in Soils and Plants, 10-13 wrzesień 2018, Leuven, Belgia
7. **Zaprezentowano poster** pt. „*Identification of transcription factors binding to PHOSPHATE2 5'-UTR in barley*” na międzynarodowej konferencji 18th International Plant Nutrition Colloquium, 19-24 sierpień 2017, Kopenhaga, Dania
8. **Zaprezentowano poster** pt. „*Searching for PHOSPHATE 2 (ubiquitin-conjugating enzyme) partner proteins in barley*” na międzynarodowej konferencji VISCEA, 26-30 czerwiec 2017, Wiedeń, Austria
9. **Zaprezentowano poster** pt. „*Phosphate transporters HvPHT1;1, HvPHT1;6 and HvPHO1 maintain Pi concentration in barley roots during heat stress conditions*” na międzynarodowej konferencji Plant Biology, 9-13 lipiec 2016, Teksas, Stany Zjednoczone
10. **Zaprezentowano poster** pt. „*PHOSPHATE 2 gene: in the hub of phosphate homeostasis in barley*” na międzynarodowej konferencji EMBO Young Scientists Forum, 2-3 lipiec 2015, Warszawa, Polska

SUMMARY / STRESZCZENIE

In the 1960s, the Food and Agriculture Organization of the United Nations (FAO) developed a programme – described as the Green Revolution – to increase agricultural productivity through the use of more efficient crop varieties and the development of agrotechnology (Pingali, 2012). As a result of this programme, food production has doubled over the next 50 years. However, this was done at the cost of deforestation on lands designated for monoculture, excessive water consumption, chemically treated with artificial fertilisers or the need to cover the growing demand for electricity. Anthropogenic changes in the natural environment, like a vicious circle, exacerbate the problems of farming, forcing the global powers to introduce modern solutions and sustainable production methods (Heffer and Prud' homme, 2013; Mehta, 2018). In 2050, the projected human population will exceed 9 billion. Together with the increase in the quality of life expected by the majority of the global population and the increased demand for animal products, agriculture is facing a huge challenge to ensure food production at an appropriate level (Millstone and Lang, 2008).

Impoverishment of agricultural soils, erosion, depletion of minerals, salinisation and, finally, environmental pollution in many parts of the world, resulted in a 12 per cent reduction in agricultural productivity (expressed in kg/ha) between 1981 and 2003 (Millstone and Lang, 2008). A report published in 2018 by the Intergovernmental Panel on Climate Change (IPCC) says that as a result of human activity, the Earth was heated by about 1°C and that 2015 was the warmest year in the last 11 000 years (Tollefson, 2018). This is reflected, among other things, in changes in temperature amplitudes around the world, extreme weather events, rising ocean levels, deoxygenation and acidification of waters, or a decline in biodiversity (Law et al., 2018; Tollefson, 2018; Xu et al., 2018). The environmental anomalies generated in this way are not without effect on plants. Plants, as representatives of sedentary organisms, can react in various ways to any adverse changes in the environment – often at the expense of reduced yield and quality of sensory characteristics. In Australia, the most popular crops are wheat, barley, maize, sunflower seeds, rapeseed and cotton. Based on data from meteorological records, between 1994 and 2019, there was a significant drop in rainfall in Australia. The worst drought that hit Australia occurred in the 21st century. Over the last two decades, due to the drought, the average annual income of Australian farms has decreased by 22 per cent (Internet source 1). Rising sea and ocean levels are flooding the low-lying fields in southern Asia with salt water. Excessive salinisation of the land is currently affecting more than one million hectares of arable land in Bangladesh, causing billions of dollars in annual losses

to the country's economy (Millstone and Lang, 2008; Islam and Harun-ur-Rashid, 2011). Whereas in Europe, in 2020, a group of scientists specially established by the governments of Denmark and the Netherlands presented a report entitled *The Northern European Enclosure Dam* (NEED). The NEED project proposes to solve the problem of rising water levels in northern Europe by building giant dams that could protect the 25 million people living on Europe's coast from flooding. The North Sea dam would connect the UK and France on one side, while the second section would connect Scotland with Shetland and Norway. In total, three sections of the 637 km long dam would absorb 51 billion tonnes of sand, and this would be the largest investment in human history (Internet source 2).

Phosphorus (P, from the Greek φωσφόρος, phōsphóros, or 'carrying light') is a macroelement, an element whose origin and presence on Earth is still a mystery to geologists and astrophysicists. In the chemical composition of the nucleus, mantle or Earth's crust, there is no point to look for phosphorus – even though it is the biogenic element that builds all living organisms. As a mineral element, phosphorus occurs in only a few places on Earth in the form of mine deposits. However, due to its functional reactivity and structural stability, phosphorus is a unique element building large biomolecules (Strap and Lauretta, 2005). Phosphorus builds adenosine triphosphate (ATP) – a molecule that stores and transfers energy in living cells, is the component of nucleic acids (DNA and RNA), is a component of cell membranes, and its presence in posttranslationally modified proteins (phosphorylation) often determines its biological activity (Bieleski, 1973). In space, phosphorus is synthesised in massive stars, where as a result of a supernova explosion it enters interstellar medium (ISM), consisting mainly of gas, plasma and dust (Koo et al., 2013). In the ISM regions, phosphorus oxide is trapped in frozen interstellar dust grains, which merge to form comets. In a 2020 scientific paper published in the leading journal entitled *Monthly Notices of the Royal Astronomical Society*, a team of ROSINA scientists headed by Prof. Kathrin Altwegg (University of Bern, Switzerland) proves that in the early stages of the Earth's formation, it was comets that provided large quantities of life enabling phosphorus (Rivilla et al., 2020). A few months later, another international group of scientists announced the discovery of hydrogen phosphide in clouds located 55 km above the surface of Venus (Greaves et al., 2020). Hydrogen phosphide (PH₃, also called phosphine) is formed during the reduction of phosphates by various species of bacteria under anaerobic conditions. So far, no non-biogenic processes have been identified that could lead to the formation of phosphine on rocky planets such as Earth or the aforementioned Venus. For this reason, in astrobiology, phosphine is treated as an indicator of biological processes

(O'Callaghan, 2020). Life on Earth started about 4 billion years ago, but we still do not fully understand the processes that made this possible.

Africa remained under the rule of local tribes until the mid-19th century. In 1884, at the invitation of Otto von Bismarck, delegations from all over the "civilised" world came to Berlin to share the map of Africa among themselves (Sabela, 2015). One colony went to Spain. They were given the right to explore the western part of Saharan Africa, an area between Morocco and Mauritania. No other country showed any willingness to explore the area due to a lack of cities, infrastructure and, as was wrongly assumed, a lack of valuable natural resources. Due to the poor economic situation, the Spaniards did not go deep into their desert colony for several decades. It was only in 1950 that a Spanish scientist, Manuel Madina, came across – as he described in his expeditionary notes – the world's largest phosphorite deposits (Sabela, 2015). To date, this deposit accounts for approximately 80 per cent (50 000 million tonnes) of the world's phosphate rock reservoir (Cooper et al., 2011). Small deposits are still being exploited in China, Algeria, Syria or the United States. Phosphorus is not renewable, and its global mining resources are being drastically depleted. In 2100, almost the entire phosphorus reservoir will remain under the control of one country, Morocco (Cooper et al., 2011). It is estimated that with only a small, i.e. 3-4% increase in demand for food, phosphorite – used in the production of artificial fertilisers – will be scarce in about 100 years, and food prices will rise by that time (Scholz et al., 2013). In the world, phosphorus is not treated sustainably. Most of it disappears from the food chain as organic waste. The issue of phosphorus has been growing in recent years, and more and more organisations are gathering together, one of them is the European Sustainable Phosphorus Platform (ESPP). The ESPP is a non-governmental organisation dealing with the issue of decreasing phosphorus resources and implementing the idea of its sustainable use in Europe. The organisation brings together large corporations, non-governmental organisations and scientific institutions exchanging views and ideas that may influence future activities (Internet source 4). The important role played by phosphorus in the European economy is demonstrated by the fact that the phosphate rock is on the list of critical raw materials published by the European Commission in September 2020 (Blengini et al., 2020).

For plants, phosphorus is the least mobile and most challenging element to access due to its great reactivity with the other components of the soil matrix. Around 67 per cent of all agricultural land in the world contains insufficient phosphorus assimilable to arable crops (Batjes, 1997; Kirkby and Johnston, 2008). More than 90 per cent of the phosphate rock extracted annually is used for soil

fertilisation (Brunner, 2010), of which only 15 per cent is taken up (in the form of orthophosphoric acid ions: H_2PO_4^- and HPO_4^{2-}) by the root system of plants. The rest reacts with organic matter and chemical compounds, including iron, calcium and aluminium oxides, creating stable and hardly soluble deposits (Lynch, 2011). The dry plant tissue contains more than 0.2 per cent of phosphorus, which is assimilated in the form of inorganic phosphate (Pi), found in standard arable soil at a concentration of about 10 μM . For comparison, the metabolically active plant cells contain Pi at a concentration of 10 000 μM , while during transport via xylem – about 400 μM (Mengel and Kirkby, 1987; Fang et al., 2009).

Barley (*Hordeum vulgare* L., monocotyledonous plant, $2n = 14$, genome size ~ 5.3 Gbp, diploid) is one of the first cereal grass species domesticated and cultivated for food purposes, in the brewing industry and as animal feed. At present, barley is grown in more than 100 countries, ranked fourth in world cereal production (Giraldo et al., 2019). In 1986, Leigh and Johnston showed that the yield of barley grown on a soil containing 0.55 kg of plant-absorbable phosphorus per hectare of land was more than 2 times higher than on a soil containing only 0.2 kg P/ha (Leigh and Johnston, 1986). Monocotyledonous plants, which are a group of angiosperms plants, are distinguished by their fibrous root system. In this group of plants, the main root quickly disappears, and the functions supplying the plant with nutrients are performed by the adventitious roots, forming the so-called bundle roots (Peret et al., 2011). The plant root system extracts phosphate ions from the soil solution, which is in balance with phosphates that are unavailable to plants, which are sorbed by minerals and colloids contained in the solid phase of the soil (Smith et al., 2003). The organic phosphorus fraction (Po) in the soil can be mineralised to assimilable Pi, through (i) biochemical mineralisation, based on the activity of phosphatases catalysing the hydrolysis of phosphoric acid esters and anhydrides [V], (ii) biological mineralisation by releasing Pi from organic matter through carbon oxidation by soil micro-organisms, and (iii) soil formation transformations due to leaching and acidity growth of the soil, which cause weathering of the primary minerals (Smeck, 1985; Rita et al., 2013). Phosphate ions are transferred to the root system of the plants by a slow diffusion process. The range of the bundle roots is significantly increased due to the presence of numerous root hairs. The soil solution penetrates, on an apoplastic pathway, into the intercellular spaces of the roots, forming an open grid in the young parts of the organ (Peterson and Cholewa, 1998). The movement of the soil solution is stopped by impermeable Casparian strips surrounding the cortical and endodermal cells of the root. These cell wall thicknesses are made of strongly hydrophobic chemicals and lignin (Perumalla and Peterson, 1986). The capture of phosphate ions from the

apoplastic to the symplastic pathway is achieved by membrane proteins acting as phosphate transporters (Smith et al., 2003). These specialised proteins enable the active transport of Pi ions from the apoplast, where the concentration of Pi is several times lower than in the cytoplasm of endoderm cells. Strong electrochemical gradients are overcome by the Pi / H⁺ PHOSPHATE TRANSPORTERS (PHT) high-affinity protein family. Plant phosphate transporters known so far include homologous sequences to the first described PHO84 transporter identified in yeast cells (*Saccharomyces cerevisiae* Meyen ex Hansen) (Bun-Ya et al., 1991). Depending on location in the cell, PHT proteins were divided into 5 families: PHT1 (cell membrane), PHT2 (chloroplasts), PHT3 (mitochondria), PHT4 (Golgi apparatus) and PHO (cell membrane responsible for loading Pi to the xylem) (Guo et al., 2007). So far, 11 members of the PHT1 protein family (HvPHT1.1-HvPHT1.11), which are involved in the uptake of Pi from the soil and its translocation to the aboveground parts of the plant, have been described in barley (Teng et al., 2017). Most phosphate transporters do not occur in one type of cell, but are located in different organs creating overlapping patterns, which indicates their complex role in the distribution of Pi within the plant (Nussaume et al., 2011). One of the basic strategies of plants adapted to living in conditions of Pi deficiency in soil is to regulate the level of proteins, including phosphate transporters, by molecular pathway, which results in a variable number of phosphate transporters saturating cell membranes. The gene encoding protein PHOSPHATE 2 (PHO2) is responsible for this process.

PHO2 is an E2-type (UBC24) ubiquitin-conjugating enzyme which, together with the appropriate E3-type ligase, catalyses the covalent binding of ubiquitin by target proteins. Such proteins are then directed to the degradation pathway. Lowering the *PHO2* gene expression level protects phosphate transporters from degradation, such as PHOSPHATE 1 (PHO1) and PHT1 family transporters (Aung et al., 2006; Park et al., 2014). In rice, PHO2 mediates the degradation of PHOSPHATE TRANSPORTER TRAFFIC FACILITATOR 1 protein (PHF1) involved in the transport of the unphosphorylated PHT1 proteins from the endoplasmic reticulum (ER) to the cell membrane (González et al., 2005) and PROTEIN PHOSPHATASE 95 (PP95), which deforms phosphate transporters within ER (Yang et al., 2020). The *pho2* knock-out mutant from *Arabidopsis thaliana* accumulates large amounts of Pi in the aboveground part, which are toxic to the plant in excess. This is due to the saturation of cell membranes with phosphate transporters and the excessive translation of Pi from roots to shoot (Delhaize and Randall, 1995). On the other hand, field experiments on wheat lines (*Triticum aestivum* L.) with the *PHO2* gene deactivated showed their higher Pi absorption capacity and increased yielding on

phosphate-poor soils than in the wild type (Ouyang et al., 2016). The importance role of the enzyme UBC24 is indicated by the preserved feedback mechanism in higher plants involving the microRNA399 molecule and long non-coding RNA *INDUCED BY PHOSPHATE STARVATION 1* (*IPS1*) (Franco-Zorrilla et al., 2007). MiR399 molecules are excised from precursor transcripts (pre-miR399) that are transcribed from 10 genomic loci in barley (Hackenberg et al., 2013). The mature isoforms of miR399 recognise six cleavage sites within the 5'-UTR region of *PHO2* transcripts (Pacak et al., 2016). Particles *IPS1* bind miR399, but due to the presence of mismatches between nucleotides in *IPS1* and miR399, this first RNA molecule does not get cleaved (Huang et al., 2011). This mechanism allows controlling the role of UBC24 in the degradation of phosphate transporters in the context of Pi availability in the soil.

Knowledge of the molecular and physiological mechanisms responsible for the ability of plants, especially cereals, to adapt to unfavourable and often changing environmental conditions is still poor. The achievements of basic research in this area to date are determined by a series of adaptations of plants such as changes in the chemical composition of phospholipid membranes, redistribution of phosphates from diseased and ageing tissues to developing and generative tissues, change in the architecture of the root system, change in hormonal management or regulation of the number and density of transmembrane phosphate transporters. In my doctoral thesis, I am studying and learning about the molecular machinery regulating phosphate management in plant tissues on the example of one of the most important genes involved in maintaining phosphate homeostasis, i.e. *PHO2* in barley.

Therefore, the main objectives of my doctoral thesis are:

- description of the role of PHR-like (*PHOSPHATE STARVATION RESPONSE*) transcription factors in maintaining plant phosphate homeostasis,
- developing a methodology to study the influence of soil phosphate availability on the expression level of barley genes,
- identification of *cis*-regulatory elements that may determine transcriptional activity of *PHO2* gene,
- identification of transcription factors that may be associated with control elements of the *PHO2* gene,
- testing the hypothesis that the 5'-UTR sequence of the *PHO2* gene functions as an expression modulator,
- investigating changes in the level of small RNAs, including microRNAs under

the influence of phosphate deficiency, using: droplet digital PCR, northern type hybridization and deep sequencing,

- identification and characterization of small RNA molecules (18-25 nt) undergoing altered expression in response to phosphorus deficiency in the root and aboveground part of barley,
- identification of target mRNAs cut with microRNAs (degradome analysis),
- identification of genes potentially related to the maintenance of phosphate homeostasis in barley,
- extensive analysis of changes in barley RNA levels to assess basic strategies for crops to survive under phosphorus deficiency conditions.

The first part of my doctoral thesis is devoted to a review, which introduces the topic of plant phosphate homeostasis. In a paper published in the *MDPI Genes* journal, I present a detailed description of the plant family of PHR proteins. PHR proteins function as transcription factors with the SANT/Myb and MYB-CC (coiled-coil) domains preserved within the plant kingdom. The PHR transcription factors identify the specific P1BS region (PHR1 binding sites, the consensus sequence of which is GnATATnC) within the regulatory regions of the Pi deficiency response genes. The PHR transcription factors function as superior regulators of the expression of plant genes involved in maintaining phosphate management. As a result of their activities, they can both promote and inhibit gene transcription. Their role in regulating the transcription of target genes is described in brief. I have paid more attention in my work to the latest reports from the last five years. I described alternative metabolic pathways and molecular molecules that may determine the activity of PHR transcription factors in the context of maintaining plant phosphate homeostasis. In my work, I took into account, among other things, the influence of phytohormones, the availability of metal ions, minerals and the role of post-translational modifications. I have also devoted part of my work to factors which can regulate the level of expression of the *PHR* genes themselves.

The second part of my doctoral dissertation relates to the methods of gene expression analysis I used during laboratory work. In the chapter of the monograph published by *Methods in Molecular Biology - Springer*, I described the methodology of analysing the expression of genes and levels of miRNA molecules by means of quantitative real-time PCR and ddPCR (droplet digital PCR). In this work, in which I am the second author, my task was to describe the whole protocol from the isolation of genetic material to the final experiment of quantitative analysis of gene expression, especially using ddPCR method. This protocol was

used by me to analyse changes in the expression of genes potentially involved in barley phosphate homeostasis, which were published in the original papers contained in subsequent parts of my doctoral thesis. The protocol I have developed to work with the ddPCR is used by others. Moreover, in the methodological work, I published for the first time the absolute number of copies of mature miR399c molecule and *PHO2* transcript from the root and aboveground part of barley established by ddPCR technique.

In the third part of my doctoral dissertation, I present experimental results extending the current state of knowledge on the regulation of *PHO2* gene transcription in barley. In the adopted research hypothesis, it was assumed that in addition to the post-transcriptional regulation of the level of *PHO2* transcripts with the participation of miR399, this level is also regulated at the transcriptional level. This was due to the fact that some of the observed changes in *PHO2* gene expression could not be explained by the effect of miR399. In the barley plant roots, I studied, despite the induction of the expression level of mature miR399 molecules under Pi deficiency stress, the expression level of the *PHO2* gene decreased, but it was not a statistically significant decrease. Using the available bioinformatics tools, I identified *cis*-regulatory elements within the promoter and the 5'-UTR region of *PHO2* gene. Selected DNA motifs were then used for "screening" in search of potential proteins that could recognise these motifs and regulate expression of the *PHO2* gene. Using the yeast single-hybrid system, I have identified two transcription factors with the characteristic SANT/Myb and MYB-CC domains corresponding to the PHR protein family. Both transcription factors are related to motifs (P1BS and P-responsive PHO element) located within the intron of region 5'-UTR of *PHO2* gene. *In silico* analyses showed that one of the identified proteins is encoded by a locus corresponding to the well-known PHR1 protein. The second protein, on the basis of homology to known Arabidopsis proteins (transcription factors), was classified and named by me as barley transcription factor ALTERED PHLOEM DEVELOPMENT (APL). Using the protocol described in part two, I have shown for the first time that Pi deficiency stress reduces the absolute number of copies of the *APL* transcript in both the root and overground parts of barley. I have demonstrated the importance of the role of the 5'-UTR region in regulating the transcription of the *PHO2* gene by using techniques both *in vitro* and *in vivo* in tobacco cells (*Nicotiana benthamiana* L.).

In part four of the dissertation, the results of comprehensive research provide data on the global changes in particle levels of both small RNA and mRNA in barley. The original work was written by me based on the results of deep sequencing from barley. It shows that only a small pool of small RNAs with altered

levels of expression under Pi deficiency conditions maps to the previously characterised miRNA molecules (based on data deposited in the miRBase). Both in the root and in the aboveground part, I observed that the increase in the level of expression in response to Pi deficiency isoforms of miRNA from two families: miR399 and miR827. Both families participate in the maintenance of plant phosphate homeostasis. MiR399 particles – as I mentioned earlier – negatively regulate the level of *PHO2* gene transcripts. In turn, miR827 in monocotyledons species participates in the post-transcriptional regulation of the expression of two genes *SPX-MFS1* and *SPX-MFS2* (the name comes from the proteins SYG1/PHO81/XPR1 and the domain Major Facility Superfamily). I have confirmed the presence of target genes for these two miRNA families in published degradome data. Our degradome platform allow for identification matches of miRNA:mRNA from both the root and the aboveground part of the barley (Rolap line) grown under Pi deficiency conditions. In this paper, I describe many interesting examples of miRNAs and small RNAs (not mapped to miRBase), which can participate in the post-transcriptional regulation of genes in response to Pi deficiency stress. Furthermore, I have identified 98 genes with significantly altered levels of expression under Pi deficiency conditions for the aboveground part of barley. Some of these can be very important in terms of protecting plants against fungal infections. I noticed a decrease in the expression of the gene encoding oxalic acid oxidase. Fungi secrete oxalic acid during infection in order to weaken the cell wall of the plant (Zhang et al., 1995). Based on the current state of knowledge and the data published in the original paper, I described all the most interesting metabolic pathways involved in maintaining plant phosphate homeostasis. I supported the detailed description with a graphical model which illustrates the scale of changes in barley at the RNA level.

The results of the doctoral dissertation were presented at scientific conferences in Poland and abroad:

1. **Oral presentation** entitled „*Integrated sRNA, degradome profiling and RNA-Seq analysis identifies phosphate starvation-responsive small RNAs and genes in barley*” at international conference 4th iPlanta, 26-28 February 2020, Athens, Greece
2. **Oral presentation** entitled „*The 5'-UTR region is necessary for efficient PHOSPHATE 2 expression in barley*” at the 5th International Conference on Research and Education Challenges for Contemporary Live Sciences BioRun, 8-13 April 2019, Poznań, Poland
3. **Oral presentation** entitled „*Global analysis of small RNA level changes in barley roots and shoots during phosphate starvation*” at international conference 2nd iPlanta, 14-16 February 2018, Poznań, Poland
4. **Oral presentation** entitled „*The importance of 5'-UTR region for the regulation of PHOSPHATE 2 gene expression in barley*” at international workshop 5th Kiel Days, 7-9 November 2018, Poznań, Poland
5. **A poster was presented**, entitled „*Global analysis of small RNA level changes in barley roots and shoots during phosphate starvation*” at the international conference Plant Biology Europe, 18-21 June 2018, Copenhagen, Denmark
6. **A poster was presented**, entitled „*Transcriptional and post-transcriptional regulation of barley PHO2 gene*” at the international conference 6th Symposium on Phosphorus in Soils and Plants, 10-13 September 2018, Leuven, Belgium
7. **A poster was presented**, entitled „*Identification of transcription factors binding to PHOSPHATE2 5'-UTR in barley*” at the 18th International Plant Nutrition Colloquium, 19-24 August 2017, Copenhagen, Denmark
8. **A poster was presented**, entitled „*Searching for PHOSPHATE 2 (ubiquitin-conjugating enzyme) partner proteins in barley*” at the VISCEA International Conference, 26-30 June 2017, Vienna, Austria
9. **A poster was presented**, entitled „*Phosphate transporters HvPHT1;1, HvPHT1;6 and HvPHO1 maintain Pi concentration in barley roots during heat stress conditions*” at the International Plant Biology Conference, 9-13 July 2016, Texas, USA
10. **A poster was presented**, entitled „*PHOSPHATE 2 gene: in the hub of phosphate homeostasis in barley*” at the international conference EMBO Young Scientists Forum, 2-3 July 2015, Warsaw, Poland

References

1. Aung K., Lin S-I., Wu C-C., Huang Y-T., Su C. and T-J. Chiou. 2006. *pho2*, a phosphate overaccumulator, is caused by a nonsense mutation in a microRNA399 target gene. *Plant Physiology* 141(3):1000-1011. doi.org/10.1104/pp.106.078063
2. Batjes N. H. 1997. A world dataset of derived soil properties by FAeUNESCO soil unit for global modelling. *Soil Use and Management* 13(1): 9-16. doi.org/10.1111/j.1475-2743.1997.tb00550.x
3. Brunner P. H. 2010. Substance flow analysis as a decision support tool for phosphorus management. *Journal of Industrial Ecology* 14(6):870-873. doi.org/10.1111/j.1530-9290.2010.00300.x
4. Bun-Ya M., Nishimura M., Harashima S., Oshima Y. 1991. The *PHO84* gene of *Saccharomyces cerevisiae* encodes an inorganic phosphate transporter. *Molecular and Cellular Biology* 11(6):3229-3238. doi.org/10.1128/MCB.11.6.3229-3238.1991
5. Cooper J., Lombardi R., Boardman D., Carliell-Marquet C. 2011. The future distribution and production of global phosphate rock reserves. *Resources, Conservation and Recycling* 57:78-86. doi.org/10.1016/j.resconrec.2011.09.009
6. Delhaize E. and P. J. Randall. 1995. Characterization of a phosphate-accumulator mutant of *Arabidopsis thaliana*. *Plant Physiology* 107(1):207-213. doi.org/10.1104/pp.107.1.207
7. Franco-Zorrilla J. M., Valli A., Todesco M., Mateos I., Puga M. I., Rubio-Somoza I., Leyva A., Weigel D., Garcia J. A. and J. Paz-Ares. 2007. Target mimicry provides a new mechanism for regulation of microRNA activity. *Nature Genetics* 39(8):1033-1037. doi.org/10.1038/ng2079
8. Giraldo P., Benavente E., Monzano-Agugliaro F. and Gimenez E. 2019. Worldwide research trends on wheat and barley: a bibliometric comparative analysis. *Agronomy* 9(7):352. doi.org/10.3390/agronomy9070352
9. González E., Solano R., Rubio V., Leyva A. and J. Paz-Ares. 2005. PHOSPHATE TRANSPORTER TRAFFIC FACILITATOR1 is a plant-specific SEC12-related protein that enables the endoplasmic reticulum exit of a high-affinity phosphate transporter in *Arabidopsis*. *Plant Cell* 17(12):3500-3512. doi.org/10.1105/tpc.105.036640
10. Guo B., Jin Y., Wussler C., Blancaflor E. B., Motes C. M. and W. K. Versaw. 2007. Functional analysis of the *Arabidopsis* PHT4 family of intracellular phosphate transporters. *New Phytologist* 177(4):889-898. doi.org/10.1111/j.1469-8137.2007.02331.x
11. Hackenberg M., Shi B-J., Gustafson P. and P. Langridge. 2013. Characterization of phosphorus-regulated miR399 and miR827 and their isomirs in barley under phosphorus-sufficient and phosphorus-deficient conditions. *BMC Plant Biology* 13:214. doi.org/10.1186/1471-2229-13-214
12. Heffer P. and M. Prud'homme. Nutrients as Limited Resources: Global Trends in Fertilizer Production and Use. In: *Improving Water and Nutrient-Use Efficiency in Food Production Systems*. Hoboken, NJ, USA: John Wiley & Sons, Inc; 2013. p. 57-78. doi.org/10.1002/9781118517994.ch4.
13. Huang C. Y., Shirley N., Genc Y., Shi B. and P. Langridge. 2011. Phosphate utilization efficiency correlates with expression of low-affinity phosphate transporters and noncoding RNA, IPS1, in barley. *Plant Physiology* 156(3):1217-1229. doi.org/10.1104/pp.111.178459
14. Islam M. S. and M. Harun-ur-Rashid. Climate change and sustainable irrigation management in Bangladesh. In: *Climate change and food security in South Asia*. Springer: Lal R., Sivakumar M. V. K., Faiz S. M. A., Rahman A. H. M. M., Islam K. R. (eds). 2011. p. 413
15. Kirkby E. A. and A. E. Johnston. Soil and fertilizer phosphorus in relation to crop nutrition. In: *The ecophysiology of plant-phosphorus interactions*. Springer: White P. J. and J. P. Hammond (eds.). 2008. p. 178
16. Koo B-C., Lee, Y-H., Moon, S-C., Yoon, S-C. and J. C. Raymond. 2013. Phosphorus in the young supernova remnant Cassiopeia A. *Science* 342(6164): pp. 1346-1348. doi.org/10.1126/science.1243823

17. Leigh R. A. and A. E. Johnston. 1986. An investigation of the usefulness of phosphorus concentrations in tissue water as indicators of the phosphorus status of field grown spring barley J. Agric. Sci. 107, 329-333
18. Law A., Saunders, J. and J. Middleton. 2018. Global warming must stay below 1.5°C. BMJ 363:k4410. doi.org/10.1136/bmj.k4410
19. Lynch J. 2011. Root phenes for enhanced soil exploration and phosphorus acquisition: tools for future crops. Plant Physiology 156(3): 1041-1049. doi.org/10.1104/pp.111.175414
20. Mehta D. 2018. The green revolution did not increase poverty and hunger for millions. Nat Plants 4(10):736. doi.org/10.1038/s41477-018-0240-8
21. Mengel K. and E. A. Kirkby. 1987. Principles of plant nutrition, fourth ed. International Potash Institute, Basel, Switzerland, pp. 687.
22. Millstone E. and T. Lang. The atlas of food. Earthscan, 2008. 22-23
23. Nussaume L., Kanno S., Javot H., Marin E., Pochon N., Ayadi A., Nakanishi T. M. and M. C. Thibaud. 2011. Phosphate import in plants: focus on the PHT1 transporters. Frontiers in Plant Science 2:83. doi.org/10.3389/fpls.2011.00083
24. Ouyang X., Hong X., Zhao X., Zhang W., He X., Ma W., Teng W. and Y. Tong. 2016. Knock out of the *PHOSPHATE 2* gene TaPHO2-A1 improves phosphorus uptake and grain yield under low phosphorus conditions in common wheat. Scientific Reports 6:29850. doi.org/10.1038/srep29850
25. Pacak A., Barciszewska-Pacak M., Świda-Barteczka A., Kruska K., Segal P., Malinowska K., Jakobsen I., Jarmolowski A. and Z. Szwejkowska-Kulińska. 2016. Heat stress affects Pi-related genes expression and inorganic phosphate deposition/accumulation in barley. Frontiers in Plant Science 7:926. doi.org/10.3389/fpls.2016.00926/full
26. Park B. S., Seo J. S. and N-H. Chua. 2014. NITROGEN LIMITATION ADAPTATION recruits PHOSPHATE2 to target the phosphate transporter PT2 for degradation during the regulation of Arabidopsis phosphate homeostasis. Plant Cell 26(1):454-64. doi.org/10.1105/tpc.113.120311
27. Pasek M. and D. Lauretta. 2005. Aqueous corrosion of phosphide minerals from iron meteorites: A highly reactive source of prebiotic phosphorus on the surface of the early earth. Astrobiology 5(4):515-535. doi.org/10.1089/ast.2005.5.515
28. Péret B., Clément M., Nussaume L. and T. Desnos. 2011. Root developmental adaptation to phosphate starvation: better safe than sorry. Trends in Plant Science 16(8):442-450. doi.org/10.1016/j.tplants.2011.05.006
29. Perumalla C. J. and C. A. Peterson. 1986. Deposition of Casparian bands and suberin lamellae in the exodermis and endodermis of young corn and onion roots. Can. J. Bot. 64, 1873-1878. doi.org/10.1139/b86-248
30. Peterson C. A. and E. Cholewa. 1998. Structural modifications of the apoplast and their potential impact on ion uptake. Z. Pflanzen- ernähr. Bodenk. 161, 521-531. doi.org/10.1002/jpln.1998.3581610505
31. Pingali P. L. 2012. Green revolution: impacts, limits, and the path ahead. Proc Natl Acad Sci U S A. 109(31):12302-8. doi.org/10.1073/pnas.0912953109
32. Rita J. C., Gama-Rodrigues, A. C., Gama-Rodrigues, E. F., Zaia, F. C. and D. A. D. Nunes. 2013. Mineralization of organic phosphorus in soil size fractions under different vegetation covers in the north of Rio de Janeiro. Revista Brasileira de Ciência do Solo 37(5):1207-1215. doi.org/10.1590/S0100-06832013000500010
33. Rivilla V. M., Drozdovskaya M. N., Altwegg K., Caselli P., Beltran M. T., Fontani F., van der Tak F. F. S., Cesaroni R., Vasyunin A., Rubin M., Lique F., Marinakis S. and L. Testi. 2020. ALMA and ROSINA detections of phosphorus-bearing molecules: the interstellar thread between star-forming regions and comets. Monthly Notices of the Royal Astronomical Society 492(1), 1190-1198. doi.org/10.1093/mnras/stz3336

34. Sabela B. 2015. Wszystkie ziarna piasku. Wydawnictwo Czarne. ISBN 978-83-8049-169-4
35. Scholz R. W., Ulrich A. E., Eilittä M. and A. Roy. 2013. Sustainable use of phosphorus: a finite resource. *Science of the Total Environment* 461-462:799-803. doi.org/10.1016/j.scitotenv.2013.05.043
36. Smeck N. E. 1985. Phosphorus dynamics in soils and landscapes. *Geoderma* 36(3-4):185-199. doi.org/10.1016/0016-7061(85)90001-1
37. Smith F. W., Mudge, S. R., Rae, A. L. and D. Glassop. 2003. Phosphate transport in plants. *Plant and Soil* 248(1):71-83. doi.org/10.1023/A:1022376332180
38. Teng W., Zhao Y-Y., Zhao X-Q., He X., Ma W-Y., Deng Y., Chen X-P. and Y-P. Tong. 2017. Genome-wide identification, characterization, and expression analysis of PHT1 phosphate transporters in wheat. *Frontiers in Plant Science* 8:543. doi.org/10.3389/fpls.2017.00543
39. Tollefson J. 2018. IPCC says limiting global warming to 1.5°C will require drastic action. *Nature* 562(7726):172-173. doi: 10.1038/d41586-018-06876-2
40. Xu Y., Ramanathan, V. and D. G. Victor. 2018. Global warming will happen faster than we think. *Nature* 564(7734):30-32. doi.org/1038/d41586-018-07586-5
41. Yang Z., Yang J., Wang Y., Wang F., Mao W., He Q., Xu J., Wu Z. and C. Mao. 2020. PROTEIN PHOSPHATASE 95 regulates phosphate homeostasis by affecting phosphate transporter trafficking in rice. *Plant Cell* 32:740-757. doi.org/10.1105/tpc.19.00685
42. Zhang Z., Collinge D. B. and H. Thordal-Christensen. 1995. Germin-like oxalate oxidase, a H₂O₂-producing enzyme, accumulates in barley attacked by the powdery mildew fungus. *Plant J.* 8(1):139-45. doi.org/10.1046/j.1365-313X.1995.08010139.x

Online sources:

1. <https://www.theguardian.com/australia-news/2019/dec/18/climate-change-has-cut-australian-farm-profits-by-22-a-year-over-past-20-years-report-says>
2. <https://www.nioz.nl/en/events/colloquium-the-northern-european-enclosure-dam-noordzeedijk-for-when-climate-change-mitigation-fails>
3. <https://www.theguardian.com/environment/2019/sep/06/phosphate-fertiliser-crisis-threatens-world-food-supply>
4. <http://phosphorusplatform.eu>

1. **Sega P.** and A. Pacak. 2019. Plant PHR Transcription Factors: Put on A Map. *Genes* (Basel) 10(12): 1018.
<https://doi.org/10.3390/genes10121018>



2. Smoczyńska A., **Sega P.**, Stępień A., Knop K., Jarmołowski A., Pacak A. and Z. Szweykowska-Kulińska. 2019. miRNA Detection by Stem-Loop RT-qPCR in Studying microRNA Biogenesis and microRNA Responsiveness to Abiotic Stresses. In: Stefan de Folter (ed.), *Plant MicroRNAs: Methods and Protocols, Methods in Molecular Biology*, vol. 1932: 131-150.
https://doi.org/10.1007/978-1-4939-9042-9_10



3. **Sega P.**, Kruszka K., Szewc Ł., Szweykowska-Kulińska Z. and A. Pacak. 2020. Identification of transcription factors that bind to the 5'-UTR of the barley *PHO2* gene. *Plant Mol Biol* 102(1-2): 73-88.
<https://doi.org/10.1007/s11103-019-00932-9>



4. **Sega P.**, Kruszka K., Bielewicz D., Karłowski W., Nuc P., Szweykowska-Kulińska Z. and A. Pacak. 2021. Pi-starvation induced transcriptional changes in barley revealed by a comprehensive RNA-Seq and degradome analyses. *BMC Genomics* 22(165).
<https://doi.org/10.1186/s12864-021-07481-w>



Review

Plant PHR Transcription Factors: Put on A Map

Paweł Segal  and Andrzej Pacak * 

Department of Gene Expression, Institute of Molecular Biology and Biotechnology, Faculty of Biology, Adam Mickiewicz University, Poznań, Uniwersytetu Poznańskiego 6, 61-614 Poznań, Poland; p.sega@amu.edu.pl

* Correspondence: apacak@amu.edu.pl; Tel.: +48-618-295-955

Received: 24 October 2019; Accepted: 5 December 2019; Published: 6 December 2019



Abstract: The phosphate starvation response (PHR) protein family exhibits the MYB and coiled-coil domains. In plants, within the either 5′ untranslated regions (UTRs) or promoter regions of phosphate starvation-induced (PSI) genes are characteristic *cis*-regulatory elements, namely PHR1 binding sequence (P1BS). The most widely studied PHR protein family members, such as AtPHR1 in *Arabidopsis thaliana* (L.) and OsPHR2 in *Oryza sativa* (L.), may activate the gene expression of a broad range of PSI genes by binding to such elements in a phosphate (Pi) dependent manner. In Pi signaling, PHR transcription factors (TFs) can be selectively activated or deactivated by other proteins to execute the final step of signal transduction. Several new proteins have been associated with the AtPHR1/OsPHR2 signaling cascade in the last few years. While the PHR TF transcriptional role has been studied intensively, here we highlight the recent findings of upstream molecular components and other signaling pathways that may interfere with the PHR final mode of action in plants. Detailed information about transcriptional regulation of the *AtPHR1* gene itself and its upstream molecular events has been reviewed.

Keywords: PHR1; phosphate signaling; protein–protein interactions; post-translational modifications

1. Introduction

Phosphorus (P) is an essential element for all living organisms. Plants acquire P as inorganic phosphate (Pi) ions. An insufficient P level in the soil is one of the most limiting factors determining crop yield and productivity. Pi rock has been mined since the late 19th century and has been used as a main source of phosphate fertilizers worldwide [1,2]. Food production experiences the effects of climate change in the form of erosion patterns that influence the pollution of surface waters, with P causing eutrophication. P is not easily available in nature because of its immobility and high reactivity with soil constituents. Thus, environmental and industrial impacts on P recycling prompt the development of balanced food production and sustainable P consumption. However, without understanding the ways in which P metabolism is regulated in eukaryotic cells, such technological efforts may not be used effectively.

The maintenance of P homeostasis in plants is strictly controlled by a molecular network regulated by a group of transcription factors (TFs). Generally, P-starved plants turn on local and long-distance signals to absorb and utilize P from either internal or external pools. Thus, the inability of live organisms to adequately adapt to P limitation allows the possibility to screen genotypes or isolate mutants for functional genomic studies. The story of P homeostasis regulators began two decades ago with the characterization of green alga *Chlamydomonas reinhardtii* (Dangeard) phosphorus-starvation response 1 (PSR1) mutants exhibiting abnormality in their response to P deprivation. Shimogawara et al. identified two mutants, *psr1-1* and *psr1-2*, that were defective in the synthesis of extracellular phosphatases and were unable to increase the rate of inorganic phosphate ion transport upon Pi scarcity [3]. They

demonstrated that both mutants possess alterations in the same gene, named *PSR1*, and such variations are recessive and allelic [3]. Later, the *PSR1* gene product was further investigated and has been recognized as a central transcriptional regulator that is needed to activate specific responses to P limitation [4,5]. Subsequent studies with higher plants revealed homologous genes, phosphate starvation response 1 (*PHR1*) in *Arabidopsis thaliana* (L.) [6], and phosphate starvation response 2 (*PHR2*) in *Oryza sativa* (L.) [7], which is orthologue of the *AtPHR1* gene. Overexpression of *AtPHR1* leads to increased Pi level in the shoot tissues, together with induction of several Pi starvation-induced (PSI) genes that encode phosphate transporters, phosphatases, or RNases [8,9]. While knockout of the *AtPHR1* gene leads to defective accumulation of anthocyanin, starch, and sugar, alteration in the root architecture and impaired induction of multiple genes are known responses to Pi scarcity [10,11]. While the transcriptional regulation of many PSI genes by PHR1 TF is clear, the mechanism regulating the *PHR1* transcript level and protein activity itself still remains largely unexplored.

Many components of the complex molecular networks are still missing. Thus, here we would like to highlight the most important findings on the PHR-like protein family and PSI gene expression regulation that may determine low-Pi tolerance in crop plants.

2. PHRs Redundancy and Dimerization

Among the eukaryotes, high functional redundancy of transcription factors is a phenomenon that is known to lead to one TF compensating for another, masking the TF knockout effect on the binding targets [12,13]. PHR-like proteins belong to the MYB-coiled-coil (MYB-CC) family of transcription factors, which are encoded by 15 genes in *Arabidopsis*, and as dimers bind an imperfect palindromic sequence (PHR1 binding sequence (P1BS); G_nATAT_nC) [6,14,15]. Characteristic P1BS *cis*-regulatory motifs may be found either in the promoter or 5' untranslated regions (UTRs) of the target genes, where PHR1 TF binds acting as an activator or repressor of transcription [16,17]. Apart from *AtPHR1*, other MYB-CC family members were found in recent studies in *Arabidopsis*: PHL1 (PHR1-like 1) [11], PHL2 and PHL3 [18], as well as PHL4 [19]. First remarks about PHR1 functional redundancy were found in *phr1 phl1* double mutant in *Arabidopsis*. The loss-of-function double mutation only partially affected the transcription of *PSI* genes indicating the synergistic effect of *PHR1/PHL1* genes and involvement of other PHR-like TFs [11].

2.1. Cooperation between PHR Family Members

In particular, studies in various plant species demonstrated the widespread species-specific functions of PHR-like TFs. Overexpression of *TaPHR1* resulted in upregulation of a subset of PSI genes following the stimulation of lateral root branching and overall grain yield promotion of *Triticum aestivum* (L.) plants under Pi scarcity [20]. On the contrary, overexpression of *BnPHR1* caused Pi accumulation in shoots and retarded growth of *Brassica napus* (L.) plants [21]. Relevant work in rice has disclosed a few more *AtPHR1* orthologues, such as *OsPHR1*, *OsPHR2*, *OsPHR3* [7,22], and *OsPHR4* [23]. In 2015, Guo et al. showed that the expression of *OsPHR3* gene was induced under Pi starvation, but not that of *OsPHR1/2* [22]. Additionally, all three *OsPHRs* exhibit different DNA-binding affinity properties, and only plants with overexpression of *OsPHR3* gene exhibited low-Pi stress tolerance under field conditions. They proved that functional redundancy exists between *OsPHR1*, *OsPHR2*, and *OsPHR3* proteins and such diversity enables them to co-regulate Pi response in rice [22]. Further, it was shown that similar to *OsPHR3*, *OsPHR4* is a Pi starvation-induced gene and its expression is directly regulated by *OsPHR1/2/3*, which can all bind to the P1BS elements located in the *OsPHR4* promoter [23]. Interestingly, *OsPHR4* could also bind to its own promoter in this study.

2.2. PHRs Work Together in a Link

Beside PHR redundancy, dimerization itself is a crucial step for PHR-like TF DNA binding capability. Previous reports showed that *AtPHR1* forms heterodimers with *AtPHL1* [11], and the interaction of *AtPHL2* and *AtPHL3* was also observed, and both can homodimerize [18]. Likewise,

Ruan et al. showed that OsPHR4 could form a heterodimer with either OsPHR1, OsPHR2, or OsPHR3, as well as homodimers [23]. The nuclear-localized homodimerization of OsPHR2 protein was also reported [7,24]. All these findings suggest that PHR-like TFs can act redundantly and form an integrated system in Pi-starvation signaling in plants.

3. The Multifunctional Role of PHR1

The main idea of this review is to point out recent findings around PHR protein family members except their self-evident DNA-binding role. However, it is worth to mention that PHR transcription factors target broad range of genes that are not connected directly with the Pi signaling. Here, we would like to present relevant studies concerning PHR1 role in various biological processes in plants.

3.1. PHR1 Affects Plant Immune System

P deficiency makes plants more sensitive and susceptible to become a host of various phytopathogens [25,26]. Thus, the plant immunity system has to react immediately to overcome the severe environmental stimuli through changing the composition of hormones and root exudates. PHR1 TF as a major regulator of *PSI* genes also affects the expression of genes involved in antimicrobial resistance. Antagonistic interactions between three plant hormones: (i) salicylic acid (SA), (ii) jasmonic acid (JA), and (iii) ethylene (ET) trigger resistance against pathogens and herbivory [27,28]. JA induction shares some typical traits observed in Pi-starved plants, such as: anthocyanin accumulation or growth reduction [29], suggesting that both signaling pathways may be connected [30].

The comprehensive data about the contribution of PHR1 to the transcriptional regulation of plant immunity-related (PIR) genes has been published in last few years. In 2016, Khan et al. showed the significant increase of JA level in *Arabidopsis* leaves and roots under low-Pi treatment [31]. Additionally, the molecular analysis of loss-of-function *phr1-1* mutant revealed that this induction may be partially controlled by the PHR1 TF. The activation of JA signaling pathway upon Pi deficiency was delayed in the *phr1-1* mutant, but not abolished completely, indicating the presence of other transcription factors that may regulate this process [31]. One year later, global ChIP-seq (chromatin immuno-precipitation-sequencing) experiment published by Castrillo et al. uncovered the significant enrichment in clusters of JA- and SA-related genes involved in plant defense, targeted by *PHR1* in *Arabidopsis* [32]. In *phr1* and *phr1 phl1* mutants most of the SA-responsive genes were upregulated compared to wild type. Where for majority of JA-responsive genes their expression was lower in *Arabidopsis* mutants than in wild type. Further, they found that *phr1 phl1* double mutants exhibit enhanced activation of plant immunity, suggesting the repressing role of AtPHR1/AtPHL1 TFs on plant immune system [32]. These results are consist with related reports showing, (i) that transcription of ET biosynthesis genes may be affected by AtPHR1 activity [11] and (ii) a group of candidate genes involved in SA, JA, and ET signal transduction were differentially expressed upon Pi deficiency in sorghum [33].

Moreover, PHR1-dependent phosphate starvation responses (PSR) may be altered by root microbial communities in *Arabidopsis*. It was shown that intact PSR suppress the root colonization by fungal root endophytes [34], where synthetic bacterial community (SynCom) triggers PHR1 activity in low-Pi conditions [32].

3.2. Metal-Phosphate Relationship Modulated by PHR1

In soils, metal cations (i.e., Ca^{2+} , Zn^{2+} , Fe^{3+}) form insoluble precipitates with the inorganic forms of phosphate impeding the availability of these elements for plants [35–37]. While in plant cells, metal homeostasis involves interactions with enzymes and organic macromolecules as well as negatively charged Pi altering its activity. Extracellular Pi level also can affect the concentration of metal ions acquired by plant root system. For example, the expression of gene encoding highly conserved *ferretin* 1 (FER1) iron-binding protein is strongly induced upon Pi scarcity [38]. Bournier et al. found that *Arabidopsis phr1 phl1* loss-of-function mutant accumulates iron upon Pi deficiency [39]. Interestingly,

the low-Pi induced expression of *AtFER1* gene was completely lost and different cellular patterns of iron distribution were observed. They showed that both PHR1 and PHL1 proteins directly bind to the P1BS motif within the promoter of *AtFER1* gene inducing its transcription under Pi deficiency, in a Pi-specific manner [39]. Cross-talk between Pi and zinc signaling has been also recognized in the PHR1-dependent manner. Usually, P and Zn elements are present in a small amount in the soils and are barely available for plants. The transcription of two genes encoding zinc transporters (*ZIP2* and *ZIP4*) is positively regulated by PHR1 TF [40]. Besides, comparative analysis of the collections of transcriptomic data highlighted the PHR1-dependent induction of candidate genes involved in calcium signaling in Pi-depleted roots as well [41].

3.3. Double-Faced Role of PHR1 in the Regulation of Sulfate Homeostasis

In addition, few reports also describe the involvement of PHR1 TF into the transcription of non-metal ions homeostasis. Rouached et al. showed the involvement of PHR1 TF into the sulfate transfer from shoot to root during Pi starvation [16]. They found the presence of P1BS motifs within two genes (*SULTR1;3* and *SULTR2;1*) encoding sulfate transporters. Further, molecular analysis of *phr1* mutant revealed that PHR1 TF plays both a positive and negative role on the expression of genes encoding sulfate transporters. They observed the induction of the *SULTR1;3* gene expression upon low-Pi, but repression of the *SULTR2;1* and *SULTR3;4* (not P1BS holder) genes expression in *Arabidopsis* [16,42].

4. Transcriptional Regulation of PHR1 Gene Expression

Broadly, signaling pathways recruit TFs, which function as a last executor in the stepwise action leading to precise changes in target gene expression. However, long distance or systemic sensing pathways trigger each other and recruit a wide range of TFs to coordinately manage the steady state of living cells. In *Arabidopsis* and barley, *PHR1* gene expression is not particularly Pi responsive and its transcript level was not seen to change in different Pi regimes [6,43].

PHR1 Promoter as a Station for Many Plant TFs

Recently, several TFs that regulate *AtPHR1* gene expression in various conditions have been uncovered. In 2017, Liu et al. identified a few *cis*-regulatory elements within the *AtPHR1* promoter, including two elongated hypocotyl 5 (HY5 TF) binding sites (ACGT-containing elements (ACEs) [44]), one far-red elongated hypocotyl 3 (FHY3 TF), and far-red-impaired response 1 (FAR1 TF) binding site (FBS; CACGCGC [45]), and a palindromic repeat sequence similar to the ethylene-insensitive 3 (EIN3 TF) binding site (EBS) [46] [47]. They observed that *AtPHR1* gene expression is induced by light. Additionally, *AtPHR1* transcript levels were positively correlated with the intensity of light, and the expression levels of eight PSI target genes, activated by PHR1, were significantly lower in dark-grown plants compared with light-grown (Figure 1). Extensive work by Liu's group proved that FHY3 and FAR1 TFs positively regulate and HY5 TF negatively regulates *AtPHR1* expression and PSI genes [47]. What is more, another analysis showed that the transcript levels of *AtPHR1* and the PSI genes were enhanced by 1-aminocyclopropane-1-carboxylate (ACC; the immediate precursor of ethylene) treatment and Pi deficiency enhances plant sensitivity to ethylene, as reflected by induction of PSI gene expression [47,48]. Such cross-talk is very likely mediated by EIN3 TF, which directly binds to the *AtPHR1* 5'-UTR and specifically recognize the EBS sequence. The FHY3 and EIN3 TFs form a complex and together coordinately regulate *AtPHR1* expression in response to both light and ethylene stimulus [47]. Recently, many groups have shown that low-Pi induced responses integrate ethylene signaling into the molecular network, which helps to remodel the root architecture and increase Pi mining capability [47,49–51]. Later, Huang et al. identified three auxin-response elements: one copy of the AuxRE (GAGACA) in 5'-UTR and two copies of the TGA (AACGAC) elements in the promoter (Figure 1). They found also that two auxin response factors, ARF7 and ARF19, bind to these DNA motifs within *AtPHR1* 5'-UTR and promoter sequences to positively regulate its gene expression. Further,

the ARF7/ARF19 expression patterns in roots are similar to that of *AtPHR1* gene [52]. Interestingly, Huang's group found auxin-response elements in the promoters of most MYB-CC family genes in *Arabidopsis*, which were confirmed to exhibit functional redundancy to *AtPHR1* protein [18,19,52]. They proposed a model in which plants exposed to Pi scarcity showed increased sensitivity of an auxin receptor, transport inhibitor response 1 (TIR1), which led to upregulation of ARF7/ARF19 TFs following the induction of *AtPHR1* expression and their *PSI* target genes in roots [52]. Year by year we get clues suggesting that in order to understand the role of PHR-like TFs in maintaining phosphate homeostasis, we need to look extensively at every single step of the signal transduction pathway.

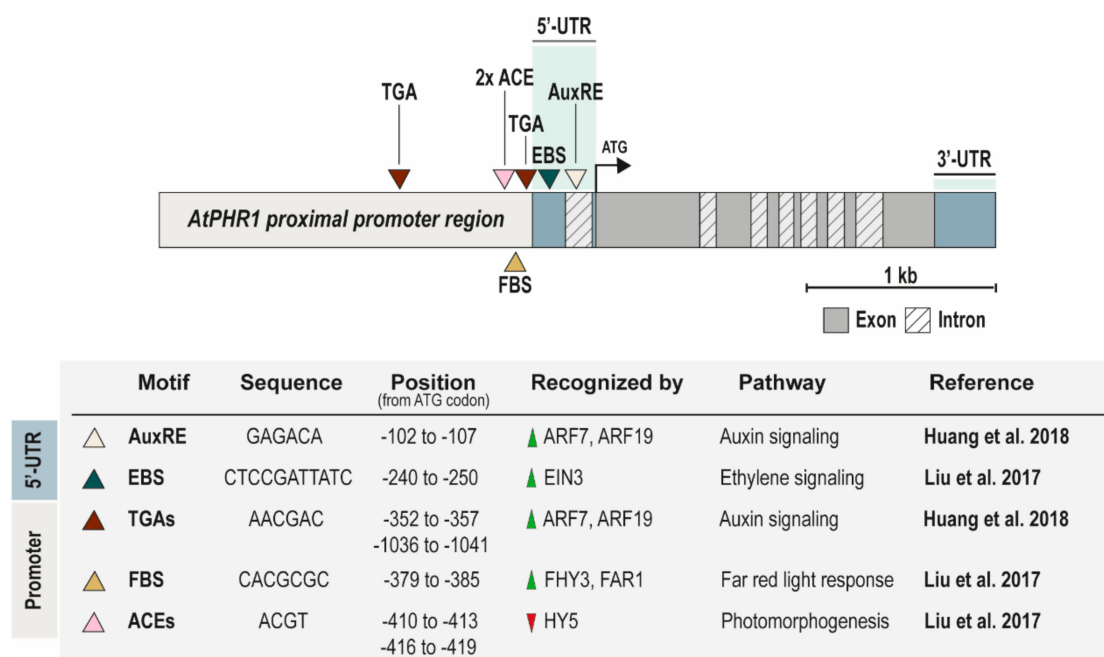


Figure 1. *Arabidopsis PHR1* gene structure with outlined major *cis*-regulatory motifs. Summary table provides detailed information about all relevant motifs published recently. Green and red triangles in column: “recognized by”, depict up- and down-regulation of *PHR1* genes expression by particular transcription factors (TFs), respectively.

5. PHR1 Post-Translational Modifications

Post-translational modification (PTM) is a biochemical modification that occurs to one or more amino acids on a translated protein. Such modification is mostly catalyzed by enzymes that recognize specific target sequences, and may determine the secondary structure of the target proteins and their subcellular localization, activity, and stability [53]. One of the most common and evolutionarily conserved PTMs in eukaryotic cells is mono- or poly-SUMOylation, which involves the binding of small ubiquitin-related modifier (SUMO) protein. The SUMO protein, with an average 10 kDa molecular mass, leads to increased target protein mass or spatial surface related to protein–protein and protein–DNA interactions [54]. Previous work established that PHR-like TFs are SUMOylated via SIZ1 (SAP and MIZ/SP-RING zinc finger domain-containing protein 1) SUMO E3 ligase in *Arabidopsis* [55], rice [56], and *Malus domestica* (Borkh.) [57]. The pioneering work of Miura's group confirmed that *AtSIZ1* is a single-gene family that encodes protein localized to nuclear speckles in *Arabidopsis* cells. The *siz1* loss-of-function mutant exhibits symptoms that are associated with Pi deficiency, such as reduced primary root growth and increased lateral root and root hair length and density, higher root/shoot mass ratio, anthocyanin accumulation, and upregulation of *PSI* gene expression [55]. There are two lysine residues within the *AtPHR1* amino acid sequence, in positions 261 and 372, that are crucial for SUMO binding, and it was proved that K261R and K372R mutations prevent SUMOylation of PHR1 [55].

The expression level of *AtPHR1* gene is relatively stable during Pi deficiency. So far, many groups have suggested that AtSIZ1-conducted SUMOylation stabilizes the level and activity of AtPHR1 protein and accelerates its binding affinity to the P1BS motifs present in the regulatory regions of PSI target genes, such as *AtHPS1* (*INDUCED BY PHOSPHATE STARVATION 1*) and *AtRNS1* (*RIBONUCLEASE 1*) [55–57]. However, mutation of *OsSIZ1* gene revealed a dual role of SIZ1 E3 ligase in the regulation of Pi homeostasis in rice. Among 13 high-affinity Pi transporters (PHT1 protein family) in rice, *OsPT1* and *OsPT8* gene expression was induced in *siz1* rice mutants under Pi deficiency. On the contrary, suppression of *PSI* genes such as *OsPT2* and *OsPT6* was also observed in this study [56]. Thus, AtSIZ1 and OsSIZ1 can act negatively or positively on the expression of *PSI* genes, even on genes that are not targeted by PHR1 transcription factors. Because of the lack of data, we can only speculate that various SIZ1-SUMOylated transcription factors work together in response to diverse environmental stresses in plants [55,58–62]. So far, there are no data on other PTMs that may affect PHR1 activity.

6. PHR1 Meets Nitrogen and Phosphate Sensors

The concentration of nutrients in the plant tissues is determined by nutrient-specific overlapping pathways that cooperate to balance nitrogen (N) and P uptake [63–65]. Fertilizers with additive N macroelement can increase the plants' P uptake and the proper N:P supply ratio, making it essential for promoting plant growth and subsequent high crop yields [66,67]. Variations in nutrient availability can alter specific gene expression levels or even activate the expression of genes that were inactive before. Related studies on OsPHR3 TF revealed that it is responsive to different forms of N irrespective of Pi regime. Sun's group raised the hypothesis that *OsPHR1/2/3/4* genes can also take part in the cross-talk between N and P [42]. In this part, we would like to point out major research breakthroughs that were made in last few years and connect PHR-mediated phosphate responses with nitrate signaling (Figure 2).

6.1. SPX Proteins Navigate PHR1 in Plant Cells

Another way the Pi-related regulation of PHR1 transcriptional activity exists is through interaction with proteins containing SPX (a name combining suppressor of yeast GPA1 (*SYG1*), CDK inhibitor in yeast PHO pathway (*Pho81*), and xenotropic and polytropic retrovirus receptor (*XPR1*)) domains [8,68–70]. There are four SPX proteins in *Arabidopsis*, AtSPX1–AtSPX4 [71–73], and six in rice, OsSPX1–OsSPX6 [8,68,74,75]. The *AtSPX* genes are highly homologous, however various expression patterns and subcellular localizations were described for them, indicating their functional diversity [70]. A nuclear protein AtSPX1 sequesters AtPHR1 in a Pi-dependent manner and inhibits its activity in *Arabidopsis*. In Pi-starved plants, AtSPX1/2/3 proteins are quickly degraded by the 26S proteasome pathway and AtPHR1 can freely regulate the expression of *PSI* genes. While the increasing Pi levels enhance the AtSPX1 protein half-life, they could preferentially interact with AtPHR1 TF, diminishing AtPHR1 binding capability to the P1BS *cis*-elements. Interestingly, SPX1–SPX3 possess P1BS motifs within their 5'-UTR and/or promoter region and serve as downstream targets of AtPHR1/OsPHR2 proteins. Thus, PHR1 can guide its own central role in Pi sensing by this negative feedback loop [70,71,76,77].

In rice, recent findings proved that contrary to nuclear AtSPX1/OsSPX1 proteins, OsSPX4 localizes in both the cell nucleus and cytoplasm, and it is not Pi-starvation responsive [24]. OsSPX4 physically interacts with OsPHR2 mainly in the cytoplasm, where such action prevents the nucleo-cytoplasmic shuttling of OsPHR2 in the presence of Pi. Afterwards, when OsPHR2 is trapped in the cytoplasm, it cannot form homodimers and binds to P1BS motifs, and in consequence the PHR-mediated signal transduction is stopped (Figure 2) [24].

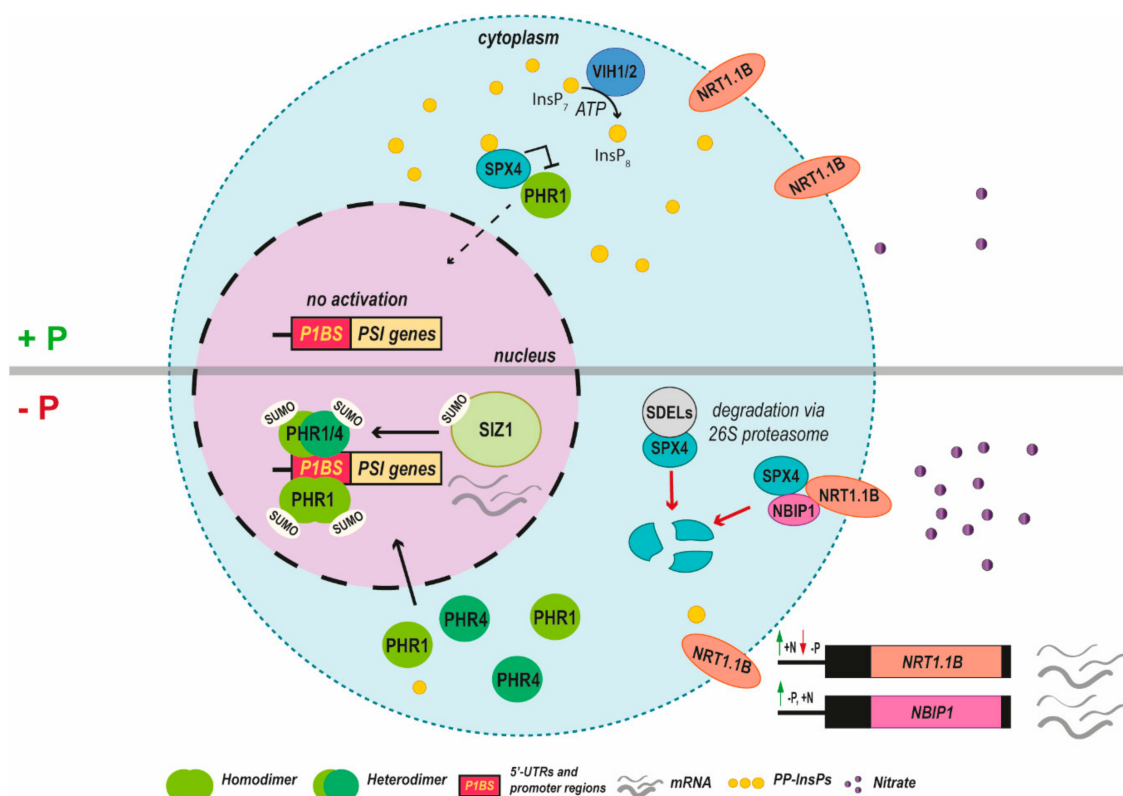


Figure 2. Graphical overview of interplays between PHR-like TFs and other cellular components under Pi scarcity in plant cells updated with current knowledge obtained from extensive research in *Arabidopsis* and rice. PHR1 TF represents both AtPHR1 and its rice orthologue OsPHR2. Under sufficient phosphate levels (+P), various inositol pyrophosphate isomers (PP-InsPs, depicted as yellow dots of different sizes) are biosynthesized to mimic the cellular Pi status. In the presence of Pi and ATP, InsP₈ messenger molecules are generated by the activity of kinase domain within VIH1/2 enzymes. Such PP-InsPs isomers (InsP₆, InsP₇, InsP₈) compete to bind to the SPX-domain containing proteins, followed by direct inhibition of AtPHR1/OsPHR2 nucleo-cytoplasmic shuttling. This leads to no activation of PSI genes. When the Pi level turns down, the protein level of specific E3 ligases, such as SPX4 degradation E3 ligases 1 or 2 (SDEL1, SDEL2), increases to target SPX-domain containing proteins for proteasomal degradation pathway. *NRT1.1B* is transcriptionally induced by high nitrate (N) or repressed by low-Pi, where *NBIP1* gene is upregulated by both low-Pi and high-N. The nitrate transporter 1.1B (*NRT1.1B*) trans-membrane nitrate sensor mediates nitrate-triggered SPX4 degradation with NBIP1 E3 ligase in phosphate signaling upon N sufficient conditions. Upon low-Pi, the PHR-like TFs are more preferentially localized in the nucleus and their structure is stabilized by SUMOylation conducted via SIZ1 activity. The PHR-like TFs, as either homo- or heterodimers, can regulate the transcript level of PSI genes by binding to the P1BS motifs present in the gene 5'-UTR or promoter regions. Green and red arrows indicate up- and down-regulation of gene expression, respectively.

6.2. Inositol Pyrophosphates (PP-InsPs) as Messenger

Throughout the paper we have shown many examples of how changes in the Pi level can affect a particular gene's expression and intracellular responses and turn the mode of action in plant development and adaptation to environmental stimuli. It raises the hypothesis that there should be a kind of universal signal element that can sense the signal transduction in response to Pi availability. Among the well-known secondary messengers for a variety of stimuli in eukaryotic cells (also common in plants) are cytosolic calcium ions, Ca²⁺. In the calcium signal transduction pathway, four Ca²⁺ ions target and activate calcium-binding messenger protein, calmodulin (CaM), which modulates subsequent protein–protein interactions [78–80]. Calcium ions were mentioned for a reason, because specific inositol 1,4,5-triophosphates (InsP₃) bind to the ligand-gated calcium channels and trigger

the release of stored Ca^{2+} ions [81,82]. InsP_3 can be further phosphorylated to InsP_4 [83], InsP_5 , InsP_6 [84–86], InsP_7 [87], and InsP_8 [88].

According to related research reports, especially the inositol pyrophosphates on the highest level of phosphorylation (PP-InsPs) play an important role coordinating cellular Pi homeostasis in plants [82,86–88]. Dong et al. showed that InsP_8 directly binds to the SPX domain and regulates the interaction between SPX1 and PHR1 in *Arabidopsis*. They demonstrated that in mutant plants exhibiting no ability to biosynthesize InsP_8 , the SPX1–PHR1 complex could not be formed, which resulted in the constitutive activation of PSI genes and overaccumulation of Pi [88]. Recently, biochemical studies have revealed various binding affinities between InsP_6 and InsP_7 to the SPX domain and competition of PP-InsP isomers prevailing over the physiological concentration of Pi. The elaborated crystal structure of SPX domain exposed some features of binding surface targeted by PP-InsPs. InsP_6 interacts with the SPX domain via variable hydrogen bond interactions, which may sense different PP-InsP isomers [87]. As far as *PHR1* gene expression is not regulated by Pi status, its activity can be fine-tuned by the presence of specific SPX-InsP complexes in an intracellular Pi-dependent manner.

The bioenergetics and signaling roles of PP-InsP molecules are evolutionarily more ancient than InsP_3 -mediated Ca^{2+} mobilization [89]. Plants exposed to low-Pi stress reprogram their metabolic pathways to compensate for cellular energetic crisis through the coordination of 5- InsP_7 or InsP_8 levels. In 2019, Zhu et al. reported that two genes encoding inositol pyrophosphate kinases/phosphatases VIP homolog 1/2 (*VIH1/2*) were able to either generate or break down PP-InsPs in *Arabidopsis* [90]. The *VIH1/2* enzymes are bifunctional, harboring an N-terminal InsP kinase and a C-terminal phosphatase domain [91]. The point mutation within the active site of the kinase domain leads to overaccumulation of Pi and constitutive Pi starvation responses. Further phosphorylated PP-InsP isomers cannot be catalyzed, and they do not mediate SPX4-PHR1/PHL1 arrest. Deletion of either *PHR1* or *PHL1* can partially rescue the *VIH1-2 VIH2-4* double-mutant phenotype, suggesting that both enzymes redundantly regulate Pi homeostasis and their PP-InsP reaction products are part of the PHR1/PHL1 signaling cascade. The dual roles of *VIH1/2* may be shaped by cellular concentration of ATP and Pi [90]. For example, plants growing in soil with sufficient Pi availability are energetically stable, and their increasing cellular level of ATP stimulates PP-InsP kinase activity. Thus, InsP_8 isomers are more abundant and act as messengers that transmit information about Pi availability throughout the plant, so PSI responses stay inactive.

Plant hormones may interplay with Pi signaling also through interactions with different InsP isomers. Recent discoveries have shown the possibility of binding either InsP_5 to the JA receptors [92] or InsP_6 to the auxin receptors [93]. Furthermore, herbivore-induced JA synthesis triggers *VIH2*-dependent increase in InsP_8 , which can be integrated into JA receptor complex [94].

6.3. SPX Proteins from the Nitrogen Perspective

Recently, two breakthrough studies appeared that extended the SPX4-PHR2 module for novel molecules that were known as nitrate sensors. Maeda's and Hu's groups revealed the mechanism by which nitrate activates both Pi and N signaling pathways in plants [75,95]. Maeda et al. found three copies of P1BS *cis*-regulatory elements in the nitrate-inducible GARP-type transcriptional repressor 1.1 (*AtNIGT1.1*) promoter, which encodes nuclear localized TF transcriptionally regulated by nitrate. Further investigation of the SPX-PHR1-NIGT1 cascade revealed their role in the modulation of nitrate uptake in a P-dependent manner. Additionally, they proved that the transmembrane protein and nitrate sensor, the nitrate transporter 1.1B (NRT1.1B), recruits SPX4 protein to facilitate its ubiquitination and degradation mediated by NRT1.1B interacting protein 1 (NBIP1) E3 ligase in the presence of N in rice (Figure 2) [75]. In *Arabidopsis*, NRT1.1 activity is positively and indirectly regulated by the phosphate 2 (PHO2) ubiquitin-conjugating (UBC) E2 enzyme [96,97]. In a short period of time, two more SPX4 degradation E3 ligases (SDEL1 and SDEL2) were discovered. Both *SDEL* genes are post-transcriptionally induced by Pi starvation, and their E3 ligase activity directs for degradation SPX4 proteins via ubiquitination of K213 and K299 lysine residues (Figure 2) [69]. Again, it was proved

that PHR-like TF functions as a master regulator to maintain nutrient homeostasis in plants. The AtPHR1/OsPHR2 TFs could compete with various E3 ligases by interacting with SPX4-PP-InsP-activated protein in either a P- or N-dependent manner, which secures SPX4 from being directed to the 26S proteasomal degradation pathway [69,75]. The plant demand for P strengthens through developmental stages in which large macromolecules, nucleic acids, and proteins are created from smaller components extensively. Inhibition of N uptake can lower the plant's demand for P and cooperatively reduce the negative impact of abiotic stresses.

7. Conclusions

Thus far, the given findings indicate that PHR1 transcription factor is a crucial component of Pi signaling in plants. Here, we emphasize the role of cooperation between signaling and hormonal pathways that are most affected by Pi-starved plants. Alterations by addition or deletion of any factor(s) from a signal transduction cascade can result in sudden cellular and molecular changes. We reviewed several breakthrough studies that should be considered during further investigation of the mechanistic picture determining plant tolerance to phosphate scarcity from the perspective of the PHR protein family. The first described PHR protein family member, PHR1 in *Arabidopsis*, redundantly cooperates with other homologous proteins (i.e., AtPHR2, AtPHL1, AtPHL2), which may equally contribute to the signaling pathway. It is believed that specific dimer sets consisting of PHR-like TFs may regulate the expression of essential genes, overcoming the negative impact of low-Pi stress.

The “phosphate problem” has recently gained much attention due to the anthropogenic impact on the environment and limited phosphorus supply. Crop improvement in current plant breeding will occur due to revealing the mechanism of Pi tolerance. Such knowledge may be used to engineer crop cultivars with improved ability to acquire and utilize Pi. In the near future, efforts should be put into investigating the relationship between different PP-InsP isomers that may coordinate cellular phosphate balance with metabolic messengers. These evolutionarily conserved signaling molecules speak directly on behalf of plants, and decoding this language may be invaluable.

Author Contributions: Conceptualization, writing—original draft preparation, editing, designing figures: P.S.; supervision and writing—review and editing: A.P.

Funding: This work was funded by the National Science Centre, Poland, grant numbers DEC-2013/11/B/NZ9/01761, UMO-2016/23/B/NZ9/00857, and UMO-2015/19/N/NZ9/00218, and by KNOW RNA Research Centre in Poznan, grant number 01/KNOW2/2014.

Conflicts of Interest: The authors declare no conflict of interest.

References

1. Vance, C.P.; Uhde-Stone, C.; Allan, D.L. Phosphorus acquisition and use: Critical adaptations by plants for securing a nonrenewable resource. *New Phytol.* **2003**, *157*, 423–447. [[CrossRef](#)]
2. Heffer, P.; Prud'homme, M. Nutrients as limited resources: Global trends in fertilizer production and use. In *Improving Water and Nutrient-Use Efficiency in Food Production Systems*; John Wiley & Sons, Inc.: Hoboken, NJ, USA, 2013; pp. 57–78, ISBN 9780813819891.
3. Shimogawara, K.; Wykoff, D.D.; Usuda, H.; Grossman, A.R. *Chlamydomonas reinhardtii* mutants abnormal in their responses to phosphorus deprivation. *Plant Physiol.* **1999**, *120*, 685–694. [[CrossRef](#)] [[PubMed](#)]
4. Wykoff, D.D.; Grossman, A.R.; Weeks, D.P.; Usuda, H.; Shimogawara, K. Psr1, a nuclear localized protein that regulates phosphorus metabolism in *Chlamydomonas*. *Proc. Natl. Acad. Sci. USA* **1999**, *96*, 15336–15341. [[CrossRef](#)] [[PubMed](#)]
5. Bajhaiya, A.K.; Dean, A.P.; Zeef, L.A.; Webster, R.E.; Pittman, J.K. PSR1 is a global transcriptional regulator of phosphorus deficiency responses and carbon storage metabolism in *Chlamydomonas reinhardtii*. *Plant Physiol.* **2016**, *170*, 1216–1234. [[CrossRef](#)] [[PubMed](#)]
6. Rubio, V.; Linhares, F.; Solano, R.; Martín, A.C.; Iglesias, J.; Leyva, A.; Paz-ares, J. A conserved MYB transcription factor involved in Phosphate starvation signaling both in vascular plants and in unicellular algae. *Genes Dev.* **2001**, *15*, 2122–2133. [[CrossRef](#)] [[PubMed](#)]

7. Zhou, J.; Jiao, F.; Wu, Z.; Li, Y.; Wang, X.; He, X.; Zhong, W.; Wu, P. OsPHR2 is involved in Phosphate-starvation signaling and excessive Phosphate accumulation in shoots of plants. *Plant Physiol.* **2008**, *146*, 1673–1686. [[CrossRef](#)]
8. Liu, F.; Wang, Z.; Ren, H.; Shen, C.; Li, Y.; Ling, H.Q.; Wu, C.; Lian, X.; Wu, P. OsSPX1 suppresses the function of OsPHR2 in the regulation of expression of OsPT2 and Phosphate homeostasis in shoots of rice. *Plant J.* **2010**, *62*, 508–517. [[CrossRef](#)]
9. Nilsson, L.; Müller, R.; Nielsen, T.H. Increased expression of the MYB-related transcription factor, PHR1, leads to enhanced Phosphate uptake in *Arabidopsis thaliana*. *Plant. Cell Environ.* **2007**, *30*, 1499–1512. [[CrossRef](#)]
10. Pant, B.D.; Burgos, A.; Pant, P.; Cuadros-Inostroza, A.; Willmitzer, L.; Scheible, W.R. The transcription factor PHR1 regulates lipid remodeling and triacylglycerol accumulation in *Arabidopsis thaliana* during phosphorus starvation. *J. Exp. Bot.* **2015**, *66*, 1907–1918. [[CrossRef](#)]
11. Bustos, R.; Castrillo, G.; Linhares, F.; Puga, M.I.; Rubio, V.; Pérez-Pérez, J.; Solano, R.; Leyva, A.; Paz-Ares, J. A central regulatory system largely controls transcriptional activation and repression responses to Phosphate starvation in *Arabidopsis*. *PLoS Genet.* **2010**, *6*, e1001102. [[CrossRef](#)]
12. Wu, W.S.; Lai, F.J. Functional redundancy of transcription factors explains why most binding targets of a transcription factor are not affected when the transcription factor is knocked out. *BMC Syst. Biol.* **2015**, *9*, S2. [[CrossRef](#)] [[PubMed](#)]
13. Kuntz, S.G.; Williams, B.A.; Sternberg, P.W.; Wold, B.J. Transcription factor redundancy and tissue-specific regulation: Evidence from functional and physical network connectivity. *Genome Res.* **2012**, *22*, 1907–1919. [[CrossRef](#)] [[PubMed](#)]
14. Jiang, M.; Sun, L.; Isupov, M.N.; Littlechild, J.A.; Wu, X.; Wang, Q.; Wang, Q.; Yang, W.; Wu, Y. Structural basis for the target DNA recognition and binding by the MYB domain of Phosphate starvation response 1. *FEBS J.* **2019**, *286*, 2809–2821. [[CrossRef](#)] [[PubMed](#)]
15. Sobkowiak, L.; Bielewicz, D.; Malecka, E.M.; Jakobsen, I.; Albrechtsen, M.; Szweykowska-Kulinska, Z.; Pacak, A. The Role of the P1BS element containing promoter-driven genes in Pi transport and homeostasis in plants. *Front. Plant Sci.* **2012**, *3*, 1–5. [[CrossRef](#)]
16. Rouached, H.; Secco, D.; Arpat, B.; Poirier, Y. The transcription factor PHR1 plays a key role in the regulation of sulfate shoot-to-root flux upon Phosphate starvation in *Arabidopsis*. *BMC Plant Biol.* **2011**, *11*, 19. [[CrossRef](#)]
17. Segal, P.; Kruszk, K.; Szewc, Ł.; Szweykowska-Kulińska, Z.; Pacak, A. Identification of transcription factors that bind to the 5'-UTR of the barley PHO2 gene. *Plant Mol. Biol.* **2019**, 1–16. [[CrossRef](#)]
18. Sun, L.; Song, L.; Zhang, Y.; Zheng, Z.; Liu, D. Arabidopsis PHL2 and PHR1 act redundantly as the key components of the central regulatory system controlling transcriptional responses to Phosphate starvation. *Plant Physiol.* **2016**, *170*, 499–514. [[CrossRef](#)]
19. Wang, Z.; Zheng, Z.; Song, L.; Liu, D. Functional characterization of *Arabidopsis* PHL4 in Plant response to Phosphate starvation. *Front. Plant Sci.* **2018**, *9*, 1432. [[CrossRef](#)]
20. Wang, J.; Sun, J.; Miao, J.; Guo, J.; Shi, Z.; He, M.; Chen, Y.; Zhao, X.; Li, B.; Han, F.; et al. A Phosphate starvation response regulator Ta-PHR1 is involved in Phosphate signalling and increases grain yield in wheat. *Ann. Bot.* **2013**, *111*, 1139–1153. [[CrossRef](#)]
21. Ren, F.; Guo, Q.Q.; Chang, L.L.; Chen, L.; Zhao, C.Z.; Zhong, H.; Li, X.B. *Brassica napus* PHR1 gene encoding a MYB-like protein functions in response to Phosphate starvation. *PLoS ONE* **2012**, *7*, e44005. [[CrossRef](#)]
22. Guo, M.; Ruan, W.; Li, C.; Huang, F.; Zeng, M.; Liu, Y.; Yu, Y.; Ding, X.; Wu, Y.; Wu, Z.; et al. Integrative comparison of the role of the PHOSPHATE RESPONSE1 subfamily in Phosphate signaling and homeostasis in rice. *Plant Physiol.* **2015**, *168*, 1762–1776. [[CrossRef](#)] [[PubMed](#)]
23. Ruan, W.; Guo, M.; Wu, P.; Yi, K. Phosphate starvation induced OsPHR4 mediates Pi-signaling and homeostasis in rice. *Plant Mol. Biol.* **2017**, *93*, 327–340. [[CrossRef](#)] [[PubMed](#)]
24. Lv, Q.; Zhong, Y.; Wang, Y.; Wang, Z.; Zhang, L.; Shi, J.; Wu, Z.; Liu, Y.; Mao, C.; Yi, K.; et al. SPX4 negatively regulates Phosphate signaling and homeostasis through its interaction with PHR2 in rice. *Plant Cell* **2014**, *26*, 1586–1597. [[CrossRef](#)] [[PubMed](#)]
25. McDonald, A.E.; Grant, B.R.; Plaxton, W.C. Phosphite (phosphorous acid): Its relevance in the environment and agriculture and influence on plant Phosphate starvation response. *J. Plant Nutr.* **2001**, *24*, 1505–1519. [[CrossRef](#)]

26. Decker, E.L.; Alder, A.; Hunn, S.; Ferguson, J.; Lehtonen, M.T.; Scheler, B.; Kerres, K.L.; Wiedemann, G.; Safavi-Rizi, V.; Nordzieke, S.; et al. Strigolactone biosynthesis is evolutionarily conserved, regulated by Phosphate starvation and contributes to resistance against phytopathogenic fungi in a moss, *Physcomitrella patens*. *New Phytol.* **2017**, *216*, 455–468. [[CrossRef](#)]
27. Robert-Seilaniantz, A.; Grant, M.; Jones, J.D. Hormone crosstalk in plant disease and defense: More than just jasmonate-salicylate antagonism. *Annu. Rev. Phytopathol.* **2011**, *49*, 317–343. [[CrossRef](#)]
28. Yang, Y.X.; Ahammed, G.J.; Wu, C.; Fan, S.Y.; Zhou, Y.H. Crosstalk among Jasmonate, Salicylate and Ethylene signaling pathways in plant disease and immune responses. *Curr. Protein Pept. Sci.* **2015**, *16*, 450–461. [[CrossRef](#)]
29. Li, T.; Jia, K.P.; Lian, H.L.; Yang, X.; Li, L.; Yang, H.Q. Jasmonic acid enhancement of anthocyanin accumulation is dependent on phytochrome A signaling pathway under far-red light in *Arabidopsis*. *Biochem. Biophys. Res. Commun.* **2014**, *454*, 78–83. [[CrossRef](#)]
30. Crombez, H.; Motte, H.; Beeckman, T. Tackling plant Phosphate starvation by the roots. *Dev. Cell* **2019**, *48*, 599–615. [[CrossRef](#)]
31. Khan, G.A.; Vogiatzaki, E.; Glauser, G.; Poirier, Y. Phosphate deficiency induces the Jasmonate pathway and enhances resistance to insect herbivory. *Plant Physiol.* **2016**, *171*, 632–644. [[CrossRef](#)]
32. Castrillo, G.; Teixeira, P.J.; Paredes, S.H.; Law, T.F.; de Lorenzo, L.; Feltcher, M.E.; Finkel, O.M.; Breakfield, N.W.; Mieczkowski, P.; Jones, C.D.; et al. Root microbiota drive direct integration of Phosphate stress and immunity. *Nature* **2017**, *543*, 513–518. [[CrossRef](#)] [[PubMed](#)]
33. Zhang, J.; Jiang, F.; Shen, Y.; Zhan, Q.; Bai, B.; Chen, W.; Chi, Y. Transcriptome analysis reveals candidate genes related to phosphorus starvation tolerance in sorghum. *BMC Plant Biol.* **2019**, *19*, 306. [[CrossRef](#)] [[PubMed](#)]
34. Hiruma, K.; Gerlach, N.; Sacristán, S.; Nakano, R.T.; Hacquard, S.; Kracher, B.; Neumann, U.; Ramírez, D.; Bucher, M.; O'Connell, R.J.; et al. Root endophyte *Colletotrichum tofieldiae* confers plant fitness benefits that are Phosphate status dependent. *Cell* **2016**, *165*, 464–474. [[CrossRef](#)] [[PubMed](#)]
35. Gupta, D.K.; Chatterjee, S.; Datta, S.; Veer, V.; Walther, C. Role of Phosphate fertilizers in heavy metal uptake and detoxification of toxic metals. *Chemosphere* **2014**, *108*, 134–144. [[CrossRef](#)] [[PubMed](#)]
36. Briat, J.F.; Rouached, H.; Tissot, N.; Gaymard, F.; Dubos, C. Integration of P, S, Fe, and Zn nutrition signals in *Arabidopsis thaliana*: Potential involvement of PHOSPHATE STARVATION RESPONSE 1 (PHR1). *Front. Plant Sci.* **2015**, *6*, 290. [[CrossRef](#)] [[PubMed](#)]
37. Mathan, K.K.; Amberger, A. Influence of iron on the uptake of phosphorus by maize. *Plant Soil* **1977**, *46*, 413–422. [[CrossRef](#)]
38. Hirsch, J.; Marin, E.; Floriani, M.; Chiarenza, S.; Richaud, P.; Nussaume, L.; Thibaud, M.C. Phosphate deficiency promotes modification of iron distribution in *Arabidopsis* plants. *Biochimie* **2006**, *88*, 1767–1771. [[CrossRef](#)]
39. Bournier, M.; Tissot, N.; Mari, S.; Boucherez, J.; Lacombe, E.; Briat, J.F.; Gaymard, F. *Arabidopsis ferritin 1 (AtFer1)* gene regulation by the Phosphate starvation response 1 (AtPHR1) transcription factor reveals a direct molecular link between iron and Phosphate homeostasis. *J. Biol. Chem.* **2013**, *288*, 22670–22680. [[CrossRef](#)]
40. Xie, X.; Hu, W.; Fan, X.; Chen, H.; Tang, M. Interactions between phosphorus, Zinc, and iron homeostasis in nonmycorrhizal and mycorrhizal plants. *Front. Plant Sci.* **2019**, *10*, 1172. [[CrossRef](#)]
41. Linn, J.; Ren, M.; Berkowitz, O.; Ding, W.; van der Merwe, M.J.; Whelan, J.; Jost, R. Root cell-specific regulators of Phosphate-dependent growth. *Plant Physiol.* **2017**, *174*, 1969–1989. [[CrossRef](#)]
42. Sun, Y.; Luo, W.; Jain, A.; Liu, L.; Ai, H.; Liu, X.; Feng, B.; Zhang, L.; Zhang, Z.; Guohua, X.; et al. OsPHR3 affects the traits governing nitrogen homeostasis in rice. *BMC Plant Biol.* **2018**, *18*, 241. [[CrossRef](#)] [[PubMed](#)]
43. Pacak, A.; Barciszewska-Pacak, M.; Świda-Barteczka, A.; Kruszka, K.; Segal, P.; Milanowska, K.; Jakobsen, I.; Jarmolowski, A.; Szwejkowska-Kulińska, Z. Heat stress affects pi-related genes expression and inorganic Phosphate deposition/accumulation in Barley. *Front. Plant Sci.* **2016**, *7*, 926. [[CrossRef](#)] [[PubMed](#)]
44. Osterlund, M.T.; Hardtke, C.S.; Wei, N.; Deng, X.W. Targeted destabilization of HY5 during light-regulated development of *Arabidopsis*. *Nature* **2000**, *405*, 462–466. [[CrossRef](#)] [[PubMed](#)]
45. Lin, R.; Ding, L.; Casola, C.; Ripoll, D.R.; Feschotte, C.; Wang, H. Transposase-derived transcription factors regulate light signaling in *Arabidopsis*. *Science* **2007**, *318*, 1302–1305. [[CrossRef](#)] [[PubMed](#)]

46. Solano, R.; Stepanova, A.; Chao, Q.; Ecker, J.R. Nuclear events in ethylene signaling: A transcriptional cascade mediated by ETHYLENE-INSENSITIVE3 and ETHYLENE-RESPONSE-FACTOR1. *Genes Dev.* **1998**, *12*, 3703–3714. [[CrossRef](#)] [[PubMed](#)]
47. Liu, Y.; Xie, Y.; Wang, H.; Ma, X.; Yao, W.; Wang, H. Light and ethylene coordinately regulate the phosphate starvation response through transcriptional regulation of *PHOSPHATE STARVATION RESPONSE1*. *Plant Cell* **2017**, *29*, 2269–2284. [[CrossRef](#)]
48. Lei, M.; Zhu, C.; Liu, Y.; Karthikeyan, A.S.; Bressan, R.A.; Raghothama, K.G.; Liu, D. Ethylene signalling is involved in regulation of Phosphate starvation-induced gene expression and production of acid phosphatases and anthocyanin in *Arabidopsis*. *New Phytol.* **2011**, *189*, 1084–1095. [[CrossRef](#)]
49. Thibaud, M.C.; Arrighi, J.F.; Bayle, V.; Chiarenza, S.; Creff, A.; Bustos, R.; Paz-Ares, J.; Poirier, Y.; Nussaume, L. Dissection of local and systemic transcriptional responses to Phosphate starvation in *Arabidopsis*. *Plant J.* **2010**, *64*, 775–789. [[CrossRef](#)]
50. Neumann, G. The role of ethylene in plant adaptations for Phosphate acquisition in soils—A review. *Front. Plant Sci.* **2016**, *6*, 1224. [[CrossRef](#)]
51. Nagarajan, V.K.; Smith, A.P. Ethylene's role in Phosphate starvation signaling: More than just a root growth regulator. *Plant Cell Physiol.* **2012**, *53*, 277–286. [[CrossRef](#)]
52. Huang, K.L.; Ma, G.J.; Zhang, M.L.; Xiong, H.; Wu, H.; Zhao, C.Z.; Liu, C.S.; Jia, H.X.; Chen, L.; Kjorven, J.O.; et al. The ARF7 and ARF19 transcription factors positively regulate *PHOSPHATE STARVATION RESPONSE1* in *Arabidopsis* roots. *Plant Physiol.* **2018**, *178*, 413–427. [[CrossRef](#)] [[PubMed](#)]
53. Mazzucotelli, E.; Mastrangelo, A.M.; Crosatti, C.; Guerra, D.; Stanca, A.M.; Cattivelli, L. Abiotic stress response in plants: When post-transcriptional and post-translational regulations control transcription. *Plant Sci.* **2008**, *174*, 420–431. [[CrossRef](#)]
54. Praefcke, G.J.; Hofmann, K.; Dohmen, R.J. SUMO playing tag with ubiquitin. *Trends Biochem. Sci.* **2012**, *37*, 23–31. [[CrossRef](#)] [[PubMed](#)]
55. Miura, K.; Rus, A.; Sharkhuu, A.; Yokoi, S.; Karthikeyan, A.S.; Raghothama, K.G.; Baek, D.; Koo, Y.D.; Jin, J.B.; Bressan, R.A.; et al. The *Arabidopsis* SUMO E3 ligase SIZ1 controls Phosphate deficiency responses. *Proc. Natl. Acad. Sci. USA* **2005**, *102*, 7760–7765. [[CrossRef](#)]
56. Wang, H.; Sun, R.; Cao, Y.; Pei, W.; Sun, Y.; Zhou, H.; Wu, X.; Zhang, F.; Luo, L.; Shen, Q.; et al. OsSIZ1, a SUMO E3 ligase gene, is involved in the regulation of the responses to Phosphate and nitrogen in rice. *Plant Cell Physiol.* **2015**, *56*, 2381–2395. [[CrossRef](#)]
57. Zhang, R.F.; Zhou, L.J.; Li, Y.Y.; You, C.X.; Sha, G.L.; Hao, Y.J. Apple SUMO E3 ligase MdSIZ1 is involved in the response to Phosphate deficiency. *J. Plant Physiol.* **2019**, *232*, 216–225. [[CrossRef](#)]
58. Park, H.C.; Kim, H.; Koo, S.C.; Park, H.J.; Cheong, M.S.; Hong, H.; Baek, D.; Chung, W.S.; Kim, D.H.; Bressan, R.A.; et al. Functional characterization of the SIZ/PIAS-type SUMO E3 ligases, OsSIZ1 and OsSIZ2 in rice. *Plant. Cell Environ.* **2010**, *33*, 1923–1934. [[CrossRef](#)]
59. Jin, J.B.; Jin, Y.H.; Lee, J.; Miura, K.; Yoo, C.Y.; Kim, W.Y.; Van Oosten, M.; Hyun, Y.; Somers, D.E.; Lee, I.; et al. The SUMO E3 ligase, AtSIZ1, regulates flowering by controlling a salicylic acid-mediated floral promotion pathway and through affects on FLC chromatin structure. *Plant J.* **2008**, *53*, 530–540. [[CrossRef](#)]
60. Zhou, L.J.; Zhang, C.L.; Zhang, R.F.; Wang, G.L.; Li, Y.Y.; Hao, Y.J. The SUMO E3 ligase MdSIZ1 targets MdbHLH104 to regulate plasma membrane H⁺-ATPase activity and iron homeostasis. *Plant Physiol.* **2019**, *179*, 88–106. [[CrossRef](#)]
61. Niu, D.; Lin, X.L.; Kong, X.; Qu, G.P.; Cai, B.; Lee, J.; Jin, J.B. SIZ1-mediated SUMOylation of TPR1 suppresses plant immunity in *Arabidopsis*. *Mol. Plant* **2019**, *12*, 215–228. [[CrossRef](#)]
62. Mishra, N.; Srivastava, A.P.; Esmaeili, N.; Hu, W.; Shen, G. Overexpression of the rice gene *OsSIZ1* in *Arabidopsis* improves drought-, heat-, and salt-tolerance simultaneously. *PLoS ONE* **2018**, *13*, e0201716. [[CrossRef](#)] [[PubMed](#)]
63. Park, B.S.; Seo, J.S.; Chua, N.H. NITROGEN LIMITATION ADAPTATION recruits PHOSPHATE2 to target the Phosphate transporter PT2 for degradation during the regulation of *Arabidopsis* Phosphate homeostasis. *Plant Cell* **2014**, *26*, 454–464. [[CrossRef](#)] [[PubMed](#)]
64. Lin, W.Y.; Huang, T.K.; Chiou, T.J. Nitrogen limitation adaptation, a target of microRNA827, mediates degradation of plasma membrane-localized Phosphate transporters to maintain phosphate homeostasis in *Arabidopsis*. *Plant Cell* **2013**, *25*, 4061–4074. [[CrossRef](#)] [[PubMed](#)]

65. Medici, A.; Marshall-Colon, A.; Ronzier, E.; Szponarski, W.; Wang, R.; Gojon, A.; Crawford, N.M.; Ruffel, S.; Coruzzi, G.M.; Krouk, G. AtNIGT1/HRS1 integrates nitrate and Phosphate signals at the *Arabidopsis* root tip. *Nat. Commun.* **2015**, *6*, 6274. [[CrossRef](#)] [[PubMed](#)]
66. Khan, F.; Khan, S.; Fahad, S.; Faisal, S.; Hussain, S.; Ali, S.; Ali, A. Effect of different levels of nitrogen and phosphorus on the phenology and yield of maize varieties. *Am. J. Plant Sci.* **2014**, *5*, 2582–2590. [[CrossRef](#)]
67. Luo, X.; Mazer, S.J.; Guo, H.; Zhang, N.; Weiner, J.; Hu, S. Nitrogen: Phosphorous supply ratio and allometry in five alpine plant species. *Ecol. Evol.* **2016**, *6*, 8881–8892. [[CrossRef](#)] [[PubMed](#)]
68. Wang, C.; Ying, S.; Huang, H.; Li, K.; Wu, P.; Shou, H. Involvement of OsSPX1 in phosphate homeostasis in rice. *Plant J.* **2009**, *57*, 895–904. [[CrossRef](#)]
69. Ruan, W.; Guo, M.; Wang, X.; Guo, Z.; Xu, Z.; Xu, L.; Zhao, H.; Sun, H.; Yan, C.; Yi, K. Two RING-finger ubiquitin E3 ligases regulate the degradation of SPX4, an internal Phosphate sensor, for Phosphate homeostasis and signaling in rice. *Mol. Plant* **2019**, *12*, 1060–1074. [[CrossRef](#)]
70. Puga, M.I.; Mateos, I.; Charukesi, R.; Wang, Z.; Franco-Zorrilla, J.M.; de Lorenzo, L.; Irigoyen, M.L.; Masiero, S.; Bustos, R.; Rodriguez, J.; et al. SPX1 is a Phosphate-dependent inhibitor of Phosphate starvation response 1 in *Arabidopsis*. *Proc. Natl. Acad. Sci. USA* **2014**, *111*, 14947–14952. [[CrossRef](#)]
71. Duan, K.; Yi, K.; Dang, L.; Huang, H.; Wu, W.; Wu, P. Characterization of a sub-family of *Arabidopsis* genes with the SPX domain reveals their diverse functions in plant tolerance to phosphorus starvation. *Plant J.* **2008**, *54*, 965–975. [[CrossRef](#)]
72. Li, Y.; Wu, H.; Fan, H.; Zhao, T.; Ling, H.Q. Characterization of the AtSPX3 promoter elucidates its complex regulation in response to phosphorus deficiency. *Plant Cell Physiol.* **2016**, *57*, 1767–1778. [[CrossRef](#)] [[PubMed](#)]
73. Osorio, M.B.; Ng, S.; Berkowitz, O.; De Clercq, I.; Mao, C.; Shou, H.; Whelan, J.; Jost, R. SPX4 acts on PHR1-dependent and -independent regulation of shoot phosphorus status in *Arabidopsis*. *Plant Physiol.* **2019**, *181*, 332–352. [[CrossRef](#)] [[PubMed](#)]
74. Zhong, Y.; Wang, Y.; Guo, J.; Zhu, X.; Shi, J.; He, Q.; Liu, Y.; Wu, Y.; Zhang, L.; Lv, Q.; et al. Rice SPX6 negatively regulates the Phosphate starvation response through suppression of the transcription factor PHR2. *New Phytol.* **2018**, *219*, 135–148. [[CrossRef](#)] [[PubMed](#)]
75. Hu, B.; Jiang, Z.; Wang, W.; Qiu, Y.; Zhang, Z.; Liu, Y.; Li, A.; Gao, X.; Liu, L.; Qian, Y.; et al. Nitrate–NRT1.1B–SPX4 cascade integrates nitrogen and phosphorus signalling networks in plants. *Nat. Plants* **2019**, *5*, 401–413. [[CrossRef](#)]
76. Qi, W.; Manfield, I.W.; Muench, S.P.; Baker, A. AtSPX1 affects the AtPHR1–DNA-binding equilibrium by binding monomeric AtPHR1 in solution. *Biochem. J.* **2017**, *474*, 3675–3687. [[CrossRef](#)]
77. Wang, Z.; Ruan, W.; Shi, J.; Zhang, L.; Xiang, D.; Yang, C.; Li, C.; Wu, Z.; Liu, Y.; Yu, Y.; et al. Rice SPX1 and SPX2 inhibit Phosphate starvation responses through interacting with PHR2 in a Phosphate-dependent manner. *Proc. Natl. Acad. Sci. USA* **2014**, *111*, 14953–14958. [[CrossRef](#)]
78. Schwartz, A. Role of Ca²⁺ and EGTA on stomatal movements in *Commelina communis* L. *Plant Physiol.* **1985**, *79*, 1003–1005. [[CrossRef](#)]
79. Tai, L.; Li, B.B.; Nie, X.M.; Zhang, P.P.; Hu, C.H.; Zhang, L.; Liu, W.T.; Li, W.Q.; Chen, K.M. Calmodulin is the fundamental regulator of NADK-mediated NAD signaling in plants. *Front. Plant Sci.* **2019**, *10*, 681. [[CrossRef](#)]
80. Yoo, C.Y.; Mano, N.; Finkler, A.; Weng, H.; Day, I.S.; Reddy, A.S.N.; Poovaiah, B.W.; Fromm, H.; Hasegawa, P.M.; Mickelbart, M.V. A Ca²⁺/CaM-regulated transcriptional switch modulates stomatal development in response to water deficit. *Sci. Rep.* **2019**, *9*, 12282. [[CrossRef](#)]
81. Allen, G.J.; Muir, S.R.; Sanders, D. Release of Ca²⁺ from individual plant vacuoles by both InsP₃ and cyclic ADP-ribose. *Science* **1995**, *268*, 735–737. [[CrossRef](#)]
82. Shears, S.B.; Ganapathi, S.B.; Gokhale, N.A.; Schenk, T.M.; Wang, H.; Weaver, J.D.; Zaremba, A.; Zhou, Y. Defining signal transduction by inositol Phosphates. *Subcell. Biochem.* **2012**, *59*, 389–412. [[PubMed](#)]
83. Hermosura, M.C.; Takeuchi, H.; Fleig, A.; Riley, A.M.; Potter, B.V.; Hirata, M.; Penner, R. InsP₄ facilitates store-operated calcium influx by inhibition of InsP₃ 5-phosphatase. *Nature* **2000**, *408*, 735–740. [[CrossRef](#)] [[PubMed](#)]
84. Menniti, F.S.; Oliver, K.G.; Putney, J.W.; Shears, S.B. Inositol Phosphates and cell signaling: New views of InsP₅ and InsP₆. *Trends Biochem. Sci.* **1993**, *18*, 53–56. [[CrossRef](#)]

85. Kuo, H.F.; Chang, T.Y.; Chiang, S.F.; Wang, W.D.; Charng, Y.Y.; Chiou, T.J. Arabidopsis inositol pentakisphosphate 2-kinase, AtIPK1, is required for growth and modulates Phosphate homeostasis at the transcriptional level. *Plant J.* **2014**, *80*, 503–515. [[CrossRef](#)] [[PubMed](#)]
86. Kuo, H.F.; Hsu, Y.Y.; Lin, W.C.; Chen, K.Y.; Munnik, T.; Brearley, C.A.; Chiou, T.J. Arabidopsis inositol Phosphate kinases IPK1 and ITPK1 constitute a metabolic pathway in maintaining Phosphate homeostasis. *Plant J.* **2018**, *95*, 613–630. [[CrossRef](#)] [[PubMed](#)]
87. Wild, R.; Gerasimaite, R.; Jung, J.; Truffault, V.; Pavlovic, I.; Schmidt, A.; Saiardi, A.; Jessen, H.J.; Poirier, Y.; Hothorn, M.; et al. Control of eukaryotic Phosphate homeostasis by inositol Polyphosphate sensor domains. *Science* **2016**, *352*, 986–990. [[CrossRef](#)]
88. Dong, J.; Ma, G.; Sui, L.; Wei, M.; Satheesh, V.; Zhang, R.; Ge, S.; Li, J.; Zhang, T.E.; Wittwer, C.; et al. Inositol Pyrophosphate InsP₈ acts as an intracellular Phosphate signal in *Arabidopsis*. *Mol. Plant* **2019**, *12*, 1463–1473. [[CrossRef](#)]
89. Shears, S.B. Inositol pyrophosphates: Why so many Phosphates? *Adv. Biol. Regul.* **2015**, *57*, 203–216. [[CrossRef](#)]
90. Zhu, J.; Lau, K.; Puschmann, R.; Harmel, R.K.; Zhang, Y.; Pries, V.; Gaugler, P.; Broger, L.; Dutta, A.K.; Jessen, H.J.; et al. Two bifunctional inositol Pyrophosphate kinases/phosphatases control plant Phosphate homeostasis. *eLife* **2019**, *8*, e43582. [[CrossRef](#)]
91. Wang, H.; Nair, V.S.; Holland, A.A.; Capolicchio, S.; Jessen, H.J.; Johnson, M.K.; Shears, S.B. Asp1 from *Schizosaccharomyces pombe* binds a [2Fe-2S]²⁺ cluster which inhibits inositol Pyrophosphate 1-phosphatase activity. *Biochemistry* **2015**, *54*, 6462–6474. [[CrossRef](#)]
92. Sheard, L.B.; Tan, X.; Mao, H.; Withers, J.; Ben-Nissan, G.; Hinds, T.R.; Kobayashi, Y.; Hsu, F.F.; Sharon, M.; Browse, J.; et al. Jasmonate perception by Inositol-Phosphate-potentiated COI1-JAZ co-receptor. *Nature* **2010**, *468*, 400–405. [[CrossRef](#)] [[PubMed](#)]
93. Tan, X.; Calderon-Villalobos, L.I.; Sharon, M.; Zheng, C.; Robinson, C.V.; Estelle, M.; Zheng, N. Mechanism of auxin perception by the TIR1 ubiquitin ligase. *Nature* **2007**, *446*, 640–645. [[CrossRef](#)]
94. Laha, D.; Johnen, P.; Azevedo, C.; Dynowski, M.; Weiß, M.; Capolicchio, S.; Mao, H.; Iven, T.; Steenbergen, M.; Freyer, M.; et al. VIH2 regulates the synthesis of Inositol Pyrophosphate InsP₈ and Jasmonate-dependent defenses in *Arabidopsis*. *Plant Cell* **2015**, *27*, 1082–1097. [[CrossRef](#)] [[PubMed](#)]
95. Maeda, Y.; Konishi, M.; Kiba, T.; Sakuraba, Y.; Sawaki, N.; Kurai, T.; Ueda, Y.; Sakakibara, H.; Yanagisawa, S. A NIGT1-centred transcriptional cascade regulates nitrate signalling and incorporates phosphorus starvation signals in *Arabidopsis*. *Nat. Commun.* **2018**, *9*, 1376. [[CrossRef](#)]
96. Medici, A.; Szponarski, W.; Dangeville, P.; Safi, A.; Dissanayake, I.M.; Saenchai, C.; Emanuel, A.; Rubio, V.; Lacombe, B.; Ruffel, S.; et al. Identification of molecular integrators shows that nitrogen actively controls the Phosphate starvation response in plants. *Plant Cell* **2019**, *31*, 1171–1184. [[CrossRef](#)]
97. Huang, T.K.; Han, C.L.; Lin, S.I.; Chen, Y.J.; Tsai, Y.C.; Chen, Y.R.; Chen, J.W.; Lin, W.Y.; Chen, P.M.; Liu, T.Y.; et al. Identification of downstream components of ubiquitin-conjugating enzyme PHOSPHATE2 by quantitative membrane proteomics in *Arabidopsis* roots. *Plant Cell* **2013**, *25*, 4044–4060. [[CrossRef](#)]



© 2019 by the authors. Licensee MDPI, Basel, Switzerland. This article is an open access article distributed under the terms and conditions of the Creative Commons Attribution (CC BY) license (<http://creativecommons.org/licenses/by/4.0/>).

Poznań, 28.09.2020

Mgr Paweł Sega
Uniwersytet im. Adama Mickiewicza w Poznaniu
Instytut Biologii Molekularnej i Biotechnologii
Zakład Ekspresji Genów
ul. Uniwersytetu Poznańskiego 6
61-614 Poznań
e-mail: pawel.sega@amu.edu.pl

Oświadczenie określające wkład w powstanie artykułu

Niniejszym oświadczam, że mój wkład w powstanie poniższego artykułu:

Paweł Sega, Andrzej Pacak. 2019. Plant PHR Transcription Factors: Put on A Map. *Genes (Basel)* 10(12):1018.

polegał na: przygotowaniu konceptu publikacji, zebraniu literatury, zaprojektowaniu oraz wykonaniu figur, napisaniu publikacji w całości, dopracowaniu manuskryptu po ocenie recenzentów


Paweł Sega

Poznań, 28.09.2020

Dr hab. Andrzej Pacak, Prof. UAM
Uniwersytet im. Adama Mickiewicza w Poznaniu
Instytut Biologii Molekularnej i Biotechnologii
Zakład Ekspresji Genów
ul. Uniwersytetu Poznańskiego 6
61-614 Poznań
e-mail: apacak@amu.edu.pl

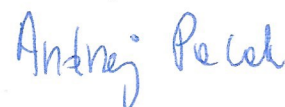
Oświadczenie określające wkład w powstanie artykułu

Niniejszym oświadczam, że mój wkład w powstanie poniższego artykułu:

Paweł Segal, **Andrzej Pacak**. 2019. Plant PHR Transcription Factors: Put on A Map. *Genes (Basel)* 10(12):1018.

polegał na: zaproponowaniu tematyki artykułu i wprowadzeniu uwag do jego treści.

Andrzej Pacak





Chapter 10

miRNA Detection by Stem-Loop RT-qPCR in Studying microRNA Biogenesis and microRNA Responsiveness to Abiotic Stresses

Aleksandra Smoczynska, Pawel Segal, Agata Stepień, Katarzyna Knop, Artur Jarmolowski, Andrzej Pacak, and Zofia Szweykowska-Kulinska

Abstract

This chapter is devoted to a PCR-based method for analyzing the expression level of mature miRNAs which utilizes the TaqMan[®] technology. Stem-loop RT-qPCR requires preparation of separate cDNA templates for each analyzed miRNA as reverse transcription occurs in the presence of a miRNA-specific stem-loop reverse primer. In quantitative analysis, SYBR[®] Green is not used but the more sensitive TaqMan[®] probe that on 5' end contains a covalently attached fluorophore and on 3' quencher. When quencher and fluorophore are spatially separated due to nucleolytic DNA polymerase activity, the signal is released and quantified. This section provides a detailed and comprehensive protocol allowing for the successful analysis of mature miRNA levels in analyzed sample. Reverse transcription combined with classic real-time PCR as well as ddPCR[™] (Droplet Digital[™] PCR) will be presented.

Key words microRNA, Stem-loop primer, RT-qPCR, RT-ddPCR, TaqMan, Probes

1 Introduction

microRNAs (miRNAs) are crucial players in all biological processes occurring in plants. The impact of miRNA activity on plant development, nutrient uptake, and adaptation to environmental conditions was shown in multiple cases [1–3]. For instance, downregulation of the *TCP4* (*TEOSINTE BRANCHED1*, *CYCLOIDEA*, and *PROLIFERATING CELL NUCLEAR ANTIGEN BINDING FACTOR 4*) transcription factor by miR319-mediated mechanism is essential for plant development. Introduction of *TCP4* gene containing mutations in the miRNA target site is lethal in most cases [4, 5]. Similarly, miR160c is important during root development. Transgenic lines overexpressing the *MIR160C* gene display reduced level of miR160c target *ARF10* (*AUXIN RESPONSE FACTOR 10*), which results in

Arabidopsis plants with shorter roots and altered root apex [6]. miRNAs are also important in plant response to abiotic stresses, such as phosphate starvation, which in *Arabidopsis* induces the expression of miR399 family members that target 5' UTR of *PHO2* (*PHOSPHATE2*) transcript. Reduction of *PHO2* helps to accumulate high amounts of inorganic phosphate in the shoots [7–9]. miRNAs are present in all tissues but display different expression patterns; that is why the level of miRNAs should be measured precisely in different tissues using appropriate methods.

One of the traditional techniques for quantifying the amount of mature miRNA is by Northern blot hybridization, where total RNA is separated on a denaturing polyacrylamide gel, transferred to a nylon membrane, UV-cross-linked, and hybridized with a radioactively labeled probe [1–3]. Unfortunately, the classical protocol is time-consuming, requires high amounts of RNA material, and often fails to identify rare miRNAs expressed at low level and to distinguish between miRNA family members. The range of modifications has been introduced to improve sensitivity of this method. Chemical cross-linking of RNA appears to be more efficient and requires almost half the amount of RNA material than the classical protocol [10]. Recently, the group of Shenghua Wang from Sichuan University published a liquid Northern hybridization protocol that uses picomolar amounts of RNA and fluorescently labeled probes. The detection process is completed in just a few hours, and multiple miRNAs can be detected in a single experiment [11]. To increase specificity of probe binding, the LNA (locked nucleic acid) oligonucleotides have been introduced [12]. LNAs are a class of nucleotide analogs containing sugar ring locked by an extra bridge connecting the 2' oxygen and 4' carbon methylene bonds in 3' endo conformation, which results in higher thermal stability when hybridized to a complementary RNA strand [13, 14]. miRNA expression level analysis can also be performed using in situ hybridization (ISH) that visualizes RNA in fixed tissue structures. ISH allows to compare expression in different cell types based on binding of labeled probe to target RNA. Different labeling can be used (fluorescent, dioxigenin, radioactive, etc.), but the tested tissue always must be fixed sufficiently, permeable, embedded in paraffin, and sliced into sections with 4–6 μm diameters [15]. Each step of tissue preparation is prone to mistakes and may cause the experiment to fail. The most challenging part of this method is the fixation of material. Individual case optimization depending on the sample is necessary as too weak fixation results in loss of signal and tissue structure, and too strong preservation will not allow the probe to penetrate. This technique is very time-consuming; the whole procedure may take up to 10 days [15]. It is worth to mention that alternative approaches in ISH technique do not necessarily utilize the final step of embedding in paraffin. Instead they use seedling root tips that after fixation are treated

with enzymes macerating plant tissue, followed by permeabilization step for RNA visualization [16].

Another tool for miRNA analysis is high-throughput sequencing of small RNA (sRNA) libraries. Next-generation sequencing (NGS) enables examination and comparison of all miRNAs derived from tested tissues in a single experiment as many samples can be processed in parallel [17]. NGS allows identification of single miRNA with the accuracy to one nucleotide. There are many commercial kits available for preparation of sRNA libraries (*see Note 1*). The procedure consists of isolation of total RNA, ligation of specific adaptors, cDNA synthesis, amplification, gel purification, and sequencing [18, 19]. Disadvantages of this method are the bias in ligation efficiency of adaptor depending on RNA sequence and structure, overrepresentation of abundant miRNAs, and underrepresentation of low-level miRNAs in the cell. This method is also still quite expensive opposed to others, especially when expression level of only one particular miRNA is analyzed.

Mature miRNAs are only about 21 nt in length. Therefore, such short sequences cannot be analyzed by classical real-time PCR because the primers used for amplification would overlap. Moreover, mature miRNAs are not polyadenylated. To overcome this issue, some modifications have been made. Poly(A) RT-PCR method uses poly(A) polymerase to extend the miRNAs by adding multiple adenylic acid residues to miRNA 3' end. In the next step, reverse transcriptase with oligo(dT) adapter produces cDNA, which allows for quantitative analysis using miRNA-specific primer and universal primer that anneals to the adaptor [20]. Another method utilizes a stem-loop reverse primer, which binds to a specific miRNA sequence and is elongated by reverse transcriptase (Fig. 1). To quantify the mature miRNA expression level more specific, TaqMan[®] Assay is used instead of SYBR[®] Green (*see Note 2*). The TaqMan[®] system is much more reliable in analysis. In this approach, apart from forward and reverse primers, a specific fluorescent probe is used (*see Note 3*). In this chapter, we will present this technique in detail.

2 Materials

The protocol is optimized for *Arabidopsis thaliana* (Col-0) seedlings and rosette leaves (wild-type (wt) plants and mutant lines of *SERRATE* (*SE*, At2g27100) (*se-1*, *se-2*) [21, 22]), *Nicotiana benthamiana* leaves, and barley shoots and roots.

2.1 Total Plant RNA Extraction

1. Liquid nitrogen, pestle, and mortar.
2. Direct-zol[™] RNA MiniPrep (Zymo Research) (*see Note 4*).
3. Plant RNA Isolation Aid (Ambion).

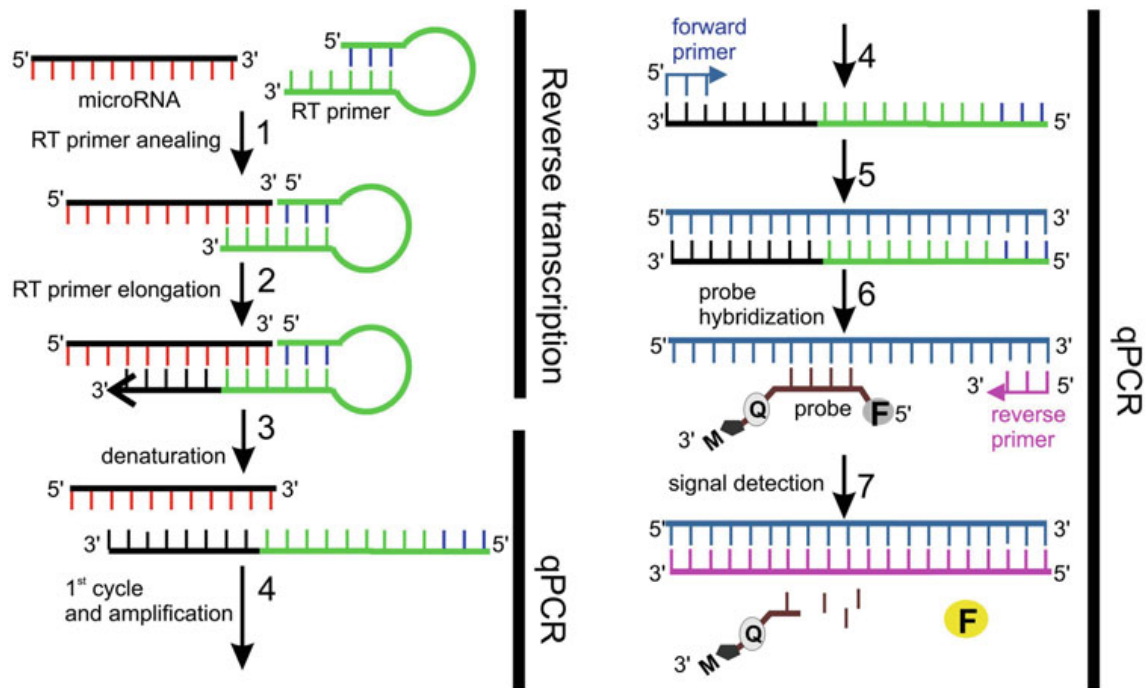


Fig. 1 The principles of reverse transcription of mature miRNA using stem-loop primer and TaqMan microRNA quantitative amplification assay. *F* reporter dye, *RT primer*, stem-loop reverse transcription primer, *Q* nonfluorescent quencher, *M* minor groove binder

- RNA extraction buffer: 0.8 M guanidine thiocyanate, 0.4 M ammonium thiocyanate, 0.1 M sodium acetate pH 5.0, 5% v/v glycerol, 38% v/v saturated acidic phenol, 5 mM EDTA, 0.5% sodium lauroylsarcosine, in diethylpyrocarbonate-treated water (DEPC).
- Pre-chilled 95–100% ethanol.
- 2× SSC (saline-sodium citrate) buffer: 0.30 M sodium citrate, 0.030 M NaCl buffer, pH = 7.0 adjusted with HCl, dissolved in diethylpyrocarbonate-treated water (DEPC).
- TURBO DNA-free™ Kit (Thermo Fisher Scientific).

2.2 cDNA Synthesis (Reverse Transcription)

- DNA-free total RNA from tissue samples.
- RNase-free and DEPC-treated water.
- TaqMan™ MicroRNA Reverse Transcription Kit (Thermo Fisher Scientific).
- TaqMan™ MicroRNA Assay: contains 5× specific reverse transcription miRNA primer and 20× TaqMan™ unique probe (Thermo Fisher Scientific) (*see Note 5*). Assay of individual miRNA level measurement can be found by their ID number:
 - miR163 (Thermo Fisher Scientific, Assay ID 000343),
 - miR171b (Thermo Fisher Scientific, Assay ID 000358),
 - miR399c (Thermo Fisher Scientific, Assay ID 000373),

- (d) miR402 (Thermo Fisher Scientific, Assay ID 001418),
- (e) miR1888a (Thermo Fisher Scientific, Assay ID 007732_mat),
- 5. Custom Small RNA Assay for U6 snRNA (*At3g14735*) level analysis: 5× specific reverse transcription primer, 20× TaqMan™ unique probe (Thermo Fisher Scientific).
- 6. Oligo(dT)18 primer (Thermo Fisher Scientific) for cDNA preparation for *Arabidopsis* actin 8 (*ACT8*, NM_103814.3), hygromycin (*ACI22368*), and barley ADP-ribosylation factor 1-like protein gene (*ARF1*, AJ508228) and *PHOSPHATE2* (*PHO2*, GQ861514.1) level determination.
- 7. SuperScript III Reverse Transcriptase (Thermo Fisher Scientific) for cDNA preparation for *ACT8*, hygromycin, *ARF1*, and *PHO2* level determination.
- 8. dNTPs' mix (10 mM each).
- 9. Power SYBR™ Green PCR Master Mix (Thermo Fisher Scientific).
- 10. GAPDH (*At1g13440*) primers for cDNA quality check (0.5 μM each):
 - (a) GAPDH 5' fragment: Fw 5'-TCTCGATCTCAATTTC GCAAAA-3' and Rev 5'-CGAAACCGTTGATTCCGA TTC-3'.
 - (b) GAPDH 3' fragment: Fw 5'-TTGGTGACAACAGGT CAAGCA-3' and Rev 5'-AAACTTGTCGCTCAATGC AATC-3'.
- 11. PCR machine ProFlex PCR System (Applied Biosystems).
- 12. qPCR machine: 7900HT Fast Real-Time PCR System or QuantStudio 7 FLEX (Applied Biosystems).

2.3 Quantitative Reverse Transcription PCR (RT-qPCR)

- 1. cDNA templates.
- 2. DNase-free water and DEPC-treated water.
- 3. TaqMan™ MicroRNA Assay specific for particular miRNA: contains 5× specific reverse transcription primer and 20× TaqMan™ unique probe (Thermo Fisher Scientific).
- 4. Custom Small RNA Assay for U6 snRNA level analysis (Thermo Fisher Scientific).
- 5. Custom TaqMan™ Gene Expression Assay for hygromycin and barley *ARF1* expression level analysis (Thermo Fisher Scientific).
- 6. TaqMan™ Gene Expression Assay for *ACT8* level analysis (Thermo Fisher Scientific, Assay ID At02270958_gH).

7. TaqMan™ Universal Master Mix II, with UNG (Applied Biosystems).
8. qPCR machine: 7900HT Fast Real-Time PCR System or QuantStudio 7 FLEX (Applied Biosystems).

2.4 Droplet Digital™ PCR (ddPCR™)

1. Undiluted miRNA cDNA and 40× diluted cDNA (for *PHO2*, *ARF1*) samples (*see* Note 6).
2. TaqMan™ MicroRNA Assay specific for particular miRNA: contains 5× specific reverse transcription primer and 20× TaqMan™ unique miRNA probe.
3. Custom TaqMan Gene Expression Assay for barley *ARF1* level analysis (Thermo Fisher Scientific).
4. 2× ddPCR™ Supermix for Probes (Bio-Rad) for miR399c and *ARF1* level determination.
5. 2× QX200 ddPCR™ EvaGreen Supermix for *PHO2* and *ARF1* level determination (Bio-Rad).
6. Droplet Generation Oil for Probes (Bio-Rad) for miR399c and *ARF1* level determination.
7. QX200 Droplet Generation Oil for EvaGreen (Bio-Rad) for *PHO2* and *ARF1* level determination.
8. ddPCR™ Plate Kit (Bio-Rad).
9. ddPCR machine: QX200™ Droplet Digital™ PCR System (Bio-Rad).

3 Methods

Firstly, unique probes for testing miRNA/noncoding/coding RNA expression level should be designed. Hence, in your website browser, open the official Thermo Fisher Scientific custom platform (<http://www.thermofisher.com/order/custom-genomic-products/tools/small-rna/>). Keep in mind that your query sequence must contain only A, C, G, T, or U bases and must be between 17 and 200 bases. Fill the “Assay Name” and “Sequence” fields and “Submit sequence(s)” to order. Once designed, probes can be searched and ordered again. Thus, go directly to the TaqMan Assay platform (<http://www.thermofisher.com/pl/en/home/life-science/pcr/real-time-pcr/real-time-pcr-assays/mirna-ncrna-taqman-assays.html>), and then search for the desired probe based either on the ID number, miRBase number (<http://www.mirbase.org>), or nucleotide sequence. Here, the “T” bases are not allowed when using nucleotide sequence for searching, and you have to replace all “T” bases into “U.” Remember to choose “TaqMan™ MicroRNA Assays” or “TaqMan™ Gene Expression Assay” option for the specific stem-loop primer approach.

3.1 Plant Total RNA Extraction

1. Transfer plant tissue into a mortar, and grind using liquid nitrogen and pestle until you see a layer of fine dust. Store homogenized material at -80°C or use immediately.
2. Into a cooled 2 mL RNase-free tube (use liquid nitrogen for cooling) weight up to 100 mg of ground plant tissue.
3. Add 1 mL of RNA extraction buffer, and homogenize mixture by vortexing thoroughly for 10–20 s.
4. Add 70 μL of Plant RNA Isolation Aid to remove any excess of polysaccharides. While white precipitates may appear, vortex vigorously your samples for 10–20 s, and incubate at room temperature for 5 min on a wheel rotator, or invert them manually.
5. Centrifuge samples at $14,000 \times g$ for 15 min at 4°C . Next, transfer the supernatant carefully into a new 2.0 mL RNase-free tube. Do not disturb the pellet.
6. Repeat centrifugation of your supernatant again until you will not see any pellet. Usually, up to 2–3 centrifugations are required.
7. Following last centrifugation, add 1 volume of chilled 95–100% ethanol to the supernatant. Here, you can leave your samples at -20°C overnight or go straight to the next step.
8. Apply up to 800 μL of the mixture from **step 7** to Zymo-Spin IIC column placed in collection tube (provided), and centrifuge at $14,000 \times g$ for 1 min at room temperature. Discard flow-through and centrifuge residual volume.
9. Transfer the column into a new collection tube (provided), and prepare the column for DNase I treatment following the manufacturer's protocol.
10. Add 400 μL RNA wash buffer to the column, and centrifuge at $14,000 \times g$ for 1 min at room temperature. Discard the flow-through. All further centrifugations should be performed under these conditions.
11. In the new RNase-free tube (not provided), mix 5 μL DNase I and 75 μL DNA digestion buffer. Add the mix directly to the column matrix. Incubate at room temperature for 15 min. Alternatively, you may perform DNase I treatment after RNA isolation and quality control (*see step 16*).
12. Add 400 μL of Direct-zol RNA PreWash buffer directly to the column and centrifuge. Discard the flow-through and repeat this step.
13. Add 700 μL RNA wash buffer to the column, and centrifuge for 2 min to ensure complete removal of the wash buffer. Transfer the column carefully into a new 1.5 mL RNase-free tube (not provided).
14. To elute RNA, add 50 μL of DNase-/RNase-Free Water directly to the column matrix, incubate for 2 min at room

temperature, and centrifuge. Quantify each sample using Nanodrop Spectrophotometer (*see Note 7*).

15. For checking RNA quality, denature 500 ng of RNA sample in 1× SSC buffer for 5 min at 70 °C. Run samples on a 1.2% agarose gel for 30 min at 10 V per cm of your gel length.

16. Alternative DNase I treatment procedure: After RNA quality control, take 30 µg of RNA, and incubate with 0.1 volume of 10× TURBO DNase Buffer and 1 µL of TURBO DNase (2 Units/µL) for 1 h at 37 °C. A typical reaction volume is 50 µL. Next, add 0.1 volume of resuspended DNase Inactivation Reagent, incubate for 5 min at room temperature, and vortex gently every 30 s. Centrifuge at 10,000 × *g* for 1.5 min at 4 °C, and transfer supernatant containing RNA to a fresh RNase-free tube (do not disturb or aspirate the pellet). Determine the RNA concentration and quality as in **steps 14** and **15**, respectively (*see Note 7*).

3.2 cDNA Synthesis

To determine the role of SERRATE (SE) in miRNA biogenesis, prepare the cDNA templates for each individual miRNA (miR163, miR171b, miR402, miR1888a) and U6 snRNA (as a control), using total RNA isolated from *A. thaliana* wild-type (wt) plants and mutant lines of *SE* (*se-1*, *se-2*).

For the analysis of active splice site influence on intronic miR402 biogenesis, prepare cDNA template from *N. benthamiana* leaves infiltrated with *Agrobacterium* carrying *MIR402* native or mutated (5' splice site or 3' splice site inactivation) construct.

3.2.1 cDNA Synthesis for miRNA and U6 snRNA Level Determination

1. Thaw the TaqMan assay/kits reagents: 5× RT Primer, dNTPs' mix, 10× RT Buffer, and RNA samples on ice.
2. Mix and briefly spin each component, and combine the following in a 0.2 mL RNase-free PCR tube (*see Note 8*):

Reagent	Volume for 15 µL single reaction
RNase-free water	4.16 µL
100 mM dNTPs' mix	0.15 µL
10× RT Buffer	1.50 µL
RNase Inhibitor 20 U/µL	0.19 µL
Multiscribe™ Reverse Transcriptase 50 U/µL	1.00 µL
Partial volume	7.00 µL

3. Keep the RT mixture on ice, and add 5 µL of total RNA (10 ng of total RNA per 15 µL reaction). Mix gently and briefly spin. Do not vortex.

4. Transfer 3 μL of the $5\times$ RT primers to the RT mixture bringing the total volume per sample to 15 μL . Mix gently and briefly spin. Do not vortex.
5. Incubate the RT mixture on ice for 5 min or until you are ready to start the thermal cycler program using PCR machine.

No. of cycles: 1

Temperature ($^{\circ}\text{C}$)	Time (min)
16	30
42	30
85	5
4	∞

6. Proceed directly after cDNA synthesis to PCR or store cDNA at -20°C .

3.2.2 cDNA Synthesis for *Arabidopsis ACT8*, *Barley PHO2*, *ARF1*, and *Hygromycin mRNA* Level Determination

1. Thaw the reagents (oligo(dT)18 primer, dNTPs' mix, $5\times$ RT Buffer, 0.1 M DTT) and total RNA samples on ice.
2. Mix and briefly spin each component, and combine the following in a 0.2 mL RNase-free PCR tube (*see Note 8*):

Reagent	Volume for 20 μL single reaction
Total RNA	3.00 μg^{a}
10 mM dNTPs' mix	1.00 μL
oligo(dT)18 primer	1.00 μL
RNase-free water	up to 13.00 μL^{a}
Partial volume	13.00 μL

^aAdd appropriate volume according to RNA sample concentration

3. Incubate for 5 min at 65°C and put reaction on ice for 2 min.
4. Collect the content of the tube by brief centrifugation, and add the rest of the RT mixture prepared as follows:

Reagent	Volume for 20 μL single reaction
$5\times$ RT buffer	4.00 μL
0.1 M DTT	1.00 μL
SuperScript III Reverse Transcriptase 200 U/ μL	1.00 μL
RNase Inhibitor 20 U/ μL	1.00 μL
Partial volume	7.00 μL

5. Mix by pipetting gently up and down and incubate for 1 h at 50 °C.
6. Inactivate the reaction by heating at 70 °C for 15 min.
7. Collect the content of the tube by brief centrifugation, and dilute three times with RNase-free water (1:2 ratio).
8. Proceed directly after cDNA synthesis to PCR or store cDNA at –20 °C.
9. To test the cDNA quality by RT-qPCR, perform independent quantitative analysis of GAPDH mRNA 5' and 3' fragments. Use separate primers for the amplification of 5' and 3' GAPDH mRNA fragments. Set up the reaction Master Mix as follows:

Reagent	Volume for 10 µL single reaction
cDNA	1.00 µL
Power SYBR™ Green PCR Master Mix	5.00 µL
Primer Mix (0.5 µM each)	4.00 µL
Total volume	10.00 µL

10. Start the RT-qPCR reaction program:

Temperature (°C)	Time
95	10 min
40 cycles:	
95	15 s
60	1 min

11. Calculate the Ct value difference for 5' and 3' GAPDH mRNA fragments. It should be lower than 1 [23].

3.3 Quantitative PCR (qPCR) for miRNA, U6 RNA, Actin, and Hygromycin cDNAs

To study the role of SE in miRNA biogenesis in *Arabidopsis*, prepare samples for each individual miRNA and U6 snRNA in wt, *se-1* and *se-2*. U6 snRNA will be used as a reference gene in further data analysis (*see* **Note 9**). You may also use another reference gene such as *ACT8* instead of U6 snRNA.

To evaluate the importance of splice sites in intronic miR402 biogenesis in tobacco, set up the reaction for miR402 as well as for hygromycin mRNA. The latter will be used for data normalization (hygromycin gene is on the same plasmid as *MIR402*).

1. Thaw all 20× TaqMan Assays as well as cDNA templates on ice. Invert tubes several times and spin them briefly.
2. Set up the reaction Master Mix as follows (*see* **Note 8**):

Reagent	Volume for 20 μ L single reaction
DNase-free water	8.00 μ L
2 \times TaqMan Universal PCR Master Mix II with UNG	10.00 μ L
20 \times TaqMan MicroRNA or Small RNA Assay (for miRNA or U6 snRNA, respectively) or 20 \times TaqMan Gene Expression Assay	1.00 μ L
Partial volume	19.00 μ L

- Pipette the mix on a 96- or 384-well plate, and add 1.00 μ L of cDNA template to each one as follows:

cDNA template	Sample
miRNA specific	miRNA level determination
U6 snRNA specific	U6 snRNA level determination
Oligo(dT)	ACT8 or hygromycin transcript level determination

- Seal the plate thoroughly to avoid evaporation, and centrifuge at $2000 \times g$ for 2 min at room temperature.
- Set the reaction program as shown below, put the plate in a qPCR machine, and start the run without melting curve.

Temperature ($^{\circ}$ C)	Time
50	2 min
95	10 min
40 cycles:	
95	15 s
60	1 min

3.4 Data Analysis After RT-qPCR

3.4.1 Determine the Levels of *A. thaliana* Intronic (*miR402*, *miR1888a*) and Exonic (*miR163*, *miR171b*) miRNAs in *wt*, *se-1* and *se-2* (Fig. 2)

- Subtract Ct values for U6 snRNA from Ct values obtained for miRNA (Δ Ct).
- Next, subtract $wt\Delta$ Ct value from all studied samples ($\Delta\Delta$ Ct).
- Use $2^{(-\Delta\Delta Ct)}$ to calculate fold change.
- Apply Student's *t*-test for statistical analyses. Use $2^{\Delta Ct}$ values for this purpose (see Note 10).

The levels of intronic miRNAs are downregulated in *se-1* compared to the *wt* plants and elevated in *se-2* in comparison to *se-1* (Fig. 2; [24, 25]). The impact of SE mutations was different in the case of exonic miRNAs, since their levels were the lowest in the *se-2* mutant [25].

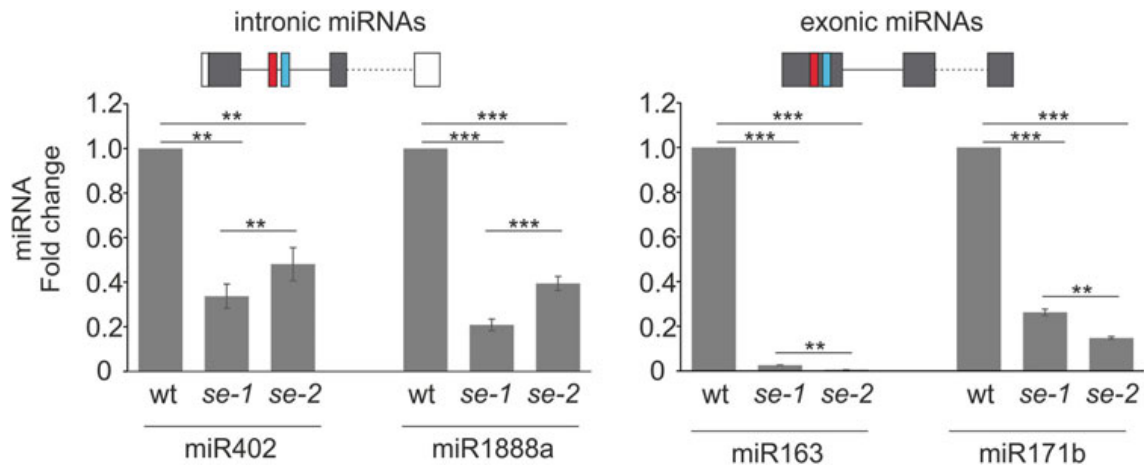


Fig. 2 The levels of intronic and exonic miRNAs in *Arabidopsis* wild-type (wt) plants and *SE* mutant lines (*se-1*, *se-2*) determined by TaqMan[®] Assay using U6 snRNA as a reference gene. Gray and white boxes in the miRNA genes represent exons and UTRs, respectively; line represents introns; red and blue boxes represent miRNA and miRNA*; p value—**<math>p < 0.01</math>, ***<math>p < 0.001</math>, [25]

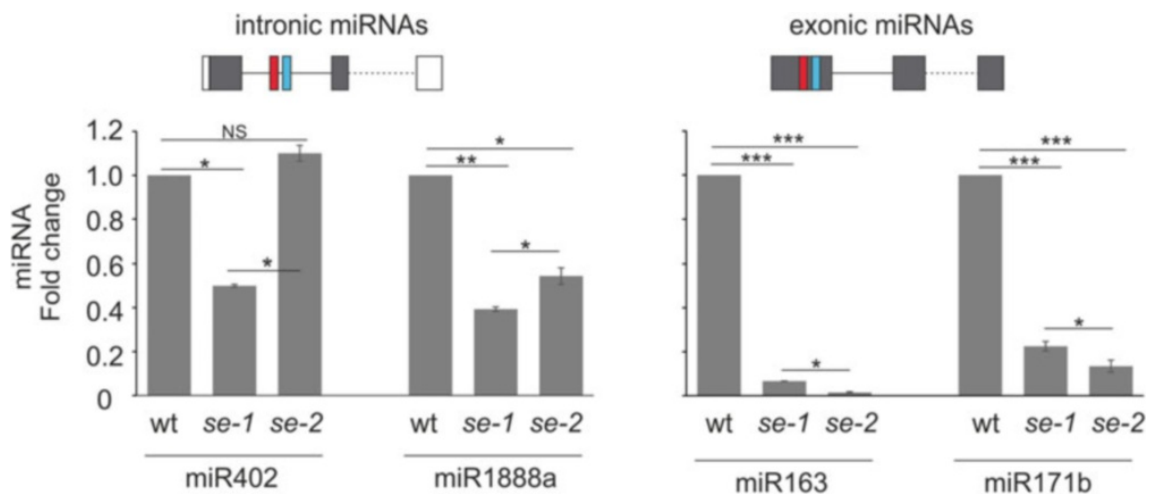


Fig. 3 The levels of intronic and exonic miRNAs in *Arabidopsis* wild-type (wt) plants and *SE* mutant lines (*se-1*, *se-2*) determined by TaqMan[®] Assay using *ACT8* as a reference gene. Gray and white boxes in the miRNA genes represent exons and UTRs, respectively; line represents introns; red and blue boxes represent miRNA and miRNA*; p value—* <math>p < 0.05</math>, **<math>p < 0.01</math>, ***<math>p < 0.001</math>

5. Perform the same analysis with the use of another reference gene, e.g., *ACT8*, and compare the results (Fig. 3).

Although the exact fold change values may be slightly different, the overall tendency and direction of changes are the same in the case of U6 snRNA and *ACT8* transcripts used as controls (Figs. 2 and 3).

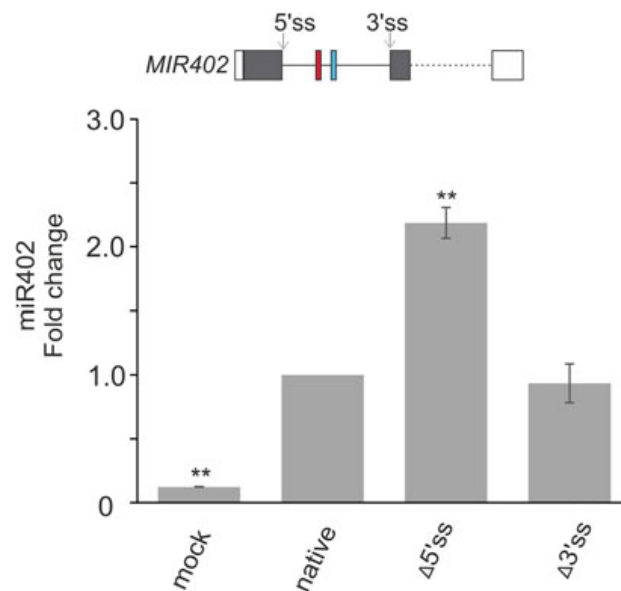


Fig. 4 The levels of intronic miR402 after splice site inactivation in transient expression assay in tobacco leaves determined by TaqMan[®] Assay. Gray and white boxes in the miRNA genes represent exons and UTRs, respectively; line represents introns; red and blue boxes represent miRNA and miRNA*, respectively; Δ5'ss and Δ3'ss indicate inactivation of 5' or 3' splice sites, respectively; *p* value—**<0.01, [25]

3.4.2 Analyze the miR402 Level After 5' or 3' Splice Site Inactivation (Fig. 4) in Transient Expression Assay in Tobacco Leaves

1. Subtract Ct values for hygromycin from Ct values obtained for miRNA (Δ Ct).
2. Subtract Δ Ct value for native construct from all samples ($\Delta\Delta$ Ct).
3. Use $2^{(-\Delta\Delta\text{Ct})}$ to calculate fold change.
4. Apply Student's *t*-test for statistical analyses. Use $2^{\Delta\text{Ct}}$ values for this purpose (see **Note 10**).

The level of miR402 is upregulated only after 5' splice site inactivation indicating a specific role of this splice site in regulation of intronic miR402 biogenesis (Fig. 4; [25]).

3.5 Droplet Digital[™] PCR (ddPCR[™])

TaqMan[®] probes can be used in miRNA detection not only with the use of classical qPCR machines but also with Droplet Digital PCR devices. The advantage of this approach is that the expression level of the particular gene as well as mature miRNA is counted based on the reactions occurring in 20,000 single droplets [26]. The final calculation data show absolute quantification of transcript level without necessity of the standard curve creation.

1. Thaw reagents on ice, invert them several times, and briefly mix. Samples for ddPCR analyses should be prepared in 1.5 mL tubes according to the following protocol:

Reagent	Volume for 22 μ L single reaction using EvaGreen for <i>PHO2</i> ² and <i>ARF1</i> ² quantification	Volume for 22 μ L single reaction using probes for miR399c ¹ and <i>ARF1</i> ² quantification
DNase-free water	6.56 μ L	7.90 μ L ¹ 5.90 μ L ²
2 \times ddPCR™ EvaGreen Supermix	11.00 μ L	–
2 \times ddPCR™ Supermix for Probes	–	11.00 μ L
20 \times TaqMan-specific probe	–	1.10 μ L
10 μ M Primer Forward	0.22 μ L	–
10 μ M Primer Reverse	0.22 μ L	–
cDNA template (<i>see Note 6</i>)	4.00 μ L ²	2.00 μ L ¹ 4.00 μ L ²
Total volume ^a	22.00 μ L	22.00 μ L

^aEach analyzed sample should be prepared in two technical repeats (prepare 2 \times 22 μ L reaction mixture). To a new 1.5 mL tube, add 40 μ L of Master Mix and 4.00 μ L of cDNA template (for miRNA cDNA). The Master Mix volume is increased to make sure that the final reaction volume is exactly 20 μ L

- Carefully apply 20 μ L of Master Mix/template to the center of one of the eight wells located in the middle part of ddPCR plastic DG8 cartridge placed in the holder (Fig. 5a, b) (*see Note 11*).
- Add 70 μ L of oil to the bottom well. After applying the sample and the oil, put a rubber cover on the cartridge (Fig. 5c).
- The entire 8-well plate must always be filled up. Even if you do not have enough samples, add the residue Master Mix or water to the remaining wells.
- Put the plate into a Droplet Generator Device, and wait few minutes to the end of the droplet generation (Fig. 5d).
- Transfer the 40 μ L of generated droplets to a new 96-well plate (provided in ddPCR™ Plate Kit) using 8-channel pipette (*see Note 11*) (Fig. 5e). Do it carefully, preferably by tilting the multichannel pipette and slowly releasing the contents on the walls of the plate wells.
- After application, cover the plate with plain transparent tape. The tape may help you to control the right order of loaded probes and to prevent evaporation.

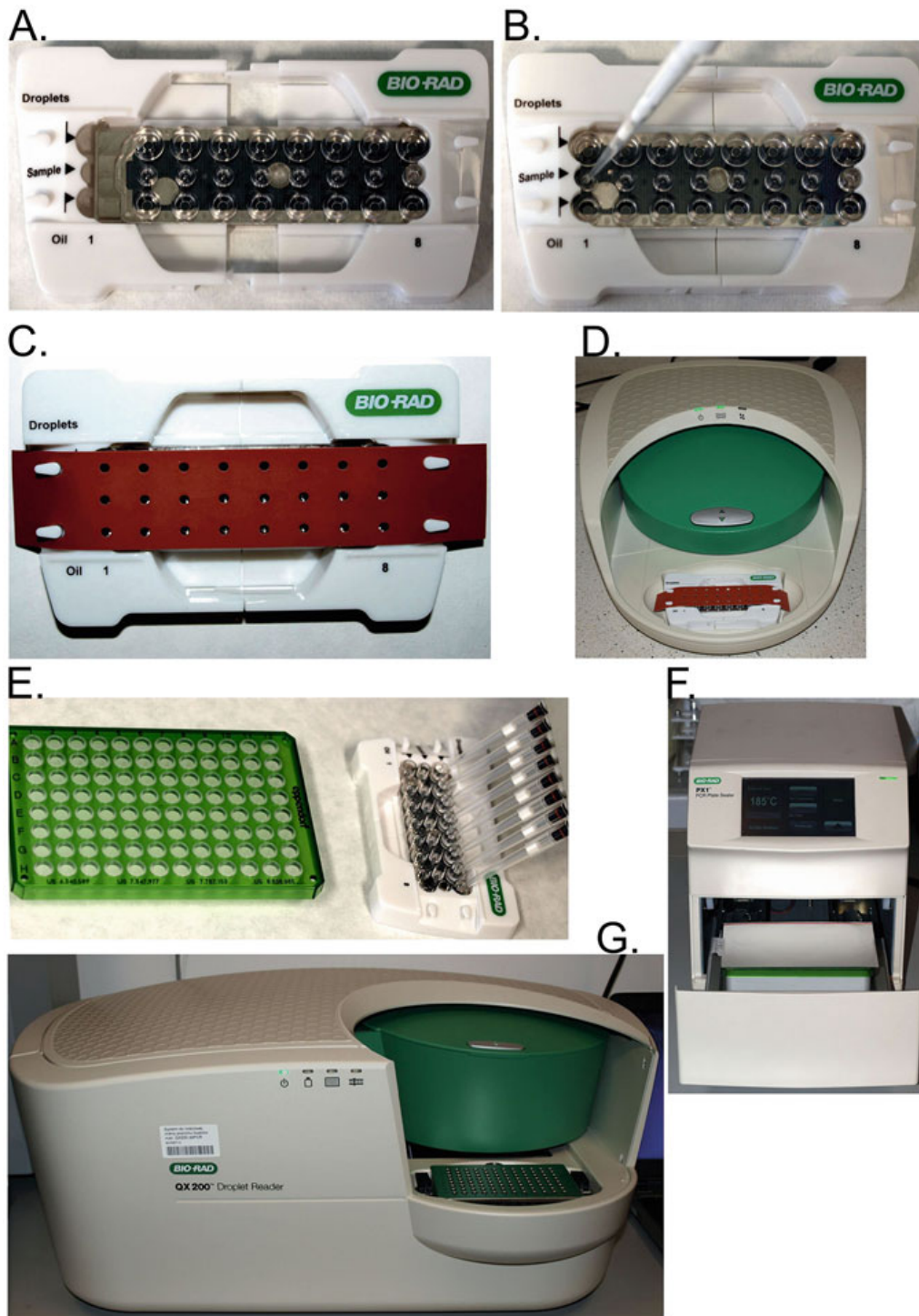


Fig. 5 Droplet generation. (a) DG8 cartridge containing 3 × 8 wells is placed in the holder. (b) 20 µL samples are loaded into central wells, and 70 µL of the appropriate oil (either for probes or for EvaGreen dye) is loaded to the bottom wells. (c) The rubber is placed on the cartridge. (d) The cartridge is placed into the QX8 Droplet Generator. (e) Droplets containing cDNA are transferred to the 96-well PCR plate. (f) Sealed using PX1 PCR plate sealer. (g) The fluorescence of PCR products is measured by QX200™ Droplet Reader

8. After transferring all samples, put foil on the 96-well plate located on the block of a sealing device (Fig. 5f).
9. Place the sealed plate into a thermocycler (used recommended Bio-Rad T100 Thermal Cycler), and run an appropriate program for TaqMan probes or EvaGreen.

PCR Program for EvaGreen Dye	
<i>Temperature (°C)</i>	<i>Time</i>
95	5 min
94	30 s
58	1 min
<i>Go to step 2 (×39)</i>	
4	5 min
90	5 min
4	∞

PCR Program for TaqMan Probe	
<i>Temperature (°C)</i>	<i>Time</i>
95	10 min
94	30 s
60	1 min
<i>Go to step 2 (×39)</i>	
98	10 min
4	∞

10. Following ddPCR reaction, apply the plate to a reading device, and use provided QuantaSoft™ program to design the plate and control the machine. Run the machine (Fig. 5g).

An example of ddPCR measurements of barley miR399 level is given below. During phosphate starvation, increased miR399 expression level is observed (Fig. 6a). MiR399 guides RISC (RNA-induced silencing complex) to *PHO2* mRNA (encoding ubiquitin-conjugating enzyme type E2) target for cleavage and leads to target transcript level downregulation in barley root and shoot (Fig. 6b).

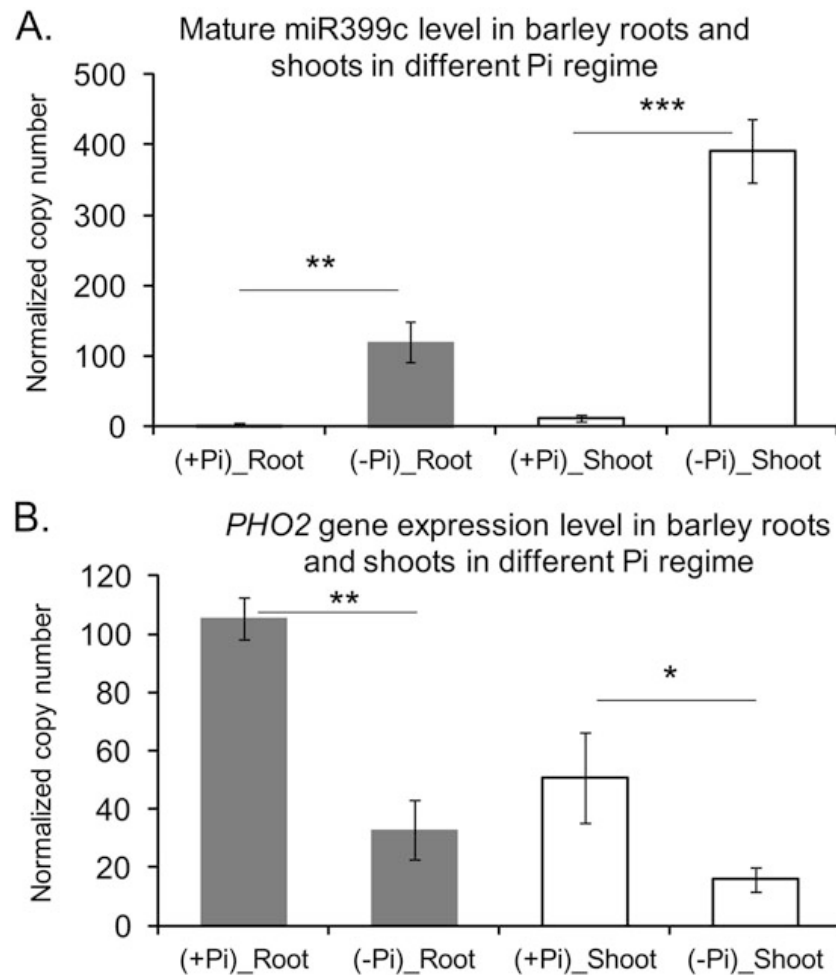


Fig. 6 ddPCR analysis using TaqMan[®] Assay. **(a)** RT stem-loop primer was used to perform reverse transcription of miR399c, and specific TaqMan[®] MicroRNA Assay was used in the ddPCR reaction. **(b)** *PHO2* gene expression level determination reaction was performed using ddPCR Supermix containing EvaGreen dye. A number of miR399c and *PHO2* copies were normalized to *ARF1* level (1000 copies). The *ARF1* copy number was calculated **(a)** using specific TaqMan[®] probe and **(b)** using specific primers and EvaGreen dye. (–Pi), low phosphate concentration; (+Pi), sufficient phosphate concentration; *p* value—* < 0.05, ** < 0.005, *** < 0.0005

4 Notes

1. TruSeq Small RNA Library Preparation Kits (Illumina), NEB-Next[®] Multiplex Small RNA Library Prep Kit for Illumina[®] (New England Biolabs), SMARTer smRNA-Seq Kit for Illumina (Clontech).
2. There is also another TaqMan[®] Advanced miRNA Assay (Applied Biosystems) in which to the 3' end of miRNA, poly (A) tail is added. Then after 5' adapter ligation reverse transcription reaction is performed using oligo(dT).

3. TaqMan unique probe is a short DNA sequence containing fluorescent dye (FAM, VIC) attached to the 5' end and nonfluorescent quencher (NFQ) together with minor groove binder (MGB) on 3' end of the probe.
4. The Direct-zol™ RNA MiniPrep is able to purify high-quality total RNA including small RNAs (17–200 nt).
5. Try to avoid multigene families or be aware of cross-hybridization between different miRNA family members. However, some probes are able to distinguish single substitutions. See the Thermo Fisher Scientific site for more information about your miRNA of interest (<http://www.thermofisher.com/pl/en/home/life-science/pcr/real-time-pcr/real-time-pcr-assays/mirna-ncrna-taqman-assays.html>). Moreover, when you search a specific TaqMan Assay using mature miRNA sequence, use uridine instead of thymidine.
6. ddPCR results are presented as number of cDNA/DNA copies per 1 μ L. Concentration calculation is performed based on the number of positive droplets and negative droplets, i.e., without cDNA/DNA signal. So, it is important to prevent saturation of the droplets with template. We recommend performing preliminary ddPCR reaction to evaluate whether the cDNA/DNA dilution fold allows for production of negative droplets. In the table we used (1) 2 μ L undiluted miRNA cDNA, which has been synthesized using stem-loop primer, for miR399 level analysis, and (2) 4 μ L 40 \times diluted cDNA for *PHO2* and *ARF1* analysis.
7. We highly recommend checking the DNA digestion efficiency by traditional PCR-based amplification using primers for 200–500 bp genomic fragment, i.e., promoter region. Set the reaction program to at least 40–45 cycles. If you notice any bands on the gel after electrophoresis, repeat the DNase I treatment as described in Subheading 3.1, step 16.
8. In the case of a larger number of samples, multiply the appropriate volumes by the number of samples “*n*” and the factor 1.1.
9. Use a proper reference gene for each assay, i.e. small/noncoding/coding RNA, in *Arabidopsis* tissue or internal gene encoded within the construct in transient expression assay in tobacco leaves. The samples for the reference gene should be prepared in parallel to the analyzed samples.
10. Data analysis. In the case of typical qPCR for miRNA expression level analysis, use relative quantification method $-\Delta\Delta Ct$. Digital PCR produces results as absolute quantification values; thus there are no ΔCt nor $\Delta\Delta Ct$ data.
11. Use accurate pipettes and low retention tips with filter. For 40 μ L droplets transferring from DG8 cartridge to 96-well PCR plate, use an 8-channel pipette.

Acknowledgment

The project is supported by the National Science Centre, Poland based on the decisions number DEC-2013/11/B/NZ9/01761, UMO-2015/19/N/NZ9/00218, 2013/10/A/NZ1/00557, UMO-2016/23/N/NZ1/00005, UMO-2016/21/B/NZ9/00550, UMO-2016/23/B/NZ9/00857 and UMO-2016/23/B/NZ9/00862, by the Foundation for Polish Science (grants START 2017 to Agata S. and Katarzyna K.), and by KNOW RNA Research Centre in Poznań (No. 01/KNOW2/2014).

References

1. Pacak A, Barciszewska-Pacak M, Swida-Barteczka A, Kruszka K, Sega P, Milanowska K, Jakobsen I, Jarmolowski A, Szweykowska-Kulinska Z (2016) Heat stress affects Pi-related genes expression and inorganic phosphate deposition/accumulation in barley. *Front Plant Sci* 7:926
2. Barciszewska-Pacak M, Milanowska K, Knop K, Bielewicz D, Nuc P, Plewka P, Pacak AM, Vazquez F, Karlowski W, Jarmolowski A, Szweykowska-Kulinska Z (2015) Arabidopsis microRNA expression regulation in a wide range of abiotic stress responses. *Front Plant Sci* 6:410
3. Kruszka K, Pacak A, Swida-Barteczka A, Nuc P, Alaba S, Wroblewska Z, Karlowski W, Jarmolowski A, Szweykowska-Kulinska Z (2014) Transcriptionally and post-transcriptionally regulated microRNAs in heat stress response in barley. *J Exp Bot* 65:6123–6135
4. Schommer C, Bresso EG, Spinelli SV, Palatnik JF (2012) Role of microRNA miR319 in plant development. In: *MicroRNAs in plant development and stress responses*. Springer, New York, pp 29–47
5. Palatnik JF, Allen E, Wu X, Schommer C, Schwab R, Carrington JC, Weigel D (2003) Control of leaf morphogenesis by microRNAs. *Nature* 425:257–263
6. Wang JW, Wang LJ, Mao YB, Cai WJ, Xue HW, Chen XY (2005) Control of root cap formation by MicroRNA-targeted auxin response factors in Arabidopsis. *Plant Cell* 17:2204–2216
7. Bari R, Datt Pant B, Stitt M, Scheible WR (2006) PHO2, microRNA399, and PHR1 define a phosphate-signaling pathway in plants. *Plant Physiol* 141:988–999
8. Pant BD, Buhtz A, Kehr J, Scheible WR (2008) MicroRNA399 is a long-distance signal for the regulation of plant phosphate homeostasis. *Plant J* 53:731–738
9. Xu F, Liu Q, Chen L, Kuang J, Walk T, Wang J, Liao H (2013) Genome-wide identification of soybean microRNAs and their targets reveals their organ-specificity and responses to phosphate starvation. *BMC Genomics* 14:66
10. Pall GS, Hamilton AJ (2008) Improved northern blot method for enhanced detection of small RNA. *Nat Protoc* 3:1077–1084
11. Wang X, Tong Y, Wang S (2010) Rapid and accurate detection of plant miRNAs by liquid northern hybridization. *Int J Mol Sci* 11:3138–3148
12. Várallyay É, Burgyán J, Havelda Z (2007) Detection of microRNAs by Northern blot analyses using LNA probes. *Methods* 43:140–145
13. Válczi A, Hornyik C, Varga N, Burgyán J, Kauppinen S, Havelda Z (2004) Sensitive and specific detection of microRNAs by northern blot analysis using LNA-modified oligonucleotide probes. *Nucleic Acids Res* 32:e175–e175
14. Yao X, Huang H, Xu L (2012) In situ detection of mature miRNAs in plants using LNA-modified DNA probes. *Methods Mol Biol* 883:143–154
15. Javelle M, Timmermans MC (2012) In situ localization of small RNAs in plants by using LNA probes. *Nat Protoc* 7:533–541
16. Niedojadło J, Deleńko K, Niedojadło K (2016) Regulation of poly (A) RNA retention in the nucleus as a survival strategy of plants during hypoxia. *RNA Biol* 13:531–543
17. Yang X, Li L (2012) Analyzing the microRNA transcriptome in plants using deep sequencing data. *Biology* 1:297–310
18. Gunaratne PH, Coarfa C, Soibam B, Tandon A (2012) miRNA data analysis: next-gen sequencing. *Methods Mol Biol* 822:273–288
19. Motameny S, Wolters S, Nürnberg P, Schumacher B (2010) Next generation sequencing of

- miRNAs—strategies, resources and methods. *Genes* 1:70–84
20. Shi R, Sun YH, Zhang XH, Chiang VL (2012) Poly(T) adaptor RT-PCR. *Methods Mol Biol* 822:53–66
 21. Prigge MJ, Wagner DR (2001) The *Arabidopsis serrate* gene encodes a zinc-finger protein required for normal shoot development. *Plant Cell* 13:1263–1279
 22. Grigg SP, Canales C, Hay A, Tsiantis M (2005) *SERRATE* coordinates shoot meristem function and leaf axial patterning in *Arabidopsis*. *Nature* 437:1022–1026
 23. Czechowski T, Stitt M, Altmann T, Udvardi MK, Scheible WR (2005) Genome-wide identification and testing of superior reference genes for transcript normalization in *Arabidopsis*. *Plant Physiol* 139:5–17
 24. Zielezinski A, Dolata J, Alaba S, Kruszka K, Pacak A, Swida-Barteczka A, Knop K, Stepień A, Bielewicz D, Pietrykowska H (2015) mirEX 2.0—an integrated environment for expression profiling of plant microRNAs. *BMC Plant Biol* 15:144
 25. Knop K, Stepień A, Barciszewska-Pacak M, Taube M, Bielewicz D, Michalak M, Borst JW, Jarmolowski A, Szweykowska-Kulinska Z (2017) Active 5′ splice sites regulate the biogenesis efficiency of *Arabidopsis* microRNAs derived from intron-containing genes. *Nucleic Acids Res* 45:2757–2775
 26. Hindson BJ, Ness KD, Masquelier DA, Belgrader P, Heredia NJ, Makarewicz AJ, Bright IJ, Lucero MY, Hiddessen AL, Legler TC, Kitano TK, Hodel MR, Petersen JF, Wyatt PW, Steenblock ER, Shah PH, Bousse LJ, Troup CB, Mellen JC, Wittmann DK, Erndt NG, Cauley TH, Koehler RT, So AP, Dube S, Rose KA, Montesclaros L, Wang S, Stumbo DP, Hodges SP, Romine S, Milanovich FP, White HE, Regan JF, Karlin-Neumann GA, Hindson CM, Saxonov S, Colston BW (2011) High-throughput droplet digital PCR system for absolute quantitation of DNA copy number. *Anal Chem* 83:8604–8610

Poznań, 28.09.2020

Mgr Paweł Segą
Uniwersytet im. Adama Mickiewicza w Poznaniu
Instytut Biologii Molekularnej i Biotechnologii
Zakład Ekspresji Genów
ul. Uniwersytetu Poznańskiego 6
61-614 Poznań
e-mail: pawel.sega@amu.edu.pl

Oświadczenie określające wkład w powstanie artykułu

Niniejszym oświadczam, że mój wkład w powstanie poniższego artykułu:

Aleksandra Smoczyńska, **Paweł Segą**, Agata Stępień, Katarzyna Knop, Artur Jarmołowski, Andrzej Pacak, Zofia Szweykowska-Kulińska. 2019. miRNA Detection by Stem-Loop RT-qPCR in Studying microRNA Biogenesis and microRNA Responsiveness to Abiotic Stresses. In: Stefan de Folter (ed.), Plant MicroRNAs: Methods and Protocols, Methods in Molecular Biology, vol. 1932

polegał na: napisaniu części metodycznej pracy (sekcje poświęcone materiałom i metodom), wykonaniu eksperymentów związanych z techniką kroplek digital PCR (ddPCR), korekcie manuskryptu po ocenach recenzentów


Paweł Segą

Poznań, 28.09.2020

Aleksandra Smoczyńska
Uniwersytet im. Adama Mickiewicza w Poznaniu
Instytut Biologii Molekularnej i Biotechnologii
Zakład Ekspresji Genów
ul. Uniwersytetu Poznańskiego 6
61-614 Poznań
e-mail: asmoczynska20@gmail.com

Oświadczenie określające wkład w powstanie artykułu

Niniejszym oświadczam, że mój wkład w powstanie poniższego artykułu:

Aleksandra Smoczyńska, Paweł Segal, Agata Stępień, Katarzyna Knop, Artur Jarmołowski, Andrzej Pacak, Zofia Szweykowska-Kulińska. 2019. miRNA Detection by Stem-Loop RT-qPCR in Studying microRNA Biogenesis and microRNA Responsiveness to Abiotic Stresses. In: Stefan de Folter (ed.), Plant MicroRNAs: Methods and Protocols, Methods in Molecular Biology, vol. 1932

polegał na: napisaniu wstępu teoretycznego do manuskryptu, korekcie manuskryptu w odpowiedzi na recenzje.


Aleksandra Smoczyńska

Poznań, 28.09.2020

Dr Agata Stępień
Uniwersytet im. Adama Mickiewicza w Poznaniu
Instytut Biologii Molekularnej i Biotechnologii
Zakład Biologii Molekularnej i Komórkowej
ul. Uniwersytetu Poznańskiego 6
61-614 Poznań
e-mail: stepiena@amu.edu.pl

Oświadczenie określające wkład w powstanie artykułu

Niniejszym oświadczam, że mój wkład w powstanie poniższego artykułu:

Aleksandra Smoczyńska, Paweł Segal, **Agata Stępień**, Katarzyna Knop, Artur Jarmołowski, Andrzej Pacak, Zofia Szweykowska-Kulińska. 2019. miRNA Detection by Stem-Loop RT-qPCR in Studying microRNA Biogenesis and microRNA Responsiveness to Abiotic Stresses. In: Stefan de Folter (ed.), Plant MicroRNAs: Methods and Protocols, Methods in Molecular Biology, vol. 1932

polegał na:

- zaplanowaniu i przeprowadzeniu analizy poziomu miRNA i genów referencyjnych u *A. thaliana* oraz w tytoniu
- współtworzeniu opisu potrzebnych materiałów i metody przeprowadzenia powyższych eksperymentów oraz analizy uzyskanych wyników
- nanoszeniu poprawek w pozostałych częściach manuskryptu



Agata Stępień

Dundee, 28.09.2020

Dr Katarzyna Knop

Division of Plant Sciences
Centre for Gene Regulation & Expression
School of Life Sciences
University of Dundee
Dow Street, Dundee, Scotland
E-mail: k.knop@dundee.ac.uk

Oświadczenie określające wkład w powstanie artykułu

Niniejszym oświadczam, że mój wkład w powstanie poniższego artykułu:

Aleksandra Smoczyńska, Paweł Segal, Agata Stępień, **Katarzyna Knop**,
Artur Jarmołowski, Andrzej Pacak, Zofia Szweykowska-Kulińska. 2019.
miRNA Detection by Stem-Loop RT-qPCR in Studying microRNA Biogenesis
and microRNA Responsiveness to Abiotic Stresses. In: Stefan de Folter
(ed.), Plant MicroRNAs: Methods and Protocols, Methods in Molecular
Biology, vol. 1932

polegał na: *korekcie manuskryptu w odpowiedzi na recenzje.*

Katarzyna Knop

Poznań, 03.03.2021

Prof. dr hab. Artur Jarmołowski
Uniwersytet im. Adama Mickiewicza w Poznaniu
Instytut Biologii Molekularnej i Biotechnologii
Zakład Ekspresji Genów
ul. Uniwersytetu Poznańskiego 6
61-614 Poznań
e-mail: artur.jarmolowski@amu.edu.pl

Oświadczenie określające wkład w powstanie artykułu

Niniejszym oświadczam, że mój wkład w powstanie poniższego artykułu:

Aleksandra Smoczyńska, Paweł Segal, Agata Stępień, Katarzyna Knop, **Artur Jarmołowski**, Andrzej Pacak, Zofia Szweykowska-Kulińska. 2019. miRNA Detection by Stem-Loop RT-qPCR in Studying microRNA Biogenesis and microRNA Responsiveness to Abiotic Stresses. In: Stefan de Folter (ed.), Plant MicroRNAs: Methods and Protocols, Methods in Molecular Biology, vol. 1932

polegał na: recenzji manuskryptu


Artur Jarmołowski

Poznań, 28.09.2020

Dr hab. Andrzej Pacak, Prof. UAM
Uniwersytet im. Adama Mickiewicza w Poznaniu
Instytut Biologii Molekularnej i Biotechnologii
Zakład Ekspresji Genów
ul. Uniwersytetu Poznańskiego 6
61-614 Poznań
e-mail: apacak@amu.edu.pl

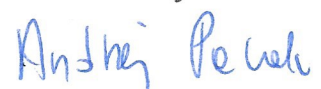
Oświadczenie określające wkład w powstanie artykułu

Niniejszym oświadczam, że mój wkład w powstanie poniższego artykułu:

Aleksandra Smoczyńska, Paweł Segą, Agata Stępień, Katarzyna Knop, Artur Jarmołowski, **Andrzej Pacak**, Zofia Szweykowska-Kulińska. 2019. miRNA Detection by Stem-Loop RT-qPCR in Studying microRNA Biogenesis and microRNA Responsiveness to Abiotic Stresses. In: Stefan de Folter (ed.), Plant MicroRNAs: Methods and Protocols, Methods in Molecular Biology, vol. 1932

polegał na: wykonaniu wspólnie z mgr Pawłem Segą reakcji ddPCR, których wyniki zostały zamieszczone w pracy, udziale w pisaniu manuskryptu w sekcji Methods oraz Notes, korekcie manuskryptu po otrzymaniu odpowiedzi od recenzentów.

Andrzej Pacak



Poznań, 03.03.2021

Prof. dr hab. Zofia Szweykowska-Kulińska
Uniwersytet im. Adama Mickiewicza w Poznaniu
Instytut Biologii Molekularnej i Biotechnologii
Zakład Ekspresji Genów
ul. Uniwersytetu Poznańskiego 6
61-614 Poznań
e-mail: zofia.szweykowska-kulinska@amu.edu.pl

Oświadczenie określające wkład w powstanie artykułu

Niniejszym oświadczam, że mój wkład w powstanie poniższego artykułu:

Aleksandra Smoczyńska, Paweł Segal, Agata Stępień, Katarzyna Knop, Artur Jarmołowski, Andrzej Pacak, **Zofia Szweykowska-Kulińska**. 2019. miRNA Detection by Stem-Loop RT-qPCR in Studying microRNA Biogenesis and microRNA Responsiveness to Abiotic Stresses. In: Stefan de Folter (ed.), Plant MicroRNAs: Methods and Protocols, Methods in Molecular Biology, vol. 1932

polegał na: stworzeniu koncepcji pracy oraz korekty manuskryptu

Zofia Szweykowska-Kulińska



Identification of transcription factors that bind to the 5'-UTR of the barley *PHO2* gene

Paweł Segal¹ · Katarzyna Kruszkas¹ · Łukasz Szewc¹ · Zofia Szweykowska-Kulińska¹ · Andrzej Pacak¹

Received: 2 September 2019 / Accepted: 9 November 2019 / Published online: 19 November 2019
© Springer Nature B.V. 2019

Abstract

In barley and other higher plants, phosphate homeostasis is maintained by a regulatory network involving the *PHO2* (*PHOSPHATE 2*) encoding ubiquitin-conjugating (UBC) E2 enzyme, the PHR1 (*PHOSPHATE STARVATION RESPONSE 1*) transcription factor (TF), *IPSI* (*INDUCED BY PHOSPHATE STARVATION 1*) RNA, and miR399. During phosphate ion (Pi) deprivation, PHR1 positively regulates *MIR399* expression, after transcription and processing mature miR399 guides the Ago protein to the 5'-UTR of *PHO2* transcripts. Non-coding *IPSI* RNA is highly expressed during Pi starvation, and the sequestration of miR399 molecules protects *PHO2* mRNA from complete degradation. Here, we reveal new *cis*- and *trans*-regulatory elements that are crucial for efficient *PHO2* gene expression in barley. We found that the 5'-UTR of *PHO2* contains two PHR1 binding sites (P1BSs) and one Pi-responsive PHO element. Using a yeast one-hybrid (Y1H) assay, we identified two candidate proteins that might mediate this transcriptional regulation: a barley PHR1 ortholog and a TF containing an uncharacterized MYB domain. Additional results classified this new potential TF as belonging to the APL (*ALTERED PHLOEM DEVELOPMENT*) protein family, and we observed its nuclear localization in barley protoplasts. Pi starvation induced the accumulation of barley *APL* transcripts in both the shoots and roots. Interestingly, the deletion of the P1BS motif from the first intron of the barley 5'-UTR led to a significant increase in the transcription of a downstream β -glucuronidase (*GUS*) reporter gene in tobacco leaves. Our work extends the current knowledge about putative *cis*- and *trans*-regulatory elements that may affect the expression of the barley *PHO2* gene.

Key Message

The 5'-UTR of the barley *PHOSPHATE 2* gene contains two P1BS motifs that can bind the transcription factor (TF) PHR1 (*PHOSPHATE STARVATION RESPONSE 1*) and the newly identified TF APL (*ALTERED PHLOEM DEVELOPMENT*)

Keywords Barley · *PHO2* · PHR1 · P1BS · MYB-domain transcription factors · Phosphate regulatory network

Accession Numbers Sequence data from this article can be found in the GenBank/EMBL data libraries (AtNSR1 (AAF05867), MYB-1 (AK373855), MYB-2/APL (AK371403), MAD57 (AK363243)) and the Ensembl Plants database for the barley genome (PHR1 (HORVU4Hr1G051080.5), PHR2 (HORVU4Hr1G051080.1), MYB-2/APL (HORVU6Hr1G031470), *PHO2* (HORVU1Hr1G085570.2)).

Electronic supplementary material The online version of this article (<https://doi.org/10.1007/s11103-019-00932-9>) contains supplementary material, which is available to authorized users.

✉ Andrzej Pacak
apacak@amu.edu.pl

¹ Department of Gene Expression, Institute of Molecular Biology and Biotechnology, Faculty of Biology, Adam Mickiewicz University, Poznań, Uniwersytetu Poznańskiego 6, 61-614 Poznań, Poland

Introduction

Phosphorus (P), which is available to plants in the form of the phosphate ion (Pi), is among the macronutrients that are essential for all living organisms. Throughout evolution, plants have developed a series of strategies that enable them to cope with Pi deficiency in the soil; mechanisms that contribute to Pi deficiency tolerance include alterations in root and shoot architecture, the induction of secondary metabolite biosynthesis, changes in phytohormone activities and responsiveness, and the promotion of symbioses with bacteria and arbuscular mycorrhizal (AM) fungi (Abel et al. 2002; Yang and Finnegan 2010). Pi is highly immobile in most soil types because these ions react with many chemical soil constituents, such as iron and aluminum oxides (Lynch

2011). For more than 30% of the arable land worldwide, as a consequence of reduced Pi availability, the uptake of Pi in the form of inorganic phosphate by the root system from the soil matrix is a limiting factor for plant growth and crop yields (Vance et al. 2003). Global Pi reserves are not renewable, and Pi is being exhausted rapidly. Total Pi reserves are predicted to last for 50–350 years, depending on fertilizer production (Heffer and Prud'homme 2013).

PHO2 (*PHOSPHATE 2*) is one of the most important genes in the control of Pi levels in plants. This gene encodes a ubiquitin-conjugating (UBC) E2 enzyme that negatively regulates the level of Pi transporter proteins, such as members of the PHT1 (*PHOSPHATE TRANSPORTER 1*) protein family, PHO1 (*PHOSPHATE 1*), and PHF1 (*PHOSPHATE TRANSPORTER TRAFFIC FACILITATOR 1*) (Liu et al. 2012; Park et al. 2014; Pacak et al. 2016). Therefore, PHO2 proteins modulate the acquisition and root-to-shoot translocation of Pi, and they protect plants from excess Pi accumulation in the shoots (Bari et al. 2006; Briat et al. 2015). The Arabidopsis *pho2* loss-of-function mutant hyperaccumulates Pi in the shoots and displays signs of Pi toxicity, such as rapid leaf senescence and reduced plant growth (Delhaize and Randall 1995). Most knowledge of the regulation of *PHO2* gene expression surrounds its post-transcriptional regulation via miR399. During Pi starvation, the *MIR399* expression level increases, which is accompanied by the downregulation of *PHO2* expression (Bari et al. 2006; Smoczynska et al. 2019). The complete feedback loop of *PHO2* and miR399 is controlled by the non-coding RNA molecule *IPS1* (*INDUCED BY PHOSPHATE STARVATION 1*), which is highly expressed in plants during Pi scarcity (Huang et al. 2011). *IPS1* RNA acts as a sponge and sequesters miR399 molecules when the *PHO2* expression level is fine-tuned. MiR399 molecules are processed from precursor transcripts (pre-miR399) that are transcribed from ten genomic loci in barley (Hackenberg et al. 2013) in a step-wise process that involves the proteins DCL1 (*DICER-Like 1*) and DRB1 (*DOUBLE-STRANDED DNA-BINDING 1*) (Hiraguri et al. 2005; Kurihara et al. 2006). Recent studies on Arabidopsis have shown that DRB protein family members, such as DRB1, DRB2, and DRB4, are involved in the production of miR399. Compared with wild-type plants, the Arabidopsis *drb1* loss-of-function mutant exhibits a weaker ability to produce anthocyanin in response to low-Pi stress, which leads to impaired maintenance of Pi homeostasis (Pegler et al. 2019). These results suggest a mechanistic picture of the post-transcriptional regulation of phosphate starvation-induced (PSI) genes and the miRNA-mediated ability of plants to overcome stress.

As mentioned above, *PHO2* gene expression is tightly controlled at the post-transcriptional level; however, little is known about the transcriptional regulation of *PHO2* gene expression. The majority of Pi-related genes have unique

DNA promoters with motifs called P1BSs (PHR1 binding sites with GnATATnC consensus sequences) that PHR1 and PHR1-like transcription factors (TFs) can bind (Rubio et al. 2001; Sobkowiak et al. 2012). Sequence analysis of rice *PHO2* isoforms revealed variation in the length of the 5'-UTR in *PHO2* transcripts that were expressed under different Pi regimes. Moreover, the presence of the P1BS motif in the second exon of the 5'-UTR was observed only in transcripts that were preferentially expressed under Pi-limited conditions (Secco et al. 2013).

In the signaling network responsible for sensing Pi availability, PHR1 (*PHOSPHATE STARVATION RESPONSE 1*)—a MYB-coiled-coil (CC)-type TF—plays a central role as a widespread leading integrator that increases the expression of many Pi-responsive genes in plants (Rubio et al. 2001; Chiou and Lin 2011; Wang et al. 2013). Most known PHR-like TFs in plants are highly similar to the PSR1 (*PHOSPHORUS STARVATION RESPONSE 1*) protein from *Chlamydomonas reinhardtii* (Wykoff et al. 1999). Knockout mutants that lack PHR1 TFs display many morphological and molecular changes, such as altered root architecture (Bustos et al. 2010), the lack of miR399 induction during Pi starvation (Khan et al. 2014), and dysregulated expression of many PSI genes, including the non-coding RNAs *AT4* (*INDUCED BY Pi STARVATION 2*) and *IPS1* (Bustos et al. 2010; Khan et al. 2014). The subcellular localization of OsPHR2 (*PHOSPHATE STARVATION RESPONSE 2*, a rice ortholog of AtPHR1) is altered because of interactions with SPX4 (*SPX DOMAIN-CONTAINING PROTEIN 4*) in response to different Pi statuses (Lv et al. 2014). Pi starvation promotes SPX4 degradation via the 26S proteasome, and OsPHR2 TFs can freely translocate from the cytosol to the nucleus to bind to the promoters of downstream PSI genes (Hu et al. 2019).

P1BS motifs have been discovered within the promoters of many crucial Pi-responsive genes, e.g., *PHT1;1* (*PHOSPHATE TRANSPORTER 1;1*) in barley (Schünmann et al. 2004a), *SPX1* (*SPX DOMAIN-CONTAINING PROTEIN 1*) in soybean (Li et al. 2015), and *IPS1* (Martín et al. 2000) and *RNS1* (*RIBONUCLEASE 1*) in Arabidopsis (Bariola et al. 1994). These genes differ in the number of P1BS motifs within their regulatory regions: the promoter of barley *PHT1;1* contains three motifs (Li et al. 2015), while two P1BS motifs are located in the promoters of the *IPS1* (Rubio et al. 2001) and *MIR399* genes in Arabidopsis (Kuo and Chiou 2011). In silico analysis revealed that P1BSs might also be present within the 5'-UTRs of genes. Many crucial genes involved in maintaining Pi homeostasis have been shown to have a 5'-UTR-localized P1BS motif (Bustos et al. 2010). Moreover, recent studies have described an important role for P1BS motif-containing 5'-UTR introns, which mediate the enhancement of *AtPHT1;4* gene expression (Karthikeyan et al. 2009). In general, the presence of the

P1BS motif within a promoter is responsible for the upregulation of gene expression.

PHR-like TFs have different binding affinities for P1BS motif variants (Ruan et al. 2015). In rice, high genetic redundancy was observed among the three PHR1 orthologous proteins in rice: OsPHR1, OsPHR2, and OsPHR3. These three rice PHR-like TFs form a network and function as activators of many Pi-related genes to regulate Pi homeostasis (Guo et al. 2015). In Arabidopsis, the PHL2 (PHR-like 2) protein was shown to act redundantly with PHR1 (Sun et al. 2016). Redundancy probably involves additional proteins of the MYB-CC family because mutations in both PHR1 and PHL1 do not fully abolish Pi starvation responses (Bustos et al. 2010). These data suggest that the molecular network that regulates the plant transcriptional response to Pi stress conditions is more complex than previously thought. It is very likely that similar homologous genes are involved in this pathway but remain uncharacterized in other crop species, including barley.

To obtain more information on the regulation of Pi homeostasis in barley, we decided to identify motifs and TFs involved in the regulation of barley *PHO2* gene transcription. To identify TFs or other *trans*-acting proteins that can bind to promoters and 5'-UTRs, we used the yeast one-hybrid (Y1H) system approach. Our analysis revealed that only sequences within the 5'-UTR could bind proteins, while those within the promoter could not. In the *PHO2* 5'-UTR, we discovered two P1BS motifs. In addition to the two P1BS motifs responsible for TF binding, the barley *PHO2* 5'-UTR contains six miR399 binding sites (Hackenberg et al. 2013; Pacak et al. 2016). The P1BS motifs are located within the 5'-UTR first intron (P1BS.1) and the second exon (P1BS.2), in which all six miR399 binding sites are found. This finding indicates that the barley *PHO2* 5'-UTR is important for the transcriptional and post-transcriptional control of *PHO2* expression levels. Here, we present a comprehensive data set that provides insight into the role of the barley *PHO2* 5'-UTR in the transcriptional regulation of this gene. Our study reveals, for the first time, the binding of Pi-related TFs to *PHO2* 5'-UTR fragments and identifies a new potential regulator of Pi homeostasis in plants.

Results

Analyses of the *PHO2* promoter and 5'-UTR and the identification of *cis*-regulatory elements

The barley *PHO2* gene has a unique structure: it contains a long 5'-UTR with cleavage sites for Pi-starvation-responsive miR399, and its structure and length are similar to those of the *PHO2* orthologs in both Arabidopsis (Kim et al. 2011) and rice (Secco et al. 2013) (Figs. S1 and S2). Just

a few examples of 5'-UTR mRNAs recognized by microRNAs have been described, including those involving barley *PHO2*, Arabidopsis *NLA* (*NITROGEN LIMITATION ADAPTATION*) (Kant et al. 2011), and rice *SPX-MFS* (*Major Facilitator Superfamily*) (Wang et al. 2012). We previously described two transcription start sites (TSSs) in the barley *PHO2* gene (Pacak et al. 2016). In silico analysis of the predicted *PHO2* proximal promoter region (TSS No. 1, total promoter length 5198 bp) using the PlantPAN 3.0 database (<http://plantpan.itps.ncku.edu.tw/>) (Chow et al. 2016) revealed the presence of many putative *cis*-regulating elements that may activate gene expression in response to various plant stresses or hormone induction (Table 1). In addition, no common consensus motifs that initiate transcription, such as the TATA-box or CAAT-box, are present 300 bp upstream of *PHO2* TSS No. 1. This situation is not unusual because the TATA-box is present in the minority of plant genes (Morton et al. 2014). In the *PHO2* promoter region, we identified a consensus sequence (CAATTAATAG, Table 1) involved in homeodomain leucine-zipper (HD-ZIP) protein binding (from –1296 to –1286 bp upstream of TSS No. 1). This motif has been identified within the soybean gene *VspB* (*VEGETATIVE STORAGE PROTEIN B*), and HD-ZIP TF binding was shown to downregulate target gene expression in response to P addition (Tang et al. 2001; Vance et al. 2003). Microarray analysis of the *PHO2* gene promoter also revealed the presence of a PHO-like element that preferentially exists in the promoter regions of Pi-responsive genes in Arabidopsis (Hammond et al. 2003). Other identified motifs are known to be involved in the regulation of photosynthesis or phytochrome gene expression (or both) in plants, such as the S1FBOXSORPSIL21 element, which was found within the promoter regions of *HvPT1;2*, *HvPHT1;4*, *HvPHT1;6*, and *HvPHT1;7*, as well as the PEHVPSBD element (Lagrange et al. 1993; Schünmann et al. 2004b). In addition, we found a dehydration-responsive element recognized by the DREB1A protein (Miura et al. 2007; Nakashima et al. 2014) and a CIACADIANLELHC element associated with circadian clock expression present in the promoter of the barley *PHT1* gene (Schünmann et al. 2004a).

An in-depth analysis of the barley *PHO2* 5'-UTR was also performed. A major reason to study the 5'-UTR of the barley *PHO2* gene is its length (2742 bp), which mostly encompasses 1602 bp of the first intron (Figs. 1a, S2). Previous studies in Arabidopsis have shown that the first intron of the 5'-UTR contains P1BS elements and is essential for *AtPHT1;4* expression in root tips in response to Pi scarcity (Karthikeyan et al. 2009). The Arabidopsis *PHO2* ortholog, which possesses two P1BS motifs within its 5'-UTR (Fig. S3), was used in this study as a reference. Additionally, the second exon of the barley *PHO2* 5'-UTR has a unique feature in that there are six potential cleavage sites for miR399 (Fig. S2). Our degradome data confirmed that during Pi

Table 1 The presence of putative *cis*-regulatory elements within the barley *PHO2* gene promoter and 5'-UTR

Y1H frag- ment	Motif	Recognized by	Position from TSS No. 1	References
pPHO2_1	PHO-like element, G(G/T/A) (C/T/A)GTGG	Pi-related motif, present in PHT1 family proteins	– 1362, – 1355	Muller et al. (2007); Schünmann et al. (2004a)
pPHO2_1	CArG, C(A/T)TTAAAAAG	MADS57	– 1352, – 1342	Guo et al. (2013)
pPHO2_1	CAATTAATAG ^a	HD-ZIP protein	– 1296, – 1286	Vance et al. (2003)
pPHO2_2	S1FBOXSORPSIL21, ATGGTA ^a	Photosynthesis and/or phy- tochrome regulation	– 1019, – 1013	Lagrange et al. (1993)
pPHO2_2	CRT/DRE motif, GCCGAC ^a	DREB1	– 910, – 904	Miura et al. (2007)
pPHO2_3	PEHVPSBD, TATTCT ^a	Photosynthesis and/or phy- tochrome regulation	– 674, – 668	Thum et al. (2001)
pPHO2_3	CIACADIANLELHC, CAATCA GACT ^a	Associated with circadian expres- sion	– 619, – 609	Piechulla et al. (1998)
pPHO2_4	GnATATnC, P1BS	PHR1, PHR1-like TFs, APL	+ 627, + 634 (1st intron)	Rubio et al. (2001)
pPHO2_5			+ 1974, + 1981 (2nd exon)	
pPHO2_4	P-responsive palindromic PHO- element, ATGCCAT ^a	PHR1, APL	+ 641, + 647 (1st intron)	Mukatira et al. (2001)

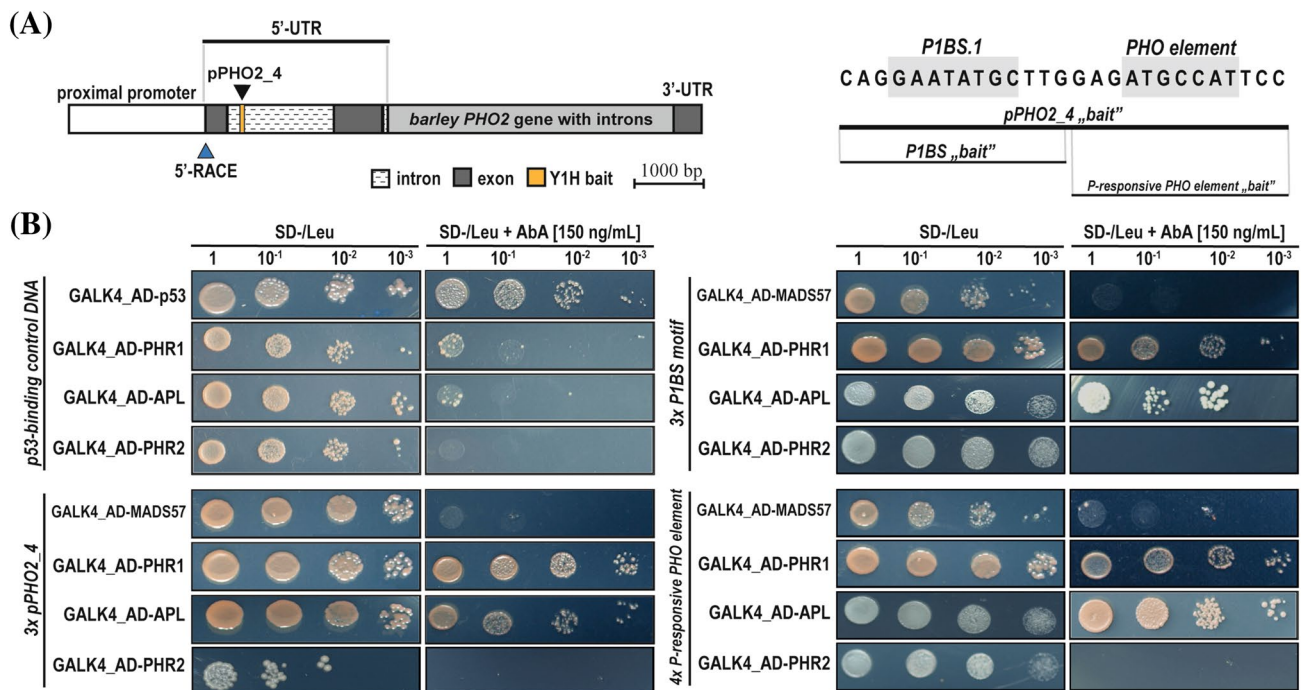
^aConsensus is identical

Fig. 1 The barley TFs PHR1 and APL interact with the first-intron “bait” fragments originating from the *PHO2* 5'-UTR in yeast cells. The structure of the barley *PHO2* gene with a marked Y1H “bait” fragment. The pPHO2_4 fragment is 27 bp in length and includes two *cis*-regulatory motifs: P1BS.1 and P-responsive PHO element, which are separated by only six nucleotides. The blue triangle indicates positions 447916090 (+) and 447916332 (+) on barley chromosome 1; the two TSSs of the *PHO2* transcripts were identified using 5'-RNA ligase-mediated rapid amplification of cDNA ends (5'RLM-RACE) and described in our previous paper (Pacak et al. 2016) (a). Images of the growing colonies of the tested Y1HGold yeast strains (TaKaRa) having “bait” fragments from the 5'-UTR first intron that

were stably introduced into the yeast genome in the form of triple tandem repeats: 3xpPHO2_4, which contains two motifs, as well as two strains having each motif separately, 3xP1BS and 4xP-responsive PHO-element. The experimental workflow was controlled using the Y1HGold-p53 yeast strain (consisting of three tandem copies of the p53 consensus binding sequence). Aureobasidin A (AbA) resistance was induced by the binding of a GAL4 activation domain (GAL4_AD) fusion protein “prey” (such as p53, MADS57, PHR1, PHR2, or APL) to the “bait” sequences. The minimal inhibitory concentration of AbA was experimentally determined to be 150 ng/mL. The barley MADS57 TF was used as a non-binding negative control (b)

starvation in barley shoots, the 5'-UTR of *PHO2* is indeed targeted and cleaved by the RNA-induced silencing complex (RISC) guided by miR399. The degradome has already shown the important role that the 5'-UTR plays in the post-transcriptional regulation of *PHO2* gene expression (Fig. S4). In silico analysis revealed (Table 1) the presence of two Pi-related motifs that are close to each other and within just 21 bp of the first intron of the *PHO2* 5'-UTR: the well-known P1BS (Rubio et al. 2001) and another motif called the P-responsive PHO element (Hammond et al. 2003). Furthermore, another P1BS element was found in the second exon (P1BS.2), making this 5'-UTR gene body even more puzzling. In this case, an equal P1BS consensus is present in the barley *RNS1* 5'-UTR and *PHT1;1* promoter region (Fig. S3). On the basis of the results of the in silico DNA motif analysis, we selected five DNA fragments for Y1H screening (Table 1).

Y1H screening of *PHO2* “bait” fragments

Whole-barley cDNA library screening was performed to identify proteins that could potentially interact with the *PHO2* proximal promoter. In this screening, none of the three tested fragments (pPHO2_1, pPHO2_2, and pPHO2_3; Table 1, Table S5) yielded any confirmed bait–prey interactions (Table S1). In the next step, we verified the hypothesis that the *PHO2* 5'-UTR might be recognized and bound by *trans*-regulatory elements. We used a Y1H system to screen two fragments: 81 bp comprising 3×27 bp of pPHO2_4 and 81 bp comprising 3×27 bp of pPHO2_5. For P1BS-containing fragments from the 5'-UTR, we utilized two strategies for Y1H screening: (i) screening the whole-barley cDNA library and (ii) directly testing pAD vectors that contain full-length coding sequences (CDSs) of potentially interacting TF candidates. These TFs were selected on the basis of the results published by Todd and his group in 2004. They used the *Psr1* sequence from *Chlamydomonas reinhardtii* as a query for the successful identification of homologs in Arabidopsis. Similarly, we used the amino acid (aa) sequence from Arabidopsis locus At3g04030 (Todd et al. 2004) (namely, *AtNSR1—NITROGEN STARVATION RESPONSE 1*) as a query to identify homologs in barley. Searching this sequence in the NCBI database, we discovered two uncharacterized barley TFs that had the highest homology: MYB-1 (Acc. No. AK373855) and MYB-2 (Acc. No. AK371403) (Fig. S5). As a result of our first strategy used in the Y1H screening, we retrieved a few polypeptides for both 5'-UTR “bait” fragments from the cDNA library, which were mapped to the barley PHR1 protein in the Ensembl Plants database. In our second strategy, we amplified the barley full-length *PHR1* coding sequence and cloned it directly into a yeast “prey” AD vector to confirm the in vivo interaction of DNA fragments with the whole PHR1 protein. We

also cloned the predicted barley *PHR2* gene (Pacak et al. 2016), as well as MYB-1 and MYB-2 candidates, into the AD vector. Our screening uncovered a novel MYB-like TF (MYB-2) that interacted directly with both fragments originating from the barley *PHO2* 5'-UTR. After examination of the protein sequence homologies, we named the MYB-like protein APL TF (ALTERED PHLOEM DEVELOPMENT). Then, the same interactions were continuously detected in synthetic leucine-dropout medium (SD/-Leu) plates supplemented with 150 ng/mL aureobasidin A (AbA) and in plated yeast with up to a 1/1000 dilution (Fig. 1b). We detected similar results for the barley PHR1 TF captured from the whole cDNA library. However, we did not detect an interaction between the 5'-UTR-derived fragments and other tested TFs, namely, the barley PHR2 TF and barley MADS57 (MADS-BOX TRANSCRIPTION FACTOR 57), which was used as a presumably non-interacting control (Fig. 1b). Positive interactions of PHR1 and APL TFs with P1BS.2 from the second exon of the barley *PHO2* 5'-UTR were also confirmed (Fig. S6).

Previous studies indicated that 5'-UTR elements, especially introns, can enhance downstream gene expression in rice (Lu et al. 2008) and petunia (Liao et al. 2013). The barley *PHO2* gene body has nine introns, two of which are present in the 5'-UTR. To study the effects of each intron from the *PHO2* transcriptional unit, we used the online tool IMEter v.2.1 to calculate the intron-mediated enhancement (IME) scores for all nine *PHO2* full-length intron sequences (Parra et al. 2011). IMEter scores represent the degree to which the oligomer composition of an individual sequence resembles that of all promoter-proximal introns (Rose et al. 2011). The IME score suggests that the first intron is crucial for *PHO2* gene expression, with 98% significance (Fig. S7). The following five of eight *PHO2* introns (from the second intron to the sixth intron) had IME scores lower than 31% (Fig. S7). In addition, we calculated IME scores using the same approach for seven consecutive ~200 bp fragments, all of which originated from the chopped first intron (5'-UTR). We clearly observed that the analyzed fragments originating from the 3' portion of the intron resulted in relatively weak IME scores: this result suggests that they are potentially less important for *PHO2* gene expression than fragments originating elsewhere. The highest scores we observed for the first four fragments (with a total length of 800 bp) were mostly above 85% (Fig. S7).

Barley PHR1 and APL TFs interact with the *PHO2* 5'-UTR in vitro

To confirm the ability of the recombinant proteins MBP-PHR1 (Maltose Binding Protein) and MBP-APL to bind to the *PHO2* 5'-UTR, we performed an electrophoretic mobility shift assay (EMSA) using biotin 5'-end-labeled

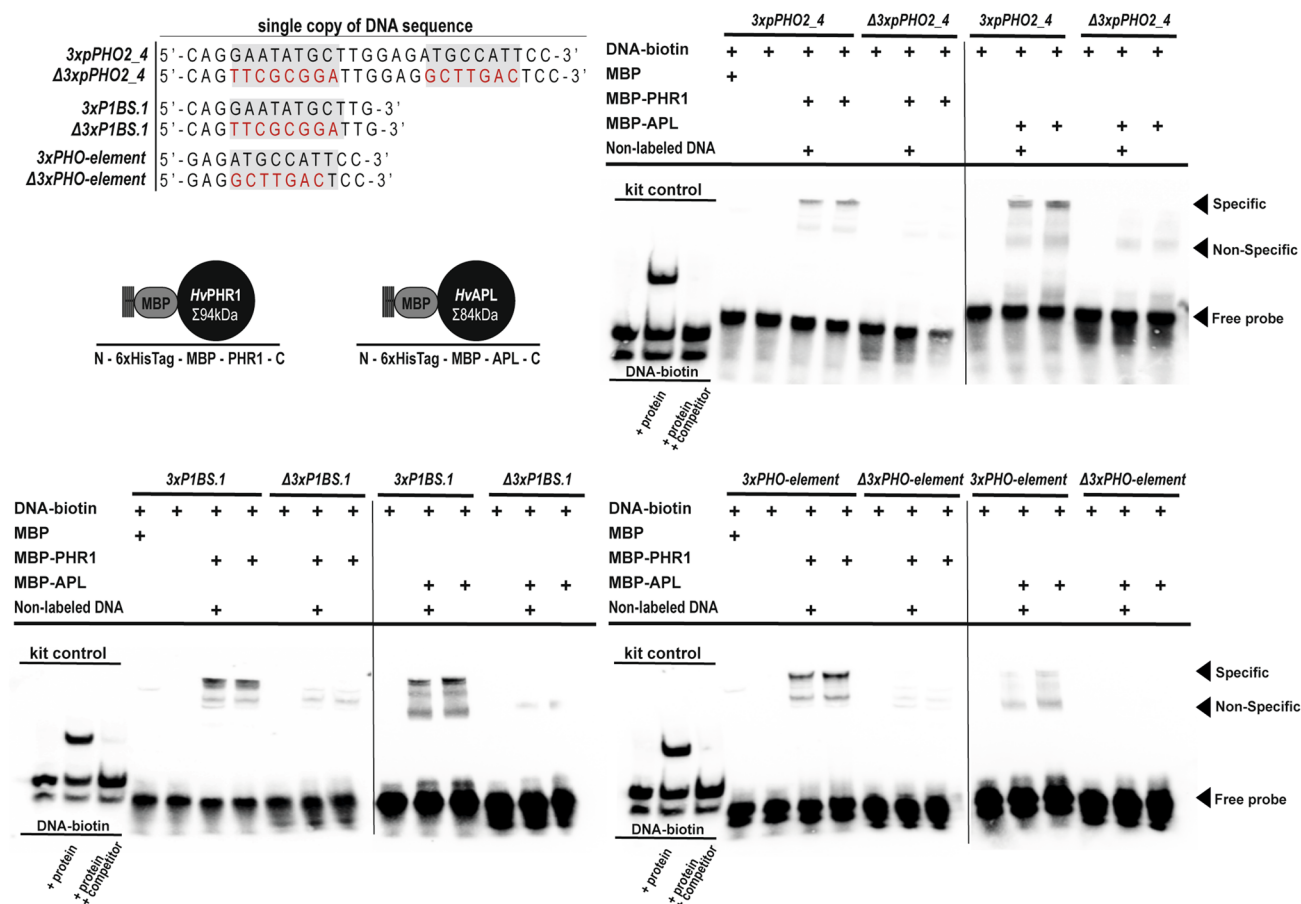


Fig. 2 Barley PHR1 and APL TFs bind to the *PHO2* 5'-UTR first intron in vitro. The EMSA results show that purified recombinant proteins MBP-APL and MBP-PHR1 bound to the biotinylated oligonucleotides that were used for Y1H tests: 3xpPHO2_4, 3xP1BS.1, and 3xPHO-element. The mutated nucleotides in Δ3xpPHO2_4, Δ3xP1BS.1, and Δ3xPHO-element are shown in red. The kit system

was controlled by the confirmed binding of Epstein-Barr nuclear antigen (EBNA) to the 60 bp of the Biotin-EBNA Control DNA (Thermo Fisher Scientific). In all tests, the 200-fold molar excess of non-labeled DNA was used in the competition reactions. The black vertical line separates two different membranes

DNA fragments for either original or mutated (containing a scrambled motif) sequences (Table S2). We first confirmed the in vitro binding of both recombinant proteins to the same DNA “bait” fragment (pPHO2_4) that we used for Y1H screening (Fig. 2). However, we did not detect specific binding of both recombinant proteins when they were incubated with the pPHO2_5 “bait” fragment containing the P1BS.2 motif. We then prepared additional DNA constructs with individual *PHO2* 5'-UTR motifs in triple tandem repeats, such as P1BS and P-responsive PHO elements, which are located close to each other within the pPHO2_4 fragment (Fig. 2). We found that MBP-PHR1 or MBP-APL could bind to the motifs originating from the pPHO2_4 fragment and that the binding efficiency decreased when a non-labeled DNA competitor was added. Additionally, there was no specific binding when MBP tags were added.

Characterization of the novel TF APL

The barley gene (HORVU6Hr1G031470) that encodes the full-length APL protein contains six exons and is located on barley chromosome number 6 on the forward strand at position 133900629–133903229. There are 26 computationally mapped potential isoforms of barley APL in the Ensembl Plants database, although, for our functional studies, we used the longest transcript variant that encodes a functional protein, which contained 368 aa residues and was mapped using our RNA-Seq results (Fig. S8). APL belongs to the protein homeobox-like domain superfamily (SSF46689), which has 402 members in the barley Ensembl Plants database. The protein structure has two conserved domains: a SANT/MYB domain (PFAM00249) at aa residues 45–93 and a MYB-CC-type LHEQLE-containing domain (PFAM14379) at aa residues 139–193 (Fig. S9). The *APL* gene is conserved in monocotyledonous plants. We found the most closely related

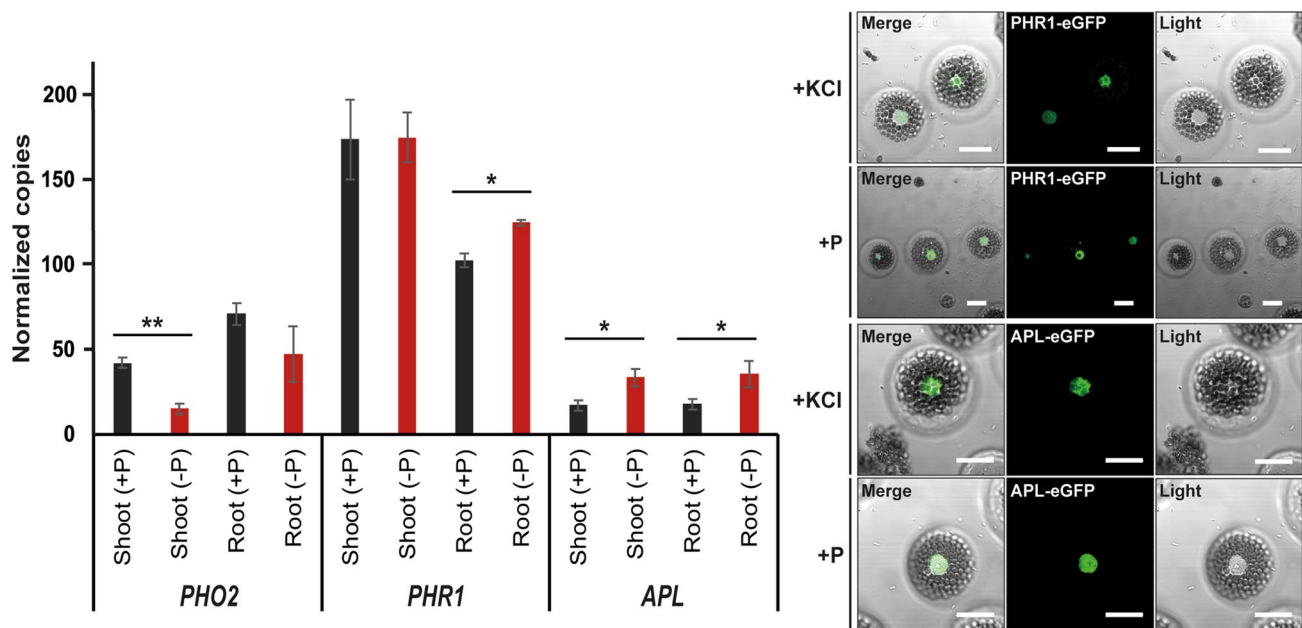


Fig. 3 The barley *APL* gene is highly expressed in Pi-deprived plants and encodes a nuclear-localized MYB-CC family protein member. Quantification by ddPCR of the absolute expression levels of the *PHO2*, *PHR1*, and *APL* genes during Pi starvation in barley shoots and roots. The black bars indicate gene expression under Pi scarcity, and the red bars indicate gene expression with Pi in the soil. The bars represent copy numbers normalized to 1000 copies of the

ARF1 reference gene; * $p < 0.05$, ** $p < 0.001$, calculated using two-tailed Student's *t*-tests for three biological and two technical replicates (**left panel**). Subcellular localization of the PHR1-eGFP and APL-eGFP recombinant proteins that were transiently expressed in protoplasts isolated from 6-day-old barley leaves (**right panel**). Scale bars = 20 μm

orthologs in *Aegilops tauschii* and *Triticum urartu* (a myb family APL-like TF (GenBank Acc. No. XP_020150564.1), a myb-related protein (AEV91195.1), and the myb family TF APL (EMS60802.1)) and in *Brachypodium distachyon* (an APL-like TF (XP_003570345.2)) (Fig. S9, Table S3).

Compared with *PSR1* in *Chlamydomonas reinhardtii*, *PHR1* in plants is a weakly Pi-responsive gene (Liu et al. 2017). Thus, we used sensitive droplet digital polymerase chain reaction (ddPCR) technology to evaluate whether barley PHR TF expression changed during Pi starvation. The ddPCR analysis revealed that *APL* gene expression was significantly upregulated during Pi starvation in barley shoots and roots. The data show that the number of *APL* transcript copies were the same in the shoots and roots of barley plants grown under control conditions, with 18 copies per 1000 copies of the *ADP-RIBOSYLATION FACTOR 1* (*ARF1*) reference gene. During Pi starvation, *APL* transcript copies were almost two times more abundant, with 34 copies ($P = 0.0292$) in the shoots and 36 copies ($P = 0.0359$) in the roots (Fig. 3). Using classic reverse-transcription quantitative PCR (RT-qPCR), we previously showed that the relative expression level of *PHR1* did not change significantly in response to low-Pi conditions (Pacak et al. 2016). When extending these results via ddPCR absolute quantification, we observed that the *PHR1* gene was affected by Pi starvation in the roots, with 103 copies detected in

the control plants and 125 copies detected in the stressed plants ($P = 0.0187$). However, this induction was found only in the roots: in the shoots, where the *PHR1* transcript is more abundant, 174 copies in the control plants and 175 copies in the stressed plants were detected (Fig. 3). Barley *PHO2* gene expression was significantly downregulated in Pi-starved shoots in the background of the barley cultivar Morex (23 days post-sowing, dps), with 42 copies in Pi-positive conditions and 15 copies in Pi-negative conditions ($P = 0.0003$). We also detected the downregulation of *PHO2* expression in the roots in response to stress, although the downregulation was not statistically significant. The results obtained for the absolute copy quantification of *PHO2* in the shoots are consistent with the data we published earlier this year for the barley line Rolap (23 dps). However, we detected a relatively more pronounced downregulation of transcripts in the roots (Smoczynska et al. 2019). We assume that such variation occurs because of the different degrees of the stress response among barley genotypes to Pi-negative conditions.

To confirm that the APL protein can bind to DNA and is present in the nucleus, we evaluated its cellular localization in barley protoplasts. Using confocal microscopy, we discovered that APL-eGFP fusion proteins localized exclusively in the cell nucleus, and their localization was not affected by the Pi status. Similarly, our data show that the PHR1 proteins were present in the nucleus (Fig. 3), but some

were also slightly visible in the cytoplasm (Fig. S10). This finding is probably explained by the PHR1 protein's post-translational modifications (such as cytoplasmic sumoylation by Siz1-SUMO ligase), which control Pi deficiency responses in plants (Miura et al. 2005), along with the cytoplasmic–nuclear shuttling of PHR-like proteins modulated by SPX4 in rice (Lv et al. 2014).

The 5'-UTR of the barley *PHO2* gene promotes transcriptional activity in tobacco leaves

To gain insight into the transcriptional activity of the 5'-UTR, we designed an experiment in which the β -glucuronidase (*GUS*) reporter gene was driven by different *PHO2* regulatory elements present in the gene promoter and 5'-UTR. After tobacco leaves were inoculated via *Agrobacterium* culture, they transiently expressed all constructs driven by (i) *pPHO2* (the native *PHO2* promoter) + the 5'-UTR, (ii) *pPHO2* and (iii) the isolated 5'-UTR (Fig. 4). Absolute quantification of the reporter gene transcripts in two independent tobacco leaves (four replicates, ddPCR analysis) confirmed the magnitude of the transcription enhancement mediated by the 5'-UTR itself. When *GUS* was expressed under the whole *PHO2* regulatory region (i), we detected 420 normalized copies per 1000 copies of the hygromycin resistance (*HygR*) gene transcript. However, with the native *PHO2* promoter (ii), the number of normalized copies significantly decreased to 265 ($P=0.009$) (Fig. 4). We detected the highest copy number when the 5'-UTR was used as a promoter sequence (iii), with 731 normalized copies per 1000 copies of the *HygR* gene transcript ($P=0.003$). Interestingly, the deletion of the first intron's P1BS.1 and P-responsive PHO elements from the *PHO2* 5'-UTR in the presence of the promoter restored the enhanced *GUS* expression (706 normalized copies, $P=0.004$) to the level observed with the 5'-UTR construct itself (Fig. 4). We did not observe the same effect when the P1BS.2 element was deleted from the second exon of the 5'-UTR (407 normalized counts versus 420). These results suggest that the promoter and the 5'-UTR act in concert and that their presence is a source of *cis*- and *trans*-regulatory elements that probably compete to alter *PHO2* gene expression in barley. The ddPCR results were consistent with those of histochemical assays, and *GUS* activity within the leaves was most visible when the full-length 5'-UTR was used as a promoter (Fig. 4).

To exclude the possibility that the P1BS motif present in the second exon of the 5'-UTR is a part of the promoter region, we mapped RNA sequencing (RNA-Seq) reads derived from barley shoots to *PHO2* cDNA (Fig. S8). The coverage of transcripts that were mapped to the 3' end of exon 1 or all of exon 2 was the same as that when the position of the start codon was located in exon 3. This result means that for the production of full-length proteins, the

PHO2 transcript requires that at least part of exon 1 and all of exon 2 contain the P1BS motif in the 5'-UTR but not in the promoter.

Discussion

In this study, we revealed new potential factors that might play significant roles in the regulation of barley *PHO2* gene expression at the transcriptional level. We identified a new APL-like TF that can bind to the P1BS motif present in the first intron and second exon of the barley *PHO2* 5'-UTR. Here, we shed new light on the regulation of *PHO2* gene expression in plants by providing the results of *in vivo* and *in vitro* studies of newly identified *cis*- and *trans*-acting regulatory elements in barley.

The average length of 5'-UTRs in plants is ~200 nucleotides and is usually much shorter than the length of 3'-UTRs (Pesole et al. 2001). Previous studies on the *PHO2* gene in rice have shown that the gene itself has an exceptionally large 5'-UTR, and alternative TSSs were identified upon Pi stress (Secco et al. 2013). Interestingly, the second exon of the *PHO2* 5'-UTR has six potential cleavage sites for miR399 (Hackenberg et al. 2013; Pacak et al. 2016), which suggests that post-transcriptional gene regulation is very broad. The Ensembl Plants database contains six *PHO2* transcript variants. Three out of six isoforms are upstream of the P1BS.1 motif located in the first intron of the 5'-UTR, one of which begins exactly where the start codon does (Fig. S1). These splicing variants have not been experimentally verified, but we can speculate their functional role. Together, our combined results suggest that some of the transcripts, if they exist, may be additionally regulated by 5'-UTR *cis*-acting elements. The role of 5'-UTRs in eukaryotes is essentially twofold and centered on post-transcriptional regulation through the stabilization of mRNA molecules and the control of mRNA nucleocytoplasmic transport (Pesole et al. 1997, 2001). Moreover, the role of 5'-UTRs in the translation process starts from the 5' cap structure, which involves the interaction of cap-binding proteins to initiate translation (Sonnenberg 1994). The 5'-UTR-mediated alteration of translation efficiency is strongly associated with the presence of binding signals for RNA-binding proteins (RBPs), upstream open reading frames (uORFs), and the ability of mRNAs to form secondary structures (Araujo et al. 2012). We did not identify a typical Kozak sequence for the barley *PHO2* AUG start codon; however, we identified a 5'-CCA TGGCGGC-3' Kozak sequence (Kozak 1987), which is a very strong translation initiation signal, within the first exon of the 5'-UTR (Fig. S2). Generally, ribosomal subunits can associate with such Kozak sequences following the activation of the upstream ORF, which can modulate the translational machinery. Furthermore, downstream of the

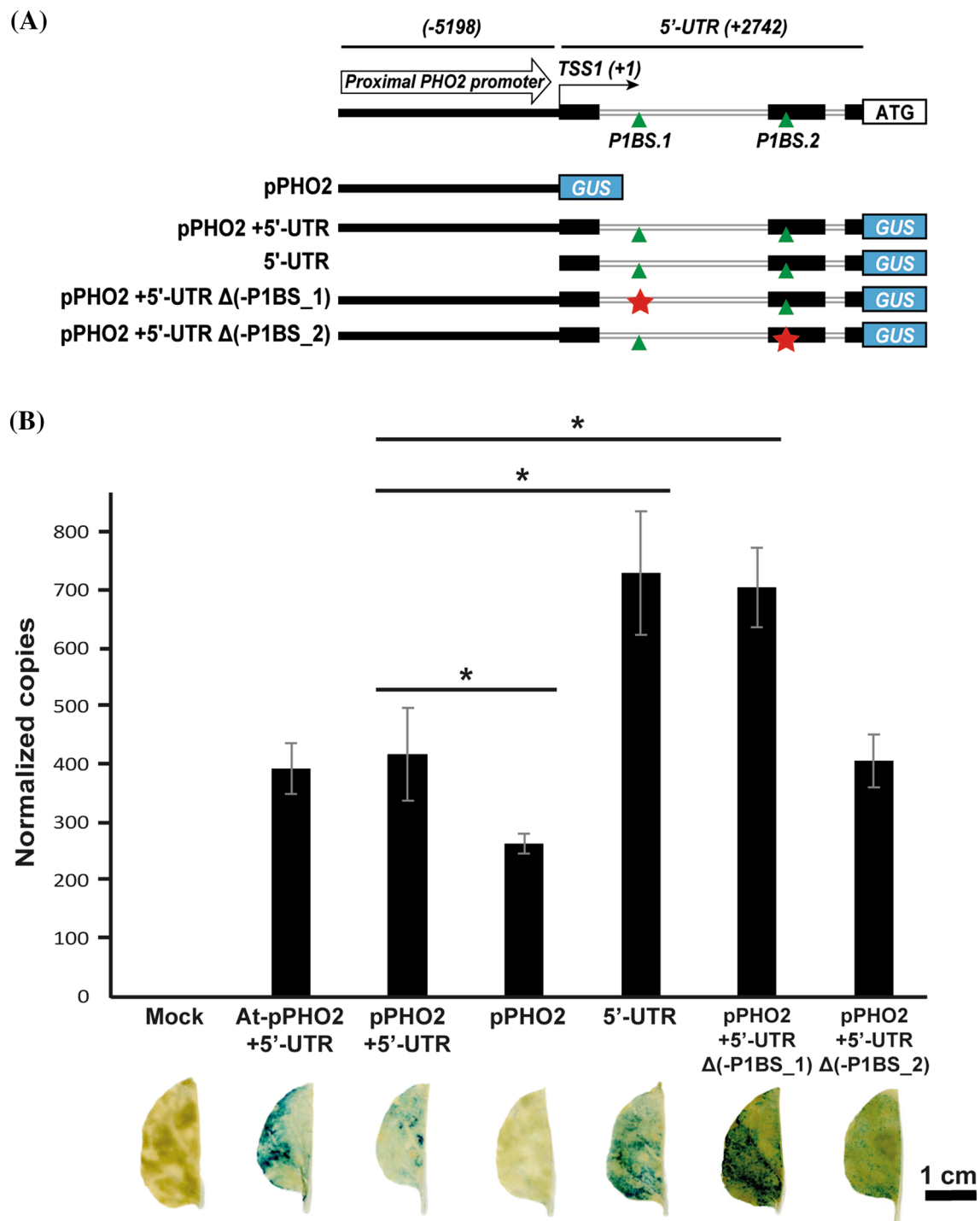


Fig. 4 The barley *PHO2* 5'-UTR ensures the high expression of downstream genes in tobacco leaves. *GUS* transient expression was determined under the following constructs: the full-length proximal *PHO2* promoter region (5198 bp), the full-length proximal *PHO2* promoter region combined with the full-length 5'-UTR (7940 bp), the *PHO2* 5'-UTR itself (2742 bp), and two P1BS deletion constructs [one without P1BS in the 5'-UTR first intron (-P1BS.1) and the other without P1BS in the 5'-UTR second exon (-P1BS.2)]. The full-length proximal *AtPHO2* promoter region combined with the 5'-UTR was used as a positive control of previously tested *PHO2* regulatory elements (6973 bp). The green triangle indicates the P1BS motif loca-

tion; the red star indicates a deleted P1BS motif (a). Plots showing the absolute quantification of *GUS* transcript copies, which were normalized to the level of 1000 copies of the *HygR* reference gene using ddPCR. Control leaves (mock plants) were inoculated with transformation buffer to eliminate unspecific *GUS* primer amplification (b). Statistical significance was determined for two biological replicates (two halves cut out from two independent leaves) and two technical replicates of RNA isolation; * $p < 0.05$, ** $p < 0.001$, calculated using two-tailed Student's *t*-tests; the other halves of the leaves were used for *GUS* staining and are presented under the bars. Scale bar for leaves = 1 cm

Kozak sequence, there are miR399 cleavage sites within the 5'-UTR that may function as another means of translational regulation of *PHO2* (Fig. S2). The level of *PHO2* transcripts is finely tuned by miR399 molecules to maintain Pi homeostasis, and such molecular activity can generate different mRNA variants. Secco et al. reported two isoforms of *OsPHO2* transcripts, designated PHO2.1 and PHO2.2, but only the PHO2.2 variant is present specifically in response to Pi scarcity in rice. Moreover, the authors observed that PHO2.1 was enriched in the non-polysomal fraction when PHO2.2 was preferentially associated with polysomes, suggesting that PHO2.2 is more actively translated into protein than the PHO2.1 isoform (Secco et al. 2013). These data support the hypothesis that additional factors may exist in plants to regulate the expression of the *PHO2* gene in response to Pi stress and promote the expression of particular isoforms; however, additional experiments are needed to verify this hypothesis. In 2010, Bustos et al. raised the possibility of an important role for the 5'-UTR in terms of transcriptional control because the highest overrepresentation of P1BS motifs was detected within the 5'-UTR of *PHR1* primary target genes (Bustos et al. 2010). Our results show that the barley *PHO2* 5'-UTR sequence contains two P1BS motifs and is sufficient on its own to activate transcription and efficiently activates the expression of the downstream *GUS* gene in tobacco leaves. On the other hand, the transcriptional activity of the *PHO2* promoter itself is 0.6 times lower, whereas the 5'-UTR alone is 1.6-fold higher, compared with the construct harboring the *PHO2* gene promoter and 5'-UTR together. The *PHO2* promoter region lacks any known Pi-responsive DNA motifs, and it does not efficiently induce downstream gene expression on its own.

In applied sciences, introns within 5'-UTRs are known to maximize gene expression and are present in various expression cassettes in commercial vectors. Such 5'-UTR introns may contain functional enhancer elements that play crucial roles that affect basal promoter activity (Bianchi et al. 2009; Gallegos and Rose 2017). The indirect role of 5'-UTR-originating introns in transcription initiation, as well as polyadenylation, protein decay, and translation, is associated with the presence of splicing signals and the activity of intron removal by the spliceosome (Chung et al. 2006; Bianchi et al. 2009). However, the hypothesis that 5'-UTR-originating introns may act as a repository for *cis*-regulatory elements to enhance or silence downstream gene expression is another phenomenon that should be considered in this context. Many groups have recently reported evidence to support this hypothesis in human cells (Melkonyan et al. 1998; Bianchi et al. 2009) and plant cells (Chung et al. 2006; Lu et al. 2008; Liao et al. 2013). For example, the 5'-UTR of the *AtP5CS1* ($\Delta 1$ -*PYRROLINE-5-CARBOXYLATE SYNTHETASE 1*) gene contains a conserved P1BS *cis*-element that is recognized and bound by both the *PHR1* and *PHL1*

TFs in *Arabidopsis* (Aleksza et al. 2017). A long intron might contain DNA motifs that are involved in the regulation of gene expression, and we assume that this region shares genetic networks with a basal promoter region to summon *trans*-acting regulators.

Transcriptional regulation of Pi-responsive genes has been reported for many plant species. The identification of new TFs in plants associated with this process is possible by homologous searching using *AtPHR1* and *CsPSR1* orthologous sequences as queries. Both of these proteins belong to a large gene family (comprising 14 proteins in *Arabidopsis*) whose members have a conserved MYB DNA-binding domain (BD) and a predicted CC domain (Rubio et al. 2001; Zhou et al. 2008). Using BLAST (Basic Local Alignment Search Tool), we identified a new TF belonging to the protein homeobox-like domain superfamily in barley and named it APL. The multiple sequence alignment of *PHR1*, *PHR2*, and the newly identified APL reveals that both MYB domains are highly conserved. However, both domains are present in the N-terminal portion of the APL aa sequence, but protein domain localization occurs via the C-terminus in the case of *PHR1* and *PHR2* (Fig. S9). This result suggests that the new TF should be considered a member of different *PHR*-like protein classes. A phylogenetic analysis of the MYB-CC family revealed two subgroups for *Arabidopsis* (Rubio et al. 2001) and three for rice (Ruan et al. 2017). Moreover, Rubio and colleagues suggested that the presence of a CC domain can promote functional heterodimeric interactions and cause partial redundancy between members of different family subgroups (Rubio et al. 2001). The APL TFs are required for phloem identity and have a dual role: they promote phloem differentiation and repress xylem differentiation during vascular development (Bonke et al. 2003; Truernit et al. 2008). APL-like proteins can activate the transcription of genes involved in Pi uptake and assimilation (Todd et al. 2004), but no data concerning their role in the regulation of Pi-starvation-responsive genes exist. Studies have shown that the expression levels of *PHR*-like TFs are stable and not affected by Pi status. However, our detailed data concerning absolute gene expression show that APL is significantly upregulated in both the shoots and roots during Pi starvation, similar to the upregulation of *PHR1* in the roots. Our results show that APL can bind both to specific DNA motifs *in vitro* in yeast cells and to biotinylated DNA fragments *in vivo* and that it is present exclusively in the barley nucleus. Moreover, phylogenetic and mutation analyses reveal functional redundancy among four *PHR1*-like proteins in rice: *OsPHR1*, *OsPHR2*, *OsPHR3*, and *OsPHR4*. Rice *PHR*-like TFs can form homo- or heterodimers with related proteins to activate target gene expression (Guo et al. 2015; Ruan et al. 2017). We believe that APL proteins are needed by plants during phosphate stress to play a redundant role with *PHR*-like proteins and that APL proteins can

probably also homo- or heterodimerize with these PHR-like proteins; however, additional studies are needed to verify this.

Materials and methods

Plant material and growth conditions

Seeds of barley (*Hordeum vulgare*) cultivar Morex (received from Agricultural Research Institute Kromeriz, Ltd., Czech Republic) and the line Rolap (obtained from the Institute of Plant Genetics of the Polish Academy of Sciences, Poznań, Poland; Devaux et al. 1992) were germinated on wet, sterile Whatman filter paper for 3 days in a growth chamber (MLR-35-1H, Sanyo, Panasonic) under long-day (16 h) conditions at 23 °C until white hypocotyls were visible. Three seedlings were then transferred to a single pot that contained a mixture of sterile low-Pi soil (8 mg P/kg) and sand (7:2 ratio). The Pi concentration in the soil was determined on the basis of the P₂O₅ method by staff at the District Chemical-Agricultural Station PN-EN ISO/IEC 17025:2015 certified laboratory in Poznań, Poland. The plants were subsequently grown under controlled conditions, which included a 16 h day/8 h night photoperiod at a temperature of 22 °C. Plant material was obtained from two different Pi regimes: Pi-depleted and Pi-sufficient, as described previously (Pacak et al. 2016).

RNA isolation and cDNA synthesis for absolute gene expression quantification

RNA extraction and cDNA synthesis for all samples collected from the Pi starvation experiment were performed as described previously (Pacak et al. 2016; Smoczynska et al. 2019). For reverse transcription, we used 1 µg of total RNA, and the final cDNA was diluted 20 times for ddPCR quantification.

ddPCR

Droplet digital PCR (ddPCR) allows precise detection of small differences in gene expression between samples since includes analysis from approximately 20 000 reactions occurring in the individual droplet per sample. By analysis of positive and negative droplets the copy numbers per 1 µL were calculated. To determine the absolute number of target cDNA copies of Pi-related genes and the expression of the *GUS* reporter gene in tobacco leaves, we performed ddPCR in accordance with the EvaGreen (Bio-Rad) approach following the protocol described by Smoczynska et al. (2019). The specific primers targeting the barley *PHO2*, *APL*, *PHR1* and *ARF1* genes as well as *GUS* reporter gene and the hygromycin resistance (*HygR*) gene are listed in Table S4.

Cis-regulatory motif prediction

A region comprising 7940 bp upstream of the *PHO2* gene start codon was amplified using the genomic DNA of the barley cultivar Morex as a template and then cloned into a pGEM-T Easy vector (Promega). The sequence itself contained a full-length 5'-UTR (2742 bp in length) as well as a predicted promoter region up to 5198 bp in length. The beginning of the promoter sequence and the TSS were determined previously using a SMARTer RACE cDNA Amplification Kit (Clontech) and GeneRacer Kit (Invitrogen, Thermo Fisher Scientific) (Pacak et al. 2016). The PlantPAN 3.0 database <http://plantpan.itsps.ncku.edu.tw> was used to search for any putative *cis*-regulatory elements within the barley *PHO2* promoter and 5'-UTR sequences (Chow et al. 2016).

IME analysis

To determine whether any of the *PHO2* intronic sequences enhance their gene expression, we used the IMEter algorithm of the IMEter v.2.1 tool (http://korflab.ucdavis.edu/cgi-bin/IMEter_2014/web-imeter2.1.pl) to screen the sequences from each of the nine *PHO2* introns (Parra et al. 2011). We also screened seven fragments that were similar in length (approximately 200 bp) and derived from the first 5'-UTR-localized intron of *PHO2*. Because the tool does not provide a unique analysis for the barley genome, we calculated each IME score for three closely related monocotyledonous species that were available for selection on the IMEter platform: *Brachypodium distachyon*, *Oryza sativa* and *Zea mays* (Fig. S7).

Y1H analysis

A Matchmaker Gold Yeast One-Hybrid screen was performed according to the manufacturer's protocol (Clontech). Each sequence used as a bait for screening was cloned into a pAbAi yeast reporter vector (Clontech) in triple tandem repeats. These triple tandem repeats were synthesized de novo using the GeneArt approach (Thermo Fisher Scientific) and provided in pUC-based vectors. The following bait strains were therefore obtained: 3xpPHO2_1, 3xpPHO2_2, 3xpPHO2_3, 3xpPHO2_4, 3xpPHO2_5 (where pPHO2 denotes the promoter of *PHO2*), and 3xP1BS.1, as well as 4xPHO-elements, with p53 serving as a control (Table S5). For each bait strain, we determined the minimal inhibitory concentration of aureobasidin A (150 ng/mL) to avoid recognition of the bait sequence by endogenous yeast TFs. Therefore, we decided to use the 4xPHO-element bait strain instead of the 3x repeated motif itself. For prey, we used the SMART cDNA library generated with poly A⁺ RNA from the shoots of Pi-starved barley cultivar Morex. In accordance with the library construction

protocol from the Matchmaker system (Clontech), we obtained barley cDNA libraries, which were used to screen all Y1H fragments listed in Table 1.

Overexpression of barley PHR1 and APL proteins

To obtain 6x His- and MBP-tagged PHR1 and APL proteins, we cloned full-length coding DNA sequences (CDSs) into pETM-41 (EMBL) vectors. The PHR1 and APL CDSs were amplified using the primers listed in Table S4 and then inserted into the pETM-41 NcoI linearized vectors using an In-Fusion HD Cloning Kit (Takara). Recombinant MBP- and His-tagged PHR1 and APL proteins were produced in *E. coli* BL21(DE3) cells transformed with the pETM-41 plasmids, and purified using HisPur Ni-NTA Resin (Thermo Fisher Scientific). All the eluted fractions, with increasing imidazole concentrations (100, 200 and 500 mM), were checked with SDS-PAGE, pooled together and then concentrated using an Amicon Ultra-4 centrifugal filter with a – 10 kDa cut-off (Merck). Size-exclusion chromatography (SEC) was then carried out on a Superdex 200 10/300GL system (GE Healthcare) in SEC buffer (10% glycerol, 20 mM HEPES, 500 mM NaCl, 10 mM 2-mercaptoethanol).

EMSA

To confirm the protein-DNA interactions, a LightShift Chemiluminescent EMSA Kit (Thermo Fisher Scientific) was used according to the manufacturer's instructions, with some modifications. We ordered both 5'-biotinylated and unlabelled oligonucleotides for each checked DNA fragment. The oligonucleotide sequences of biotin-labeled and unlabeled probes are listed in (Table S2). Mutated oligonucleotides were generated using the GenScript online tool (<https://www.genscript.com/tools/create-scrambled-sequence>). All the oligonucleotides were purified via gel extraction; electrophoresis was performed on a 15% (19:1) acrylamide/bisacrylamide denaturing gel with 8 M urea. After purification, both DNA strands were pooled together to final concentrations described in the LightShift protocol and denatured for 20 min at 95 °C before use. For each tested DNA-protein interaction, we applied 400 ng of MBP-PHR1 protein or 1000 ng of MBP-APL protein (Fig. 2). The same protein amounts were applied of MBP tag alone. The biotin end-labelled DNA was then detected using a Chemiluminescent Nucleic Acid Detection Module (Thermo Fisher Scientific).

Histochemical GUS assays and detection of barley pPHO2 activity

To evaluate the activity of the reporter *GUS* gene under different *PHO2* gene promoters and 5'-UTR fragments,

we amplified various pPHO2 + 5'-UTR fragments from the genomic DNA of barley cultivar Morex and cloned them into pENTR/SD/D-Topo (Invitrogen) vectors before they were recombined into pMDC163 destination vectors (Curtis and Grossniklaus 2003). To investigate the necessity of *P1BS* elements for *GUS* expression, the *P1BS* elements were deleted via an In-Fusion Cloning System (Takara), resulting in pPHO2 + 5'-UTRΔ(-*P1BS*₁) and pPHO2 + 5'-UTRΔ(-*P1BS*₂) mutation constructs. For a positive control in this experiment, we used the construct containing the full-length (6973 bp) sequence of the *PHO2* promoter and the 5'-UTR from *Arabidopsis*. The vectors were then transformed into *Agrobacterium tumefaciens* strain AGL1. Transient expression in tobacco leaves and GUS staining were subsequently performed according to a protocol described by Ishizaki and Nonomura (2012).

Subcellular localization of PHR1 and APL in barley protoplasts

Gene-specific primers (Table S4) were used to amplify the *PHR1* and *APL* CDSs from barley cultivar Morex cDNA material. The genes were cloned into pENTR/SD/D-Topo (Invitrogen) vectors before they were recombined into either the 5'- or 3'-end of the eGFP-tagging vectors pSU5 and pSU3 (Knop et al. 2017). Barley protoplasts were isolated according to the protocol described by Susann Frank (2017), whereas low Pi experiments were performed according to Hu et al. (2019). Images were taken using a confocal scanning microscope (Nikon A1Rsi).

RNA-seq

To analyse the abundance of barley *PHO2*, *PHR1* and *APL* transcript isoforms, paired-end RNA-seq analysis was performed. A library was constructed using an mRNA-Seq Library Prep Kit v2 (Lexogen) and RNA isolated from the shoots of barley line Rolap growing in soil with sufficient Pi concentrations. RNA-seq was performed at Fasteris SA (Switzerland) via an Illumina HiSeq 3000/4000 approach. The reads were mapped to the full-length transcripts using CLC Genomics Workbench (QIAGEN) software.

Parallel analysis of RNA ends (PARE)

To analyse the barley *PHO2* degradome profile, the methods described by German et al. (2009) and Alaba et al. (2015) were applied. In brief, mRNA fragments derived from the barley line Rolap growing at a low-Pi concentration were ligated to the 5' RNA adapter-containing sequence recognized by the restriction enzyme MmeI. After cDNA production, PCR was performed to produce dsDNA degradome fragments. The PCR products were digested using the MmeI

enzyme and ligated to a 3' adapter. The purified fragment ligation products were then used as a template for PCR. The prepared degradome library was sequenced at Fasteris SA (Switzerland) using the HiSeq 2500 Illumina technique. PAREsnip2 software was used for degradome t-plot construction in conjunction with three databases: the degradome library, *PHO2* cDNA library (HORVU1Hr1G085570.2, Ensembl Plants database) and the set of low-Pi-responsive barley microRNAs (Thody et al. 2018).

Acknowledgements The authors wish to thank Dr. Iver Jakobsen (University of Copenhagen, Copenhagen, Denmark) for providing low-P soil and Prof Tzzy-Jen Chiou (Agricultural Biotechnology Research Center, Academia Sinica, Taiwan) for the construct containing the *AtPHO2* promoter and the 5'-UTR. We thank Michał Taube and Przemysław Wiecek for their help with the protein overexpression and purification protocols and Mateusz Bajczyk for all his advice.

Author contributions PS performed most of the experiments and wrote the manuscript under the supervision of AP. AP prepared the degradome and transcriptome libraries. LS performed the protein subcellular localization. All authors reviewed the manuscript.

Funding This work was funded by the National Science Centre, Poland, on the basis of DEC-2013/11/B/NZ9/01761, UMO-2016/23/B/NZ9/00857, and UMO-2015/19/N/NZ9/00218 and by KNOW RNA Research Centre in Poznań 01/KNOW2/2014.

Compliance with ethical standards

Conflict of interest All authors declare that they have no conflict of interest.

References

- Abel S, Ticconi CA, Delatorre CA (2002) Phosphate sensing in higher plants. *Physiol Plant* 115(1):1–8. <https://doi.org/10.1034/j.1399-3054.2002.1150101.x>
- Alaba S, Piszczalka P, Pietrykowska H, Pacak AM, Sierocka I, Nuc PW, Singh K, Plewka P, Sulkowska A, Jarmolowski A, Karłowski WM, Szwejkowska-Kulinska Z (2015) The liverwort *Pellia endivifolia* shares microtranscriptomic traits that are common to green algae and land plants. *New Phytol* 206(1):352–367. <https://doi.org/10.1111/nph.13220>
- Aleksza D, Horváth GV, Sándor G, Szabados L (2017) Proline accumulation is regulated by transcription factors associated with phosphate starvation. *Plant Physiol* 175:555–567. <https://doi.org/10.1104/pp.17.00791>
- Araujo PR, Yoon K, Ko D, Smith AD, Qiao M, Suresh U, Burns SC, Penalva LO (2012) Before it gets started: regulating translation at the 5' UTR. *Comp Funct Genomics* 2012:475731. <https://doi.org/10.1155/2012/475731>
- Bari R, Datt Pant B, Stitt M, Scheible WR (2006) *PHO2*, *MicroRNA399*, and *PHR1* define a phosphate-signaling pathway in plants. *Plant Physiol* 141:988–999. <https://doi.org/10.1104/pp.106.079707>
- Bariola PA, Howard CJ, Taylor CB, Verburg MT, Jaglan VD, Green PJ (1994) The *Arabidopsis* ribonuclease gene *RNS1* is tightly controlled in response to phosphate limitation. *Plant J* 6:673–685. <https://doi.org/10.1046/j.1365-313X.1994.6050673.x>
- Bianchi M, Crinelli R, Giacomini E, Carloni E, Magnani M (2009) A potent enhancer element in the 5'-UTR intron is crucial for transcriptional regulation of the human ubiquitin C gene. *Gene* 448:88–101. <https://doi.org/10.1016/j.gene.2009.08.013>
- Bonke M, Thitamadee S, Mahonen AP, Hauser MT, Helariutta Y (2003) APL regulates vascular tissue identity in *Arabidopsis*. *Nature* 426:181–186. <https://doi.org/10.1038/nature02100>
- Briat JF, Rouached H, Tissot N, Gaymard F, Dubos C (2015) Integration of P, S, Fe, and Zn nutrition signals in *Arabidopsis thaliana*: potential involvement of PHOSPHATE STARVATION RESPONSE 1 (PHR1). *Front Plant Sci* 6:290. <https://doi.org/10.3389/fpls.2015.00290>
- Bustos R, Castrillo G, Linhares F, Puga MI, Rubio V, Pérez-Pérez J, Solano R, Leyva A, Paz-Ares J (2010) A central regulatory system largely controls transcriptional activation and repression responses to phosphate starvation in *Arabidopsis*. *PLoS Genet* 6(9):e1001102. <https://doi.org/10.1371/journal.pgen.1001102>
- Chiou TJ, Lin SI (2011) Signaling network in sensing phosphate availability in plants. *Annu Rev Plant Biol* 62:185–206. <https://doi.org/10.1146/annurev-arplant-042110-103849>
- Chow CN, Zheng HQ, Wu NY, Chien CH, Huang HD, Lee TY, Chiang-Hsieh YF, Hou PF, Yang TY, Chang WC (2016) PlantPAN 2.0: an update of plant promoter analysis navigator for reconstructing transcriptional regulatory networks in plants. *Nucleic Acids Res* 44:D1154–D1160. <https://doi.org/10.1093/nar/gkv1035>
- Chung BY, Simons C, Firth AE, Brown CM, Hellens RP (2006) Effect of 5' UTR introns on gene expression in *Arabidopsis thaliana*. *BMC Genomics* 7:120. <https://doi.org/10.1186/1471-2164-7-120>
- Curtis MD, Grossniklaus U (2003) A gateway cloning vector set for high-throughput functional analysis of genes in plants. *Plant Physiol* 133(2):462–469. <https://doi.org/10.1104/pp.103.027979>
- Delhaize E, Randall PJ (1995) Characterization of a phosphate-accumulator mutant of *Arabidopsis thaliana*. *Plant Physiol* 107(1):207–213. <https://doi.org/10.1104/pp.107.1.207>
- Devaux P, Adamski P, Surma M (1992) Inheritance of seed set in crosses of spring barley and *Hordeum bulbosum* L. *Crop Sci* 32(1):269–271. <https://doi.org/10.2135/cropsci1992.0011183X003200010054x>
- Frank S (2017) Die Cysteinpeptidase HvPAP14 der Gerste und ihre Rolle beim Abbau plastidärer Proteine. PhD thesis, Kiel University. Retrieved from https://macau.uni-kiel.de/receive/dissertation_diss_00020524
- Gallegos JE, Rose AB (2017) Intron DNA sequences can be more important than the proximal promoter in determining the site of transcript initiation. *Plant Cell* 29(4):843–853. <https://doi.org/10.1105/tpc.17.00020>
- German MA, Luo S, Schroth G, Meyers BC, Green PJ (2009) Construction of parallel analysis of RNA ends (PARE) libraries for the study of cleaved miRNA targets and the RNA degradome. *Nat Protoc* 4:356–362. <https://doi.org/10.1038/nprot.2009.8>
- Guo S, Xu Y, Liu H, Mao Z, Zhang C, Ma Y, Zhang Q, Meng Z, Chong K (2013) The interaction between OsMADS57 and OsTB1 modulates rice tillering via DWARF14. *Nat Commun* 4:1566. <https://doi.org/10.1038/ncomms2542>
- Guo M, Ruan W, Li C, Huang F, Zeng M, Liu Y, Yu Y, Ding X, Wu Y, Wu Z, Mao C, Yi K, Wu P, Mo X (2015) Integrative comparison of the role of the PHOSPHATE RESPONSE1 subfamily in phosphate signaling and homeostasis in rice. *Plant Physiol* 168:1762–1776. <https://doi.org/10.1104/pp.15.00736>
- Hackenberg M, Shi BJ, Gustafson P, Langridge P (2013) Characterization of phosphorus-regulated miR399 and miR827 and their isomirs in barley under phosphorus-sufficient and

- phosphorus-deficient conditions. *BMC Plant Biol* 13:214. <https://doi.org/10.1186/1471-2229-13-214>
- Hammond JP, Bennett MJ, Bowen HC, Broadley MR, Eastwood DC, May ST, Rahn C, Swarup R, Woolaway KE, White PJ (2003) Changes in gene expression in Arabidopsis shoots during phosphate starvation and the potential for developing smart plants. *Plant Physiol* 132(2):578–596. <https://doi.org/10.1104/pp.103.020941>
- Heffer P, Prud'homme M (2013) Nutrients as limited resources: global trends in fertilizer production and use. In: Rengel Z (ed) Improving water and nutrient-use efficiency in food production systems. Wiley, Hoboken, NJ, pp 57–78
- Hiraguri A, Itoh R, Kondo N, Nomura Y, Aizawa D, Murai Y, Koiwa H, Seki M, Shinozaki K, Fukuhara T (2005) Specific interactions between Dicer-like proteins and HYL1/DRB- family dsRNA-binding proteins in *Arabidopsis thaliana*. *Plant Mol Biol* 57(2):173–188. <https://doi.org/10.1007/s11103-004-6853-5>
- Hu B, Jiang Z, Wang W, Qiu Y, Zhang Z, Liu Y, Li A, Gao X, Liu L, Qian Y, Huang X, Yu F, Kang S, Wang Y, Xie J, Cao S, Zhang L, Wang Y, Xie Q, Kopriva S, Chu C (2019) Nitrate–NRT1.1B–SPX4 cascade integrates nitrogen and phosphorus signalling networks in plants. *Nat Plants* 5:401–413. <https://doi.org/10.1038/s41477-019-0384-1>
- Huang CY, Shirley N, Genc Y, Shi B, Langridge P (2011) Phosphate utilization efficiency correlates with expression of low-affinity phosphate transporters and noncoding RNA, IPS1, in barley. *Plant Physiol* 156(3):1217–1229. <https://doi.org/10.1104/pp.111.178459>
- Ishizaki K, Nonomura M, Kato H, Yamato KT, Kohchi T (2012) Visualization of auxin-mediated transcriptional activation using a common auxin-responsive reporter system in the liverwort *Marchantia polymorpha*. *J Plant Res* 125(5):643–651. <https://doi.org/10.1007/s10265-012-0477-7>
- Kant S, Peng M, Rothstein SJ (2011) Genetic regulation by NLA and MicroRNA827 for maintaining nitrate-dependent phosphate homeostasis in Arabidopsis. *PLoS Genet* 7(3):e1002021. <https://doi.org/10.1371/journal.pgen.1002021>
- Karthikeyan AS, Ballachanda DN, Raghothama KG (2009) Promoter deletion analysis elucidates the role of cis elements and 5'UTR intron in spatiotemporal regulation of AtPht1;4 expression in Arabidopsis. *Physiol Plant* 136(1):10–18. <https://doi.org/10.1111/j.1399-3054.2009.01207.x>
- Khan GA, Bouraine S, Wege S, Li Y, de Carbonnel M, Berthomieu P, Poirier Y, Rouached H (2014) Coordination between zinc and phosphate homeostasis involves the transcription factor PHR1, the phosphate exporter PHO1, and its homologue PHO1;H3 in Arabidopsis. *J Exp Bot* 65(3):871–884. <https://doi.org/10.1093/jxb/ert444>
- Kim W, Ahn HJ, Chiou TJ, Ahn JH (2011) The role of the miR399-PHO2 module in the regulation of flowering time in response to different ambient temperatures in *Arabidopsis thaliana*. *Mol Cells* 32(1):83–88. <https://doi.org/10.1007/s10059-011-1043-1>
- Knop K, Stepien A, Barciszewska-Pacak M, Taube M, Bielewicz D, Michalak M, Borst JW, Jarmolowski A, Szweykowska-Kulinska Z (2017) Active 5' splice sites regulate the biogenesis efficiency of Arabidopsis microRNAs derived from intron-containing genes. *Nucleic Acids Res* 45:2757–2775. <https://doi.org/10.1093/nar/gkw895>
- Kozak M (1987) An analysis of 5'-noncoding sequences from 699 vertebrate messenger RNAs. *Nucleic Acids Res* 15(20):8125–8148. <https://doi.org/10.1093/nar/15.20.8125>
- Kuo HF, Chiou TJ (2011) The role of microRNAs in phosphorus deficiency signaling. *Plant Physiol* 156(3):1016–1024. <https://doi.org/10.1104/pp.111.175265>
- Kurihara Y, Takashi Y, Watanabe Y (2006) The interaction between DCL1 and HYL1 is important for efficient and precise processing of pri-miRNA in plant microRNA biogenesis. *RNA* 12(2):206–212. <https://doi.org/10.1261/rna.2146906.2>
- Lagrange T, Franzetti B, Axelos M, Mache R, Lerbs-Mache S (1993) Structure and expression of the nuclear gene coding for the chloroplast ribosomal protein L21: developmental regulation of a housekeeping gene by alternative promoters. *Mol Cell Biol* 13(4):2614–2622. <https://doi.org/10.1128/mcb.13.4.2614>
- Li LH, Guo N, Wu ZY, Zhao JM, Sun JT, Wang XT, Xing H (2015) P1BS, a conserved motif involved in tolerance to phosphate starvation in soybean. *Genet Mol Res* 14(3):9384–9394. <https://doi.org/10.4238/2015.August.14.2>
- Liao L, Ning G, Liu C, Zhang W, Bao M (2013) The intron from the 5'-UTR of the FBP11 gene in petunia displays promoter- and enhancer-like functions. *Sci Hortic (Amsterdam)* 154:96–101. <https://doi.org/10.1016/j.scienta.2013.02.009>
- Liu TY, Huang TK, Tseng CY, Lai YS, Lin SI, Lin WY, Chen JW, Chiou TJ (2012) PHO2-dependent degradation of PHO1 modulates phosphate homeostasis in Arabidopsis. *Plant Cell* 24(5):2168–2183. <https://doi.org/10.1105/tpc.112.096636>
- Liu Y, Xie Y, Wang H, Ma X, Yao W, Wang H (2017) Light and ethylene coordinately regulate the phosphate starvation response through transcriptional regulation of PHOSPHATE STARVATION RESPONSE1. *Plant Cell* 29(9):2269–2284. <https://doi.org/10.1105/tpc.17.00268>
- Lu J, Sivamani E, Azhakanandam K, Samadder P, Li X, Qu R (2008) Gene expression enhancement mediated by the 5' UTR intron of the rice rubi3 gene varied remarkably among tissues in transgenic rice plants. *Mol Genet Genom* 279(6):563–572. <https://doi.org/10.1007/s00438-008-0333-6>
- Lv Q, Zhong Y, Wang Y, Wang Z, Zhang L, Shi J, Wu Z, Liu Y, Mao C, Yi K, Wu P (2014) SPX4 negatively regulates phosphate signaling and homeostasis through its interaction with PHR2 in rice. *Plant Cell* 26(4):1586–1597. <https://doi.org/10.1105/tpc.114.123208>
- Lynch JP (2011) Root phenes for enhanced soil exploration and phosphorus acquisition: tools for future crops. *Plant Physiol* 156(3):1041–1049. <https://doi.org/10.1104/pp.111.175414>
- Martín AC, del Pozo JC, Iglesias J, Rubio V, Solano R, de La Peña A, Leyva A, Paz-Ares J (2000) Influence of cytokinins on the expression of phosphate starvation responsive genes in Arabidopsis. *Plant J* 24(5):559–567. <https://doi.org/10.1046/j.1365-3113X.2000.00893.x>
- Melkonyan H, Hofmann HA, Nacken W, Sorg C, Klempt M (1998) The gene encoding the myeloid-related protein 14 (MRP14), a calcium-binding protein expressed in granulocytes and monocytes, contains a potent enhancer element in the first intron. *J Biol Chem* 273(41):27026–27032. <https://doi.org/10.1074/jbc.273.41.27026>
- Miura K, Rus A, Sharkhuu A, Yokoi S, Karthikeyan AS, Raghothama KG, Baek D, Koo YD, Jin JB, Bressan RA, Yun DJ, Hasegawa PM (2005) The Arabidopsis SUMO E3 ligase SIZ1 controls phosphate deficiency responses. *Proc Natl Acad Sci USA* 102(21):7760–7765. <https://doi.org/10.1073/pnas.0500778102>
- Miura K, Jin JB, Lee J, Yoo CY, Stirn V, Miura T, Ashworth EN, Bressan RA, Yun DJ, Hasegawa PM (2007) SIZ1-mediated sumoylation of ICE1 controls CBF3/DREB1A expression and freezing tolerance in Arabidopsis. *Plant Cell* 19(4):1403–1414. <https://doi.org/10.1105/tpc.106.048397>
- Morton T, Petricka J, Corcoran DL, Li S, Winter CM, Carda A, Benfey PN, Ohler U, Megraw M (2014) Paired-end analysis of transcription start sites in Arabidopsis reveals plant-specific promoter signatures. *Plant Cell* 26(7):2746–2760. <https://doi.org/10.1105/tpc.114.125617>

- Mukitira UT, Liu C, Varadarajan DK, Raghothama KG (2001) Negative regulation of phosphate starvation-induced genes. *Plant Physiol* 127(4):1854–1862. <https://doi.org/10.1104/pp.010876>
- Muller R, Morant M, Jarmer H, Nilsson L, Nielsen TH (2007) Genome-wide analysis of the Arabidopsis leaf transcriptome reveals interaction of phosphate and sugar metabolism. *Plant Physiol* 143(1):156–171. <https://doi.org/10.1104/pp.106.090167>
- Nakashima K, Yamaguchi-Shinozaki K, Shinozaki K (2014) The transcriptional regulatory network in the drought response and its crosstalk in abiotic stress responses including drought, cold, and heat. *Front Plant Sci* 5:170. <https://doi.org/10.3389/fpls.2014.00170>
- Pacak A, Barciszewska-Pacak M, Swida-Barteczka A, Kruska K, Segal P, Milanowska K, Jakobsen I, Jarmolowski A, Szweykowska-Kulinska Z (2016) Heat stress affects Pi-related genes expression and inorganic phosphate deposition/accumulation in barley. *Front Plant Sci* 7:926. <https://doi.org/10.3389/fpls.2016.00926>
- Park BS, Seo JS, Chua NH (2014) NITROGEN LIMITATION ADAPTATION recruits PHOSPHATE2 to target the phosphate transporter PT2 for degradation during the regulation of Arabidopsis phosphate homeostasis. *Plant Cell* 26(1):454–464. <https://doi.org/10.1105/tpc.113.120311>
- Parra G, Bradnam K, Rose AB, Korf I (2011) Comparative and functional analysis of intron-mediated enhancement signals reveals conserved features among plants. *Nucleic Acids Res* 39(13):5328–5337. <https://doi.org/10.1093/nar/gkr043>
- Pegler JL, Oultram MJ, Grof CPL, Eamens AL (2019) DRB1, DRB2 and DRB4 are required for appropriate regulation of the microRNA399/PHOSPHATE2 expression module in *Arabidopsis thaliana*. *Plants (Basel)* 8(5):124. <https://doi.org/10.3390/plants8050124>
- Pesole G, Liuni S, Grillo G, Saccone C (1997) Structural and compositional features of untranslated regions of eukaryotic mRNAs. *Gene* 205(1–2):95–102. [https://doi.org/10.1016/s0378-1119\(97\)00407-1](https://doi.org/10.1016/s0378-1119(97)00407-1)
- Pesole G, Mignone F, Gissi C, Grillo G, Licciulli F, Liuni S (2001) Structural and functional features of eukaryotic mRNA untranslated regions. *Gene* 276(1–2):73–81. [https://doi.org/10.1016/s0378-1119\(01\)00674-6](https://doi.org/10.1016/s0378-1119(01)00674-6)
- Piechulla B, Merforth N, Rudolph B (1998) Identification of tomato Lhc promoter regions necessary for circadian expression. *Plant Mol Biol* 38(4):655–662. <https://doi.org/10.1023/A:1006094015513>
- Rose AB, Emami S, Bradnam K, Korf I (2011) Evidence for a DNA-based mechanism of intron-mediated enhancement. *Front Plant Sci* 2:98. <https://doi.org/10.3389/fpls.2011.00098>
- Ruan W, Guo M, Cai L, Hu H, Li C, Liu Y, Wu Z, Mao C, Yi K, Wu P, Mo X (2015) Genetic manipulation of a high-affinity PHR1 target cis-element to improve phosphorous uptake in *Oryza sativa* L. *Plant Mol Biol* 87(4–5):429–440. <https://doi.org/10.1007/s11103-015-0289-y>
- Ruan W, Guo M, Wu P, Yi K (2017) Phosphate starvation induced OsPHR4 mediates Pi-signaling and homeostasis in rice. *Plant Mol Biol* 93(3):327–340. <https://doi.org/10.1007/s11103-016-0564-6>
- Rubio V, Linhares F, Solano R, Martín AC, Iglesias J, Leyva A, Paz-Ares J (2001) A conserved MYB transcription factor involved in phosphate starvation signaling both in vascular plants and in unicellular algae. *Genes Dev* 15(16):2122–2133. <https://doi.org/10.1101/gad.204401>
- Schünmann PH, Richardson AE, Smith FW, Delhaize E (2004a) Characterization of promoter expression patterns derived from the Pht1 phosphate transporter genes of barley (*Hordeum vulgare* L.). *J Exp Bot* 55(398):855–865. <https://doi.org/10.1093/jxb/erh103>
- Schünmann PH, Richardson AE, Vickers CE, Delhaize E (2004b) Promoter analysis of the barley Pht1;1 phosphate transporter gene identifies regions controlling root expression and responsiveness to phosphate deprivation. *Plant Physiol* 136(4):4205–4214. <https://doi.org/10.1104/pp.104.045823>
- Secco D, Jabnour M, Walker H, Shou H, Wu P, Poirier Y, Whelan J (2013) Spatio-temporal transcript profiling of rice roots and shoots in response to phosphate starvation and recovery. *Plant Cell* 25(11):4285–4304. <https://doi.org/10.1105/tpc.113.117325>
- Smoczynska A, Segal P, Stepień A, Knop K, Jarmolowski A, Pacak A, Szweykowska-Kulinska Z (2019) miRNA detection by stem-loop RT-qPCR in studying microRNA biogenesis and microRNA responsiveness to abiotic stresses. *Methods Mol Biol* 1932:131–150. https://doi.org/10.1007/978-1-4939-9042-9_10
- Sobkowiak L, Bielewicz D, Malecka EM, Jakobsen I, Albrechtsen M, Szweykowska-Kulinska Z, Pacak A (2012) The role of the P1BS element containing promoter-driven genes in Pi transport and homeostasis in plants. *Front Plant Sci* 3:58. <https://doi.org/10.3389/fpls.2012.00058>
- Sonenberg N (1994) mRNA translation: influence of the 5' and 3' untranslated regions. *Curr Opin Genet Dev* 4(2):310–315. [https://doi.org/10.1016/s0959-437x\(05\)80059-0](https://doi.org/10.1016/s0959-437x(05)80059-0)
- Sun L, Song L, Zhang Y, Zheng Z, Liu D (2016) Arabidopsis PHL2 and PHR1 act redundantly as the key components of the central regulatory system controlling transcriptional responses to phosphate starvation. *Plant Physiol* 170(1):499–514. <https://doi.org/10.1104/pp.15.01336>
- Tang Z, Sadka A, Morishige DT, Mullet JE (2001) Homeodomain leucine zipper proteins bind to the phosphate response domain of the soybean VspB tripartite promoter. *Plant Physiol* 125(2):797–809. <https://doi.org/10.1104/pp.125.2.797>
- Thody J, Folkes L, Medina-Calzada Z, Xu P, Dalmay T, Moulton V (2018) PAREsnip2: a tool for high-throughput prediction of small RNA targets from degradome sequencing data using configurable targeting rules. *Nucleic Acids Res* 46(17):8730–8739. <https://doi.org/10.1093/nar/gky609>
- Thum KE, Kim M, Morishige DT, Eibl C, Koop HU, Mullet JE (2001) Analysis of barley chloroplast psbD light-responsive promoter elements in transplastomic tobacco. *Plant Mol Biol* 47(3):353–366. <https://doi.org/10.1023/A:1011616400264>
- Todd CD, Zeng P, Huete AM, Hoyos ME, Polacco JC (2004) Transcripts of MYB-like genes respond to phosphorous and nitrogen deprivation in Arabidopsis. *Planta* 219(6):1003–1009. <https://doi.org/10.1007/s00425-004-1305-7>
- Truernit E, Bauby H, Dubreucq B, Grandjean O, Runions J, Barthélémy J, Palauqui JC (2008) High-resolution whole-mount imaging of three-dimensional tissue organization and gene expression enables the study of phloem development and structure in Arabidopsis. *Plant Cell* 20:1494–1503. <https://doi.org/10.1105/tpc.107.056069>
- Vance CP, Uhde-Stone C, Allan DL (2003) Phosphorus acquisition and use: critical adaptations by plants for securing a nonrenewable resource. *New Phytol* 157(3):423–447. <https://doi.org/10.1046/j.1469-8137.2003.00695.x>
- Wang C, Huang W, Ying Y, Li S, Secco D, Tyerman S, Whelan J, Shou H (2012) Functional characterization of the rice SPX-MFS family reveals a key role of OsSPX-MFS1 in controlling phosphate homeostasis in leaves. *New Phytol* 196(1):139–148. <https://doi.org/10.1111/j.1469-8137.2012.04227.x>
- Wang J, Sun J, Miao J, Guo J, Shi Z, He M, Chen Y, Zhao X, Li B, Han F, Tong Y, Li Z (2013) A phosphate starvation response regulator Ta-PHR1 is involved in phosphate signalling and increases grain yield in wheat. *Ann Bot* 111(6):1139–1153. <https://doi.org/10.1093/aob/mct080>
- Wykoff DD, Grossman AR, Weeks DP, Usuda H, Shimogawara K (1999) Psl1, a nuclear localized protein that regulates phosphorus metabolism in Chlamydomonas. *Proc Natl Acad Sci USA* 96(26):15336–15341. <https://doi.org/10.1073/pnas.96.26.15336>

- Yang XJ, Finnegan PM (2010) Regulation of phosphate starvation responses in higher plants. *Ann Bot* 105(4):513–526. <https://doi.org/10.1093/aob/mcq015>
- Zhou J, Jiao F, Wu Z, Li Y, Wang X, He X, Zhong W, Wu P (2008) OsPHR2 is involved in phosphate-starvation signaling and

excessive phosphate accumulation in shoots of plants. *Plant Physiol* 146(4):1673–1686. <https://doi.org/10.1104/pp.107.111443>

Publisher's Note Springer Nature remains neutral with regard to jurisdictional claims in published maps and institutional affiliations.

Poznań, 28.09.2020

Mgr Paweł Sega
Uniwersytet im. Adama Mickiewicza w Poznaniu
Instytut Biologii Molekularnej i Biotechnologii
Zakład Ekspresji Genów
ul. Uniwersytetu Poznańskiego 6
61-614 Poznań
e-mail: pawel.sega@amu.edu.pl

Oświadczenie określające wkład w powstanie artykułu

Niniejszym oświadczam, że mój wkład w powstanie poniższego artykułu:

Paweł Sega, Katarzyna Kruszką, Łukasz Szewc, Zofia Szweykowska-Kulińska, Andrzej Pacak. 2020. Identification of transcription factors that bind to the 5'-UTR of the barley *PHO2* gene. *Plant Mol Biol* 102(1-2):73-88.

polegał na: wykonaniu niemal wszystkich eksperymentów, w tym: odkrycie motywów DNA w obrębie regionu 5'-UTR genu *PHO2*, przygotowanie bibliotek cDNA do systemu jednohybrydowego drożdży, przygotowanie konstruktów (w tym również do mikroskopii), odkrycie nowego białka APL oddziałującego z regionem 5-UTR genu *PHO2*, nadanie nazwy białku na podstawie analiz filogenetycznych, nadekspresja białek, oczyszczanie białek, określenie oddziaływania białko:DNA przy użyciu EMSY, analizie ekspresji genów techniką ddPCR, analizie aktywności promotora oraz regionu 5'-UTR w tytoniu, analizie aktywności intronów, analizy bioinformatyczne otrzymanych wyników, stworzeniu konceptu pracy, napisaniu publikacji, zaprojektowaniu oraz wykonaniu figur znajdujących się w publikacji, korekcie manuskryptu po ocenach recenzentów


Paweł Sega

Poznań, 03.03.2021

Dr Katarzyna Kruszka
Uniwersytet im. Adama Mickiewicza w Poznaniu
Instytut Biologii Molekularnej i Biotechnologii
Zakład Ekspresji Genów
ul. Uniwersytetu Poznańskiego 6
61-614 Poznań
e-mail: katarzyna.kruszka@amu.edu.pl

Oświadczenie określające wkład w powstanie artykułu

Niniejszym oświadczam, że mój wkład w powstanie poniższego artykułu:

Paweł Sega, **Katarzyna Kruszka**, Łukasz Szewc, Zofia Szweykowska-Kulińska, Andrzej Pacak. 2020. Identification of transcription factors that bind to the 5'-UTR of the barley *PHO2* gene. *Plant Mol Biol* 10(12):1018.

polegał na: edycji manuskryptu

Katarzyna Kruszka

Poznań, 28.09.2020

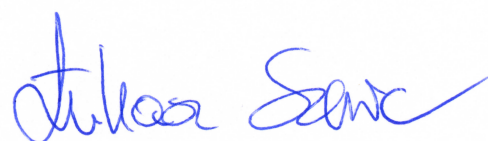
Łukasz Szewc
Uniwersytet im. Adama Mickiewicza w Poznaniu
Instytut Biologii Molekularnej i Biotechnologii
Zakład Ekspresji Genów
ul. Uniwersytetu Poznańskiego 6
61-614 Poznań
e-mail: luksze1@amu.edu.pl

Oświadczenie określające wkład w powstanie artykułu

Niniejszym oświadczam, że mój wkład w powstanie poniższego artykułu:

Paweł Segal, Katarzyna Kruska, **Łukasz Szewc**, Zofia Szweykowska-Kulińska, Andrzej Pacak. 2020. Identification of transcription factors that bind to the 5'-UTR of the barley *PHO2* gene. *Plant Mol Biol* 10(12):1018.

polegał na: wykonaniu analiz mikroskopowych celem sprawdzenia lokalizacji białek rekombinowanych, GFP-PHR1 oraz GFP-APL -
- w izolowanych protoplastach z jęczmienia.



Poznań, 03.03.2021

Prof. dr hab. Zofia Szweykowska-Kulińska
Uniwersytet im. Adama Mickiewicza w Poznaniu
Instytut Biologii Molekularnej i Biotechnologii
Zakład Ekspresji Genów
ul. Uniwersytetu Poznańskiego 6
61-614 Poznań
e-mail: zofia.szweykowska-kulinska@amu.edu.pl

Oświadczenie określające wkład w powstanie artykułu

Niniejszym oświadczam, że mój wkład w powstanie poniższego artykułu:

Paweł Sega, Katarzyna Kruszką, Łukasz Szewc, **Zofia Szweykowska-Kulińska**, Andrzej Pacak. 2020. Identification of transcription factors that bind to the 5'-UTR of the barley *PHO2* gene. *Plant Mol Biol* 10(12):1018.

polegał na: dyskusji uzyskanych wyników i korekty manuskryptu

Zofia Szweykowska-Kulińska

Poznań, 28.09.2020

Dr hab. Andrzej Pacak, Prof. UAM
Uniwersytet im. Adama Mickiewicza w Poznaniu
Instytut Biologii Molekularnej i Biotechnologii
Zakład Ekspresji Genów
ul. Uniwersytetu Poznańskiego 6
61-614 Poznań
e-mail: apacak@amu.edu.pl

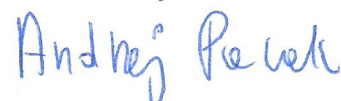
Oświadczenie określające wkład w powstanie artykułu

Niniejszym oświadczam, że mój wkład w powstanie poniższego artykułu:

Paweł Sega, Katarzyna Kruszka, Łukasz Szewc, Zofia Szweykowska-Kulińska, **Andrzej Pacak**. 2020. Identification of transcription factors that bind to the 5'-UTR of the barley *PHO2* gene. *Plant Mol Biol* 10(12):1018.

polegał na: przygotowaniu grantu w ramach, którego były realizowane publikowane badania, edytowaniu manuskryptu, wykonaniu bibliotek degradomowych oraz transkryptomowych do głębokiego sekwencjonowania.

Andrzej Pacak



Supplemental Table 1. List of proteins obtained from Y1H experiments

Fragment pPHO2_1 (Proximal promoter)			
Lp	Protein name	Acc. No.	Confirmation
1	TFIID, transcription initiation factor TFIID subunit 2	AK374504	-
2	PGL4, 6-Phosphogluconolactonase 4	AK368025	-
3	COV 2-like, Continuous vascular ring	AK369087	-
4	HSP90, Activator of 90kDA heat shock protein ATPase-like	AK363076	-
5	H-ACA, H/ACA ribonucleoprotein complex subunit1-like protein 1	AK353763	-
6	PMT13, probable methyltransferase	AK365482	-

Fragment pPHO2_2 (Proximal promoter)			
Lp	Protein name	Acc. No.	Confirmation
1	<i>No colonies</i>		

Fragment pPHO2_3 (Proximal promoter)			
Lp	Protein name	Acc. No.	Confirmation
1	<i>No colonies</i>		

Fragment pPHO2_4 (5'-UTR)			
Lp	Protein name	Acc. No.	Confirmation
1	APL	AK357363	+
2	PHR1	AK358314	+
3	Uncharacterized protein (potential MYB-like TF)	AK373372	-
4	Squalene monooxygenase	AK355681	-
5	Polyadenylate-binding protein RBP47-like	AK362249	-
6	Oxygen evolving protein	AK354253	-
7	PSMD1, 26S proteasome non-ATPase regulatory subunit 1	AK361326	-

Fragment pPHO2_5 (5'-UTR)			
Lp	Protein name	Acc. No.	Confirmation
1	Uncharacterized protein (potential E3 Cullin Ligase)	AK358608	-
2	Uncharacterized protein (potential histone H2B)	AK375744	-
3	APL	AK357363	+
4	PHR1	AK358314	+

(+) indicates positive interaction confirmed afterwards via full-length CDSs

(-) indicates potential false positives

Supplemental Table 2. Synthetic oligonucleotides used for EMSA experiments

Name	Sequence (5'-3')	Description
PS132-F	5'-BIOTIN- CAGGAATATGCTTGGAGATGCCATTCCCAGGAATATGCTTGGAGATGCCATTCCCAGGAATATGCTTGGAGATGCCATTCC-3'	Fragment pPHO2_4 Forward+5' BIOTIN
PS133-R	5'-BIOTIN- GGAATGGCATCTCCAAGCATATTCTGGGAATGGCATCTCCAAGCATATTCTGGGAATGGCATCTCCAAGCATATTCTG -3'	Fragment pPHO2_4 Reverse+5'BIOTIN
PS134-F	5'-BIOTIN- CAGTTCGCGGATTGGAGGCTTGACTCCAGTTCGCGGATTGGAGGCTTGACTCCAGTTCGCGGATTGGAGGCTTGACTCC-3'	Mutated fragment pPHO2_4 Forward+5' BIOTIN
PS135-R	5'-BIOTIN- GGAGTCAAGCCTCCAATCCGCGAACTGGGAGTCAAGCCTCCAATCCGCGAACTGGGAGTCAAGCCTCCAATCCGCGAACTG-3'	Mutated fragment pPHO2_4 Reverse+5'BIOTIN
PS136-F	5'-CAGGAATATGCTTGGAGATGCCATTCCCAGGAATATGCTTGGAGATGCCATTCCCAGGAATATGCTTGGAGATGCCATTCC-3'	Fragment pPHO2_4 Forward, unlabeled
PS137-R	5'-GGAATGGCATCTCCAAGCATATTCTGGGAATGGCATCTCCAAGCATATTCTGGGAATGGCATCTCCAAGCATATTCTG-3'	Fragment pPHO2_4 Reverse, unlabeled
PS138-F	5'-CAGTTCGCGGATTGGAGGCTTGACTCCAGTTCGCGGATTGGAGGCTTGACTCCAGTTCGCGGATTGGAGGCTTGACTCC-3'	Mutated fragment pPHO2_4 Forward, unlabeled
PS139-R	5'-GGAGTCAAGCCTCCAATCCGCGAACTGGGAGTCAAGCCTCCAATCCGCGAACTGGGAGTCAAGCCTCCAATCCGCGAACTG-3'	Mutated fragment pPHO2_4 Reverse, unlabeled
PS319-F	5'-BIOTIN- TTGGGTGGTGGCATATTCTCTGATGGCTTGGGTGGTGGCATATTCTCTGATGGCTTGGGTGGTGGCATATTCTCTGATGGC-3'	Fragment pPHO2_5 Forward+5' BIOTIN
PS320-R	5'-BIOTIN- GCCATCAGAGAATATGCCACCACCAAGCCATCAGAGAATATGCCACCACCAAGCCATCAGAGAATATGCCACCACCA-3'	Fragment pPHO2_5 Reverse+5' BIOTIN
PS321-F	5'-TTGGGTGGTGGCATATTCTCTGATGGCTTGGGTGGTGGCATATTCTCTGATGGCTTGGGTGGTGGCATATTCTCTGATGGC-3'	Fragment pPHO2_5 Forward, unlabeled
PS322-R	5'-GCCATCAGAGAATATGCCACCACCAAGCCATCAGAGAATATGCCACCACCAAGCCATCAGAGAATATGCCACCACCA-3'	Fragment pPHO2_5 Reverse, unlabeled
PS323-F	5'-BIOTIN- TTGGGTGGTGGATTCAAGTCTGATGGCTTGGGTGGTGGATTCAAGTCTGATGGCTTGGGTGGTGGATTCAAGTCTGATGGC-3'	Mutated fragment pPHO2_5 Forward+5' BIOTIN
PS324-R	5'-BIOTIN- GCCATCAGACTTGAATCCACCACCAAGCCATCAGACTTGAATCCACCACCAAGCCATCAGACTTGAATCCACCACCA-3'	Mutated fragment pPHO2_5 Reverse+5'BIOTIN
PS325-F	5'-TTGGGTGGTGGATTCAAGTCTGATGGCTTGGGTGGTGGATTCAAGTCTGATGGCTTGGGTGGTGGATTCAAGTCTGATGGC-3'	Mutated fragment pPHO2_4 Forward, unlabeled
PS326-R	5'-GCCATCAGACTTGAATCCACCACCAAGCCATCAGACTTGAATCCACCACCAAGCCATCAGACTTGAATCCACCACCA-3'	Mutated fragment pPHO2_4 Reverse, unlabeled
PS327-F	5'-BIOTIN-CAGGAATATGCTTGCAGGAATATGCTTGCAGGAATATGCTTG-3'	Fragment pPHO2_4-derived P1BS motif Forward+5' BIOTIN
PS328-R	5'-BIOTIN-CAAGCATATTCTGCAAGCATATTCTGCAAGCATATTCTG-3'	Fragment pPHO2_4-derived P1BS motif Reverse+5' BIOTIN
PS329-F	5'-CAGGAATATGCTTGCAGGAATATGCTTGCAGGAATATGCTTG-3'	Fragment pPHO2_4-derived P1BS motif Forward, unlabeled
PS330-R	5'-CAAGCATATTCTGCAAGCATATTCTGCAAGCATATTCTG-3'	Fragment pPHO2_4-derived P1BS motif Reverse, unlabeled
PS331-F	5'-BIOTIN-CAGTTCGCGGATTGCAGTTCGCGGATTGCAGTTCGCGGATTG-3'	Mutated fragment pPHO2_4-derived P1BS motif Forward+5' BIOTIN

PS332-R	5'-BIOTIN-CAATCCGCGAACTGCAATCCGCGAACTGCAATCCGCGAACTG-3'	Mutated fragment pPHO2_4-derived P1BS motif Reverse+5' BIOTIN
PS333-F	5'-CAGTTCGCGGATTGCAGTTCGCGGATTGCAGTTCGCGGATTG-3'	Mutated fragment pPHO2_4-derived P1BS motif Forward, unlabeled
PS334-R	5'-CAATCCGCGAACTGCAATCCGCGAACTGCAATCCGCGAACTG-3'	Mutated fragment pPHO2_4-derived P1BS motif Reverse, unlabeled
PS335-F	5'-BIOTIN-GAGATGCCATTCCGAGATGCCATTCCGAGATGCCATTCC-3'	Fragment pPHO2_4-derived P-resp PHO motif Forward+5' BIOTIN
PS336-R	5'-BIOTIN-GGAATGGCATCTCGGAATGGCATCTCGGAATGGCATCTC-3'	Fragment pPHO2_4-derived P-resp PHO motif Reverse+5' BIOTIN
PS337-F	5'-GAGATGCCATTCCGAGATGCCATTCCGAGATGCCATTCC-3'	Fragment pPHO2_4-derived P-resp PHO motif Forward, unlabeled
PS338-R	5'-GGAATGGCATCTCGGAATGGCATCTCGGAATGGCATCTC-3'	Fragment pPHO2_4-derived P-resp PHO motif Reverse, unlabeled
PS339-F	5'-BIOTIN-GAGGCTTGACTCCGAGGCTTGACTCCGAGGCTTGACTCC-3'	Mutated fragment pPHO2_4-derived P-resp PHO motif Forward+5' BIOTIN
PS340-R	5'-BIOTIN-GGAGTCAAGCCTCGGAGTCAAGCCTCGGAGTCAAGCCTC-3'	Mutated fragment pPHO2_4-derived P-resp PHO motif Reverse+5' BIOTIN
PS341-F	5'-GAGGCTTGACTCCGAGGCTTGACTCCGAGGCTTGACTCC-3'	Mutated fragment pPHO2_4-derived P-resp PHO motif Forward, unlabeled
PS342-R	5'-GGAGTCAAGCCTCGGAGTCAAGCCTCGGAGTCAAGCCTC-3'	Mutated fragment pPHO2_4-derived P-resp PHO motif Reverse, unlabeled

Supplemental Table 3. List of selected proteins used for the phylogenetic analysis of the HvAPL TF

Name	Description	GenBank	Organism
HvAPL	APL predicted protein	BAJ88577	<i>Hordeum vulgare</i>
AtaAPL	Myb family transcription factor APL-like isoform X1	XP_020150563	<i>Aegilops tauschii</i>
AtaMyb	Uncharacterized myb-related protein	AEV91195	<i>Aegilops tauschii</i>
TuAPL	Myb family transcription factor APL	TEMS60802	<i>Triticum urartu</i>
PhAPL	Myb family transcription factor APL	XP_025799290	<i>Panicum hallii</i>
DoAPL	Myb family transcription factor APL	OEL24427	<i>Dichanthelium oligosanthes</i>
SiAPL	Myb family transcription factor APL	XP_004951748	<i>Setaria italica</i>
BdAPL	Myb family transcription factor APL isoform X1	XP_003570345	<i>Brachypodium distachyon</i>
PmAPL	Myb family transcription factor APL	RLN08131	<i>Panicum miliaceum</i>
SbAPL	Myb family transcription factor APL isoform X1	XP_021314094	<i>Sorghum bicolor</i>
ZmUp	Uncharacterized protein Zm00014a_016771	PWZ24855	<i>Zea mays</i>
ZmAPL	Myb family transcription factor APL isoform X1	XP_008645294	<i>Zea mays</i>
OsMyb	Myb family transcription factor-like	BAD26189	<i>Oryza sativa Japonica Group</i>
OsAPL	Myb family transcription factor APL isoform X1	XP_015624013	<i>Oryza sativa Japonica Group</i>
VvAPL	Potential APL-like transcription factor	RVW36819	<i>Vitis vinifera</i>
HvPHR2	Predicted HvPHR2 protein	BAJ94688	<i>Hordeum vulgare</i>
HvPHR1	Predicted HvPHR1 protein	BAJ89528	<i>Hordeum vulgare</i>
TaPHR1	Predicted TaPHR1 protein	AGG55850	<i>Triticum aestivum</i>
BdPHR1	Predicted BdPHR1 protein	XP_010228678	<i>Brachypodium distachyon</i>
ZmPi	Uncharacterized phosphate starvation protein	AEH96380	<i>Zea mays</i>
AthPHL1	Potential AtPHL1 protein	NP_568512	<i>Arabidopsis thaliana</i>
AthPp	Potential homeodomain-like superfamily protein	NP_849905	<i>Arabidopsis thaliana</i>
AthPHR1	Predicted AtPHR1 protein	NP_194590	<i>Arabidopsis thaliana</i>
OsPHR1	Predicted OsPHR1 protein	B8ANX9	<i>Oryza sativa Japonica Group</i>
OsPHR2	Predicted OsPHR2 protein	XP_015647735	<i>Oryza sativa Japonica Group</i>
OsPHR3	Predicted OsPHR3 protein	A2X0Q0	<i>Oryza sativa Japonica Group</i>
OsPHR4	Predicted OsPHR4 protein	XP_015644151	<i>Oryza sativa Japonica Group</i>
AtPHL2	Potential AtPHL2 protein	NP_566744	<i>Arabidopsis thaliana</i>
AthNSR1	Predicted NSR1 (Nitrogen Stress Response 1) Protein	NP_001118567	<i>Arabidopsis thaliana</i>
HvMyb	Potential Myb family transcription factor	BAJ96936	<i>Hordeum vulgare</i>

Supplemental Table 4. Primers used in this paper

Name	Sequence (5'-3')	Product size (bp)	Destiny
PS361-F	GAAGAGGTCCAGCCAGTACG	195	<i>Primers for ddPCR gene expression analysis of HvAPL</i>
PS362-R	CCTCTGCTCCCAGTTGAGTC		
PS496-F	TGTAGAAACCCCAACCCGTG	111	<i>Primers for ddPCR gene expression analysis of GUS reporter gene</i>
PS500-R	TCTTGTAACGCGCTTTCCAC		
PS498-F	ATTTGCGCTCCAACAATGTC	104	<i>Primers for ddPCR gene expression analysis of HygR</i>
PS499-R	GATGTTGGCGACCTCGTATT		
APO387-F	CGTGACGCTGTGTTGCTTGT	61	<i>Primers for ddPCR gene expression analysis of HvARF1</i>
APO388-R	CCGCATTATCATGCATTAGG		
APO700-F	CAAAGGCAACTGACGAGTGA	187	<i>Primers for ddPCR gene expression analysis of HvPHR1</i>
APO701-R	ATGACTGAGGAGCGAAAGGA		
APO792-F	GCGAACCTCCTTTGACACTAA	115	<i>Primers for ddPCR gene expression analysis of HvPHO2</i>
APO793-F	GCACACTTTAGTCCTAATGCC		
PS72-F	CGGAATTCATGAGGAGGTGTGATCTGAGACAG	1356	<i>Primers for amplification of HvPHR1 full-length coding sequence and cloning via EcoRI site into pGADT7 vector</i>
PS73-R	CGGGATCCTTAACATCATGCACCCTTCGG		
PS154-F	CGGAATTCATGTTCTCTTCCAAGAAGGCCAC	1107	<i>Primers for amplification of HvAPL full-length coding sequence and cloning via EcoRI site into pGADT7 vector</i>
PS155-R	CGGGATCCTTACCCGTAGATCACCGACGG		
PS391-F	ATAAGAATGCGGCCGCcATGAGGAGGTGTGATCTGAGACAG	1356	<i>Primers for amplification of HvPHR1 full-length coding sequence and cloning via NdeI/AscI sites into pENTR/SD/D-Topo vector</i>
PS392-R	TTGGCGCGCCcTTAACTATCATGCACCCTTCGGCA		
PS393-R	TTGGCGCGCCcACTATCATGCACCCTTCGGCA	1353	<i>Reverse primer for amplification of HvPHR1 full-length coding sequence (without STOP codon) and cloning via NdeI/AscI sites into pENTR/SD/D-Topo vector</i>
PS393-F	ATAAGAATGCGGCCGCcATGTTCTCTTCCAAGAAGGCCAC	1107	<i>Primers for amplification of HvAPL full-length coding sequence and cloning via NdeI/AscI sites into pENTR/SD/D-Topo vector</i>
PS395-R	TTGGCGCGCCcTTACCCGTAGATCACCGACGG		
PS396-R	TTGGCGCGCCcCCCGTAGATCACCGACGG	1104	<i>Reverse primer for amplification of HvAPL full-length coding sequence (without STOP codon) and cloning via NdeI/AscI sites into pENTR/SD/D-Topo vector</i>

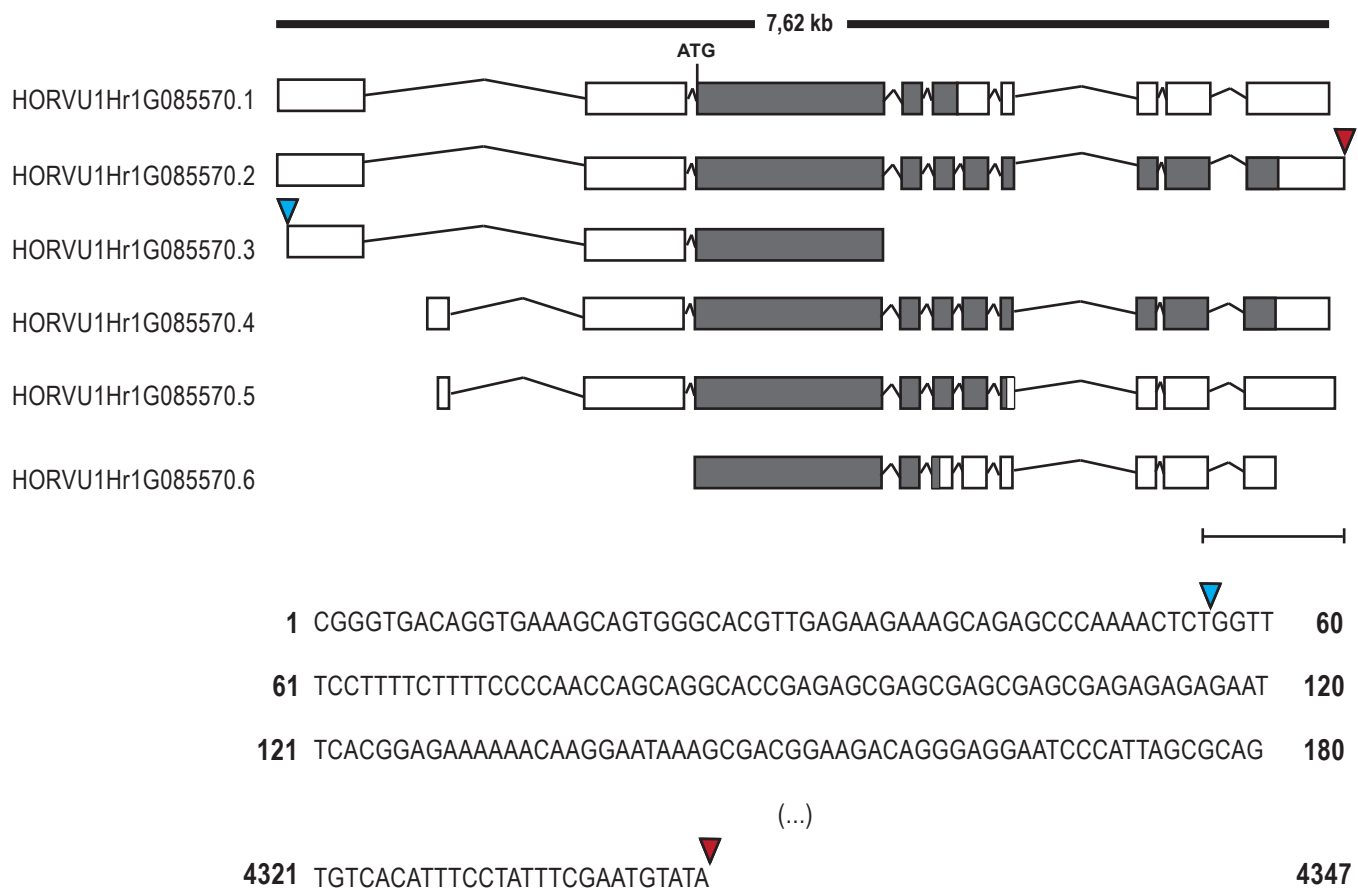
*The yellow mark indicates nucleotides used for restriction cloning

*The red font colour indicates additional nucleotides necessary to maintain the right ORF after cloning

Supplemental Table 5. Y1H “bait” sequences derived from *PHO2* gene fragments used for screening. The grey colour indicates the presence of motifs, which are described in Table 1

Y1H part	Sequence 5’-3’	Genomic location
1	GTGTAGATTCACTCATTTTGCTTCGTATATAGTCTGTAGTGGGAATCTCTAAAAAGACTTATATTTAGGAATGATGGGA GTAAATTACATGCATTGATCCTTCAATTAATAGATGAAGTCTAATTAATATGCATG	chr1 from 535890253 to 535890386 (+)
2	CTTATAGAGAATATGGCACCTCCGGAATGAGCTGGTACATGGTAAATCAATCCCTCCGACAGAGGTATCCTGCTCCT TCCTCCTCAGCTACTATAACACCTTCAATCAGATTTACGGGGTGTGGATGAGATTATCAAGGGCAAGTCGCCGACG TTCTCTG	chr1 from 535890593 to 535890753 (+)
3	GCTACATGCTATTCTAGAAGGTATTAACTAACAATTGAACATTCCAACCCATAATCATGGTGCAATCAGACTGCGC CGTAGCCCTTAAAGCTATATCTG	chr1 from 535890967 to 535891067 (+)
4	CAGGAATATGCTTGGAGATGCCATTCC	chr1 from 535892276 to 535892302 (+)
5	TTGGGTGGTGGCATATTCCTCTGATGGC	chr1 from 535893616 to 535893642 (+)
P1BS	CAGGAATATGCTTG	chr1 from 535892276 to 535892289 (+)
PHO- element	GAGATGCCATTCC	chr1 from 535892289 to 535892302 (+)

*The grey mark indicates the presence of motifs, which are described in Table 1



Supplementary Fig. S1. The graph showing all six *PHO2* transcript variants from the Ensembl Plants database and RNA-Seq results.

There are six *PHO2* protein-coding transcripts that are present in the barley Ensembl Plants database: HORVU1Hr1G085570.1 (544 aa), HORVU1Hr1G085570.2 (847 aa), HORVU1Hr1G085570.3 (445 aa), HORVU1Hr1G085570.4 (847 aa), HORVU1Hr1G085570.5 (606 aa), and HORVU1Hr1G085570.6 (491 aa). The lower panel displays the cDNA sequences of the first 180 bp from the HORVU1Hr1G085570.1 variant and the last 26 bp of the HORVU1Hr1G085570.2 variant to show the 5' (blue arrow) and 3' (red arrows) ends obtained in our RNA-Seq analysis. The white boxes indicate the untranslated region, and the gray boxes indicate the coding region. Scale bar = 1000 bp.

>barley *PHO2* 5'-UTR genomic sequence

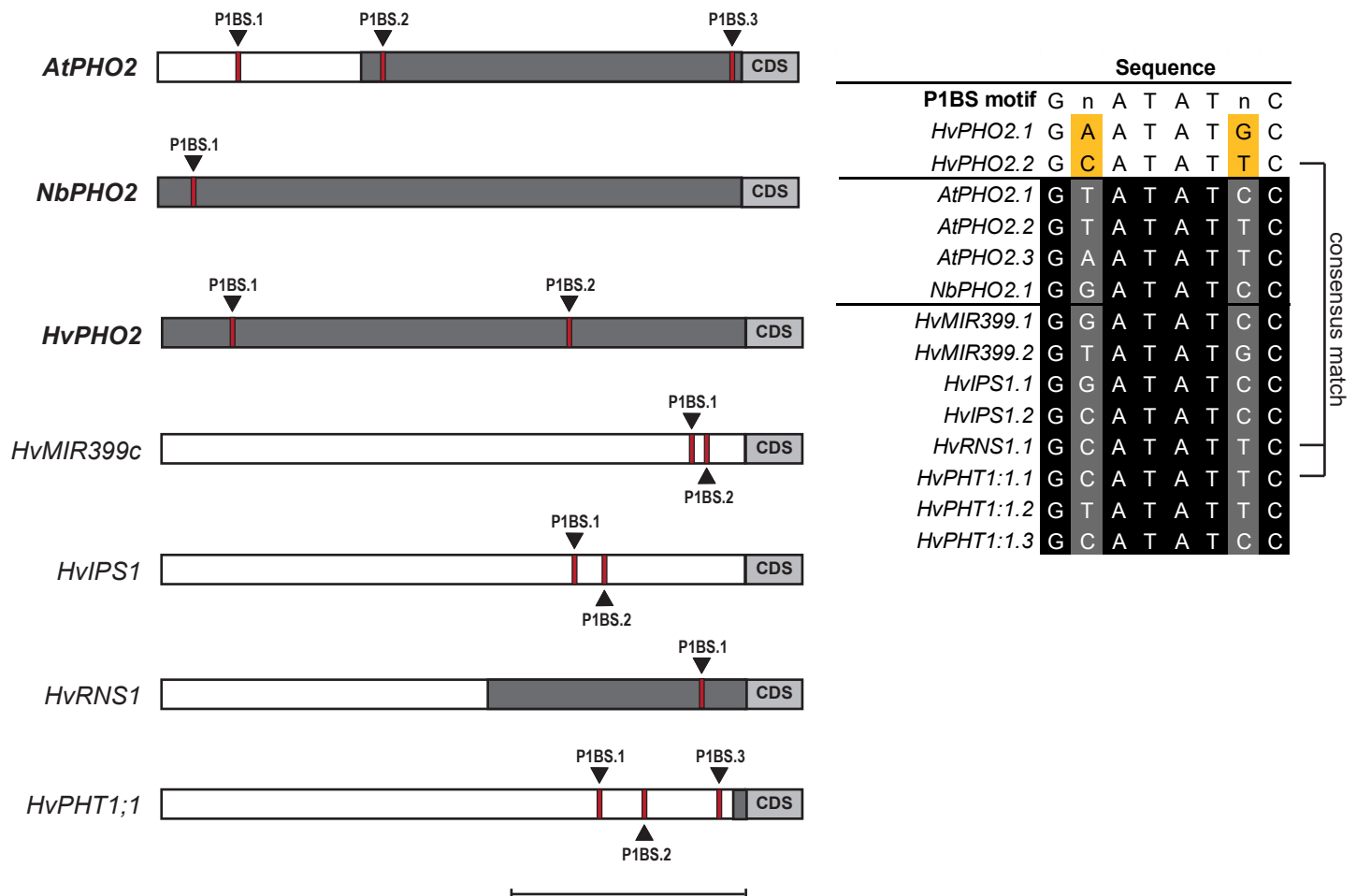
```

1 ATCATCATCCATCGTCGCCATTACGAGCAGCAGCGCCGAGCACCCAGCAGAGAAGCCTT 60
61 CCCGTTCCCTCTACCCTCTTTCTCCCTCTCCAGGCGCGCTCTCTCCTCCTCCCGCCGCCG 120
121 CGCCGCGCTGAGATTTGGTTCGGAGGAGGAGGAGGAGCAGGCGGCGGCGGCCGAGCTGGTC 180
181 GTTTCTTGGAGGGGGCGGAGGGGGGACGGGCTTGCTGGCCATGGTCCACGGGCTCCGGGAT 240
241 GGA CTGAGGCGCGGGGGGAGGGGAGGCCTGCTCCCTCTTCTTCA GTGACCGAGCGG CCAT 300
Kozak signal
301 GGCGGC GGGCTGGGCTTGGCACAG GTACTGCCAATCTGCCATTCTGAGCTCACTTTTTTC 360
361 CTATTCATTTGCGATTGCGAGTCGAGCCGCCGCCGCCGCCGCCGACTTCCCGACGGCGG 420
421 CCCTCCCTTTCTTTGCGCGCGCCCATGTGCTTGTTTACTACTCCTAGGAGGATGCGTGCA 480
481 CTCAAATGTCCGATTTCTAGTACAGCAGGAGCATATTAACTCGCACCGTCGGTGTCAT 540
541 GCCTGCAGGGCGAAATTTAGTCAGAACGATGCATGCCAATCCGAGAACATGGCCATCAAA 600
601 CCTACGCCACCCCGATTCTCGGAAACAG GAATATGC P1BS.1TTGGAG ATGCCAT PHO elementTCCGATCCGT 660
661 CTTGCCCCAATTCAGTTGTGCGAGCCCCCAACTAGATTGCGCAAACGTCCCTGTCTTCA 720
721 GTCTTGACCATGTGCAATCAAACAATATTATTACCCTGGGTCAGCCCAGATGGATTGGAC 780
781 ATAAGCAGGGGAGGCT*CTGGTAGTCTGGTTGAGCAGTAGTAGCTGAAGTGCTGAACACAG 840
841 CTTATCC CAGCGGCGACGCACACCGGCAACCTACCGTGGCGAAGGCGCCTCCGACCAGTA 900
901 AATTTGGGTGGCTCAG GTGTTATGTCGATGGTAGCTTCTTACAGTTTGTAGCGAAACATC 960
961 TGGGTTTTTGTGGCCGCGCGTAGGAATTGGTGGAGTGGATGATATTTTGCCGTTTTTCGGAT 1020
1021 GTGGTGGTATGGGGTGCAAGGTTTTAGTTTGTGCTTTTGTGTTGCCGGTTTTAGGAGAT 1080
1081 CATAATGAGCACGGAAGCTGTTGTTTTGATCGGATTTGTTTGGCAGGCTTATCCATAGGT 1140
1141 AGGTTGTCTTTTAGCTGTTTTCGGATCGGCTATGATGCTGAACTATGTGCTGCTTTGTCA 1200
1201 TCTTTGTTGTTGTTGCTATGAAAAGATCCAAAACCTTCCGTGTCGATATATAGAATCAATG 1260
1261 TTTGCTAGCTGAAAAC TAGGTTCTCAGATCAGACCAATTATACCCAGCCATGTTTTTGA 1320
1321 TTACATAATTTAATAAGTAGATAGTTTTGATACTCCAATCTCTATTTGTTGCGTTATGCT 1380
1381 TTAACATGGATTTT CAGCTGTTCCATCTATGT CAGTTTTTATTTT GCCCTGCCTATT CAC 1440
1441 GTGTTTGAAGGCATCCTAACATCTATTGGTGAAGAACCTTTTACCTGTTTATTTACAAA 1500
1501 TTTTTTAGCGATGTAAGCATGCAAGCGGTGTTAAAAGATAAACACACCATTCTGAACAAA 1560
1561 TTTTAGTTT CATGTCCACTGCGGGATTGATCCTTGTGACACAAATTGGCTCTTGCGCCTAC 1620
1621 TATGTGTTTTT TGAATAAATTCACAGGAAGTCTTTACGGATTAGTGTCTCTACTATTATT 1680
1681 GCACGATATCTACTTTTATATTATTAGATATCGTAAGTCTCTTACTATTATATGCTAGAA 1740
1741 TGTGCTAACATGGCCCTGATGCCCGCAGTTTTTTTTTTTACCATGAATTTTAATTAAGA 1800
1801 AATTGGTTTAACTTACAACCGTGTTTATTGAAACTATGCAAAAAAAGTCTATTTATCAA 1860
1861 CTCCAGTTGTGTTGTTCTATTAAGAAGATAAGCAGTTGGACTAACATTCTTTTGATATTA 1920
1921 TTGCAGGATCAGCTAATCTGAACAGTTGTTGGTTGAATATTGGTCATTGGGTGGTG P1BS.2GCAT 1980
1981 ATTCTCTGATGGCTTCTCATGTCTGGTGATCATCGAAAGCGAACACATTTCA TTCGGACT 2040
2041 TTCCTCTGGAAATCATCTCCTGTGACAATCCATTCCCTAGTTT TAGGGCAAATCTCCTTTG mir399 cleavage site 1 2100
2101 GCGCTGAACATTT CAGATAGT GACTGTTCTGTAGTTCTTCTGGAAGCTCCCTTGGCGAAC 2160
2161 ATTT CAGACAGT GACTGTTCTGTAAGTTCTT CGGGGCAAATCTCCTTTGGCA AACCTACC mir399 cleavage site 2 2220
2221 GATAGTT CGGGGCAAATCTCCTTTTGGCA AAACCTACCTACGTACCTATAG TTGCGGCAA mir399 cleavage site 3 2280
2281 ATCTCCTTTGGCA site 4 AATCTACCTAGTTCTTCTGATCTCCTTCTTACATATGCTTTCTCTT 2340
2341 CTGATTGCTCCCTGGACAAATCTCCTTCGACATTAGCTTTAGCTATCGATTGCTAT CTTG mir399 cleavage site 6 2400
2401 GCACTTCTCCTTTGGCA CTAGGTTTAGCGTCAGTCCTGTCTGGGCGAACCTCCTTTGACA 2460
2461 CTAAATCTTACTGTTTCTTATTTGCTAT CTGGGCAAATCTCCTTTGGCG GTTACTGTTAC mir399 cleavage site 5 2520
2521 TGTATCAGGGATCCTTTGGCATTAGGACTAAAGTGTGCTGACCTTACAAGTTGGTCGGAA 2580
2581 CTTAACCTGCTGTTCAAAGGCTGCTCCTGAGTTTATCATATCATCACAGAACACAGCTTG 2640
2641 TTACAAAAG GTGGGGACGAATTTAATCTAATATTTATGAACACAATTGGTTGTTTCATA 2700
2701 TCATACAAAATGACAAAATGTGGTGTGTCAG GGCTTGCAGAC START codon (+1) 2742

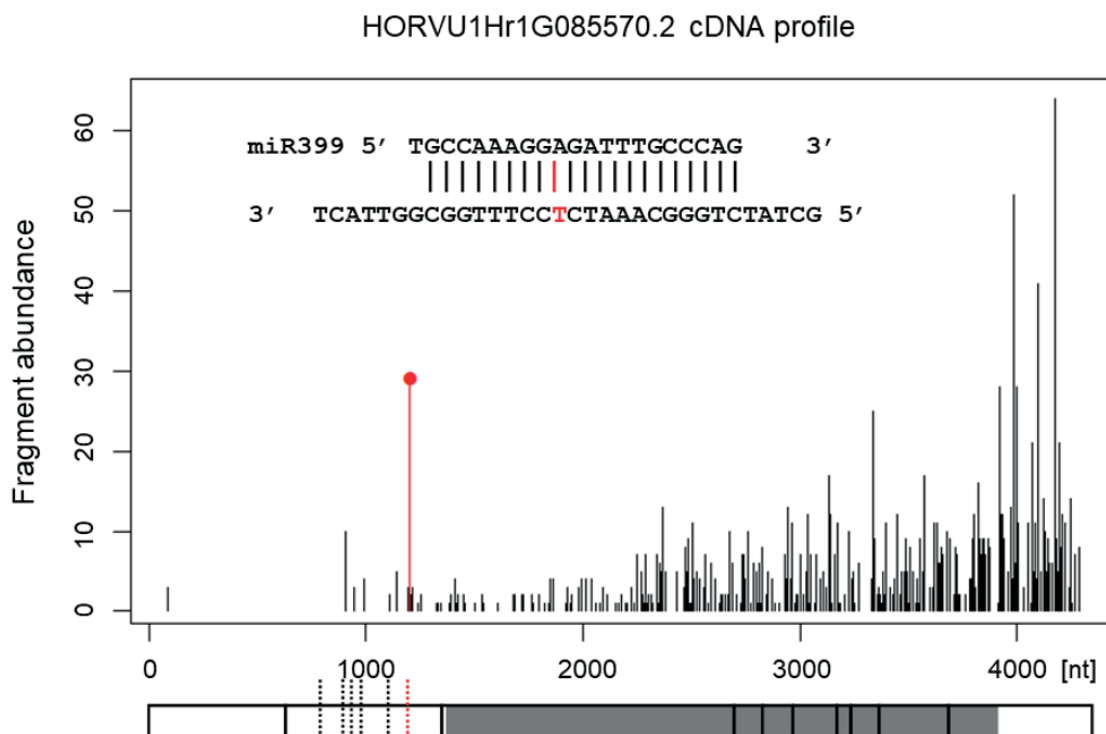
```

Supplementary Fig. S2. The genomic sequence of the barley *PHO2* 5'-UTR region used in this study.

The validated genomic sequence of the barley *PHO2* 5'-UTR region (2742 bp) that was cloned and sequenced from the Morex genotype (Ensembl Plants database: chr1H:535891650:535894391:1). Denoted are the *cis*-regulatory motifs that were identified in this study, in addition to six miR399 potential cleavage sites. The yellow boxes indicate the locations of exons. The black star indicates the additional exon within the 5'-UTR that is present only in barley *PHO2* isoforms 5 and 6.



Supplementary Fig. S3. The P1BS motif is evolutionarily conserved and present in various PSI genes in barley. The genomic localization of P1BS motifs within regulatory sequences of the barley Pi-starvation-responsive genes *PHO2*, *MIR399c*, *IPS1*, *RNS1*, and *PHT1;1*. The *Arabidopsis thaliana* (*AtPHO2*) and *Nicotiana benthamiana* (*NbPHO2*) *PHO2* gene orthologs were used as a reference to show the P1BS motif positions within barley *PHO2* regulatory sequences relative to those within the other plant species used in this study. The gray box depicts the 5'-UTR; the white box depicts the promoter; the red line indicates the position of the P1BS motif. Scale bar = 1000 bp (left). Comparison of the sequences of all P1BS motifs that are present in the left panel (right). The yellow box indicates the specific nucleotide within the motif consensus; the consensus match connects barley *PHO2* motifs with P1BS motifs that are the same but present within the regulatory sequences of other genes.



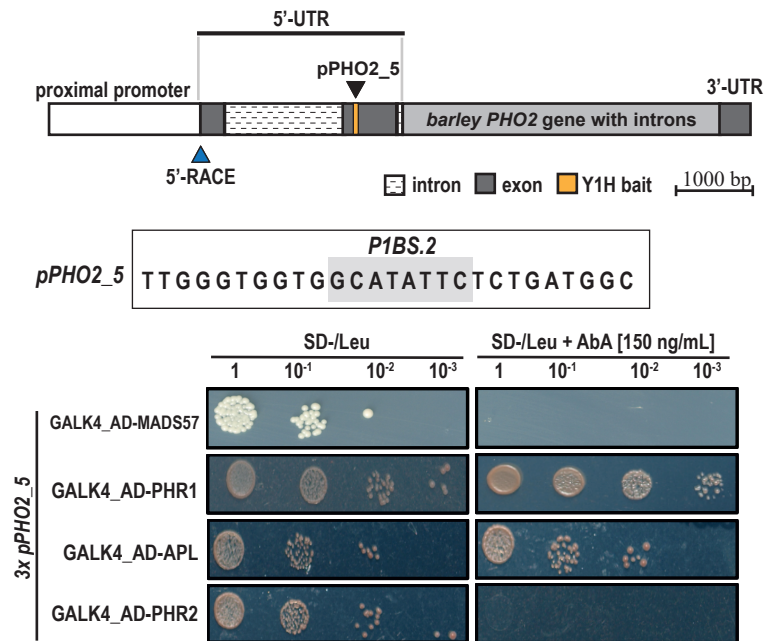
Supplementary Fig. S4. The barley *PHO2* transcript is cleaved within its 5'-UTR.

The red vertical line shows the cleavage position directed by miR399; the cleavage position 1203 is within exon No. 2 in the 5'-UTR of the *PHO2* transcript (HORVU1Hr1G085570.2, length of 4347 nt). The black vertical lines on the graph show the positions within the *PHO2* cDNA to which 20 nt degradome fragments (reads) were mapped. The number of such reads (fragment abundance) is depicted by the height of the red and black lines. Below the graph, the structure of the *PHO2* transcript is presented. The white boxes denote UTRs, the gray boxes denote CDSs, and the dotted vertical lines denote cleavage sites within the 5'-UTR.

Query_At3g04030	1	MYYNQH-----QGKNILS-----SSRMHITSERHPFLR-----
HvMYB-1_	1	ME-----
HvMYB-2_	1	MFSSKKA-----TS-----SSAGAVVAVQGE--R-----
HvPHR1_	1	MRRCDLRQCHNSRVSGMSSSLPILPNSLKETFHGPYNPQLTPMQRQLTSDFVPLYQSACPSATLPRAGAMRSSYSASL
HvPHR2_	1	-----
consensus	1	.
Query_At3g04030	30	-----GNSP----
HvMYB-1_	3	-----SCENNIGSN-----
HvMYB-2_	23	-----GAPICVQ-----
HvPHR1_	81	GYSANPLDSVPNHERQSMVAPFAPQSSDIEVFQALSNNIPGGHTEATWFPGSADSLSDYRDNIPAGSGSIQNSGPAITSD
HvPHR2_	1	-----
consensus	81	.
Query_At3g04030	34	GDSGLIL-----STDAKPERLKWTPDL
HvMYB-1_	12	DGPNSKA-----SLAAEQRLRWTDDEL
HvMYB-2_	31	GDSGLVL-----TDPKPERLRWTVEL
HvPHR1_	161	VVAKQNEWWADIMNDDWRDILDATAADPQSKSMVQPSNSAASQPAVNQPASSHGGEICNVASPPNGNSAAKQRMWRWTPDEL
HvPHR2_	1	-----MRWTPDEL
consensus	161*
Query_At3g04030	55	HERFTEAVNQLGGADKATPKTITKVMGIPGLTIYHKSHLQKYRLSKNLNGQANN-SFNKIGIMTMMEKTPDAETQSE
HvMYB-1_	33	HEQFEVAVTQLGGPDATPKGVLRIMGTPGLTIYHVKSHLQKYRLAKYIPIS-----SADGNKADNKDPGDSLA--
HvMYB-2_	52	HERFVDAVQLGGPDKATPKTITMRVMGVKGLTIYHKSHLQKRLKQPHKDFNDHAVKDAAAAMEMHNAASSGILGR
HvPHR1_	241	HECFVDSVNLGGSEKATPKGVLRIMKVDGLTIYHVKSHLQKYRTARYKPIV-----T-EGTADKRTTTEE--L--
HvPHR2_	8	HERFVDAVNLLGGSEKATPKGVLRIMKADNLTIIYHVKSHLQKYRTARYRPL-----S-EGSSERLEASKEDLP--
consensus	241	***.....*.....*.....*.....*.....*.....*.....*.....*.....*
Query_At3g04030	134	NLSIGPQPN-KNSPTGEALQMQIEVQRRLEQLEVQRRLQRLRIEAGQKYLQSVLEKAQETLCRQNLCAAG---IEAAKVQ
HvMYB-1_	102	----GLDGS-SGMQISEALRLQMEVQKRLHEQLEVQRQLQRLRIEAGQKYLKKIIEEQQR-FC-GIKS-----ETPG
HvMYB-2_	132	N-----NDRNVHMEARLQMEVQKRLHEQLEVQKRLQRLRIEAGQKYQSTIEKAYQTLATGIVASPTAGYKSLGSH
HvPHR1_	307	----TLDLK-SSVLDLALRLQMEVQKRLHEQLEVQRQLQRLRIEAGQKYLQMMFEKQSK-SN-TEK-----QDLS
HvPHR2_	76	----SIDLK-GNFDLALRLQLELQKRLHEQLEVQRSLQRLRIEAGKCLQIMTEQQCN-PA-ADKA-----LDAS
consensus	321*.....*.....*.....*.....*.....*.....*.....*
Query_At3g04030	210	LSELVSKVSAEYENSSFLPEKEL-----QNLCSQMQTNYPPDCSLESCLTSSBCTQKNSKMLENNRLGLRTYIGDST
HvMYB-1_	166	AGATVVIASSDQFPDSE-----RTDPSTPAPT-----SESASQCA-----AFKRD-S
HvMYB-2_	206	AGVLDVCSIKDIGPASMGFPSLQDLHLYGGGHLD-----LQQQQPMESFFACSDGGGIGS-----LGKKR
HvPHR1_	371	SGAT-TTSSDPHSA-----NRRNDRN-----DAED-----DLHRT-G
HvPHR2_	140	TSLEGSKLPSDPPSS-----T-----VK-----DVPNN-S
consensus	401*.....*.....*
Query_At3g04030	283	SECKEIMEEPLFQRMELTWTE-GLRCNPYISTMVSEAEQRISYSERSPGRLSIGVGLHGHSQHQQCNNEHDHKLLETNRNK
HvMYB-1_	206	GSQTEAIIKSECHDEPLLTADSNCHGSPTEISPKHERAA-----KRQRSSDAEFPEAELSLEPQ
HvMYB-2_	266	SSQYAGGKSEPMWGDDEDE-DDKGDQLIQMAPPMDDMSIAGVYEAKPMMTMSGDSTGSRGFDGGMG-SKLERPSPR
HvPHR1_	402	EN-----PVSAEI-GET-----SMHAGCNREMAETESSDEL
HvPHR2_	165	QN-----CTI-----ERAESCDK-----
consensus	481
Query_At3g04030	362	GMDSTTELDLNTHTVENYCTTRTKQFDLNGFSWN
HvMYB-1_	263	HI-----FESSSGPEFQQCSVPYFSGH
HvMYB-2_	344	RP-----HMGAQRMGSPSVIYG
HvPHR1_	432	AN-----TNDGSKAPQEKCRRVHD--S
HvPHR2_	178	-----E
consensus	561	

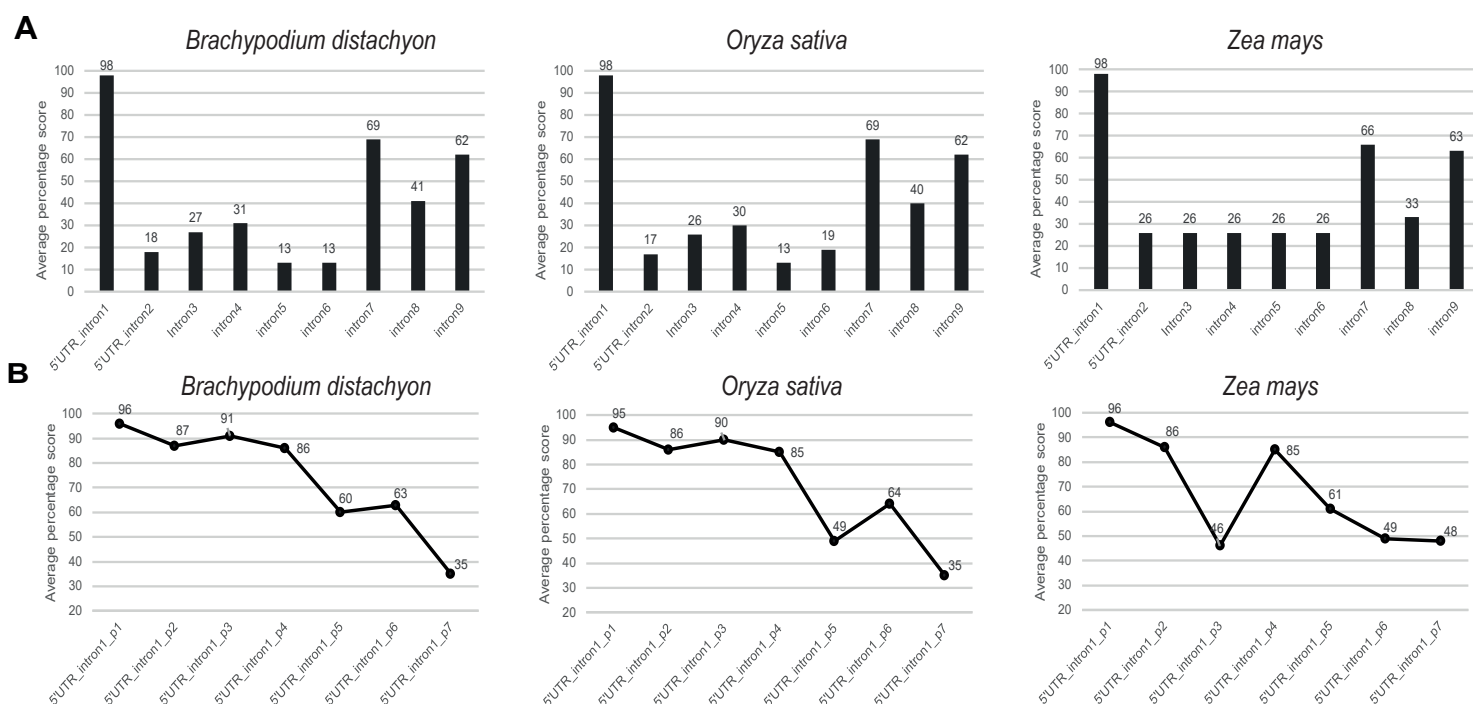
Supplementary Fig. S5. The multiple sequence alignment for PHR-like TFs in which the AtNSR1 protein sequence was used as a query.

On the basis of the results published by Todd and his group in 2004, we selected two MYB-like TFs (temporarily named MYB-1 and MYB-2) that exhibited the highest homology to the AtNSR1 protein (At3g04030) and analyzed them in a Y1H screening assay. The orange box indicates the SANT/MYB protein domain, and the green box indicates the MYB-CC domain.



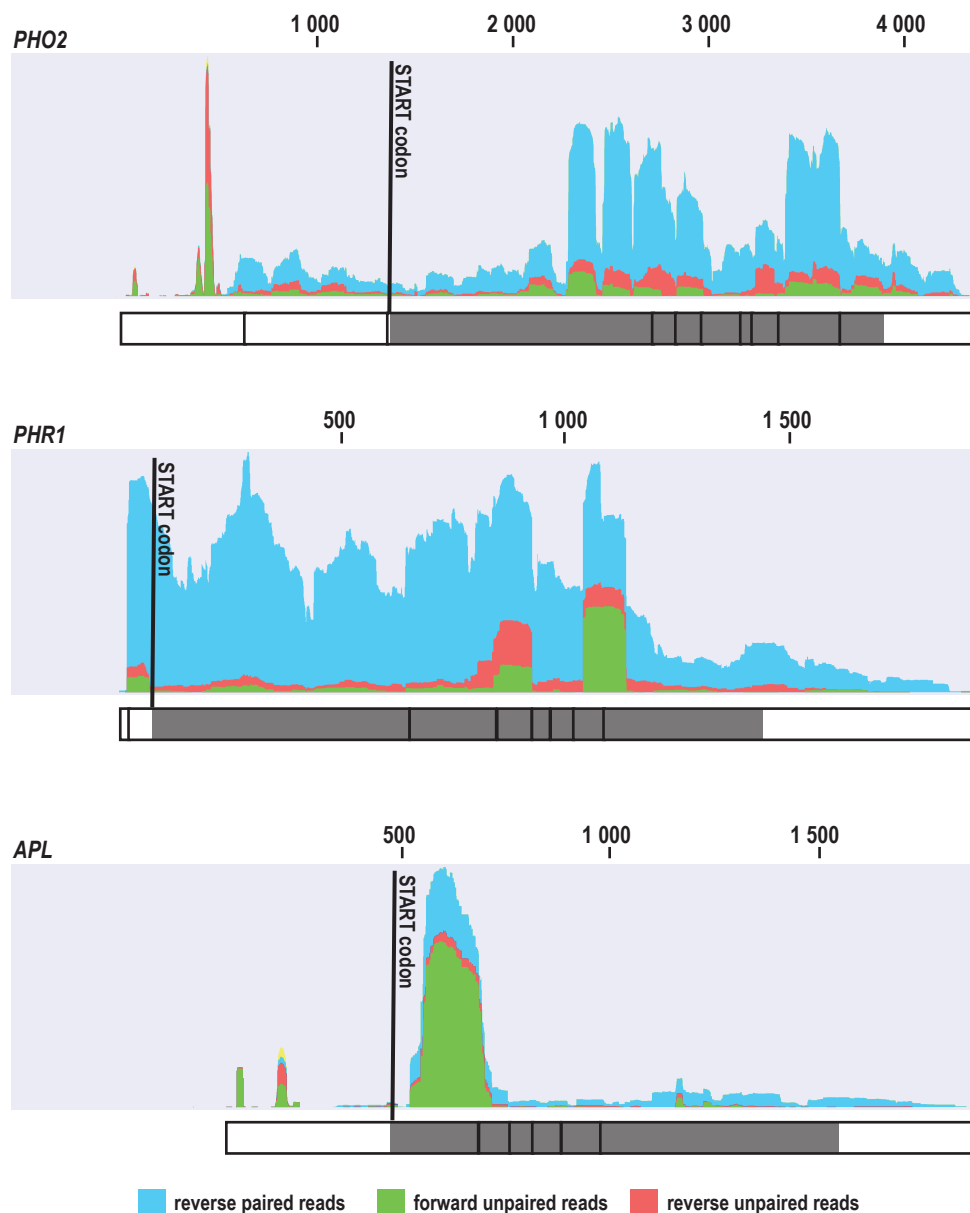
Supplementary Fig. S6. The barley TFs PHR1 and APL interact with the second exon “bait” fragment originating from the *PHO2* 5'-UTR in yeast cells.

The structure of the barley *PHO2* gene with marked a Y1H “bait” fragment. The pPHO2_5 fragment is 27 bp in length and includes the P1BS.2 motif. The blue triangle indicates positions 447916090 (+) and 447916332 (+) on barley chromosome 1; the two TSSs of the *PHO2* transcripts were identified using 5'RLM-RACE. The lower panel contains images of the growing colonies of the tested Y1HGold yeast strain having the “bait” fragment from the *PHO2* 5'-UTR second exon. The barley MADS57 TF was used as a non-binding negative control.



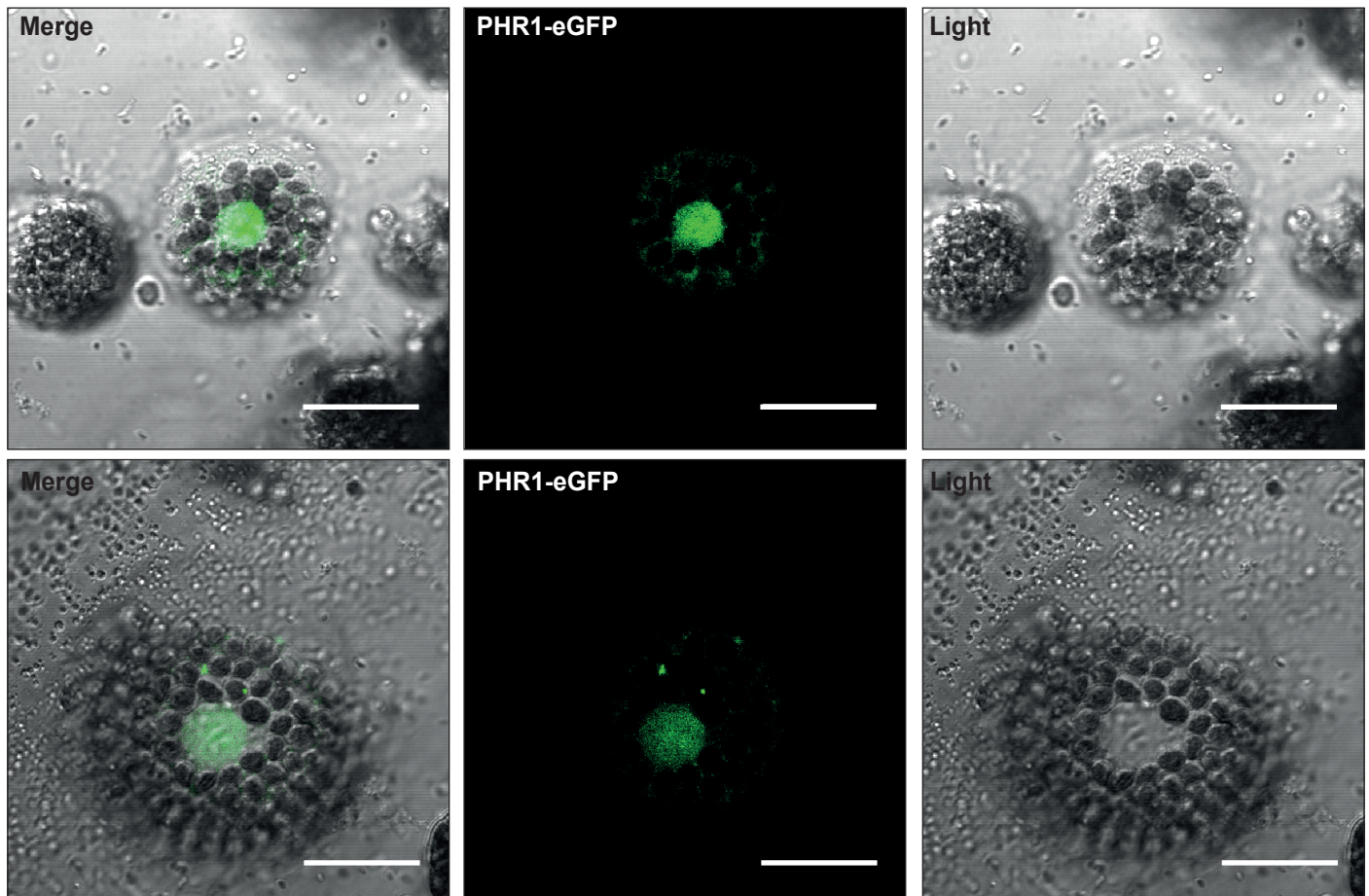
Supplementary Fig. S7. The first intron originating from the barley *PHO2* 5'-UTR contains signals that help increase gene expression.

The distribution of IMETER scores for either (A) all nine *PHO2*-related introns (the first two introns are located within 5'-UTR region) or (B) seven fragments approximately 200 bp in length chopped from the first intron of the *PHO2* 5'-UTR. Each ~200 bp fragment is designated with an additional prefix from p1 to p7, where the p1 fragment is located on the first intron 5'-end, and p7 is located on its 3'-end. The plots show percentage scores, which were calculated on the basis of the results from three monocotyledonous plant species: *Brachypodium distachyon*, *Oryza sativa*, and *Zea mays*.



Supplementary Fig. S8. *PHO2*, *PHR1*, and *APL* transcript coverage.

RNA-Seq paired reads were mapped to the *PHO2* (HORVU1Hr1G085570.2, Ensembl Plants database), *PHR1* (HORVU4Hr1G051080.5), and *APL* (HORVU6Hr1G031470.1) transcripts. Blue indicates the reverse paired reads, green indicates forward unpaired reads, and red indicates reverse unpaired reads; the black vertical line denotes the ATG start codon. Below the graph, the structures of the transcript are presented. The white boxes denote UTRs, and the gray boxes denote CDSs.



Supplementary Fig. S10. The cellular localization of PHR1–eGFP fusion proteins in barley protoplasts.

Exclusive images that show the localization of recombinant proteins transiently expressed in protoplasts isolated from 6-day-old barley leaves. Slight expression of PHR1–eGFP proteins in the cytoplasm was observed in one out of every five cells. The protoplasts shown here were incubated overnight in standard W5 buffer (without extra KH_2PO_4 , a source of Pi). Microscopic analyses were repeated three times, and similar patterns were imaged. Scale bars = 20 μm

RESEARCH ARTICLE

Open Access



Pi-starvation induced transcriptional changes in barley revealed by a comprehensive RNA-Seq and degradome analyses

Paweł Sega¹, Katarzyna Kruszk¹, Dawid Bielewicz^{1,2}, Wojciech Karłowski³, Przemysław Nuc¹, Zofia Szwejkowska-Kulińska¹ and Andrzej Pacak^{1*}

Abstract

Background: Small RNAs (sRNAs) are 20–30 nt regulatory elements which are responsible for plant development regulation and participate in many plant stress responses. Insufficient inorganic phosphate (Pi) concentration triggers plant responses to balance the internal Pi level.

Results: In this study, we describe Pi-starvation-responsive small RNAs and transcriptome changes in barley (*Hordeum vulgare* L.) using Next-Generation Sequencing (NGS) RNA-Seq data derived from three different types of NGS libraries: (i) small RNAs, (ii) degraded RNAs, and (iii) functional mRNAs. We find that differentially and significantly expressed miRNAs (DEMs, Bonferroni adjusted p -value < 0.05) are represented by 15 molecules in shoot and 13 in root; mainly various miR399 and miR827 isomiRs. The remaining small RNAs (i.e., those without perfect match to reference sequences deposited in miRBase) are considered as differentially expressed other sRNAs (DESS, p -value Bonferroni correction < 0.05). In roots, a more abundant and diverse set of other sRNAs (DESS, 1796 unique sequences, 0.13% from the average of the unique small RNA expressed under low-Pi) contributes more to the compensation of low-Pi stress than that in shoots (DESS, 199 unique sequences, 0.01%). More than 80% of differentially expressed other sRNAs are up-regulated in both organs. Additionally, in barley shoots, up-regulation of small RNAs is accompanied by strong induction of two nucleases (S1/P1 endonuclease and 3'-5' exonuclease). This suggests that most small RNAs may be generated upon nucleolytic cleavage to increase the internal Pi pool. Transcriptomic profiling of Pi-starved barley shoots identifies 98 differentially expressed genes (DEGs). A majority of the DEGs possess characteristic Pi-responsive *cis*-regulatory elements (P1BS and/or PHO element), located mostly in the proximal promoter regions. GO analysis shows that the discovered DEGs primarily alter plant defense, plant stress response, nutrient mobilization, or pathways involved in the gathering and recycling of phosphorus from organic pools.

(Continued on next page)

* Correspondence: apacak@amu.edu.pl

¹Department of Gene Expression, Faculty of Biology, Institute of Molecular Biology and Biotechnology, Adam Mickiewicz University, Poznań, Uniwersytetu Poznańskiego 6, 61-614 Poznań, Poland
 Full list of author information is available at the end of the article



© The Author(s). 2021 **Open Access** This article is licensed under a Creative Commons Attribution 4.0 International License, which permits use, sharing, adaptation, distribution and reproduction in any medium or format, as long as you give appropriate credit to the original author(s) and the source, provide a link to the Creative Commons licence, and indicate if changes were made. The images or other third party material in this article are included in the article's Creative Commons licence, unless indicated otherwise in a credit line to the material. If material is not included in the article's Creative Commons licence and your intended use is not permitted by statutory regulation or exceeds the permitted use, you will need to obtain permission directly from the copyright holder. To view a copy of this licence, visit <http://creativecommons.org/licenses/by/4.0/>. The Creative Commons Public Domain Dedication waiver (<http://creativecommons.org/publicdomain/zero/1.0/>) applies to the data made available in this article, unless otherwise stated in a credit line to the data.

(Continued from previous page)

Conclusions: Our results provide comprehensive data to demonstrate complex responses at the RNA level in barley to maintain Pi homeostasis and indicate that barley adapts to Pi-starvation through elicitation of RNA degradation. Novel P-responsive genes were selected as putative candidates to overcome low-Pi stress in barley plants.

Keywords: Phosphate regulatory network, Barley, Small RNAs, Degradome, RNA-Seq

Background

Barley (*Hordeum vulgare* L.) is one of the most commonly cultivated crop plants worldwide. It is a diploid plant with a low chromosome number ($n = 7$) and large genome size (haploid genome size of ~ 5.3 Gbp). In recent years, many resources essential to barley genomic studies have been developed, including a barley genome assembly in Ensembl Plants [1], a large number of expressed sequence tags (ESTs) [2], DNA markers, and useful techniques for stable or transient transformation of barley [3]. The simplicity of cross-breeding and cultivation in a wide range of climatic conditions makes barley a model crop plant in the study of desirable agronomic traits [4]. Studies on the responses of barley to abiotic stresses can help to better its cultivation in variable and adverse conditions. Environmental stressors cause crop damage and reduction of yields, which result in financial losses for agricultural businesses. In plants, abiotic stresses trigger specific stress-induced molecular pathways that often involve different classes of small RNAs (sRNAs) [5–7].

Small RNAs (sRNA) are non-translating into protein class of RNA (20–30 nt) [8]. Best known are siRNA (small interfering RNAs) and miRNA (microRNAs, 18–25 nt) - a class of RNA, which may target chromatin or transcripts to regulate both the genome and transcriptome [9, 10]. Plant small RNAs tend to bind to Argonaute (AGO) family proteins to form either RNA-induced silencing complexes (RISC) for post-transcriptional gene silencing (PTGS) [11] or RNA-induced initiation of transcriptional silencing (RITS) complex for transcriptional gene silencing [12]. Recently, many studies have emerged about various sRNA types, biogenesis, targets, and functions [13–15]. Based on the biogenesis pathway, small RNAs have been classified into miRNAs, siRNAs, phasiRNA and tRFs (tRNA-derived RNA fragments) [16]. Among them, miRNAs and siRNAs are the most extensively studied sRNAs in plants.

Plant *MIR* genes represent independent transcriptional units, which are transcribed by RNA polymerase II (RNA Pol II). Primary transcripts (pri-miRNAs) mature in a two-step process in the cell nucleus [17]: Firstly, pri-microRNAs are diced out by the DCL1 (DICER-LIKE 1) protein from a stem-loop precursors [18]. The next

step of DCL1 protein action leads to the generation of a double-stranded molecule composed of a guide miRNA strand and the passenger miRNA* (star) strand (called the miRNA/miRNA* duplex). Different DCL family members produce miRNA molecules of different lengths; however, the majority of plant miRNAs are 21 nucleotides in length [19]. The miRNA is assembled together with AGO1 (ARGONAUTE 1), in order to create RISC in the cytoplasm which is responsible for mRNA slicing. The cleavage position is precisely determined and occurs in the target mRNA between nucleotides complementary to the 10th and 11th nucleotides of the related miRNA, counting from the miRNA's 5'-end [20]. Ultimately, target mRNA recognized by the specific miRNA molecule is degraded by 5'-to-3' exonucleases and the overall pool of valid mRNA transcripts is decreased [21]. Such a mechanism exists in plants to modulate the expression levels of crucial stress-responsive genes [22].

In plants, there are many types of siRNAs, including (i) nat-siRNAs (natural-antisense siRNAs), which are produced from overlapping regions of natural sense-antisense mRNA pairs; (ii) ta-siRNAs (trans-acting siRNAs), processed from non-coding RNA precursors; and (iii) ra-siRNAs (repeat-associated siRNAs), generated from transposable and repetitive elements to mediate further steps of RNAi [9, 23]. tRFs may be produced after cleavage of tRNA ends (to generate 5'-tRF and 3'-tRF) by RNase T2 [24], as well as DCL (DICER-LIKE) processing in plants [25]. Both miRNAs and siRNAs mediate RNA interference (RNAi) in plants, but there are subtle differences between them. As an endogenous molecule miRNA is diced-out from microRNA precursor folded in stem-loop structure [26], while siRNA is a double-stranded RNA derived from the host genome or directly from viruses or transgenes [27].

The expression of sRNAs changes in response to environmental factors [7, 28] or viral infection [29–31]. Mentioned above classes of sRNAs appear to play important roles in plant growth, development regulation, and adaptation to various stresses. In barley, miRNAs have been shown to (i) mediate tolerance to heat stress [32], (ii) confer drought tolerance [33], (iii) regulate low-potassium tolerance [34], (iv) respond to aluminum stress [35], and (v) maintain inorganic phosphate (Pi)

homeostasis [36]. On the other hand, siRNAs mostly function as a defenders of genome integrity in response to foreign nucleic acids [37]. The *TAS3* gene expresses ta-siRNAs, which may negatively regulate auxin signaling by targeting AUXIN RESPONSE FACTOR 3 (ARF3) transcripts [38] and moderate floral architecture in response to drought stress in *Arabidopsis thaliana* L. [39]. The TAS-ARF pathway has been shown to be involved either in the development process of maize (*Zea mays* L.) [40] or regulating lateral root growth in *Arabidopsis* [41]. In addition, tRNA-derived small RNAs have been shown to accumulate in *Arabidopsis* roots under Pi-starvation [42], while rhizobial tRFs can regulate nodule formation in soybean (*Glycine max* L.) [13].

Changes in soil nutrient concentrations lead to aberrations in the set of sRNAs, with respect to the prevailing severe environmental conditions [6]. One of the most important macronutrients, which is indispensable for proper plant growth, is phosphorus (P) [43, 44]. P is a component of DNA, RNA, phospholipids, and ATP, and is involved in several biochemical processes such as protein phosphorylation, energy storage and transfer, and regulation of protein synthesis [45]. From soil matrices, P is acquired by the root system in the form of inorganic phosphate ions. Insufficient Pi supply leads to barley growth inhibition [46, 47]. Plant transcriptome response to Pi-starvation involves protein coding genes, sRNAs, and long non-coding RNAs that form regulatory feedback loops. The most widely studied molecules in this context—miRNA399 molecules—are up-regulated in barley shoots and roots under low-Pi conditions [36]. MiRNA399 targets the 5'-UTR of the barley *PHO2* (*PHOSPHATE 2*) transcripts [48], encoding an ubiquitin-conjugating E2 enzyme (UBC24), a negative regulator of Pi uptake and root-to-shoot translocation. *PHO2* is involved in ubiquitination of PHOSPHATE TRANSPORTER 1 (PHT1) family [49] and PHOSPHATE TRANSPORTER TRAFFIC FACILITATOR 1 (PHF1) [49]. Transgenic *Arabidopsis* plants over-expressing miR399 accumulate excessive Pi in shoots and display Pi over-accumulation toxic symptoms. Likewise, such a phenotype has been reported for the *pho2* loss-of-function *Arabidopsis* mutant [50, 51]. Thus, plants have developed a strategy to regulate the level of miR399 in the cytoplasm. The non-coding RNA molecule, *IPS1* (*INDUCED BY PHOSPHATE STARVATION 1*), has been shown to be highly expressed in plants exposed to Pi-starvation [52–54]. *IPS1* is a non-cleavable miR399 target which inhibits miR399-mediated down-regulation of *PHO2* mRNA by target mimicry [54]. Thus, the RNAi effect of miRNA activity may be counterbalanced by other RNAs, in a stress-dependent manner.

Deep sequencing of sRNAs has uncovered up-regulation of miRNAs like miR156, miR778, miR827, and miR2111, and down-regulation of miR169, miR395,

and miR398 in *Arabidopsis* plants upon Pi deprivation [42, 55]. In rice (*Oryza sativa* L.), Pi-starvation induced the expression level of miR827 molecules, which dysregulate the transcript level of two genes encoding the SPX-MFS (named after proteins SYG1/PHO81/XPR1 and the protein domain Major Facility Superfamily) protein family members SPX-MFS1 and SPX-MFS2 [56, 57]. These two SPX-MFS membrane transporters mediate Pi transport and control Pi homeostasis in shoot [58]. In *Arabidopsis*, the level of mature miR778 was up-regulated in shoots and roots in low-Pi conditions, while its target gene expression *SUVH6* (*SU(VAR)3–9 HOMOLOG 6*) was accordingly reduced [59]. The *SUVH6* gene encodes a histone H3 lysine 9 (H3K9) methyltransferase, which may enable plants to adapt to environmental conditions by changing their chromatin structure [60]. miR2111 functions as an activator of rhizobial nodulation, which is strictly correlated with the balanced assimilation of nitrogen (N) and P in plants [61, 62]. However, there is still a gap in understanding how Pi-starvation affects the quantity and quality of sRNAs distributed in barley shoots and roots. What kind of sRNAs are preferentially induced? What is the role of sRNAs in responding to Pi-starvation? What are the mRNA targets recognized by those sRNAs in barley?

In this paper, we analyzed changes in the expression levels of RNAs in barley growing under Pi-starvation, as compared to control/Pi sufficient conditions. Our results support the hypothesis that Pi-starvation triggers underlying molecular mechanisms and the expression level of key genes involved in maintaining proper barley growth and development. Combined deep sequencing data (sRNAs, degradome and mRNAs) reveals the widespread importance of low-Pi-dependent miRNAs and genes representing various biological pathways. Using degradome analysis, we identified mRNAs targeted by sRNAs identified in this study. Among these sRNAs, only a small fraction maps perfectly to miRNA sequences deposited in miRBase. Our degradome data show that most sRNAs produced upon Pi-starvation are not involved in gene silencing. In addition, we performed transcriptome analysis of the protein-coding gene expression in barley shoots upon Pi-starvation. Subsequent analyses were performed (GO analysis, chromosomal mapping, and Pi-responsive motifs localization) to characterize specific stress responses in barley plants to accomplish Pi homeostasis.

Results

Barley plants display low-Pi symptoms at the morphological and molecular levels

Severe low-Pi responses were induced in the barley plant line Rolap grown in the soil containing 8 mg P/kg. P undernourishment caused over 2-fold reduction

of plant shoot biomass (Fig. 1a). Shoot fresh weight of plants at 23rd day post-sowing (dps) was significantly reduced, in comparison with control plants, with average mass 8.8 g for stressed plants and 18.5 g for plants growing under Pi-sufficient conditions ($p = 0.001$) (Fig. 1b). We observed a significantly decreased concentration of Pi ions, with only 0.48 μmol Pi per g of fresh root weight (FW) and 4.2 μmol Pi per g of shoot FW, when compared with the control plants having 3.84 ($p = 0.0056$) and 24.35 μmol Pi/g FW ($p = 0.0001$), respectively (Fig. 1c). To examine the induction of changes at a molecular level by low-Pi stress in barley plants, we measured the absolute gene expression of the low-Pi-responsive marker gene *IPS1*. The barley *IPS1* gene is highly expressed under Pi-deficient conditions in the plant line Rolap. At the tillering stage (23 dps), we detected 4191 copies of *IPS1* RNA for low-Pi treated roots, normalized per 1000 copies of *ADP-RIBOSYLATION FACTOR 1-LIKE* (*ARF1*) reference gene, in comparison to the control

plants, with only 58 copies of *IPS1* RNA ($p = 0.00006$) (Additional file 1). Taking validated plant material, we performed tripartite deep-sequencing analysis to: (i) identify Pi-responsive sRNAs, (ii) elucidate changes in the barley transcriptome upon Pi starvation, and (iii) identify mRNA targets for Pi-responsive sRNAs through degradome sequencing (Fig. 2).

Identification of barley differentially expressed miRNAs (DEMs) under low-Pi

We performed small RNA deep-sequencing to find out which small RNAs are up- or down-regulated by Pi starvation in barley shoots and roots. The average of 30.4 mln reads for roots and 25.2 mln reads for shoots were generated in 50 nt single-read Illumina sequencing (Additional file 2). After adapter and quality trimming, we mapped reads to the miRBase Sequence Database (release 22) to annotate miRNA-derived sequences [63]. A set of parameters were used to define the pool of

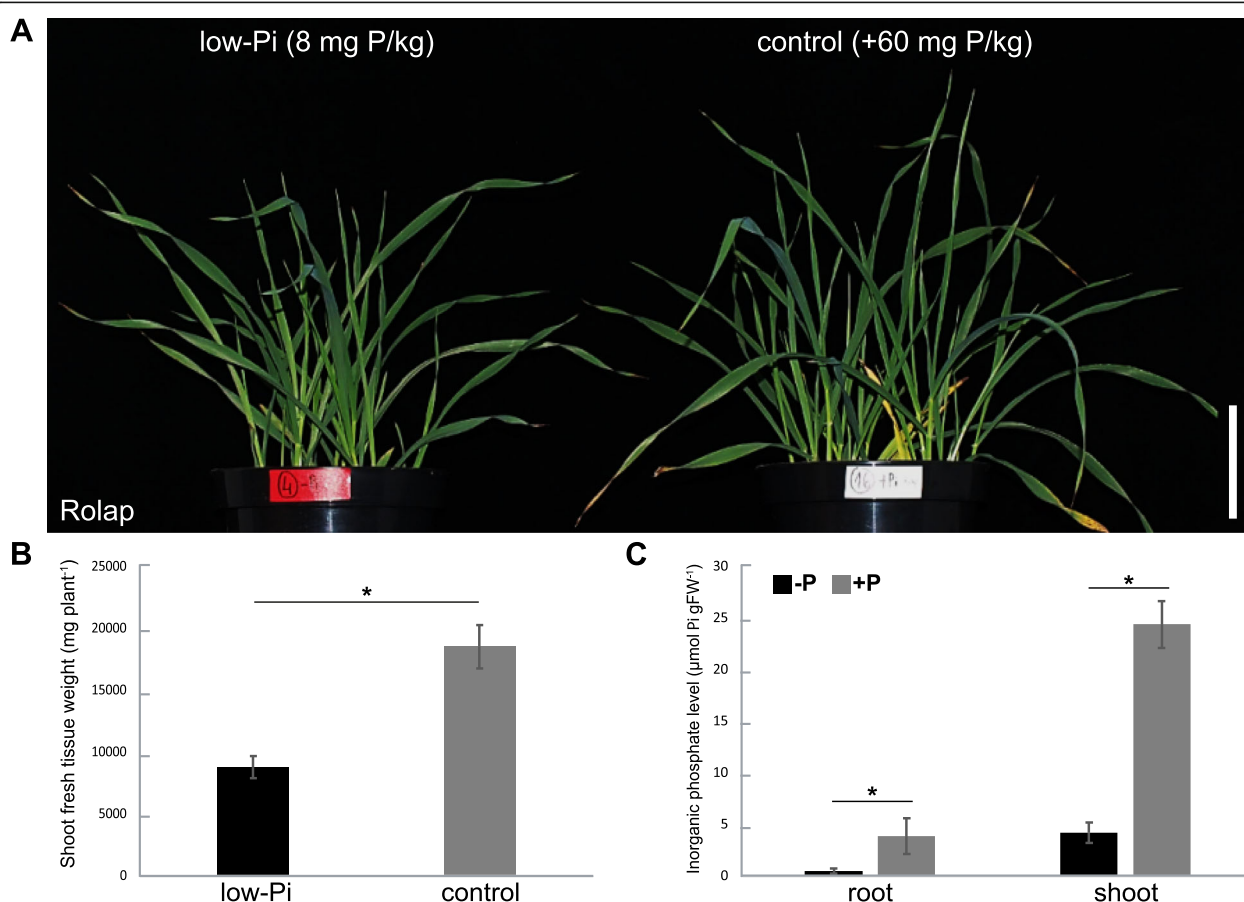
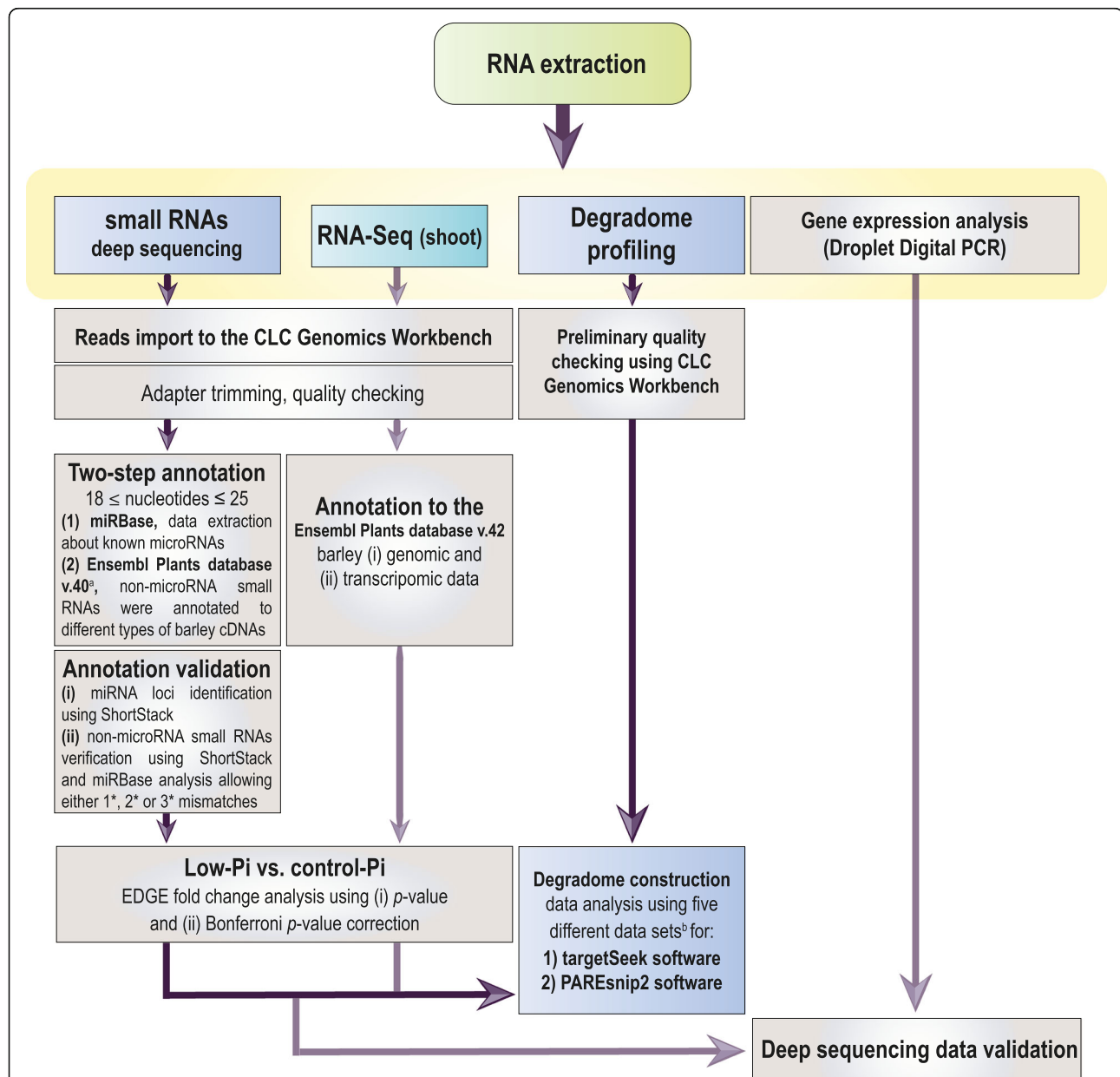


Fig. 1 The validation of barley line Rolap plant material under low-Pi stress. **a** Pictures of the plants ($n = 3$) collected on the 23rd day after sowing, grown under low-Pi, 8 mg P/kg soil (left) and control-Pi, addition of 60 mg P/kg soil (right), conditions. **b** Shoot fresh tissue weight ($n = 3$). **c** The Pi concentration measurements performed for barley roots and shoots ($n = 3$). Asterisks indicate a significant difference (* p -value < 0.05) calculated using two-tailed Student's t -tests. Scale bar = 10 cm. Error bars = SD



^a Ensembl Plants v.40; *Hordeum vulgare* genes (IBSC v2), 42 859 genes classified as: (i) antisense RNA – 22, (ii) nontranslating RNA – 2 340, (iii) pre-miRNA – 77, (iv) protein coding – 37 705, (v) pseudogene – 100, (vi) RNase – 1, (vii) rRNA – 1 385, (viii) sense intronic – 173, (ix) snoRNA – 455, (x) snRNA – 192, (xi) SRP_RNA – 11, (xii) tRNA – 688

^b (i) microRNA reads with significant *p*-value from roots and shoots (Bonferroni corrected), (ii) small RNA reads with significant (Bonferroni corrected) *p*-value from roots and shoots, (iii) protein coding cDNAs annotated to Ensembl Plants database, (iv) transcripts of 98 genes with significant expression changed upon low-Pi and (v) degradome profiles from roots and shoots.

Fig. 2 The framework illustrating the data generation protocols used in this study. The low-Pi stress-specific subsets of RNAs were generated following (i) deep sequencing of small RNAs from barley shoots and roots, (ii) transcriptomic RNA-Seq for barley shoots, and (iii) degradome profiling for barley shoots and roots. The obtained data sets were mapped to the references collected from miRBase and Ensembl Plants databases. The log₂ scale for fold change and Bonferroni corrections were calculated to pick the significantly changed sequences under Pi-deficient and Pi-sufficient conditions

differentially expressed miRNAs: (i) no mismatches with the reference sequences in the miRBase were allowed; (ii) different types of miRNA sequences were permitted, whether they were annotated as precursor, mature, or isomiR; (iii) miRNA sequences were named accordingly to the name of the assigned reference miRNA; and (iv) significance of fold change (p -value < 0.05) was additionally verified using a restricted Bonferroni p -value adjustment (Fig. 2).

We found 162 and 138 differentially expressed miRNAs (DEMs) annotated to the miRBase (p -value < 0.05) in barley shoots and roots, respectively. Only 25 DEMs were expressed in both examined barley organs (Additional file 3). However, restricted Bonferroni p -value correction narrowed down set of miRNAs to 15 in shoots and 13 in roots (Table 1). Those 28 annotated miRNAs were comprehensively analyzed using ShortStack tool to obtain useful annotations for 5 miRNAs. Among them, 3 out of 5 represent DEMs identified in both tested organs: miR399b (root ID: 75, shoot ID: 2019), miR399a (root ID: 105, shoot ID: 2063), miR827 (root ID: 114, shoot ID: 2073). The ShortStack analysis supports two more miRNAs identified in barley shoot: miR399b (ID: 2060) and miR827 (ID: 2096) (Table 1, Additional file 4).

sRNA-Seq (small RNA Sequencing) data were experimentally validated by complex analysis of mature miR827 derived from 3' arm (root ID: 114, shoot ID: 2073) in all samples taken for deep sequencing. The absolute expression level of miR827 is significantly up-regulated in both shoots and roots under a low-Pi regime (Fig. 3a). The \log_2 fold change of miR827 molecules defined by deep-sequencing in shoot was found on the same level in root, $\log_2(fc) = 3.05$ and 3.01 , respectively (Fig. 3a). The ddPCR results were consistent with NGS data showing up-regulation of mature miR827 molecule in both tested organs. These data were confirmed by northern blot hybridization (Fig. 3b).

Barley plants express an organ-specific set of microRNAs in response to low-Pi conditions

In both organs, majority of the DEMs were significantly up-regulated. Interestingly, out of 15 miRNA, only miRNA166d (ID: 2004) was down-regulated in shoot under low-Pi ($\log_2(\text{fold change}) = -1.18$). In our previous work, we showed that miRNA166 is expressed in barley during different developmental stages reaching the highest level in 2-week-old plants [65]. miRNA166 plays an important role in plant development, including root and leaf patterning, by targeting mRNA encoding HOMEODOMAIN LEUCINE-ZIPPER CLASS III (HD-ZIP III) transcription factors [66]. Similarly, only miRNA319b (ID: 51) out of 13 DEMs was down-regulated in low-Pi treated roots ($\log_2(\text{fold change}) = -1.28$). In a previous

study, we presented data that Arabidopsis miR319 is a multi-stress responsiveness miRNA [22]. For example, *MIR319b* gene expression was down-regulated in response to drought, heat, and salinity, but up-regulated in response to copper and sulfur deficiency stresses [22].

A specific set of miRNAs was expressed in barley shoot or root under low-Pi (Table 1). In shoot, only two miRNA families, miRNA399 and miRNA827, were induced, while in root we observed a more diverse response. Apart from miRNA399/miRNA827 induction, we found the following additional miRNA to be up-regulated in root: two miRNA5083 (ID: 3, and ID: 4), miRNA1511 (ID: 6), two miRNA9779 (ID: 16, and ID: 17), two miRNA156 (ID: 65, and ID: 69), and miRNA5072 (ID: 118). Among these eight miRNAs, only miR156 has been reported before as Pi-responsive in Arabidopsis [42, 55]. The miR156 isomiRs were also found dysregulated in shoot, but none of them pass the Bonferroni test (Additional file 3). Our results suggest that there is a more complex response to low-Pi stress regarding miRNA expression in roots than in shoots, where the miRNA action is directed to control the transcript level of either *PHO2*, *SPX-MFS1*, or *SPX-MFS2* by just two miRNA families.

Different classes of small RNAs in barley accumulate in an organ-specific manner under low-Pi regime

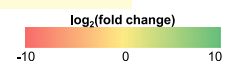
The small RNAs which did not map to miRBase were mapped to particular classes of barley cDNAs derived from the Ensembl Plants database (release 40). Each small RNA was annotated to (i) each class of cDNA in separate analysis, and (ii) to all cDNA classes in a single analysis (Fig. 2). These two-fold annotation provide in-depth analysis and delivers more reliable data about the localization of particular small RNA in barley genome. All sequences mapped to barley cDNAs are listed in Additional file 3. We found that small RNAs, other than miRNAs, differentially expressed sRNAs (DESS) in barley under Pi starvation were represented by 199 unique sequences identified in shoot (0.01% of the average of unique small RNA found in shoots of barley growing under Pi starvation (Additional file 5) and by 1796 (0.13%, respectively) unique sequences identified in roots (Fig. 4a, Additional file 6).

We analyzed whether different lengths (taking sequences from 18 to 25 nt in length) and classes of small RNAs contributed to either root or shoot response to low-Pi conditions. In roots, the length distribution of DESS remained balanced, from 10.91% for the representation of 24 nt sequences to 15.26% for the 18 nt sequences, which were the most abundant (including 274 DESS) (Fig. 4b). In shoots, the representations of DES lengths fluctuated more than in roots. The 19 nt sequences were the most visible (21.11%), while three

Table 1 List of differentially expressed miRNAs (DEMs, Bonferroni adjusted p -value < 0.05) identified in this study. The ID number specifies the miRNA sequence according to data sets obtained in sRNA-Seq (Additional file 3). The given fold change is shown as a \log_2 value in the column $\log_2(\text{FC})$. Predicted target genes are presented in the table based on dual degradome profiling (Additional files 15, 17, 19 and 23). Type categorizes miRNAs based on the sequences deposited in miRBase without mismatches, isomiRs include miRNAs with nucleotide shift (super or sub) at their 5', 3', or at both ends [64]

	ID	Name	Size	Sequence (from 5' to 3')	ShortStack	$\log_2(\text{FC})$	Type	Target locus	Cut	Target annotation	Score	MFE
SHOOT	>1966	miR399b	21	CAGGGCGCTTCTCCTTTGGCA	N/A	7.92	mature 5'	N/A	-	-	-	-
	>2031	miR399a	21	GTGCAGTTCTCCTCTGGCATG	N/A	6.57	precursor	N/A	-	-	-	-
	>2019	miR399b†	21	GGGCGCTTCTCCTTTGGCACG	+	5.63	isomiR	N/A	-	-	-	-
	>2074	miR827	22	TTAGATGACCATCAGCAACAT	N/A	5.49	isomiR	HORVU2Hr1G094690.14 ^{PS} HORVU6Hr1G065710.5 ^{TS}	378 217	SPX-MFS1 SPX-MFS2	3 5	-27.3 -26.0
	>1957	miR399b//miR399a	18	CAAGGAGAATTGCCCTG	N/A	5.31	precursor	N/A	-	-	-	-
	>2060	miR399b//miR399a	21	TGCCAAGGAGAATTGCCCTG	+	4.49	mature 3'	HORVU1Hr1G085570.3 ^{PS}	857 1154	PHO2	2.5 3.5	-35.0 -32.6
	>2072	miR827†	20	TTAGATGACCATCAGCAAC	N/A	4.08	isomiR	HORVU2Hr1G094690.14 ^{PS} HORVU6Hr1G065710.5 ^{TS}	378 217	SPX-MFS1 SPX-MFS2	2 2	-25.9 -26.0
	>1958	miR399b//miR399c	18	CAAGGAGAGTTGCCCTG	N/A	4.04	precursor	N/A	-	-	-	-
	>2091	miR827	21	TTTGTGGTTGCATCTAACC	N/A	4.02	isomiR	N/A	-	-	-	-
	>2096	miR827	22	TTTTGTGGTTGCATCTAACC	+	3.77	mature 5'	N/A	-	-	-	-
	>2063	miR399a†	21	TGCCAAGGAGAGTTGCCCTG	+	3.71	mature 5'	HORVU1Hr1G085570.3 ^{PS}	857 1154	PHO2	2.5 3.5	-35.0 -32.6
	>1970	miR399b//miR399a	19	CAAGGAGAATTGCCCTG	N/A	3.29	isomiR	N/A	-	-	-	-
	>2073	miR827†	21	TTAGATGACCATCAGCAACA	+	3.05	mature 3'	HORVU2Hr1G094690.14 ^{PS} HORVU6Hr1G065710.5 ^{TS}	378 217	SPX-MFS1 SPX-MFS2	3 3.5	-27.3 -26.0
	>2036	miR827	20	TAGATGACCATCAGCAACA	N/A	3.02	isomiR	HORVU6Hr1G065710.5 ^{TS} HORVU2Hr1G094690.14 ^{TS}	217 378	SPX-MFS2 SPX-MFS1	3.5 5	-25.0 -24.9
	>2004	miR166d	21	GGAATGTTGTCTGGCTCGGGG	N/A	-1.18	mature 5'	N/A	-	-	-	-
ROOT	>113	miR827†	20	TTAGATGACCATCAGCAAC	N/A	4.05	isomiR	HORVU6Hr1G065710.10 ^{TS}	185	SPX-MFS2	2	-26.0
	>75	miR399b†	21	GGGCGCTTCTCCTTTGGCACG	+	3.30	isomiR	N/A	-	-	-	-
	>114	miR827†	21	TTAGATGACCATCAGCAACA	+	3.01	mature 3'	HORVU6Hr1G065710.10 ^{TS}	185	SPX-MFS2	3.5	-26.0
	>17	miR9779	22	ACCTATGATGAGTTGCGAAGCTG	N/A	2.57	precursor	N/A	-	-	-	-
	>3	miR5083	24	AAACCAATGGATCCTCTGAGCCT	N/A	2.24	precursor	N/A	-	-	-	-
	>16	miR9779	21	ACCTATGATGAGTTGCGAAGCT	N/A	2.09	precursor	N/A	-	-	-	-
	>4	miR5083	25	AAACCAATGGATCCTCTGAGCCTG	N/A	2.04	precursor	N/A	-	-	-	-
	>65	miR156c	22	GCTCACTGCTCTATCTGTACCC	N/A	2.02	mature 3'	N/A	-	-	-	-
	>6	miR1511	18	AACCTGGCTCTGATACCA	N/A	2.00	precursor	N/A	-	-	-	-
	>105	miR399a†	21	TGCCAAGGAGAGTTGCCCTG	+	1.87	mature 5'	HORVU1Hr1G085570.3 ^{PS} HORVU1Hr1G085570.3 ^{TS}	1154 857	PHO2	3.5 4.5	-32.6 -31.5
	>69	miR156e	22	GCTCACTTCTCTCTGTGTCAGC	N/A	1.65	mature 3'	N/A	-	-	-	-
	>118	miR5072	18	TCCCCAGCGGAGTCGCC	N/A	1.53	precursor	N/A	-	-	-	-
	>51	miR319b	22	CTTGGACTGAAGGGTGCTCCCT	N/A	-1.28	isomiR	HORVU2Hr1G060120.1 ^{PS} HORVU3Hr1G079490.2 ^{TS} HORVU7Hr1G027370.1 ^{TS}	1673 1521 1002	PCF6 transcription factor GAMyb transcription factor GAMyb transcription factor	2.5 8 9.5	-36.1 -30.2 -28.8

† = miRNA expressed in both organs; + = miRNA detected by ShortStack tool; TS = TargetSeek approach; PS = PAREsnip2 approach; N/A = not available



† = miRNA expressed in both organs; + = miRNA detected by ShortStack tool; TS = TargetSeek approach, PS = PAREsnip2 approach, N/A = not available

representations did not score more than 10%: the 22 nt (9.55%), 23 nt (8.54%), and 25 nt (3.52%) sequences (Fig. 4b, Additional file 7).

In roots, 1070 unique small RNAs were mapped to cDNA sequences annotated in the Ensembl Plants

databases (non-translating, protein-coding, pseudogenes, rRNA, snoRNA, snRNA, sRP-RNA, tRNA), while 726 unique sequences remained without match (Additional file 6). The DESs obtained from low-Pi roots were mostly annotated to protein-coding mRNAs (38.54%),

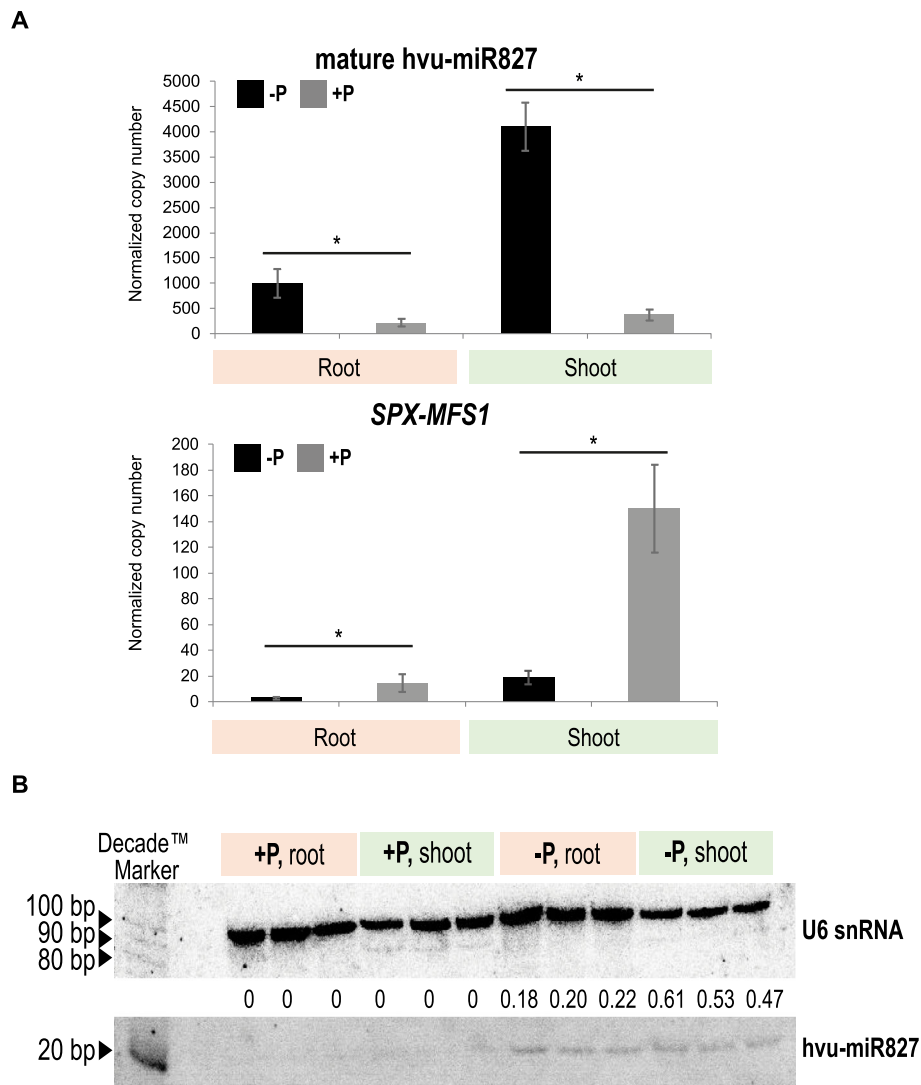


Fig. 3 The induced expression level of miR827 (root ID: 114, shoot ID: 2073) correlates with downregulation of its target SPX-MFS1 in barley. **a** The absolute gene expression quantification of identified mature hvu-miR827 and its predicted target gene *SPX-MFS1* using ddPCR. The bars represent copy numbers normalized to 1000 copies of the *ARF1* reference gene; * *p*-value < 0.05, calculated using two-tailed Student's *t*-tests for three biological and two technical replicates. Error bars = SD. **b** Detection of hvu-miR827 expression pattern in barley samples used in this study for NGS analysis. Specific probes for hvu-miR827 mature sequence and U6 reference gene were used for Northern hybridization performed on a single membrane. The number represents hvu-miR827 band intensity compared to U6 snRNA. The blots were cropped and original, full-length blots are presented in Additional files 32 and 33

rRNAs (34.17%), and non-translating RNAs (19.49%). Below 5% of overall DESs, we found a number of remaining cDNA classes, such as snoRNAs (2.49%), tRNAs (2.47%), SRP-RNAs (1.17%), snRNAs (0.95%), and pseudogenes (0.65%). While in shoot, we found 199 DESs under the low-Pi regime. Altogether, 116 out of 199 differentially expressed small RNAs (DESs) were annotated to the barley Ensembl Plants database, where 83 sequences remained without match (Additional file 5). In the case of shoot samples, 85% of annotated DESs represented only protein-coding mRNAs (47.87%) and non-translating RNAs (36.49%) (Fig. 4a; Additional file 8).

We did not find any DESs annotated to the snRNAs, SRP-RNAs, or tRNAs from barley shoot upon low-Pi. In addition, total numbers of 166 DESs (83%) in shoots and 1560 DESs (87%) in roots were significantly up-regulated after exposure to low-Pi stress (Additional files 5 and 6). Among the unannotated sRNAs in roots, the highest fold change was observed for a 19 nt DES ID: 388 ($\log_2(-\text{fold change}) = 8.02$, induction) and a 22 nt DES ID: 1133 (-5.87 , repression). The BLAST (Basic Local Alignment Search Tool) analysis of first (19 nt) molecule showed a perfect match to either the intergenic region of barley chromosome no. 5, soil bacteria (*mesorhizobium*), or

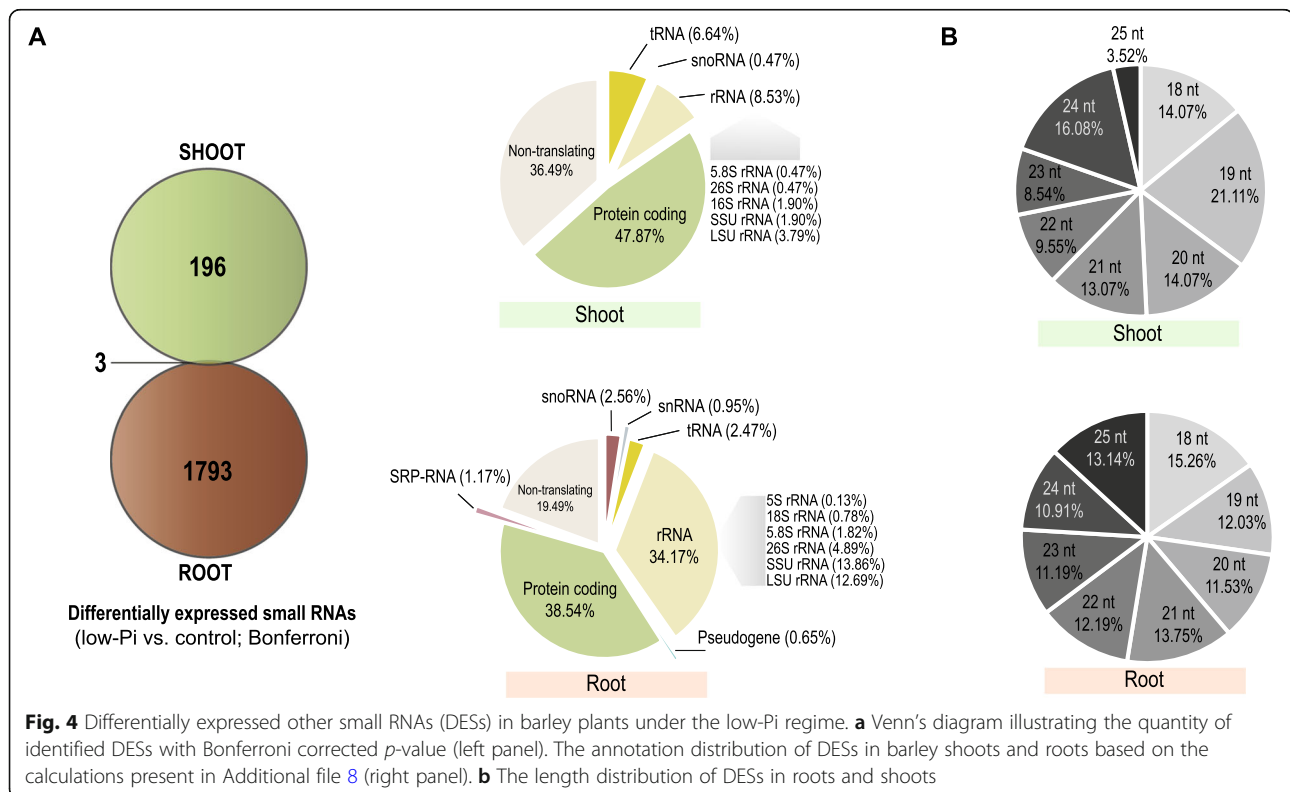


Fig. 4 Differentially expressed other small RNAs (DEs) in barley plants under the low-Pi regime. **a** Venn's diagram illustrating the quantity of identified DEs with Bonferroni corrected p -value (left panel). The annotation distribution of DEs in barley shoots and roots based on the calculations present in Additional file 8 (right panel). **b** The length distribution of DEs in roots and shoots

Linum usitatissimum L., while the second molecule (22 nt) mapped to RNA encodes 16S rRNA. Furthermore, in roots, the most abundant small RNA was a 25 nt DES ID: 331 (15,847.7 and 65,590.5 mean of normalized counts in barley root in control and low-Pi conditions, $\log_2(fc) = 2.82$). This small RNA matched several barley loci encoding SSU (small subunit) rRNAs (Additional file 6).

In our results from low-Pi treated shoot samples, the highest fold change was represented by a 24 nt DES ID: 2112 ($\log_2(fc) = 8.72$, induction). This 24 nt molecule is a part of transcript encoding a putative pentatricopeptide repeat (PPR) protein. The PPR protein family facilitates the processing, splicing, editing, stability, and translation of RNAs in plants [67]. The most abundant small RNA was a 19 nt DES ID: 2216 (9471.5 and 49,914.1 normalized mean counts in barley shoot in control and low-Pi, respectively, $\log_2(fc) = 2.45$). This sRNA was mapped to the barley genomic loci (EPIHVUG00000039813), which encodes arginyl-tRNA (trnR-ACG) and a cDNA encoding uncharacterized protein (HORVU2Hr1G084630) which is likely involved in carbon fixation. Interestingly, the pool of DEs was selective, considering organ-specific expression change, providing only three unique sequences that were significantly changed in both barley organs under low-Pi regime (Fig. 4a, left panel). These molecules were: (i) 20 nt DES ID: 2143 ($\log_2(fc) = 2.01$ in root and 1.16 in shoot, respectively) annotated to the

26S rRNAs, (ii) 24 nt DES ID: 2161 (3.69 in root and 2.07 in shoot) annotated to the RNA encoding the barley MYB21 transcription factor, and (iii) 21 nt DES ID: 2265 (4.64 in root and 6.27 in shoot) mapped to the intergenic region of barley chromosome no. 3 (Additional file 5).

The proper annotation of DEs was confirmed by ShortStack analysis. Among DES representatives only one small RNA (shoot ID: 2265, root ID: 1813, unannotated) has features of potential miRNA molecule and it is upregulated in both tested organs (Additional file 9). All DES molecules were once again annotated to miRbase allowing either 1, 2, or 3 mismatches. The new potential miRNA has one mismatch and belongs to miR399 family. Less restricted annotation revealed two more miR399 molecules (ids = 2141, 2222) and three miR827 (ids = 2279, 2280, 2281) expressed in shoot. In root we found three miR9779 (ids = 396, 645, 1629), two miR1511 (ids = 140, 141), two miR9653a (ids = 403, 404), miR319b (ID: 1266) and miR9675 (ID: 556) (Additional files 5 and 6). Nonetheless, all of them were classified as unannotated.

The results obtained in this study show again that barley roots exhibit a more diverse pool of Pi-responsive small RNAs which may trigger developmental adaptation of the root to Pi-starvation. Additionally, 613 rRNA-derived sRNAs are up-regulated, whereas 176 rRNA-derived sRNAs are down-regulated in barley roots (Additional file 6). We believe that such sRNA may be further

processed, serving as a Pi source to compensate Pi deficiency.

Identification of barley genes responsive to Pi-starvation

Since we observed, that most of the other sRNAs in shoot were derived from either protein-coding mRNAs or non-translating RNAs, we checked whether this observation is correlated with gene expression changes of polyadenylated RNAs in barley shoot under Pi-starvation. Among 98 of identified DEGs, the transcripts of 56 annotated loci were significantly up-regulated, while those derived from 42 loci were down-regulated in Pi-starved barley shoots (Table 2). Repressed loci were found to be preferentially located at barley chromosome no. 2, while induced loci were found mostly at barley chromosomes no. 3, no. 5 and no. 6 (Additional file 10).

The highest enrichment of shoot DEGs was found in the GO terms, either (i) belonging to the cellular components of the chloroplasts; (ii) showing catalytic activity, either ion or chlorophyll binding properties; and (iii) involved in the various biological and metabolic processes related to photosynthesis, stress response and plant defense (Fig. 5, Additional file 11). A major set of up-regulated DEGs represent genes involved in the Pi signaling. Among them, we found genes encoding: *IPSI* ($\log_2(fc) = 5.89$) [54], inorganic pyrophosphatase (PPase, 4.01) [68], SPX-domain containing protein 5 (SPX5, 3.44) [69], phosphate transporter PHOSPHATE 1–3 (PHO1–3, 2.97) [70], SPX-MFS2 (2.79) [56], haloacid dehalogenase-like hydrolase (HAD1, 1.95), [71] and five different purple acid phosphatases (PAPs) (Table 2) [72]. Interestingly, four genes were induced to a higher extent than the low-Pi stress marker, *IPSI* gene. These genes encode ferredoxin (FD1, $\log_2(fc) = 14.20$), mitochondrial-processing peptidase (13.35), chlorophyll a/b binding protein (8.90), and alpha-amylase (7.30), and are engaged in photosynthesis, redox reactions, reactive oxygen species (ROS) homeostasis, and co-ordinated mobilization of nutrients. Chloroplasts and mitochondria are the organelles with the highest Pi requirements. Strong *FDI* gene up-regulation most likely reflects the accumulation of reduced ferredoxin in chloroplasts. Low-Pi lowers the capacity to process incoming light and enhances starch accumulation in chloroplasts, thereby leading to photo-inhibition [73, 74]. Within the category of genes that were significantly down-regulated, most of them were related to stress and defense responses (Table 2); for instance, uncharacterized protein (HORVU2Hr1G030090, – 6.50), oxalate oxidase (– 4.41) [75], betasessquiphellandrene synthase (– 3.41), glutamate carboxypeptidase (– 3.17), chalcone synthase (– 3.05) [76], or caleosin-like protein (– 2.95). Only two repressed genes are known to be directly involved in Pi signaling and metabolism, *SPX-MFS1* (– 2.58), targeted by miR827

[57] and probable inactive purple acid phosphatase (– 1.75). Additionally, two genes encoding laccases (*LAC19-like*, Table 2), cell wall-localized multi-copper oxidases, were significantly down-regulated (– 2.10 and – 2.44) in our mRNA RNA-Seq data. Laccases are involved in copper homeostasis and lignin biosynthesis, and have been shown to be targeted by miR397 in maize [77] and Arabidopsis [78]. Furthermore, key genes encoding proteins involved in the nitrate and phosphate cross-talk were affected by low-Pi conditions in barley shoots, such as *NIGT1* (NITRATE-INDUCIBLE, GARP-TYPE TRANSCRIPTIONAL REPRESSOR 1) transcription factor (3.80) [79, 80] and nitrite reductase (1.98), as well as high-affinity nitrate transporter *NRT2.1* (NITRATE TRANSPORTER 2.1) (– 2.60) [81].

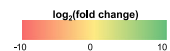
Absolute quantification of a few selected transcripts was performed to validate RNA-Seq data obtained in this study. Two genes which were highly induced (encoding endonuclease S1/P1 and 3'-5'-exonuclease) and two which were severely repressed (encoding oxalate oxidases) under the low-Pi regime were taken for ddPCR (droplet digital PCR) analysis (Fig. 6a). We confirmed statistically significant changes ($p < 0.05$) in normalized copy number (per 1000 copies of the *ARF1* reference gene) of all genes taken for analysis.

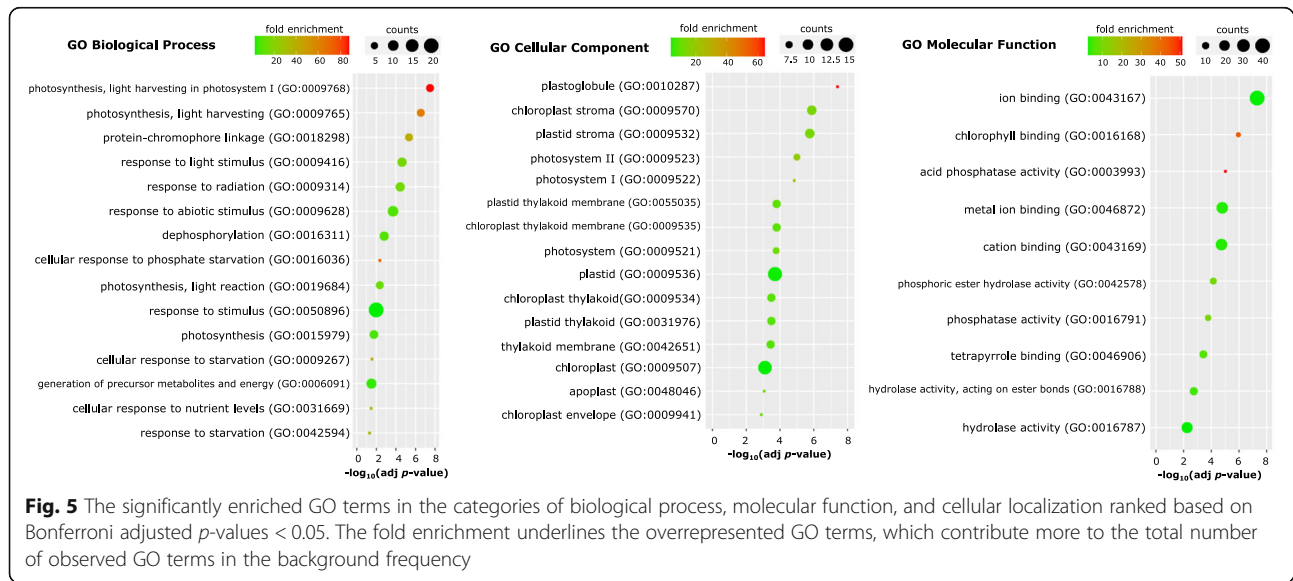
Pi-responsive motifs found in the promoters of DEGs

In general, genes that are affected by Pi status possess characteristic *cis*-regulatory elements within either promoter or 5'-UTR regions [82]. Previously, we have shown the importance of the P1BS motif (PHR1 binding sequence, consensus GnATATnC, [83]) and P-responsive PHO elements (consensus ATGCCAT, [84]) in the expression efficiency of the barley *PHO2* gene [48]. Both motifs may bind PHR-like (PHOSPHATE STARVATION RESPONSE) transcription factors (TFs) and act as activators or repressors of downstream gene expression in a Pi-dependent manner [85]. Likewise, we hypothesized that regulatory regions of the identified DEGs had Pi-responsive motifs, which may be bound by PHR TFs, causing gene expression dysregulation. To confirm this hypothesis, we analyzed DNA sequences from the 2000 bp region upstream of the predicted transcription start sites from all 98 DEGs (Additional file 12). In the next step, promoter data were directly screened for P1BS and P-responsive PHO element consensus sequences by multiple promoter analysis using the PlantPAN3.0 tool. We confirmed the presence of Pi-dependent motif in 55 out of 98 DEGs promoters. An in silico approach detected 46 DEGs having at least one P1BS motif (Additional file 13) and 17 DEGs with at least one P-responsive PHO element (Fig. 6b, Additional file 14). The most over-represented motifs were found in the promoters of genes encoding

Table 2 List of 98 DEGs from barley shoots (low-Pi vs. control/sufficient Pi) identified in this study

#	Gene ID	Chr.	log ₂ (FC)	Encodes	GO: biological process	P1BS	P-resp. PHO element
1	HORVU4Hr1G002520	chr4H	14.20	Ferredoxin	Response to high light intensity		
2	HORVU0Hr1G008980	chrUn	13.35	Mitochondrial-processing peptidase beta subunit	Targeting to mitochondrion		
3	HORVU1Hr1G078380	chr1H	8.90	Chlorophyll a/b binding protein of LHClI type 1-like	Photosynthesis		
4	HORVU6Hr1G080790	chr6H	7.30	Alpha-amylase	Carbohydrate metabolism	GgATATcC; GcATATcC	1562; 1694
5	HORVU4Hr1G079600	chr4H	5.89	IP51	Pi signaling		
6	HORVU3Hr1G079900	chr3H	5.78	Glycerophosphodiester phosphodiesterase, GDDP1	Lipid metabolism		
7	HORVU4Hr1G044140	chr4H	5.27	Monogalactosyl diacylglycerol synthase 2	Lipid metabolism		
8	HORVU5Hr1G062450	chr5H	5.14	Uncharacterized protein	N/A		
9	HORVU5Hr1G066300	chr5H	4.48	O-fucosyltransferase 31-like isoform X2	Fucose metabolism		
10	HORVU3Hr1G091170	chr3H	4.30	Protein kinase domain-containing protein	Protein phosphorylation		ATGCCAT 1188; 1783
11	HORVU3Hr1G017440	chr3H	4.21	Sn1-specific diacylglycerol lipase alpha isoform X1	Lipid catabolism	GaATATcC; GgATATgC	1828; 1872
12	HORVU5Hr1G023710	chr5H	4.21	Uncharacterized protein	N/A		
13	HORVU3Hr1G068380	chr3H	4.01	Inorganic pyrophosphatase 1-like	Pi signaling	GaATATcC	1904
14	HORVU7Hr1G113020	chr7H	3.89	Uncharacterized protein	N/A	GgATATcC; GaATATcC	849; 1923
15	HORVU2Hr1G020140	chr2H	3.80	NIGT1 transcription factor	Nitrate signaling	GgATATcC	1693
16	HORVU3Hr1G010540	chr3H	3.74	Sulfoquinovosyl transferase SQD2-like	Lipid biosynthesis	GcATATcC; GaATATcC; GaATATaC	1099; 1132; 1352
17	HORVU6Hr1G007360	chr6H	3.72	2'-5' exonuclease domain-containing protein	Nucleic acid catabolism	GaATATcC	188
18	HORVU3Hr1G068390	chr3H	3.48	Inorganic pyrophosphatase 1-like	Pi signaling	GaATATcC; GcATATgC	1811; 1917
19	HORVU2Hr1G031400	chr2H	3.44	SPX domain-containing protein 5, SPX5	Pi signaling	GIATATcC	599
20	HORVU2Hr1G112830	chr2H	3.11	Endonuclease, S1/P1 nuclease	Nucleic acid catabolism	GcATATgC	1624
21	HORVU7Hr1G047210	chr7H	2.97	Phosphate transporter PHO1-3	Pi transport		
22	HORVU2Hr1G116250	chr2H	2.93	AB hydrolase-1 domain-containing protein	Lipid metabolism	GIATATcC	1992
23	HORVU4Hr1G022630	chr4H	2.80	CBL-interacting protein kinase 14	Signal transduction		
24	HORVU6Hr1G065710	chr6H	2.79	OsSPX-MFS2 orthologue	Pi signaling		ATGCCAT 128
25	HORVU2Hr1G108290	chr2H	2.64	Uncharacterized protein	N/A		
26	HORVU5Hr1G055570	chr5H	2.60	Purple acid phosphatase (PAP)	Pi signaling	GaATATcC	1970
27	HORVU3Hr1G078360	chr3H	2.49	Purple acid phosphatase (PAP)	Pi signaling	GgATATaC; GgATATaC; GcATATgC	1726; 1758; 1827
28	HORVU5Hr1G066460	chr5H	2.49	Uncharacterized protein	N/A	GcATATaC	1632
29	HORVU2Hr1G097150	chr2H	2.42	MFS-domain containing transmembrane protein	Transmembrane transport		
30	HORVU3Hr1G013890	chr3H	2.38	Putative cytochrome P450	Oxidation-reduction process		
31	HORVU1Hr1G075570	chr1H	2.29	Carotenoid 9,10(9',10')-cleavage dioxygenase (CDD)	Cytoskeleton organisation	GaATATcC	1891
32	HORVU5Hr1G055740	chr5H	2.28	Carotenoid 9,10(9',10')-cleavage dioxygenase (CDD)	Carotene catabolism	GgATATcC	1946
33	HORVU7Hr1G091060	chr7H	2.25	TLC domain-containing protein	Defense response		
34	HORVU5Hr1G124430	chr5H	2.15	Ribosome-binding factor PSRP1, chloroplastic	Translation regulation		
35	HORVU3Hr1G076060	chr3H	2.14	Purple acid phosphatase (PAP)	Pi signaling	GcATATaC	1669
36	HORVU5Hr1G051160	chr5H	2.12	Probable tyrosine-protein phosphatase (DSP4)	Defense response	GaATATcC	657
37	HORVU3Hr1G034460	chr3H	2.10	Purple acid phosphatase (PAP)	Pi signaling		
38	HORVU5Hr1G028140	chr5H	2.08	Heptahelical transmembrane protein 4	Abiotic stress response		ATGCCAT 1408
39	HORVU6Hr1G016850	chr6H	2.04	Chlorophyll a/b binding protein, chloroplastic	Photosynthesis		
40	HORVU6Hr1G016880	chr6H	2.02	Chlorophyll a/b binding protein, chloroplastic	Photosynthesis		
41	HORVU6Hr1G080750	chr6H	1.98	Nitrite reductase (NIR)	Nitrate signaling		
42	HORVU2Hr1G110540	chr2H	1.95	Molybdate transporter 2 (MOT2)	Molybdate ion transport	GgATATcC	585
43	HORVU1Hr1G054430	chr1H	1.95	Halocacid dehalogenase-like hydrolase domain-containing protein (HAD1)	Pi signaling	GcATATaC	1861
44	HORVU5Hr1G097130	chr5H	1.94	Peroxidase 57-like	Response to oxidative stress	GaATATaC	642
45	HORVU7Hr1G053940	chr7H	1.90	Uridine kinase	Nucleoside metabolism		
46	HORVU2Hr1G116180	chr2H	1.87	AB hydrolase-1 domain-containing protein	Lipid metabolism		
47	HORVU5Hr1G079600	chr5H	1.84	Uncharacterized protein	N/A	GgATATcC; GcATATcC; GcATATgC	733; 741; 1859
48	HORVU6Hr1G016940	chr6H	1.79	Uncharacterized protein	N/A	GaATATgC; GaATATgC; GaATATcC	293; 329; 1670
49	HORVU6Hr1G058780	chr6H	1.79	Phosphoenolpyruvate carboxylase kinase 2 (PPCK2)	Signal transduction		
50	HORVU1Hr1G089180	chr1H	1.79	Chlorophyll a/b binding protein, chloroplastic	Photosynthesis		
51	HORVU7Hr1G089910	chr7H	1.78	SPX domain-containing protein 1, SPX1	Pi signaling	GcATATgC; GaATATcC; GcATATcC	857; 1765; 1795
52	HORVU1Hr1G089920	chr1H	1.75	Chlorophyll a/b binding protein, chloroplastic	Photosynthesis	GgATATcC; GaATATaC; GcATATgC	249; 1132; 1480
53	HORVU6Hr1G016890	chr6H	1.75	Inositol hexakisphosphate and diphosphoinositol-pentakisphosphate kinase (VIP1)	Pi signaling	GIATATaC	887
54	HORVU3Hr1G076320	chr3H	1.73	Phosphoenolpyruvate carboxylase 1-like	Pi signaling	GaATATcC	503
55	HORVU3Hr1G029200	chr3H	1.73	Purple acid phosphatase 5 (PAP5)	Pi signaling	GcATATgC; GIATATgC; GaATATcC	734; 754; 1704
56	HORVU5Hr1G044460	chr5H	1.63	Purple acid phosphatase 5 (PAP5)	Pi signaling	GaATATcC; GaATATaC	1267; 1982
57	HORVU5Hr1G106010	chr5H	-1.40	Pathogenesis-related protein 1-like	Defense response	GIATATcC; GIATATgC; GaATATcC	4; 25; 721
58	HORVU3Hr1G108100	chr3H	-1.43	Carotenoid 9,10(9',10')-cleavage dioxygenase 1 (CDD1)	Carotene catabolism	GIATATaC	1653
59	HORVU3Hr1G065320	chr3H	-1.49	ABC transmembrane type-1 domain-containing protein	ATPase activity		ATGCCAT 1870
60	HORVU2Hr1G115730	chr2H	-1.50	Stress enhanced protein 2, chloroplastic	Response to high light intensity		
61	HORVU5Hr1G077920	chr5H	-1.50	Beta-glucosidase 31-like	Carbohydrate metabolism	GIATATcC	383
62	HORVU3Hr1G103950	chr3H	-1.54	Protein-rich receptor-like protein kinase 10	Protein phosphorylation	GgATATcC	400
63	HORVU0Hr1G038320	chrUn	-1.73	Prx4L endopeptidase-like	Metabolism of peptides	GIATATgC	899
64	HORVU5Hr1G081950	chr5H	-1.75	Probable inactive purple acid phosphatase 29	Pi signaling		
65	HORVU2Hr1G024460	chr2H	-1.80	Uncharacterized protein	N/A		
66	HORVU7Hr1G010990	chr7H	-1.91	Aromatic-L-amino-acid decarboxylase-like	Metabolism of amino acids		
67	HORVU3Hr1G077950	chr3H	-1.91	Subtilisin-like protease (SBT3)	Defense response		ATGCCAT 7
68	HORVU1Hr1G089620	chr1H	-1.92	Caffeic acid-3-O-methyltransferase (COMT)	Stress response		ATGCCAT 197
69	HORVU2Hr1G112230	chr2H	-1.96	Zinc transporter 8-like (ZnT8)	Zinc transport		
70	HORVU2Hr1G012980	chr2H	-1.97	Premnaspirodiene oxygenase-like	Oxidation-reduction process	GgATATcC	1849
71	HORVU1Hr1G089520	chr1H	-1.98	Flavonoid 7-O-methyltransferase	Defense response		
72	HORVU2Hr1G112060	chr2H	-2.01	Glycine-rich protein 2-like	Stress response		
73	HORVU4Hr1G071300	chr4H	-2.02	Aminotransferase (ALD1 homolog)	Defense response	GIATATgC	968
74	HORVU2Hr1G038940	chr2H	-2.04	Photosystem II 10 kDa polypeptide, chloroplastic	Photosynthesis		
75	HORVU4Hr1G001250	chr4H	-2.05	Tricetin 3',4',5'-O-trimethyltransferase-like (OMT2)	Stress response	GgATATcC	1162
76	HORVU4Hr1G044460	chr4H	-2.09	Potential tubulin alpha-6 chain	Cytoskeleton organisation	GaATATgC; GIATATgC	2; 1347
77	HORVU3Hr1G097860	chr3H	-2.10	Laccase (LAC19-like)	Copper homeostasis		
78	HORVU6Hr1G083050	chr6H	-2.13	Alpha-aminoacidic semialdehyde synthase	L-lysine catabolism		
79	HORVU6Hr1G008780	chr6H	-2.17	Papain-like cysteine proteinase	Stress response		
80	HORVU1Hr1G065150	chr1H	-2.19	Putative proteinase inhibitor (wrsi5-1)	Stress response		
81	HORVU3Hr1G070540	chr3H	-2.20	Probable glutamate carboxypeptidase 2	Defense response		
82	HORVU0Hr1G008640	chrUn	-2.34	Tyrosine-specific transport protein-like	Transport of amino acids		
83	HORVU1Hr1G081410	chr1H	-2.39	Chaperone protein dnaJ C76, chloroplastic isoform X1	Stress response	GcATATgC	284
84	HORVU1Hr1G019750	chr1H	-2.44	Laccase(LAC19-like)	Copper homeostasis		
85	HORVU5Hr1G081860	chr5H	-2.49	Chaperone protein CtpD1, chloroplastic	Stress response		
86	HORVU7Hr1G116080	chr7H	-2.51	Endoplasmic reticulum metalloproteinase 1	Stress response	GcATATcC	1316
87	HORVU6Hr1G012090	chr6H	-2.52	S-(+)-linalol synthase, chloroplastic-like	Defense response		
88	HORVU2Hr1G094690	chr2H	-2.58	OsSPX-MFS1 orthologue	Pi signaling	GIATATgC	1823
89	HORVU6Hr1G005720	chr6H	-2.60	High-affinity nitrate transporter 2.1-like (NRT2.1)	Nitrate signaling	GcATATaC; GcATATaC	291; 345
90	HORVU2Hr1G070220	chr2H	-2.61	Alanine-glyoxylate aminotransferase-2-like	Biosynthesis of amino acids	GaATATaC; GaATATaC; GaATATcC	1456; 1506; 1763
91	HORVU4Hr1G005440	chr4H	-2.62	Oxalate oxidase (germin-like protein)	Defense response	GIATATaC	728
92	HORVU2Hr1G006830	chr2H	-2.62	Indole-2-monooxygenase-like	Oxidation-reduction process	GaATATgC	9
93	HORVU2Hr1G088640	chr2H	-2.95	Peroxygenase-like	Defense response		
94	HORVU1Hr1G089540	chr1H	-3.05	Chalcone synthase 2	Stress response		ATGCCAT 120
95	HORVU3Hr1G020960	chr3H	-3.17	Probable glutamate carboxypeptidase 2	Defense response		
96	HORVU2Hr1G007600	chr2H	-3.41	Beta-essiquipellandrene synthase-like	Defense response		
97	HORVU4Hr1G005380	chr4H	-4.41	Oxalate oxidase 2 (germin-like protein)	Defense response	GaATATcC	1579
98	HORVU2Hr1G030090	chr2H	-6.50	Uncharacterized protein	N/A		ATGCCAT 1314; 1662; 1700





sulfoquinovosyl transferase SQD2-like ($\log_2(\text{fc}) = 3.74$) [86], phosphoenolpyruvate carboxylase 1-like ($\log_2(\text{fc}) = 1.73$) [87], and pyridoxal phosphate-dependent transferase ($\log_2(\text{fc}) = -2.61$) [88]. Each of the genes harbor three PIBSs and one P-responsive PHO element, as well (Table 2).

Degradome profiling describes post-transcriptional regulatory network of identified DEMs

After identification of (i) differentially expressed miRNAs (DEMs), (ii) other sRNAs (DESSs), and (iii) mRNAs (DEGs), we used this comprehensive data together with cDNAs annotated in the Ensembl Plants database to identify the sRNAs directly involved in RNA degradation. The DESSs were also examined, because we assumed that there may have been putative miRNAs that were not mapped to the miRbase, due to restricted query settings allowing no mismatch or that there are other small RNAs which could be involved in mRNA degradation. It was shown that human Ago proteins are associated with short RNA originated from non-miRNA sequences (mRNA, snRNA, snoRNA, tRNA, vRNA) [89]. Molecules which exhibited a single mismatch (or more) may still function as miRNA in barley. Degradome libraries were carried out for root, as well as for shoot, and sequenced using an Illumina System. The received data were analyzed using two independent in silico approaches: PAREsnip2 (PS) and TargetSeek (TS) (Fig. 2). At times, the different algorithms used elicited different miRNA targets; however, the general degradome pattern was equivalent for both approaches (Table 1, Additional files 15, 16, 17, 18, 19, 20, 21, 22, 23, 24, 25 and 26).

In order to determine the potential cleavage activity of miRNAs identified in shoot and root we performed

degradome analysis. Firstly, we searched for the potential target mRNAs for differentially expressed miRNAs with significant fold change (Bonferroni adjusted p -value), taking 15 DEMs from shoot and 13 DEMs from root, respectively (Table 1). A total of 168 scores were obtained for shoot DEMs (113 using the TargetSeek approach and 55 using PAREsnip2) (Additional files 15, 19 and 20), while in root there were 26 records (24 and 2, respectively) (Additional files 17, 23 and 24).

None of the DEM annotated as part of the pre-miRNA was found in the degradome platform. While 10 out of 19 DEMs annotated as mature/isomiR molecule scored for target prediction. In shoot, a majority of records corresponded to different miR399 and/or miR827 isomiRs and their known targets PHO2 or SPX-MFS1/SPX-MFS2, respectively. One of the best scoring miRNA:mRNA match was found for mature miRNA827 (21 nt, ID: 2073), which guides cleavage within the 5'-UTR of *SPX-MFS1* mRNA (isoform no. 4) in position 192 ($p = 0.014$) (Fig. 7). In roots, the most downregulated miR319b (22 nt, ID: 51) has predicted three different target loci in barley. The miR319b guides for cleavage PCF6 TF and two GaMyb-like TFs (Table 1). The plant GAMyb TFs, have been shown to activate gibberellin-responsive gene expression of α -amylase in barley [90, 91].

Putative regulatory small RNAs identified in degradome data

Degradome profiling was performed to test whether any of the sequences from the 1796 DESSs found in roots or 199 DESSs found in shoots contribute to the complexity of gene regulation during low-Pi stress. A total of 759

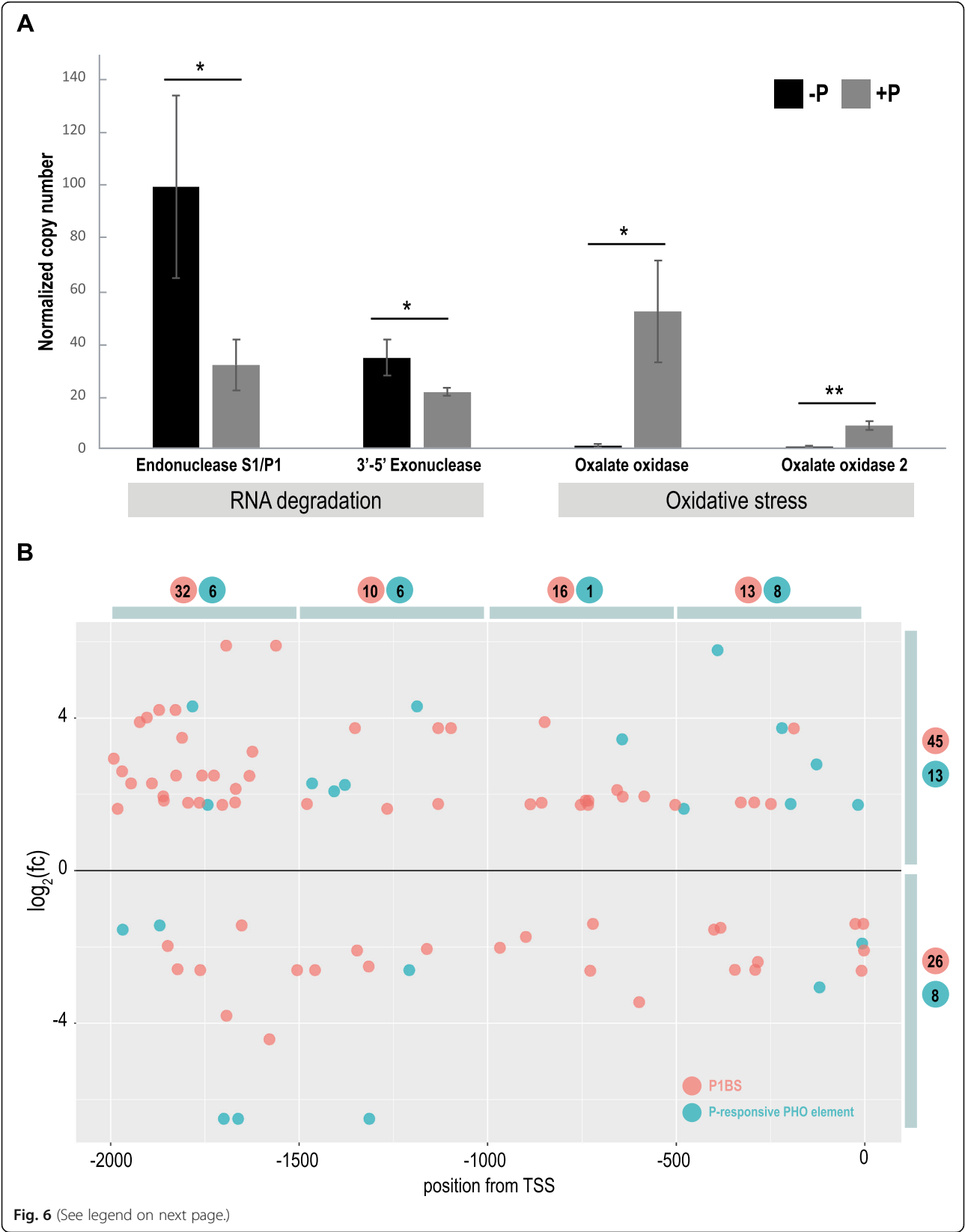


Fig. 6 (See legend on next page.)

(See figure on previous page.)

Fig. 6 Molecular characterization of identified DEGs from barley shoot. **a** Quantification by ddPCR of the absolute expression levels of the DEGs belonging to two selected pathways in barley shoots. Two up-regulated DEGs, which encode endonuclease S1/P1 and 3'-5' exonuclease, are involved in nucleic acid metabolism and further RNA degradation. Two down-regulated DEGs, which encode two different oxalate oxidases, are involved in the reduction of oxidative stress. The bars represent copy numbers normalized to 1000 copies of the *ARF1* reference gene; **p*-value < 0.05, ***p*-value < 0.001, calculated using two-tailed Student's *t*-tests for three biological and two technical replicates. **b** Localization of all P1BS and P-responsive PHO *cis*-regulatory elements within the 2000 bp upstream from the DEG TSSs. On the graph, grouped motifs are specifically located in every 500 bp, induced ($\log_2(\text{fc}) > 0$), or repressed ($\log_2(\text{fc}) < 0$). The motif quantity in each group is shown in either red (P1BS) or blue (PHO elements) dots

records (245 using the TargetSeek approach and 514 using PAREsnip2) were found in the degradome profiles matching root DESs (Additional files 18, 25 and 26) and 160 records (87 and 73, respectively) matching shoot DESs (Additional files 16, 21 and 22). Taking only either the most up-regulated or the most down-regulated sRNAs for degradome screening, we found six promising target genes in shoot and five in root (Table 3). For example, in roots, the highly up-regulated 20 nt DES ID: 348 ($\log_2(\text{fc}) = 6.46$) binds to the 3'-UTR region of the MYB44 TF's mRNA and guides/promotes cleavage in the 1037 position (PAREsnip2: score = 4; MFE = -33.3) (Table 3). RNA-Seq data for potato (*Solanum tuberosum* L.) proved that expression of the MYB44 gene is highly downregulated under low-Pi in roots [92], which may be the result of miRNA-guided PTGS. Studies in potato have indicated that MYB44 TF may

form a regulatory complex together with WRKY6 TF, which negatively regulates Pi transport by suppressing *PHO1* expression [92]. Other degradome records in this study, among the most differentially expressed sRNAs, were found to target mRNAs of the V-ATPase assembly factor (VMA21-like) and three barley genomic loci encoding uncharacterized proteins (HORVU7Hr1G053570, HORVU1Hr1G027340, and HORVU0Hr1G023910) (Table 3). For example, the potential cleavage activity was predicted for 24 nt DES ID: 463 ($\log_2(\text{fc}) = -3.58$), which may target the mRNA encoding uncharacterized protein with unknown PTHR47188 domain (Fig. 8).

Analogous degradome screening was done for shoot data. Among all identified DESs, we found that the most upregulated sequence, 24 nt DES ID: 2112 ($\log_2(\text{fc}) = 8.72$), targets the 3'-UTR of mRNA encoding multiple

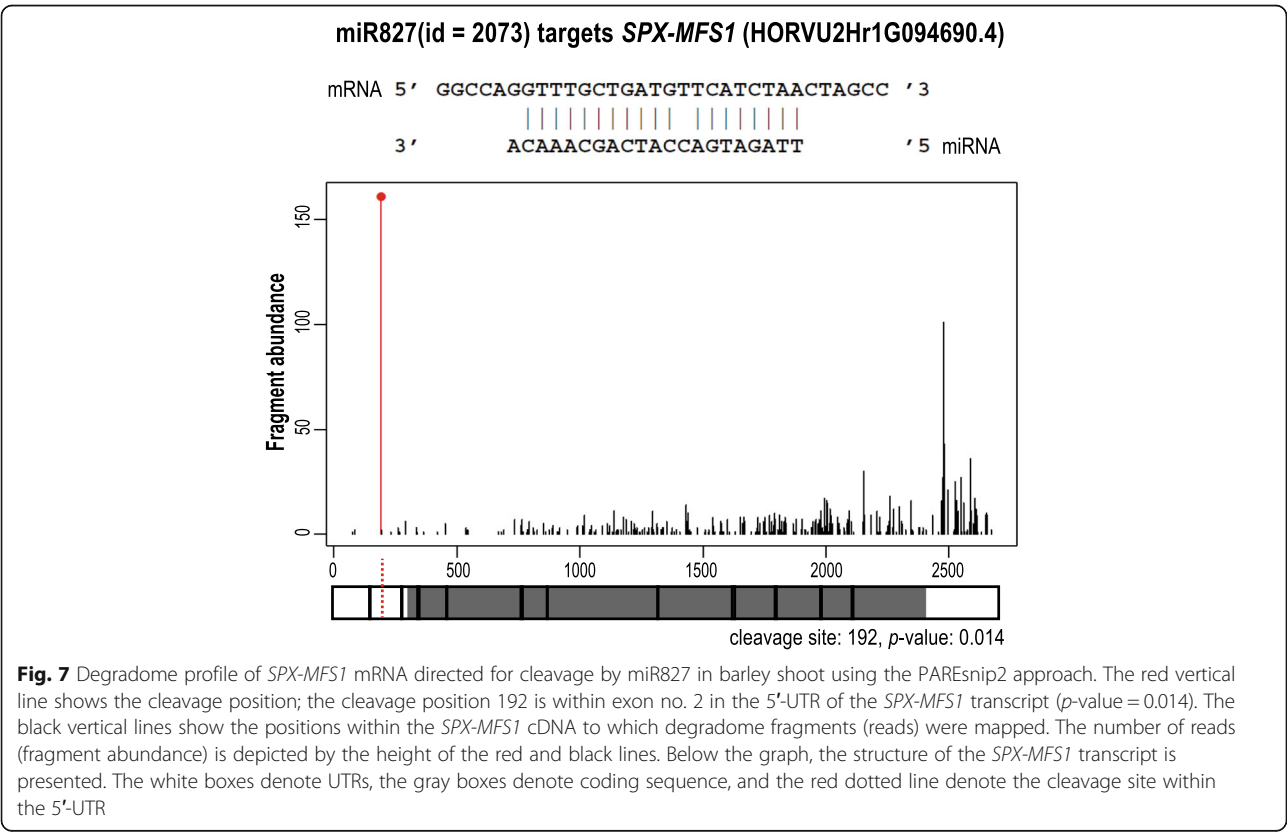


Table 3 List of genes predicted in degradome analysis to be guided for cleavage by the most up- and down-regulated DES identified in this study

ID	Sequence	Lenght	DES annotation	log ₂ (FC)	Target	Cut	Score	MFE
SHOOT	>2112 AAGATTGGTTGGTTGGTTGGTCT	24	Unannotated	8.72	HORVU7Hr1G073170,1 ^{TS} HORVU7Hr1G073170,3 ^{TS} HORVU7Hr1G073170,7 ^{TS} HORVU7Hr1G073170,9 ^{PS}	730 628 704 562	16.5 16.5 16.5 16.5	-28.1 -28.1 -28.1 -28.1
	>2265 TGCCAAAGGAGAACTGCCCTG	21	*miR399b/miR399a	6.27	HORVU1Hr1G085570,3 ^{PS} HORVU6Hr1G028940,8 ^{PS} HORVU6Hr1G028940,11 ^{PS} HORVU6Hr1G028940,17 ^{PS}	857 1497 1321 792	6 / 3.5 3.5 3.5 3.5	-29.9 / -33.4 -24.2 -24.2 -24.2
	>2113 AAGCTCGGATTGATTACA	19	Protein-coding	4.68	HORVU1Hr1G093760,10 ^{PS} HORVU1Hr1G093760,11 ^{PS} HORVU1Hr1G093760,12 ^{PS} HORVU1Hr1G093760,13 ^{PS}	511 360 294 294	4 4 4 4	-27.6 -27.6 -27.6 -27.6
	>2146 ATAGTCGGTGCTGCTGCA	18	Protein-coding	4.5	HORVU3Hr1G036970,1 ^{TS} HORVU3Hr1G036970,2 ^{TS} HORVU3Hr1G036970,3 ^{TS} HORVU3Hr1G036970,4 ^{TS}	781 637 745 479	12 12 12 12	-43.2 -43.2 -43.2 -43.2
	>2137 AGGAGGCGCGCGCGCGCTG	21	rRNA	-1.26	Uncharacterized protein with transmembrane domain	637	12	-43.2
	>2225 GGGGGATCTACCGTCGTGATG	24	Unannotated	-4.49	Lysine-specific demethylase 5A (LSD)	1082	3	-42.0
	348 ACCGACCTACTTGACCCCTC	20	Unannotated	6.46	MYB44 transcription factor	1037	4	-33.3
	1804 TGAAAGGACTTTGAAAGAGAGT	24	Protein-coding	-3.48	Vacuolar ATPase, VMA21 homolog	2402 2304 295 164 404 284	13 13 0 0 0 0	-21.9 -21.9 -49.4 -49.4 -49.4 -49.4
	463 AGAGGAACTCTGGTGGAGGCTCG	24	rRNA	-3.58	Uncharacterized protein with unknown PTHR47188 domain	156 748 1614 2020 321	0 0.5 0 0 0	-48.4 -48.5 -49.4 -49.4 -49.4
ROOT								

* = annotated to miRbase with at least one mismatch; TS = TargetSeek; PS = PAREsnip2

log₂(fold change)

* = annotated to miRbase with at least one mismatch; TS = TargetSeek, PS = PAREsnip2

organellar RNA editing factor 9 (MORF9, HORVU7Hr1G073170, TargetSeek: score = 16.5, MFE = -28.1) (Table 3). MORF9 proteins are required for RNA editing in plastid mRNAs, which may contribute to stress adaptation in plants [93, 94]. In both approaches, we found that the 21 nt DES ID: 2265 (log₂(fc) = 6.27) targeted the same isoform of *PHO2* mRNA (HORVU1Hr1G085570.3, TargetSeek: score = 6, MFE = -29.9, PAREsnip2: score = 3.5, MFE = -33.4). When we browsed the miRBase using this 21 nt sRNA as a query, we found high similarity to the osa-miR399a, exhibiting

only one mismatch. Thus, we suspect that such sRNA may function as another miR399 isomiR in barley. Most dysregulated DESs were also found to target mRNAs encoding methyltransferase type 11 domain-containing protein (MT11), AAA-ATPase (At3g50940-like), lysine-specific demethylase 5A (LSD), or an uncharacterized protein with a predicted transmembrane domain (HORVU3Hr1G036970). The best scoring degradome records were found for the 21 nt DES ID: 2279 (log₂(fc) = 3.11), which targets mRNAs encoding SPX-MFS1 (PAREsnip2: score = 2.5, MFE = -27.5) and SPX-MFS2 (TargetSeek:

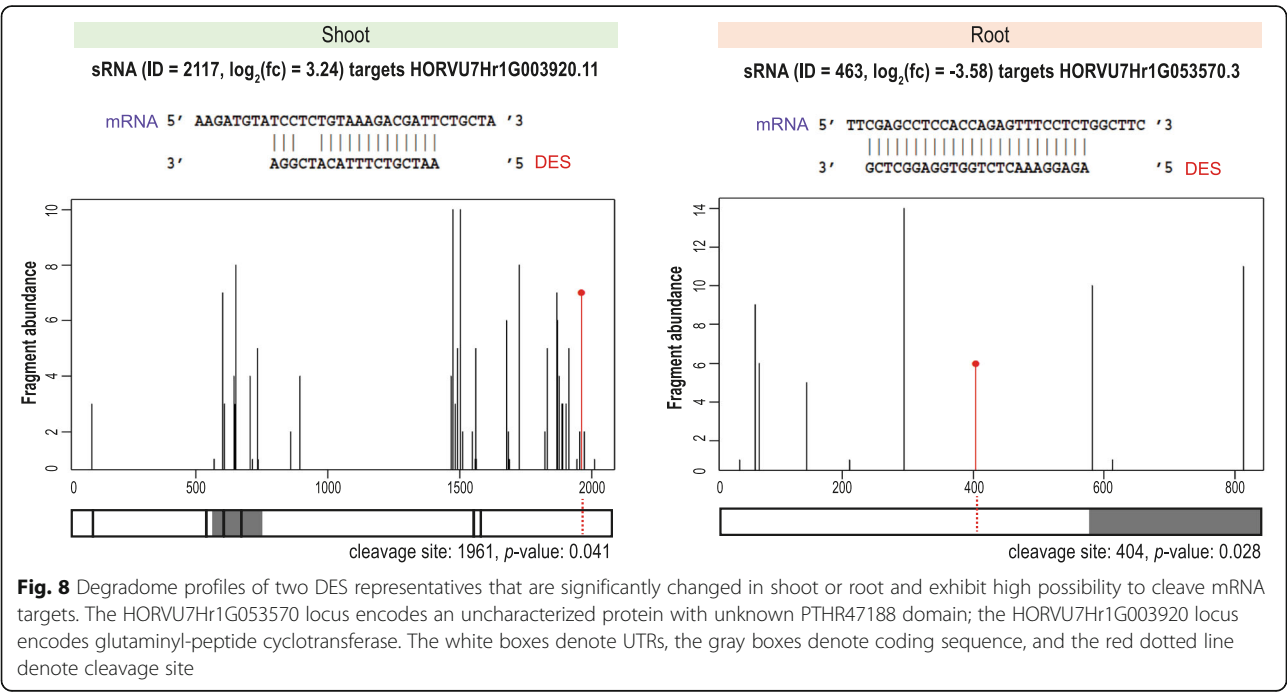


Fig. 8 Degradome profiles of two DES representatives that are significantly changed in shoot or root and exhibit high possibility to cleave mRNA targets. The HORVU7Hr1G053570 locus encodes an uncharacterized protein with unknown PTHR47188 domain; the HORVU7Hr1G003920 locus encodes glutaminy-peptide cyclotransferase. The white boxes denote UTRs, the gray boxes denote coding sequence, and the red dotted line denote cleavage site

score = 3.5, MFE = -26) (Additional file 27). Further analysis revealed that such DES annotates to osa-miR827 with one mismatch. This result suggests that such sRNA may exist as another miR827 isomiR in barley. Moreover, this is consistent with the screening made for differentially expressed miRNAs, where miR827 targeted both SPX-MFS proteins, depending on the approach we used. In addition, the 18 nt DES ID: 2117 ($\log_2(fc) = 3.24$) was found to target mRNA encoding glutamyl-peptide cyclotransferase (HORVU7Hr1G003920, PAREsnip2: score = 2.0, MFE = -19.6) (Fig. 8), which may be involved in plant defense reactions [95].

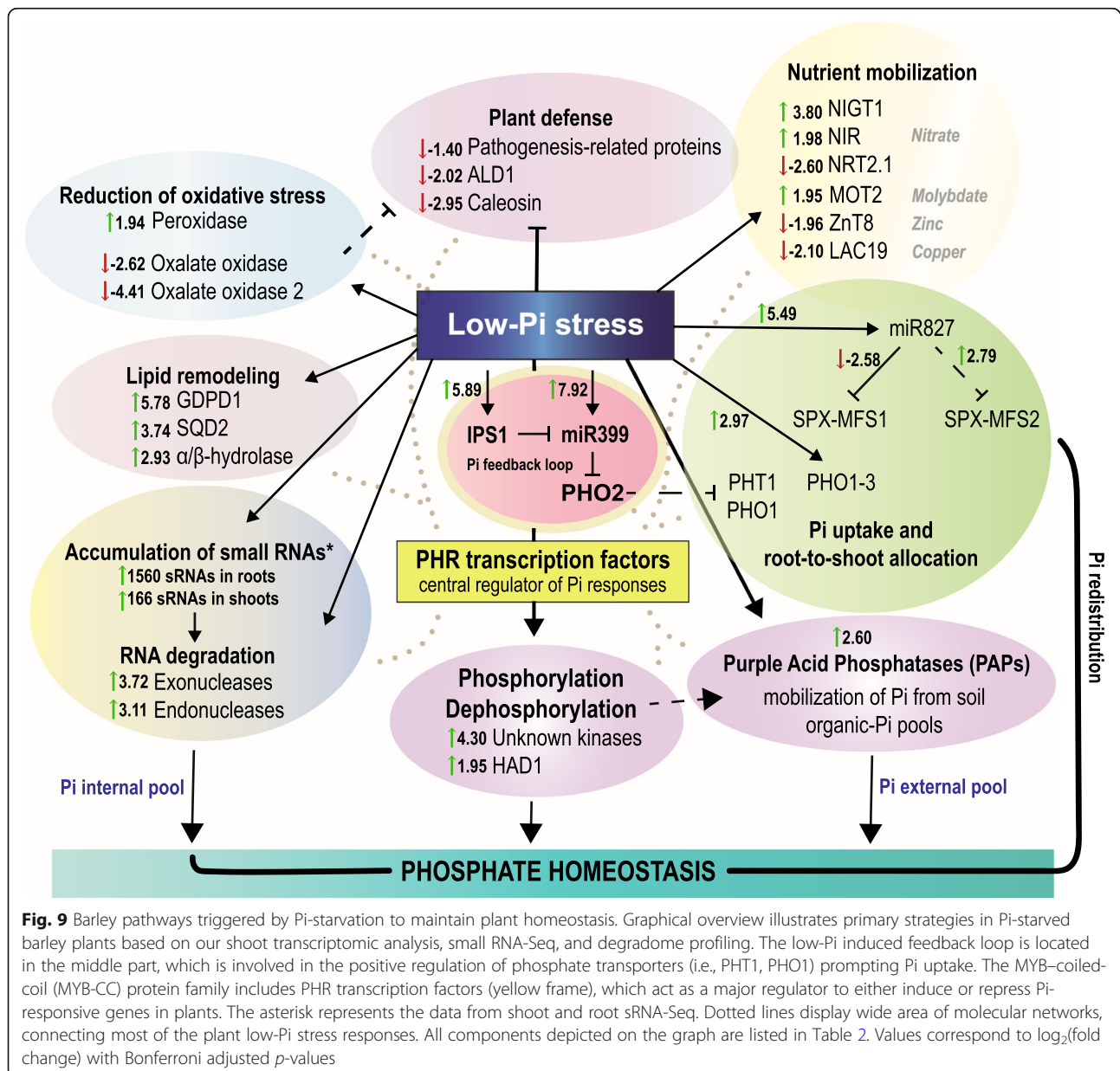
Some other interesting Pi-related targets which are recognized by DESs were found in our root degradome data, but the prediction scores were weaker than those in the examples described above. For instance: nitrate reductase (HORVU6Hr1G003300), high-affinity nitrate transporter-activating protein (HORVU5Hr1G115500), MYB-like TF (HORVU7Hr1G027370), and stress-induced TF NAC1 (HORVU5Hr1G11590) were found. Interestingly, among the 98 DEGs identified in this study, only two of them (SPX-MFS1 and SPX-MFS2) were found as putative targets of miRNA guided activity. In addition, none of the DEGs gene IDs were found to match with any of the identified IDs classified for differentially expressed small RNAs.

Discussion

In this study, we used a tripartite approach (sRNA-Seq, mRNA-Seq, and degradome-seq) to describe the set of small RNAs differentially expressed in barley roots and shoots under low-Pi stress. We detailed the sophisticated responses of barley shoots and roots involved in the maintaining of Pi homeostasis (Fig. 9). Integrated deep-sequencing data were used to describe organ-specific adaptations to low-Pi through either activation or repression of different classes of 18–25 nt small RNAs. Additionally, the mRNA-Seq analysis of low-Pi treated barley shoot was performed to analyze the correlation between shoot-derived small RNAs, annotated to either protein-coding mRNAs (47.87%) or non-translating RNAs (36.49%), and gene expression changes of polyadenylated RNAs. We identified a total of 28 differentially expressed miRNAs (Bonferroni adjusted *p*-value) annotated to miRBase (release 22) without mismatches and a total of 1995 differentially expressed other small RNAs (Bonferroni adjusted *p*-value).

In plants, a limited number of miRNA have been shown to be specifically and strongly induced by Pi limitation, including miRNA399 [96], miRNA778 [59], miRNA827 [55], and miRNA2111 [55, 97]. In this work, the majority of DEMs represent various miR399 and miR827 isomiRs in both tested organs. Our results are

consistent with sRNA sequencing data published for Arabidopsis [42, 55] and *Nicotiana benthamiana* L. [98]. In both plant species, authors have shown that the number of various miR399 isomiRs was the most abundant in shoots and roots under low-Pi. Eight of the 15 DEMs (after Bonferroni *p*-value adjustment) we found in barley shoots belonged to the miR399 family. However, in root, miR399 was represented only by two DEMs; the miR399a and miR399b (Table 1). Previously, our absolute copy number analysis of mature miR399 demonstrated that its normalized expression level is 4-fold downregulated in barley roots, as compared to in shoots, under a low-Pi regime [99]. The long-distance movement of signal molecules is known to be crucial for Pi recycling and allocation from root to shoot. The root system is responsible for Pi acquisition conducted by phosphate transporters belonging to PHT1 family, which saturate cell membranes during Pi deficiency [100]. The level of PHT1 proteins is negatively controlled by the PHO2, which is suppressed by miR399 (see model in Fig. 9) [101]. A high level of miR399 molecules was detected in Arabidopsis wild type rootstocks grafted with miR399-overexpressing scions [42, 102]. Thus, miR399 is involved in a plant's systemic response to low-Pi conditions and acts as a long-distance signal, moving from shoot to root to control Pi homeostasis [102]. In Arabidopsis, miR827 has been shown in multiple studies to target the 5'-UTR of the *NITROGEN LIMITATION ADAPTATION* (*NLA*) gene [103, 104]. In rice, the *OsNLA* mRNA has a 'degenerate' osa-miR827 potential cleavage site, that is why miR827 does not cleave the *OsNLA* transcript in vivo [56, 57, 105]. Likewise, we did not find *NLA* mRNAs to be targeted by any of the identified hvu-miR827 isomiRs in our barley degradome records. The *NLA* gene encodes an E3 ubiquitin-protein ligase with RING and SPX domains, which interacts with the PHO2 to prevent the excessive accumulation of Pi [106]. In roots, a more diverse set of miRNAs contributed to the compensation of low-Pi stress, compared to that in shoots. We found six up-regulated miRNA molecules (DEMs) in roots mapped to pre-miRNAs, such as: two miR9779, two miR5083, miR1511 and miR5072. In addition, none of them was found in our degradome analysis. The differentially expressed other small RNAs in roots (DESs, 1796 molecules) were represented by 90% of the total set of other sRNAs (DESs from both organs), annotated to all classes of cDNAs taken for analysis. Among the identified set of DESs, we found non-miRNA small RNAs with high probabilities to target various mRNAs involved in plant adaptations to abiotic stresses, plant defense, and/or transcription (Table 3, Additional file 27). Further analysis will be performed to experimentally validate the in silico predicted PTGS role of Pi-responsive small RNAs found in this study, as well.



In this paper, we detailed the shoot differentially expressed genes (DEGs) harboring Pi-responsive *cis*-regulatory elements, involving various molecular pathways and biological processes. These DEGs were mostly engaged in Pi mobilization and utilization upon Pi-starvation in barley shoots. Other sRNAs selected from shoots were much less abundant and represent sequences belonging mostly to non-translating and/or protein-coding mRNAs. None of the sRNAs mapped to the differentially expressed mRNAs found in the transcriptomic analysis, suggesting that they may inhibit gene expression through translational repression or may serve as a Pi source for developing plant organs. Plants are adapted to recycle nutrients from senescing organs.

For example, class II RNases are involved in the degradation of housekeeping rRNAs before cell death occurs [107]. During senescence extracellular class I RNases were shown to degrade RNA during Pi-starvation in Arabidopsis as well [108]. In 2018, Ren et al. published RNA-Seq data describing the barley transcriptome under low-Pi stress [109]. The authors compared the transcriptomes of two barley genotypes with contrasting low-Pi stress tolerance. In roots, they observed 28 DEGs classified into the following functional groups: Pi transport, transcription, lipid metabolism, metabolism, and phosphorylation/dephosphorylation [109]. Likewise, our mRNA-Seq data from barley shoot discovered the DEGs involved in all mentioned functional groups. In our shoot

transcriptome analysis, we found the same four DEGs: (i) *GLYCEROPHOSPHODIESTER PHOSPHODIESTERASE 1* (*GDPD1*) gene (HORVU3Hr1G079900, $\log_2(\text{fc}) = 5.78$), (ii) *MONOGALACTOSYLDIACYLGLYCEROL SYNTHASE 2* gene (*MGD2*, HORVU4Hr1G044140, 5.27), (iii) *SPX5* (HORVU2Hr1G031400, 3.44), and (iv) *SPX1* (HORVU7Hr1G089910, 1.78). Furthermore, Ren et al. found three genes encoding purple acid phosphatases (PAPs) [109]; however, they appeared from different barley genome loci than the five PAPs we found in our study. It was shown that vacuolar and secreted PAPs are involved in Pi scavenging and remobilization during Pi-starvation and leaf senescence. Other related RNA-Seq data published for either wheat (*Triticum aestivum* L.) [110], rice [111], soybean [112], *Plantago major* L. [113], and maize [114] demonstrated similar molecular patterns to those in our study (Table 2). Based on our work we propose a model of barley adaptations to Pi-starvation (Fig. 9). Interestingly, the presence of crucial Pi-responsive *cis*-regulatory elements within the promoter regions of more than 50% of identified DEGs may indicate their essential and direct role in conditioning low-Pi tolerance (Fig. 6b). The most widely studied PHR TFs, such as PHR1 in Arabidopsis [83] and PHR2 in rice [115], bind to P1BS elements present in the promoter of a broad range of Pi-related genes. Moreover, the PHR protein family exhibits high functional redundancy and its protein members may cooperatively form a regulatory network to maintain Pi homeostasis in plants [85]. In our previous paper, we showed that, within the 5'-UTR of the *PHO2* gene, there is another Pi-responsive motif called the PHO element in close proximity to the P1BS [48]. The PHO element can be bound by PHR-like transcription factors in barley plants, as well [48], and has been found in the promoters of many DEGs in independent Arabidopsis [116, 117] or soybean [112] studies.

The elevated abundance of sRNAs has been associated with the up-regulation of two types of nucleases (endonuclease S1/P1 and 3'-5' exonuclease), which may catalyze the degradation of RNA into shorter fragments [118, 119] and play a relevant role in nutrient mobilization under Pi-starvation. It seems likely that sRNA production upon Pi-starvation is an effect of RNA degradation by different types of nucleases. Thus, degraded RNA may serve as a source of Pi necessary in emerging plant organs. We found also two genes encoding oxalate oxidases, the expression of which was significantly downregulated during Pi-starvation. This class of genes is responsible for the inactivation of oxalic acid, which mediates fungal-plant pathogenesis in barley [120].

Conclusion

To conclude, our studies provide comprehensive data sets, which may serve as a rich platform for the

characterization of barley responses to Pi-starvation at an RNA level. Furthermore, our data may be used as a reference tool for parallel studies in other crop plants.

Materials and methods

Plant material

Three biological replicates of barley root and shoot samples were analyzed. One replicate consisted of three plants growing in a single pot containing 1.5 kg of soil mixed with sand in a 7:2 ratio. Material was collected from the barley line Rolap (obtained from the Institute of Plant Genetics of the Polish Academy of Sciences, Poznań, Poland [121]) growing under low-Pi (8 mg P/kg soil) and Pi-sufficient conditions (after addition of 60 mg P/kg soil), as described before [48]. On the 23rd day after sowing plant shoots (Zadoks decimal code 22–23 [122]), they were cut off and fresh tissue weight was measured. Immediately afterwards, shoots and roots were collected and frozen in liquid nitrogen to be kept at -80°C until use.

Pi concentration measurements

Measurements of inorganic phosphate level were performed according to the protocol we have described before [46]. The samples were measured in two technical and three biological replicates using an Infinite F200 Pro (TECAN, Switzerland).

RNA isolation

Four procedures of RNA isolation were used, depending on the following experiments: (i) small RNA expression level analysis (ddPCR using TaqMan™ MicroRNA assays, NGS of small RNAs, Northern hybridization); (ii) shoot transcriptome analysis; (iii) degradome - PARE (Parallel Analysis of RNA Ends) [123] analysis for mRNA cleaved by miRNA; or (iv) validation of RNA-Seq data using ddPCR.

(i) Small RNA expression level analysis

RNA isolation was performed using a modified method allowing enrichment of small RNAs, according to the detailed protocol we published before [65].

(ii) RNA for RNA-Seq

RNA was extracted from a 100 mg of shoot sample using RNA extraction buffer [99] and a Direct-Zol RNA MiniPrep Kit (Zymo Research). According to the Lexogen's SENSE mRNA-Seq Library prep kit v2 user guide DNase treatment step was omitted to avoid RNA hydrolysis.

(iii) RNA for degradome analysis

Procedure of RNA isolation from barley root and shoot (growing in low-Pi conditions) used for degradome profiling was performed using a method described by German et al. using RNA extraction buffer [123], along with some modifications that we have described previously [65, 124].

(iv) mRNA-Seq data validation

To validate the transcript level of significantly changed genes, we used precise dd-PCR analysis. To isolate RNA for these analyses, we used a Direct-Zol RNA MiniPrep Kit (Zymo Research) with some modifications that we have described in detail previously [99]. The RNA material was treated using DNase I enzyme from the above kit (Zymo Research).

Preparation of NGS libraries

We prepared three different NGS libraries: (i) small RNA, (ii) transcriptome - mRNA, and (iii) degradome.

(i) Small RNA libraries

Small RNA libraries were prepared using a TruSeq Small RNA Library Prep Kit (Illumina). In brief, small RNAs of 15–30 nt in length were separated on denaturing 8 M urea 15% polyacrylamide (PA) gel and purified and ligated to 3' and 5' RNA adapters. Next, the RNA fragments were reverse transcribed to run PCR: PCR products were indexed by utilization of specific RNA PCR Index Primers and PCR profile, according to the Illumina protocol (RPI, Illumina). PCR products were separated on 7% PA gel containing 1% glycerol. After 10' staining by SYBR[™] Gold Nucleic Acid Gel Stain (Invitrogen, Thermo Fisher Scientific)/0.5xTBE buffer, DNA fragments of 140–160 bp in length were cut and eluted using 400 µl elution buffer (50 mM Mg-acetate, 0.5 M ammonium acetate, 1 mM EDTA, 0.1% SDS) after O/N incubation, 28 °C, 400 rpm. Then, chloroform/phenol pH = 8.0 purification libraries were precipitated using 1.5 µl GlycoBlue[™] coprecipitant (15 mg/mL) (Ambion, Thermo Fisher Scientific) and three volumes of 100% ethanol. Purified libraries were quantified using a Qubit[®] dsDNA HS Assay kit (Invitrogen, Thermo Fisher Scientific) and Qubit 3.0 Fluorometer (Invitrogen, Thermo Fisher Scientific). The quality of the libraries was analyzed using a High Sensitivity D1000 ScreenTape Assay (Agilent Technologies) and a 2200 TapeStation (Agilent Technologies). A total of 12 libraries were pooled together in equal molar ratio and sequenced by Fasteris SA (Switzerland).

(ii) Degradome library construction

Degradome library construction was performed according to PARE technique described by German et al. [123]. Ligation was performed using a Rapid DNA Ligation Kit (Roche), according to the manufacturer instructions. The ligation mixture was composed of MmeI-digested PCR product and 3' DNA Adapter, kept for 6 h at RT and at 4 °C overnight, then purified using phenol/chloroform extraction. PCR reaction was performed in a 50 µl volume containing MmeI fragment-3'Adapter template, appropriate index-containing primer (0.5 µM final concentration), MmeI Universal Fwd primer (0.5 µM final concentration), 350 µM dNTPs, Q5 reaction buffer, and Q5[®] Hot Start High-Fidelity DNA Polymerase (New England Biolabs), using the following steps: 94 °C for 2 min; 94 °C for 30 s, 60 °C for 30 s, 72 °C for 30 s—14 cycles; and 72 °C for 7 min. PCR products were separated on 8% PA gel containing 1% glycerol. Appropriate in length bands were cut and eluted O/N. Quantitative analysis of the purified libraries was performed using a Qubit[®] dsDNA HS Assay kit (Invitrogen, Thermo Fisher Scientific) and a Qubit 3.0 Fluorometer (Invitrogen, Thermo Fisher Scientific). Finally, the quality of the libraries was analyzed using a High Sensitivity D1000 ScreenTape Assay (Agilent Technologies) and a 2200 TapeStation (Agilent Technologies). Each library possessed an individual specific index. The four libraries were pooled together in equal molar ratio and sequenced by Fasteris SA (Switzerland). In present study two degradome libraries were analyzed.

(iii) mRNA libraries

Shoot transcriptome libraries were carried out using a SENSE mRNA-Seq library prep kit v2 (Lexogen), according to the manufacturer's protocol and as previously described [48]. A 420 pg of Spike-In RNA Variants SIRV-set3 (Lexogen) was added to 1500 ng of total RNA. ERCC mix was used for Spike-in analysis.

Library sequencing

Sequencing of small RNAs was performed (i) internally, using a MiSeq paired-end kit to check the library quality using a MiSeq[®] Reagent Kit v3 (Illumina) at the Laboratory of High Throughput Technologies, Adam Mickiewicz University, Poznań, Poland. Received data showed proper library quality and low-Pi induced changes in small RNA levels. (ii) The main deep sequencing (12 small RNA libraries, degradome, mRNA) was performed externally by Fasteris SA (Switzerland).

Data analysis

Differences in small RNAs, RNAs levels, and preliminary degradome data analysis were performed using a CLC Genomics Workbench (Qiagen Aarhus A/S).

Small RNA data analysis

The trimming procedure was used with default settings for quality trimming (quality score limit 0.02), adapter trimming, and for removal of small RNAs longer than 25 nt and shorter than 18 nt. Reads were extracted, counted, and normalized per 1,000,000 reads. Then, we set up the Experiment analysis for samples derived from roots and shoots separately (two-group comparison, unpaired). Empirical analysis of DGE (EDGE) was used to find significant fold changes in small RNA expression levels between samples derived from different treated barley. Moreover, we performed EDGE Bonferroni and EDGE FDR *p*-value correction calculation. First, all small RNAs were annotated to miRBase (release 22) without mismatches and with strand-specific alignment. Then, unannotated small RNAs (i.e., those not identified in miRbase) were sorted according to the lowest *p*-value. The annotation reports for shoot small RNAs are present in Additional file 28 and for root small RNAs in Additional file 29. All identified differentially expressed sRNAs were annotated with internal ID numbers: IDs from 1 to 138 represent miRNAs identified in roots, and successfully mapped to miRBase (*p*-value < 0.05); IDs 139–1934 represent other small RNAs identified in roots (Bonferroni *p*-value correction < 0.05); IDs 1935–2096 represent miRNAs identified in shoots, and successfully mapped to miRBase (*p*-value < 0.05), and IDs represent 2097–2295 other small RNAs identified in shoots (Bonferroni *p*-value correction < 0.05).

Annotation validation

ShortStack version 3.8.5 [125] was used for the identification of potential microRNA molecules. The software was run with: mismatches - 0, fold size - 400 parameters. The input files for the analysis were: fastq files containing small RNA sequences after adapter removal and fasta file with *Hordeum vulgare* genome (IBSC_v2) from Ensembl Plants database. The forna tool was used to visualize secondary structure of RNA [126].

Degradome data analysis

Degradome construction was performed using two different approaches, which allowed for a more in-depth analysis (Fig. 2). In the first method, the raw sequencing reads were processed by Cutadapt program (<https://cutadapt.readthedocs.io/en/stable/>) to trim low-quality and adapter sequences. Only sequences of length 15 nt and above were selected for further analyses. The processed sequencing reads were aligned to the reference sequences using bowtie. The count of 5'-end marked cleavage sites was scored by Perl script and normalized to the depth of sequencing and total signal for each of the reference transcripts. The putative miRNA:target pairs were predicted by a custom program (targetSeek) which included the following steps: (i) calculation of perfect match MFE (minimum free energy); (ii) RNAplex-based (Vienna

package) screening for sRNA:transcript pairs; (iii) filtering number of bulges and length of sequence overhangs by MFE (percent of the perfect MFE match); and (iv) calculation of prediction score using a penalty schema for loops, bulges, and G:U wobble pairing. In the second approach, we used the PAREsnip2 software [127] to generate t-plots in conjunction with five databases (Fig. 2). Potential miRNA targets are classified into one of five categories, where category 0 indicates the best miRNA-target match. The lower the alignment score, the better the alignment between the sRNA and the target site [127]. During PAREsnip2 analysis, we set the Fahlgren and Carrington targeting rules to permit a mismatch or G:U wobble at position 10 [128].

Identification of DEGs

Experiments were performed in three biological replicates of plants grown under low-Pi and control conditions. Paired-end sequencing reactions of the 150 nt reads were performed using an Illumina System. Total read numbers from six samples were mapped to the barley reference genome from Ensembl Plants Genes 42 (*Hordeum vulgare* IBSC v2). The library's quality and sequencing accuracy were verified carefully (i) by adding Spike-in RNA Variant Control Mixes (Lexogen) (Additional file 30) and (ii) by quality trimming. RNA-Seq analysis was performed using following normalization method - TPM expression values. TPM (Transcripts Per Million) is computed with the following equation $TPM = \frac{RPKM \times 10^6}{\sum RPKM}$. RPKM (Reads Per Kilobase of exon model per Million mapped reads) is computed using following equation $RPKM = \frac{\text{total exon reads}}{\text{mapped reads (millions)} \times \text{exon length (kb)}} \cdot \text{RNA-Seq reads}$. RNA-Seq reads were mapped to the gene track = *Hordeum vulgare*. IBSC_v2.42(Gene), mRNA track = *Hordeum vulgare*. IBSC_v2.42 (RNA) using the CLC Genomics Workbench (QIAGEN) software, as previously described [48]. Differentially expressed genes (DEGs) were selected using Differential Expression in Two Groups tool (present in CLC Genomics Workbench software). This tool uses multi-factorial statistics based on a negative binomial Generalized Linear Model (GLM). Among potential differentially expressed transcripts only those which went through restricted Bonferroni *p*-value adjustment (< 0.05) were considered as differentially expressed genes (DEGs).

GO analysis

Gene ontology (GO) analyses were performed using the gProfiler tool (version e102_eg49_p15_7a9b4d6) [129]. The over-representation binomial tests classified DEGs within GO domains (cellular component, biological process, and molecular function) with Bonferroni adjusted *p*-value < 0.05. Fold enrichment was calculated as described before [130]: ((number of genes annotated to

specific term/term size)/(total number of inputted genes/total number of genes used for selection)). The calculations are present in Additional file 11. The plots were generated using already published protocol [131].

cis-regulatory motif localization within DEG promoters

To analyze the enrichment of Pi-related *cis*-regulatory motifs, we extracted 2000 bps upstream of transcription start site from each identified DEG. Such data were directly screened to look for any either P1BS- or P-responsive PHO element consensus sequences using multiple promoter analysis with the PlantPAN3.0 tool [132].

ddPCR

To determine the absolute copy number of genes encoding *IPS1*, *SPX-MFS1*, endonuclease *S1/P1*, 3'-5' exonuclease, oxalate oxidase, and oxalate oxidase 2, we performed ddPCR using either EvaGreen Supermix (Bio-Rad) or TaqMan Assay (Bio-Rad) for mature miR827, according to the protocols previously described [48, 99]. TaqMan Small RNA Assay ID 008386_mat (Thermo Fisher Scientific) was used to detect and quantify mature 3' miR827 molecule (sequence ID: 2073). To normalize the copy number of miR827, we ran ddPCR for the *ARF1* reference gene using the TaqMan Assay ID: AIMS IL4 (Thermo Fisher Scientific). Absolute gene expression was shown as normalized copy number per 1000 copies of the barley *ARF1* reference gene. All specific primers and probes (mature miR827, U6 snRNA) used in this paper are listed in Additional file 31.

Northern blot of mature miR827

To determine the mature miR827 expression level, we performed northern blot hybridization using a specific probe for analysis. All steps of these experiments were done according to a detailed protocol as described previously [65]. 10 µg of each RNA sample was run alongside a radioactively labelled Decade Marker (Invitrogen, Thermo Scientific) on a 15% polyacrylamide gel with 8 M urea. The miR827 and U6 probe sequences are available in Additional file 31. The Decade Marker (Ambion) was loaded to control the length of the tested RNAs. Original blots are presented in Additional files 32 and 33. To calculate band intensity, we used the ImageQuant TL 8.1 software (GE Healthcare Life Sciences).

Abbreviations

sRNA: Small RNA; siRNA: Small interfering RNA; Pi: Inorganic phosphate; NGS: Next-Generation Sequencing; RNA-Seq: RNA Sequencing; DEM: Differentially expressed miRNA; DES: Differentially expressed small RNA; DEG: Differentially expressed gene; GO: Gene ontology; miRBase: The microRNA database; BLAST: Basic Local Alignment Search Tool; ddPCR: Droplet digital Polymerase Chain Reaction; P1BS: PHR1 binding sequence; TF: Transcription factor; PARE: Parallel Analysis of RNA Ends; EDGE: Empirical analysis of Differential Gene Expression; FDR: False discovery rate; MFE: Minimum free energy; TPM: Transcripts per million; RPKM: Reads per kilo base of exon model per million mapped reads

Supplementary Information

The online version contains supplementary material available at <https://doi.org/10.1186/s12864-021-07481-w>.

Additional file 1 Normalized copy numbers of barley *IPS1* gene transcript in low-Pi treated root material. DdPCR was performed to examine the absolute gene expression of the barley *IPS1* gene. Obtained copy numbers were normalized per 1000 copies of the *ARF1* reference gene transcript. Asterisks indicate a significant differences (**p*-value < 0.05) calculated using two-tailed Student's *t*-tests.

Additional file 2. Characteristic of reads obtained from small RNA deep sequencing.

Additional file 3 MicroRNAs and small RNAs (other) for which expression is significantly changed during Pi-starvation in barley roots and shoots. ID numbers 1–138: miRNAs identified in roots (*p*-value < 0.05); ID numbers 139–1934: other small RNAs identified in roots (Bonferroni *p*-value correction < 0.05); ID numbers 1935–2096: miRNAs identified in shoots (*p*-value < 0.05); ID numbers 2097–2295: other small RNAs identified in shoots (Bonferroni *p*-value correction < 0.05). Samples R4–R6 = low-Pi root; R16–R18 = control; S4–S6 = low-Pi shoot; S16–S18 = control shoot. NaN means “Not a Number”, describing molecules that were exclusively expressed in low-Pi or control samples. Yellow color marks DEMs with Bonferroni adjusted *p*-value < 0.05. Data created using CLC Genomics Workbench.

Additional file 4. Identification of differentially expressed miRNAs (DEMs) in barley plants under low-Pi regime. The graph illustrates step-by-step annotation of unique small RNAs obtained in this study. The table summarizes the ShortStack output data.

Additional file 5 List of differentially expressed other small RNAs (ID 2097–2295) in barley shoots (low-Pi vs. control) identified in this study (Bonferroni corrected *p*-value < 0.05). Based on the available Ensembl Plants database, we classified each sequence into best-matching functional classes of cDNAs. DESs were also mapped to miRBase allowing 1, 2 or 3 mismatches.

Additional file 6 List of differentially expressed other small RNAs (ID 139–1934) in barley roots (low-Pi vs. control) identified in this study (Bonferroni corrected *p*-value < 0.05). Based on the available Ensembl Plants database, we classified each sequence into best-matching functional classes of cDNAs. DESs were also mapped to miRBase allowing 1, 2 or 3 mismatches.

Additional file 7. Length distribution of DESs identified in barley roots and shoots.

Additional file 8. Annotation distribution of DESs identified in barley roots and shoots.

Additional file 9. The output of DES ShortStack analysis (upper panel) and RNA secondary structure visualization of potential new miRNA generated by forna tool (lower panel). Red color marks miRNA; yellow color marks miRNA star.

Additional file 10. Chromosomal mapping of 98 DEGs identified in this study. Lower panel illustrates the percentage between quantitative distribution of either up-regulated or down-regulated genes under low-Pi conditions and total number of protein-coding genes in each barley chromosome. Scale bar for chromosomes = 160 Mbp.

Additional file 11. The extracted data from GO analysis for 98 DEGs used as a query.

Additional file 12 Upstream sequences (2 kb) extracted from all 98 DEGs used for *cis*-regulatory motif prediction analysis.

Additional file 13. List of identified P1BS motifs within the DEG promoters.

Additional file 14. List of identified P-responsive PHO motifs within the DEG promoters.

Additional file 15. Degradome profile (TargetSeek approach) demonstrates potential mRNA targets for differentially expressed miRNAs (DEMs) identified in barley shoots (low-Pi vs. control). The lower the alignment score, the more reliable the prediction.

Additional file 16. Degradome profile (TargetSeek approach) demonstrates potential mRNA targets for differentially expressed other sRNAs (DESS) identified in barley shoots (low-Pi vs. control). The lower the alignment score, the more reliable the prediction.

Additional file 17. Degradome profile (TargetSeek approach) demonstrates potential mRNA targets for differentially expressed miRNAs (DEMs) identified in barley roots (low-Pi vs. control). The lower the alignment score, the more reliable the prediction.

Additional file 18. Degradome profile (TargetSeek approach) demonstrates potential mRNA targets for differentially expressed other sRNAs (DESS) identified in barley roots (low-Pi vs. control). The lower the alignment score, the more reliable the prediction.

Additional file 19. Degradome profile (PAREsnip2 approach) demonstrates potential mRNA targets for differentially expressed miRNAs (DEMs) identified in barley shoots (low-Pi vs. control). The lower the alignment score, the more reliable the prediction.

Additional file 20. The t-plots generated by PAREsnip2 software showing the potential mRNA targets for differentially expressed miRNAs (DEMs) identified in barley shoots (low-Pi vs. control).

Additional file 21. Degradome profile (PAREsnip2 approach) demonstrates potential mRNA targets for differentially expressed other sRNAs (DESS) identified in barley shoots (low-Pi vs. control). The lower the alignment score, the more reliable the prediction.

Additional file 22. The t-plots generated by PAREsnip2 software showing the potential mRNA targets for differentially expressed other sRNAs (DESS) identified in barley shoots (low-Pi vs. control).

Additional file 23. Degradome profile (PAREsnip2 approach) demonstrates potential mRNA targets for differentially expressed miRNAs (DEMs) identified in barley roots (low-Pi vs. control). The lower the alignment score, the more reliable the prediction.

Additional file 24. The t-plots generated by PAREsnip2 software showing the potential mRNA targets for differentially expressed miRNAs (DEMs) identified in barley roots (low-Pi vs. control).

Additional file 25. Degradome profile (PAREsnip2 approach) demonstrates potential mRNA targets for differentially expressed other sRNAs (DESS) identified in barley roots (low-Pi vs. control). The lower the alignment score, the more reliable the prediction.

Additional file 26. The t-plots generated by PAREsnip2 software showing the potential mRNA targets for differentially expressed other sRNAs (DESS) identified in barley roots (low-Pi vs. control).

Additional file 27. List of genes predicted in degradome analysis to be guided for cleavage by putative regulatory sRNAs (identified as DES) with best scoring matches.

Additional file 28. miRbase annotation report from CLC Workbench (QIAGEN) analysis of shoot small RNAs.

Additional file 29. miRbase annotation report from CLC Workbench (QIAGEN) analysis of root small RNAs.

Additional file 30. Spike-in quality control of RNA-Seq samples from barley shoots (low-Pi vs. control). Correlation between known and measured spike-in concentrations.

Additional file 31. List of primers and probes used in this study.

Additional file 32. Original, full-length blot of mature hvu-miR827 analysis. Lane 1: Decade™ Marker System (Invitrogen, Thermo Fisher Scientific); Lane 2: empty space (no sample loaded); Lane 3–5: RNA samples from root (Pi sufficient); Lane 6–8: shoot (Pi sufficient); Lane 9–11: root (low-Pi); Lane 12–14: shoot (low-Pi).

Additional file 33. Original, full-length blot of U6 snRNA analysis. Lane 1: Decade™ Marker System (Invitrogen, Thermo Fisher Scientific); Lane 2: empty space (no sample loaded); Lane 3–5: RNA samples from root (Pi sufficient); Lane 6–8: shoot (Pi sufficient); Lane 9–11: root (low-Pi); Lane 12–14: shoot (low-Pi).

Acknowledgements

The authors wish to thank Dr. Halina Pietrykowska (Adam Mickiewicz University, Poznań, Poland) for help with the degradome libraries preparation

and Piotr Kopec (Adam Mickiewicz University, Poznań, Poland) for help in cDNA data preparation. MiSeq paired-read of small RNA deep sequencing (three replicas) was performed at the Laboratory of High-throughput Technologies (IBMiB, Faculty of Biology at the Adam Mickiewicz University, Poznań) funded by National Multidisciplinary Laboratory of Functional Nanomaterials NanoFun nr POIG.02.02.00-00-025/09 (Innovative Economy Operational Programme, Priority Axis 2: R&D Infrastructure, Action 2.2: Support of Formation of Common Research Infrastructure of Scientific Units).

Authors' contributions

Conceptualization, writing - original draft preparation, writing - original draft editing, designing and preparing figures, plant material generation, Pi concentration measurements, ddPCR analysis, NGS data analysis, promoters' analysis, funding acquisition: P.S.; conceptualization, supervision and writing - original draft preparation, writing - original draft editing, NGS libraries preparation, NGS data analysis, degradome data analysis, ddPCR analysis, Northern-blot analysis, funding acquisition: A.P.; NGS data analysis, visualization, preparing figures: D.B.; NGS libraries preparation, original draft review: K.K.; NGS libraries preparation, original draft review: P.N., degradome data analysis, original draft review: W.K.; results discussion and original draft review: Z.S.K. The authors read and approved the final manuscript.

Funding

This work was funded by the National Science Centre, Poland, on the basis of DEC-2013/11/B/NZ9/01761, UMO-2016/23/B/NZ9/00857, and UMO-2015/19/N/NZ9/00218.

Availability of data and materials

The datasets generated and/or analyzed during the current study have been submitted to GEO database (SuperSeries GSE145427 contain following SubSeries: degradome RNA-Seq - GSE145423, sRNA-Seq - GSE145425, shoot transcriptome mRNA-Seq - GSE145426). All accession numbers mentioned in this study or listed in the tables and additional files can be found in the open-access Ensembl Plants database (<http://plants.ensembl.org>) for the barley genome.

Declarations

Ethics approval and consent to participate

Not applicable.

Consent for publication

Not applicable.

Competing interests

The authors declare that they have no competing interests.

Author details

¹Department of Gene Expression, Faculty of Biology, Institute of Molecular Biology and Biotechnology, Adam Mickiewicz University, Poznań, Uniwersytetu Poznańskiego 6, 61-614 Poznań, Poland. ²Center for Advanced Technology, Adam Mickiewicz University, Poznań, Uniwersytetu Poznańskiego 10, 61-614 Poznań, Poland. ³Department of Computational Biology, Faculty of Biology, Institute of Molecular Biology and Biotechnology, Adam Mickiewicz University, Poznań, Uniwersytetu Poznańskiego 6, 61-614 Poznań, Poland.

Received: 17 February 2020 Accepted: 25 February 2021

Published online: 09 March 2021

References

1. International Barley Genome Sequencing Consortium, Mayer KF, Waugh R, Brown JW, Schulman A, Langridge P, et al. A physical, genetic and functional sequence assembly of the barley genome. *Nature*. 2012; 491(7426):711–6.
2. Jo W-S, Kim H-Y, Kim K-M. Development and characterization of polymorphic EST based SSR markers in barley (*Hordeum vulgare*). *3 Biotech*. 2017;7(4):265.
3. Harwood WA. An introduction to barley: the crop and the model. *Methods Mol Biol*. 2019;1900:1–5.
4. Saisho D, Takeda K. Barley: emergence as a new research material of crop science. *Plant Cell Physiol*. 2011;52(5):724–7.

5. Phillips JR, Dalmay T, Bartels D. The role of small RNAs in abiotic stress. *FEBS Lett.* 2007;581(19):3592–7.
6. Sunkar R, Chinnusamy V, Zhu J, Zhu JK. Small RNAs as big players in plant abiotic stress responses and nutrient deprivation. *Trends Plant Sci.* 2007;12(7):301–9.
7. Banerjee S, Sirohi A, Ansari AA, Gill SS. Role of small RNAs in abiotic stress responses in plants. *Plant Gene.* 2017;11:180–9.
8. Großhans H, Filipowicz W. Molecular biology: the expanding world of small RNAs. *Nature.* 2008;451(7177):414–6.
9. Guleria P, Mahajan M, Bhardwaj J, Yadav SK. Plant small RNAs: biogenesis, mode of action and their roles in abiotic stresses. *Genomics Proteomics Bioinformatics.* 2011;9(6):183–99.
10. Borges F, Martienssen RA. The expanding world of small RNAs in plants. *Nat Rev Mol Cell Biol.* 2015;16(12):727–41.
11. Zhang H, Xia R, Meyers BC, Walbot V. Evolution, functions, and mysteries of plant ARGONAUTE proteins. *Curr Opin Plant Biol.* 2015;27:84–90.
12. Bhattacharjee S, Roche B, Martienssen RA. RNA-induced initiation of transcriptional silencing (RITS) complex structure and function. *RNA Biol.* 2019;16(9):1133–46.
13. Ren B, Wang X, Duan J, Ma J. Rhizobial tRNA-derived small RNAs are signal molecules regulating plant nodulation. *Science.* 2019;365(6456):919–22.
14. Khraiweh B, Zhu J-K, Zhu J. Role of miRNAs and siRNAs in biotic and abiotic stress responses of plants. *Biochim Biophys Acta.* 2012;1819(2):137–48.
15. Jacobs TB, Lawler NJ, LaFayette PR, Vodkin LO, Parrott WA. Simple gene silencing using the trans-acting siRNA pathway. *Plant Biotechnol J.* 2016;14(1):117–27.
16. Komiya R. Biogenesis of diverse plant phasiRNAs involves an miRNA-trigger and Dicer-processing. *J Plant Res.* 2017;130(1):17–23.
17. Xie Z, Allen E, Fahlgren N, Calamar A, Givan SA, Carrington JC. Expression of Arabidopsis MIRNA genes. *Plant Physiol.* 2005;138(4):2145–54.
18. Kurihara Y, Watanabe Y. Arabidopsis micro-RNA biogenesis through Dicer-like 1 protein functions. *Proc Natl Acad Sci U S A.* 2004;101(34):12753–8.
19. Budak H, Akpinar BA. Plant miRNAs: biogenesis, organization and origins. *Funct Integr Genomics.* 2015;15(5):523–31.
20. Fang X, Qi Y. RNAi in plants: an Argonaute-centered view. *Plant Cell.* 2016;28(2):272–85.
21. Valencia-Sanchez MA, Liu J, Hannon GJ, Parker R. Control of translation and mRNA degradation by miRNAs and siRNAs. *Genes Dev.* 2006;20(5):515–24.
22. Barciszewska-Pacak M, Milanowska K, Knop K, Bielewicz D, Nuc P, Plewka P, et al. Arabidopsis microRNA expression regulation in a wide range of abiotic stress responses. *Front Plant Sci.* 2015;6:410.
23. Meister G, Tuschl T. Mechanisms of gene silencing by double-stranded RNA. *Nature.* 2004;431(7006):343–9.
24. Megel C, Hummel G, Lalande S, Ubrig E, Cognat V, Morelle G, et al. Plant RNases T2, but not Dicer-like proteins, are major players of tRNA-derived fragments biogenesis. *Nucleic Acids Res.* 2019;47(2):941–52.
25. Martinez G, Choudury SG, Slotkin RK. tRNA-derived small RNAs target transposable element transcripts. *Nucleic Acids Res.* 2017;45(9):5142–52.
26. Palatnik JF, Allen E, Wu X, Schommer C, Schwab R, Carrington JC, et al. Control of leaf morphogenesis by microRNAs. *Nature.* 2003;425(6955):257–63.
27. Doench JG, Petersen CP, Sharp PA. siRNAs can function as miRNAs. *Genes Dev.* 2003;17(4):438–42.
28. Borsani O, Zhu J, Verslues PE, Sunkar R, Zhu J-K. Endogenous siRNAs derived from a pair of natural cis-antisense transcripts regulate salt tolerance in Arabidopsis. *Cell.* 2005;123(7):1279–91.
29. Li J, Zheng H, Zhang C, Han K, Wang S, Peng J, et al. Different virus-derived siRNAs profiles between leaves and fruits in cucumber green mottle mosaic virus-infected *Lagenaria siceraria* plants. *Front Microbiol.* 2016;7:1797.
30. Li J, Andika IB, Shen J, Lv Y, Ji Y, Sun L, et al. Characterization of rice black-streaked dwarf virus- and rice stripe virus-derived siRNAs in singly and doubly infected insect vector *Laodelphax striatellus*. *PLoS One.* 2013;8(6):e66007.
31. Zhang B, Li W, Zhang J, Wang L, Wu J. Roles of small RNAs in virus-plant interactions. *Viruses.* 2019;11(9):e827.
32. Kruska K, Pacak A, Swida-Barteczka A, Nuc P, Alaba S, Wroblewska Z, et al. Transcriptionally and post-transcriptionally regulated microRNAs in heat stress response in barley. *J Exp Bot.* 2014;65(20):6123–35.
33. Zhou H, Hussain SS, Hackenberg M, Bazanova N, Eini O, Li J, et al. Identification and characterisation of a previously unknown drought tolerance-associated microRNA in barley. *Plant J.* 2018;95(1):138–49.
34. Zeng J, Ye Z, He X, Zhang G. Identification of microRNAs and their targets responding to low-potassium stress in two barley genotypes differing in low-K tolerance. *J Plant Physiol.* 2019;234–235:44–53.
35. Wu L, Yu J, Shen Q, Huang L, Wu D, Zhang G. Identification of microRNAs in response to aluminum stress in the roots of Tibetan wild barley and cultivated barley. *BMC Genomics.* 2018;19(1):560.
36. Hackenberg M, Shi B, Gustafson P, Langridge P. Characterization of phosphorus-regulated miR399 and miR827 and their isomirs in barley under phosphorus-sufficient and phosphorus-deficient conditions. *BMC Plant Biol.* 2013;13:214.
37. Carthew RW, Sontheimer EJ. Origins and mechanisms of miRNAs and siRNAs. *Cell.* 2009;136(4):642–55.
38. Fahlgren N, Montgomery TA, Howell MD, Allen E, Dvorak SK, Alexander AL, et al. Regulation of AUXIN RESPONSE FACTOR3 by TAS3 ta-siRNA affects developmental timing and patterning in Arabidopsis. *Curr Biol.* 2006;16(9):939–44.
39. Matsui A, Mizunashi K, Tanaka M, Kaminuma E, Nguyen AH, Nakajima M, et al. tasiRNA-ARF pathway moderates floral architecture in Arabidopsis plants subjected to drought stress. *Biomed Res Int.* 2014;2014:303451.
40. Dotto MC, Petsch KA, Aukerman MJ, Beatty M, Hammell M, Timmermans MC. Genome-wide analysis of leafbladeless1-regulated and phased small RNAs underscores the importance of the TAS3 ta-siRNA pathway to maize development. *PLoS Genet.* 2014;10(12):e1004826.
41. Marin E, Jouanet V, Herz A, Lokerse AS, Weijers D, Vaucheret H, et al. miR390, Arabidopsis TAS3 tasiRNAs, and their AUXIN RESPONSE FACTOR targets define an autoregulatory network quantitatively regulating lateral root growth. *Plant Cell.* 2010;22(4):1104–17.
42. Hsieh L-C, Lin S-I, Shih A-C, Chen J-W, Lin W-Y, Tseng C-Y, et al. Uncovering small RNA-mediated responses to phosphate deficiency in Arabidopsis by deep sequencing. *Plant Physiol.* 2009;151(4):2120–32.
43. Abel S, Ticconi C, Delatorre CA. Phosphate sensing in higher plants. *Physiol Plant.* 2002;115(1):1–8.
44. Poirier Y, Bucher M. Phosphate transport and homeostasis in Arabidopsis. *Arabidopsis Book.* 2002;1:e0024.
45. Yang XJ, Finnegan PM. Regulation of phosphate starvation responses in higher plants. *Ann Bot.* 2010;105(4):513–26.
46. Pacak A, Barciszewska-Pacak M, Swida-Barteczka A, Kruska K, Sega P, Milanowska K, et al. Heat stress affects Pi-related genes expression and inorganic phosphate deposition/accumulation in barley. *Front Plant Sci.* 2016;7:926.
47. Mimura T, Dietz K-J, Kaiser W, Schramm MJ, Kaiser G, Heber U. Phosphate transport across biomembranes and cytosolic phosphate homeostasis in barley leaves. *Planta.* 1990;180(2):139–46.
48. Sega P, Kruska K, Szewc L, Szwejkowska-Kulinska Z, Pacak A. Identification of transcription factors that bind to the 5'-UTR of the barley *PHO2* gene. *Plant Mol Biol.* 2020;102(1–2):73–88.
49. Huang T-K, Han C-L, Lin S-I, Chen Y-J, Tsai Y-C, Chen Y-R, et al. Identification of downstream components of ubiquitin-conjugating enzyme PHOSPHATE2 by quantitative membrane proteomics in Arabidopsis roots. *Plant Cell.* 2013;25(10):4044–60.
50. Aung K, Lin S-I, Wu C-C, Huang Y-T, Su C-L, Chiou T-J. *pho2*, a phosphate overaccumulator, is caused by a nonsense mutation in a microRNA399 target gene. *Plant Physiol.* 2006;141(3):1000–11.
51. Chiou T-J, Aung K, Lin S-I, Wu C-C, Chiang S-F, Su C-L. Regulation of phosphate homeostasis by microRNA in Arabidopsis. *Plant Cell.* 2006;18(2):412–21.
52. Pacak A, Geisler K, Jørgensen B, Barciszewska-Pacak M, Nilsson L, Nielsen TH, et al. Investigations of barley stripe mosaic virus as a gene silencing vector in barley roots and in *Brachypodium distachyon* and oat. *Plant Methods.* 2010;6:26.
53. Wang C, Ying S, Huang H, Li K, Wu P, Shou H. Involvement of OsSPX1 in phosphate homeostasis in rice. *Plant J.* 2009;57(5):895–904.
54. Franco-Zorrilla JM, Valli A, Todesco M, Mateos I, Puga MI, Rubio-Somoza I, et al. Target mimicry provides a new mechanism for regulation of microRNA activity. *Nat Genet.* 2007;39(8):1033–7.
55. Pant BD, Musialak-Lange M, Nuc P, May P, Buhtz A, Kehr J, et al. Identification of nutrient-responsive Arabidopsis and rapeseed microRNAs by comprehensive real-time polymerase chain reaction profiling and small RNA sequencing. *Plant Physiol.* 2009;150(3):1541–55.
56. Wang C, Huang W, Ying Y, Li S, Secco D, Tyerman S, et al. Functional characterization of the rice SPX-MFS family reveals a key role of OsSPX-MFS1 in controlling phosphate homeostasis in leaves. *New Phytol.* 2012;196(1):139–48.

57. Lin S-I, Santi C, Jobet E, Lacut E, El Kholti N, Karłowski WM. Etal. Complex regulation of two target genes encoding SPX-MFS proteins by rice miR827 in response to phosphate starvation. *Plant Cell Physiol.* 2010;51(12):2119–31.
58. Liu T-Y, Huang T-K, Yang S-Y, Hong Y-T, Huang S-M, Wang F-N, et al. Identification of plant vacuolar transporters mediating phosphate storage. *Nat Commun.* 2016;7:11095.
59. Wang L, Zeng J, HQ, Song J, Feng SJ, Yang ZM. miRNA778 and SUVH6 are involved in phosphate homeostasis in Arabidopsis. *Plant Sci.* 2015;238:273–85.
60. Ebbs ML, Bartee L, Bender J. H3 lysine 9 methylation is maintained on a transcribed inverted repeat by combined action of SUVH6 and SUVH4 methyltransferases. *Mol Cell Biol.* 2005;25(23):10507–15.
61. Míguez-Montero MA, Valentine A, Pérez-Fernández MA. Regulatory effect of phosphorus and nitrogen on nodulation and plant performance of leguminous shrubs. *AoB Plants.* 2020;12(1):plz047.
62. Tsikou D, Yan Z, Holt DB, Abel NB, Reid DE, Madsen LH, et al. Systemic control of legume susceptibility to rhizobial infection by a mobile microRNA. *Science.* 2018;362(6411):233–6.
63. Kozomara A, Birgaoanu M, Griffiths-Jones S. miRBase: from microRNA sequences to function. *Nucleic Acids Res.* 2019;47(D1):D155–62.
64. Shi J, Dong M, Li L, Liu L, Luz-Madrugal A, Tsonis PA, et al. mirPro-a novel standalone program for differential expression and variation analysis of miRNAs. *Sci Rep.* 2015;5:14617.
65. Kruska K, Pacak A, Swida-Barteczka A, Stefaniak AK, Kaja E, Sierocka I, et al. Developmentally regulated expression and complex processing of barley pri-microRNAs. *BMC Genomics.* 2013;14:34.
66. Singh A, Roy S, Singh S, Das SS, Gautam V, Yadav S, et al. Phytohormonal crosstalk modulates the expression of miR166/165s, target class III HD-ZIPs, and KANADI genes during root growth in *Arabidopsis thaliana*. *Sci Rep.* 2017;7(1):3408.
67. Manna S. An overview of pentatricopeptide repeat proteins and their applications. *Biochimie.* 2015;113:93–9.
68. May A, Berger S, Hertel T, Köck M. The Arabidopsis thaliana phosphate starvation responsive gene AtPPase1 encodes a novel type of inorganic pyrophosphatase. *Biochim Biophys Acta.* 2011;1810(2):178–85.
69. Secco D, Wang C, Arpat BA, Wang Z, Poirier Y, Tyerman SD, et al. The emerging importance of the SPX domain-containing proteins in phosphate homeostasis. *New Phytol.* 2012;193(4):842–51.
70. Secco D, Baumann A, Poirier Y. Characterization of the rice PHO1 gene family reveals a key role for OsPHO1;2 in phosphate homeostasis and the evolution of a distinct clade in dicotyledons. *Plant Physiol.* 2010;152(3):1693–704.
71. Pandey BK, Mehra P, Verma L, Bhadouria J, Giri J. OSHAD1, a haloacid dehalogenase-like APase, enhances phosphate accumulation. *Plant Physiol.* 2017;174(4):2316–32.
72. Tran HT, Hurlay BA, Plaxton WC. Feeding hungry plants: the role of purple acid phosphatases in phosphate nutrition. *Plant Sci.* 2010;179(1–2):14–27.
73. Heber U, Vilj J, Neimanis S, Mimura T, Dietz K-J. Photoinhibitory damage to chloroplasts under phosphate deficiency and alleviation of deficiency and damage by photorespiratory reactions. *Z Naturforsch C.* 1989;44:524–36.
74. Hernández I, Munné-Bosch S. Linking phosphorus availability with photo-oxidative stress in plants. *J Exp Bot.* 2015;66(10):2889–900.
75. Ma T-L, Wu W-H, Wang Y. Transcriptome analysis of rice root responses to potassium deficiency. *BMC Plant Biol.* 2012;12:161.
76. Gho Y-S, Kim S-J, Jung K-H. Phenylalanine ammonia-lyase family is closely associated with response to phosphate deficiency in rice. *Genes Genomics.* 2020;42(1):67–76.
77. Thiebaut F, Rojas CA, Grativol C, Motta MR, Vieira T, Regulski M, et al. Genome-wide identification of microRNA and siRNA responsive to endophytic beneficial diazotrophic bacteria in maize. *BMC Genomics.* 2014;15:766.
78. Khandal H, Singh AP, Chattopadhyay D. MicroRNA397b-LACCASE2 module regulates root lignification under water- and phosphate deficiency. *Plant Physiol.* 2020;182(3):1387–403.
79. Maeda Y, Konishi M, Kiba T, Sakuraba Y, Sawaki N, Kurai T, et al. A NIGT1-centred transcriptional cascade regulates nitrate signalling and incorporates phosphorus starvation signals in Arabidopsis. *Nat Commun.* 2018;9(1):1376.
80. Medici A, Marshall-Colon A, Ronzier E, Szponarski W, Wang R, Gojon A, et al. AtNIGT1/HRS1 integrates nitrate and phosphate signals at the Arabidopsis root tip. *Nat Commun.* 2015;6:6274.
81. Hu B, Jiang Z, Wang W, Qiu Y, Zhang Z, Liu Y, et al. Nitrate-NRT1.1B-SPX4 cascade integrates nitrogen and phosphorus signalling networks in plants. *Nat Plants.* 2019;5(4):401–13.
82. Bustos R, Castrillo G, Linhares F, Puga MI, Rubio V, Pérez-Pérez J, et al. A central regulatory system largely controls transcriptional activation and repression responses to phosphate starvation in Arabidopsis. *PLoS Genet.* 2010;6(9):e1001102.
83. Rubio V, Linhares F, Solano R, Martín AC, Iglesias J, Leyva A, et al. A conserved MYB transcription factor involved in phosphate starvation signaling both in vascular plants and in unicellular algae. *Genes Dev.* 2001;15(16):2122–33.
84. Mukatira UT, Liu C, Varadarajan DK, Raghothama KG. Negative regulation of phosphate starvation-induced genes. *Plant Physiol.* 2001;127(4):1854–62.
85. Sega P, Pacak A. Plant PHR transcription factors: put on a map. *Genes (Basel).* 2019;10(12):e1018.
86. Kuo H-F, Chang T-Y, Chiang S-F, Wang W-D, Charng Y-Y, Chiou T-J. Arabidopsis inositol pentakisphosphate 2-kinase, AtIPK1, is required for growth and modulates phosphate homeostasis at the transcriptional level. *Plant J.* 2014;80(3):503–15.
87. Nimmo HG, Fontaine V, Hartwell J, Jenkins GI, Nimmo GA, Wilkins MB. PEP carboxylase kinase is a novel protein kinase controlled at the level of expression. *New Phytol.* 2001;151(1):91–7.
88. Percudani R, Peracchi A. A genomic overview of pyridoxal-phosphate-dependent enzymes. *EMBO Rep.* 2003;4(9):850–4.
89. Burroughs AM, Ando Y, de Hoon ML, Tomaru Y, Suzuki H, Hayashizaki Y, et al. Deep-sequencing of human Argonaute-associated small RNAs provides insight into miRNA sorting and reveals Argonaute association with RNA fragments of diverse origin. *RNA Biol.* 2011;8(1):158–77.
90. Swida-Barteczka A, Szwejkowska-Kulinska Z. Micromanagement of developmental and stress-induced senescence: the emerging role of microRNAs. *Genes (Basel).* 2019;10(3):e210.
91. Gubler F, Chandler PM, White RG, Llewellyn DJ, Jacobsen JV. Gibberellin signaling in barley aleurone cells. Control of SLN1 and GAMYB expression. *Plant Physiol.* 2002;129(1):191–200.
92. Zhou X, Zha M, Huang J, Li L, Imran M, Zhang C. StMYB44 negatively regulates phosphate transport by suppressing expression of PHOSPHATE1 in potato. *J Exp Bot.* 2017;68(5):1265–81.
93. Zhang A, Jiang X, Zhang F, Wang T, Zhang X. Dynamic response of RNA editing to temperature in grape by RNA deep sequencing. *Funct Integr Genomics.* 2020;20:421–32.
94. Takenaka M, Zehrmann A, Verbitskiy D, Kugelmann M, Härtel B, Brennicke A. Multiple organellar RNA editing factor (MORF) family proteins are required for RNA editing in mitochondria and plastids of plants. *Proc Natl Acad Sci U S A.* 2012;109(13):5104–9.
95. Schilling S, Stenzel I, von Bohlen A, Wermann M, Schulz K, Demuth H-U, et al. Isolation and characterization of the glutamyl cyclases from *Solanum tuberosum* and *Arabidopsis thaliana*: implications for physiological functions. *Biol Chem.* 2007;388(2):145–53.
96. Bari R, Pant BD, Stitt M, Scheible W-R. PHO2, microRNA399, and PHR1 define a phosphate-signaling pathway in plants. *Plant Physiol.* 2006;141(3):988–99.
97. Thomas HR, Frank MH. Connecting the pieces: uncovering the molecular basis for long-distance communication through plant grafting. *New Phytol.* 2019;223(2):582–9.
98. Huen A, Bally J, Smith P. Identification and characterisation of microRNAs and their target genes in phosphate-starved *Nicotiana benthamiana* by small RNA deep sequencing and 5'RACE analysis. *BMC Genomics.* 2018;19(1):940.
99. Smoczynska A, Sega P, Stepien A, Knop K, Jarmolowski A, Pacak A, et al. miRNA detection by stem-loop RT-qPCR in studying microRNA biogenesis and microRNA responsiveness to abiotic stresses. In: de Folter S. (eds) *plant MicroRNAs. Methods Mol Biol.* 2019;1932:131–50.
100. Jost R, Pharmawati M, Lapis-Gaza HR, Rossig C, Berkowitz O, Lambers H, et al. Differentiating phosphate-dependent and phosphate-independent systemic phosphate-starvation response networks in *Arabidopsis thaliana* through the application of phosphite. *J Exp Bot.* 2015;66(9):2501–14.
101. Kim W, Ahn HJ, Chiou T-J, Ahn JH. The role of the miR399-PHO2 module in the regulation of flowering time in response to different ambient temperatures in *Arabidopsis thaliana*. *Mol Cells.* 2011;32(1):83–8.
102. Lin S-I, Chiang S-F, Lin W-Y, Chen J-W, Tseng C-Y, Wu P-C, et al. Regulatory network of microRNA399 and PHO2 by systemic signaling. *Plant Physiol.* 2008;147(2):732–46.

103. Kant S, Peng M, Rothstein SJ. Genetic regulation by NLA and microRNA827 for maintaining nitrate-dependent phosphate homeostasis in Arabidopsis. *PLoS Genet*. 2011;7(3):e1002021.
104. Lin W-Y, Huang T-K, Chiou T-J. NITROGEN LIMITATION ADAPTATION, a target of microRNA827, mediates degradation of plasma membrane-localized phosphate transporters to maintain phosphate homeostasis in Arabidopsis. *Plant Cell*. 2013;25(10):4061–74.
105. Yang S-Y, Lu W-C, Ko S-S, Sun C-M, Hung J-C, Chiou T-J. Upstream open reading frame and phosphate-regulated expression of rice OsNLA1 controls phosphate transport and reproduction. *Plant Physiol*. 2020;182(1):393–407.
106. Park BS, Seo JS, Chua N-H. NITROGEN LIMITATION ADAPTATION recruits PHOSPHATE2 to target the PHOSPHATE transporter PT2 for degradation during the regulation of Arabidopsis phosphate homeostasis. *Plant Cell*. 2014;26(1):454–64.
107. Stigter KA, Plaxton WC. Molecular mechanisms of phosphorus metabolism and transport during leaf senescence. *Plants*. 2015;4(4):773–98.
108. Bariola PA, MacIntosh GC, Green PJ. Regulation of S-like ribonuclease levels in Arabidopsis. Antisense inhibition of RNS1 or RNS2 elevates anthocyanin accumulation. *Plant Physiol*. 1999;119(1):331–42.
109. Ren P, Meng Y, Li B, Ma X, Si E, Lai Y, et al. Molecular mechanisms of acclimatization to phosphorus starvation and recovery underlying full-length transcriptome profiling in barley (*Hordeum vulgare* L.). *front. Plant Sci*. 2018;9:500.
110. Oono Y, Kobayashi F, Kawahara Y, Yazawa T, Handa H, Itoh T, et al. Characterisation of the wheat (*Triticum aestivum* L.) transcriptome by de novo assembly for the discovery of phosphate starvation-responsive genes: gene expression in Pi-stressed wheat. *BMC Genomics*. 2013;14:77.
111. Oono Y, Kawahara Y, Yazawa T, Kanamori H, Kuramata M, Yamagata H, et al. Diversity in the complexity of phosphate starvation transcriptomes among rice cultivars based on RNA-Seq profiles. *Plant Mol Biol*. 2013;83(6):523–37.
112. Zeng H, Zhang X, Zhang X, Pi E, Xiao L, Zhu Y. Early transcriptomic response to phosphate deprivation in soybean leaves as revealed by RNA-sequencing. *Int J Mol Sci*. 2018;19(7):E2145.
113. Huang J, Huang Z, Zhou X, Xia C, Imran M, Wang S, et al. Tissue-specific transcriptomic profiling of Plantago major provides insights for the involvement of vasculature in phosphate deficiency responses. *Mol Gen Genomics*. 2019;294(1):159–75.
114. Du Q, Wang K, Xu C, Zou C, Xie C, Xu Y, et al. Strand-specific RNA-Seq transcriptome analysis of genotypes with and without low-phosphorus tolerance provides novel insights into phosphorus-use efficiency in maize. *BMC Plant Biol*. 2016;16(1):222.
115. Zhou J, Jiao F, Wu Z, Li Y, Wang X, He X, et al. OsPHR2 is involved in phosphate-starvation signaling and excessive phosphate accumulation in shoots of plants. *Plant Physiol*. 2008;146(4):1673–86.
116. Hammond JP, Bennett MJ, Bowen HC, Broadley MR, Eastwood DC, May ST, et al. Changes in gene expression in Arabidopsis shoots during phosphate starvation and the potential for developing smart plants. *Plant Physiol*. 2003;132(2):578–96.
117. Müller R, Morant M, Jarmer H, Nilsson L, Nielsen TH. Genome-wide analysis of the Arabidopsis leaf transcriptome reveals interaction of phosphate and sugar metabolism. *Plant Physiol*. 2007;143(1):156–71.
118. Diaz-Baena M, Galvez-Valdivieso G, Delgado-García E, Pineda M, Piedras P. Nuclease and ribonuclease activities in response to salt stress: identification of PvRNS3, a T2/S-like ribonuclease induced in common bean radicles by salt stress. *Plant Physiol Biochem*. 2020;147:235–41.
119. Zheng J, Wang Y, He Y, Zhou J, Li Y, Liu Q, et al. Overexpression of an S-like ribonuclease gene, OsRNS4, confers enhanced tolerance to high salinity and hyposensitivity to phytochrome-mediated light signals in rice. *Plant Sci*. 2014;214:99–105.
120. Zhang Z, Collinge DB, Thordal-Christensen H. Germin-like oxalate oxidase, a H₂O₂-producing enzyme, accumulates in barley attacked by the powdery mildew fungus. *Plant J*. 1995;8(1):139–45.
121. Devaux P, Adamski T, Surma M. Inheritance of seed set in crosses of spring barley and *Hordeum bulbosum* L. *Crop Sci*. 1992;32(1):269–71.
122. Zadoks JC, Chang TT, Konzak CF. A decimal code for the growth stages of cereals. *Weed Res*. 1974;14(6):415–21.
123. German MA, Luo S, Schroth G, Meyers BC, Green PJ. Construction of parallel analysis of RNA ends (PARE) libraries for the study of cleaved miRNA targets and the RNA degradome. *Nat Protoc*. 2009;4(3):356–62.
124. Alaba S, Piszczalka P, Pietrykowska H, Pacak AM, Sierocka I, Nuc PW, et al. The liverwort *Pellia endiviifolia* shares microtranscriptomic traits that are common to green algae and land plants. *New Phytol*. 2015;206(1):352–67.
125. Axtell MJ. ShortStack: comprehensive annotation and quantification of small RNA genes. *RNA*. 2013;19(6):740–51.
126. Kerpedjiev P, Hammer S, Hofacker IL. Forna (force-directed RNA): simple and effective online RNA secondary structure diagrams. *Bioinformatics*. 2015;31(20):3377–9.
127. Thody J, Folkes L, Medina-Calzada Z, Xu P, Dalmay T, Moulton V. PAREsnip2 : a tool for high-throughput prediction of small RNA targets from degradome sequencing data using configurable targeting rules. *Nucleic Acids Res*. 2018;46(17):8730–9.
128. Fahlgren N, Carrington JC. miRNA target prediction in plants. *Methods Mol Biol*. 2010;592(8):51–7 B.C. Meyers and P.J. Green (eds.) *Plant microRNA Methods*.
129. Raudvere U, Kolberg L, Kuzmin I, Arak T, Adler P, Peterson H, et al. G:profiler: a web server for functional enrichment analysis and conversions of gene lists (2019 update). *Nucleic Acids Res*. 2019;47(W1):91–8.
130. Min X-L, Wang T-Y, Cao Y, Liu J, Li J-T, Wang T-H. MicroRNAs: a novel promising therapeutic target for cerebral ischemia/reperfusion injury? *Neural Regen Res*. 2015;10(11):1799.
131. Bonnot T, Gillard MB, Nagel DH. A simple protocol for informative visualization of enriched gene ontology terms. *Bio-101*. 2019;9(22):e3429.
132. Chow C-N, Lee T-Y, Hung Y-C, Li G-Z, Tseng K-C, Liu Y-H, et al. PlantPAN3.0: a new and updated resource for reconstructing transcriptional regulatory networks from ChIP-seq experiments in plants. *Nucleic Acids Res*. 2019;47(D1):D1155–63.

Publisher's Note

Springer Nature remains neutral with regard to jurisdictional claims in published maps and institutional affiliations.

Ready to submit your research? Choose BMC and benefit from:

- fast, convenient online submission
- thorough peer review by experienced researchers in your field
- rapid publication on acceptance
- support for research data, including large and complex data types
- gold Open Access which fosters wider collaboration and increased citations
- maximum visibility for your research: over 100M website views per year

At BMC, research is always in progress.

Learn more biomedcentral.com/submissions



Poznań, 09.03.2020


Mgr Paweł Segą
Uniwersytet im. Adama Mickiewicza w Poznaniu
Instytut Biologii Molekularnej i Biotechnologii
Zakład Ekspresji Genów
ul. Uniwersytetu Poznańskiego 6
61-614 Poznań
e-mail: pawel.sega@amu.edu.pl

Oświadczenie określające wkład w powstanie artykułu

Niniejszym oświadczam, że mój wkład w powstanie poniższego artykułu:

Paweł Segą, Katarzyna Kruszką, Dawid Bielewicz, Wojciech Karłowski, Przemysław Nuc, Zofia Szweykowska-Kulińska, Andrzej Pacak. 2021. Pi-starvation induced transcriptional changes in barley revealed by a comprehensive RNA-Seq and degradome analyses. BMC Genomics 22 (165), doi: 10.1186/s12864-021-07481-w

polegał na: wykonaniu części eksperymentów, w tym: analizy fenotypowe oraz fizjologiczne roślin jęczmienia po traktowaniu stresem niedoboru fosforu, wygenerowanie, zebranie oraz zabezpieczenie materiału biologicznego, pomiary zawartości fosforu w tkankach roślinnych, identyfikacja motywów DNA w obrębie zidentyfikowanych genów o zmienionej ekspresji, analiza ekspresji genów przy użyciu ddPCR, opracowaniu ontologii genów wraz z analizą statystyczną, analizie danych pochodzących z głębokiego sekwencjonowania, analizy bioinformatyczne otrzymanych wyników, współtworzeniu konceptu publikacji, zebraniu literatury, napisaniu publikacji, wizualizacji danych, zaprojektowaniu oraz wykonaniu figur znajdujących się w publikacji, korekcie manuskryptu po ocenach recenzentów


Paweł Segą

Poznań, 03.03.2021

Dr Katarzyna Kruszka
Uniwersytet im. Adama Mickiewicza w Poznaniu
Instytut Biologii Molekularnej i Biotechnologii
Zakład Ekspresji Genów
ul. Uniwersytetu Poznańskiego 6
61-614 Poznań
e-mail: katarzyna.kruszka@amu.edu.pl

Oświadczenie określające wkład w powstanie artykułu

Niniejszym oświadczam, że mój wkład w powstanie poniższego artykułu:

Paweł Sega, **Katarzyna Kruszka**, Dawid Bielewicz, Wojciech Karłowski, Przemysław Nuc, Zofia Szweykowska-Kulińska, Andrzej Pacak. 2021. Pi-starvation induced transcriptional changes in barley revealed by a comprehensive RNA-Seq and degradome analyses. BMC Genomics 22 (165), doi: 10.1186/s12864-021-07481-w

polegał na: udziale w przygotowaniu bibliotek do głębokiego sekwencjonowania, edycji manuskryptu

Katarzyna Kruszka

Poznań, 03.03.2021

Dr Dawid Bielewicz
Uniwersytet im. Adama Mickiewicza w Poznaniu
Instytut Biologii Molekularnej i Biotechnologii
Zakład Ekspresji Genów
ul. Uniwersytetu Poznańskiego 6
61-614 Poznań
e-mail: dawid.bielewicz@amu.edu.pl

Dr Dawid Bielewicz
Uniwersytet im. Adama Mickiewicza w Poznaniu
Instytut Biologii Molekularnej i Biotechnologii
Zakład Ekspresji Genów
ul. Uniwersytetu Poznańskiego 6
61-614 Poznań
e-mail: dawid.bielewicz@amu.edu.pl

Oświadczenie określające wkład w powstanie artykułu

Niniejszym oświadczam, że mój wkład w powstanie poniższego artykułu:

Paweł Segal, Katarzyna Kruszk, **Dawid Bielewicz**, Wojciech Karłowski, Przemysław Nuc, Zofia Szweykowska-Kulińska, Andrzej Pacak. 2021. Pi-starvation induced transcriptional changes in barley revealed by a comprehensive RNA-Seq and degradome analyses. BMC Genomics 22 (165), doi: 10.1186/s12864-021-07481-w

polegał na: pomocy w wizualizacji wybranych figur, analizie danych pochodzących z głębokiego sekwencjonowania, recenzji manuskryptu

Dawid Bielewicz
Dawid Bielewicz

Poznań, 03.03.2021

Prof. dr hab. Wojciech Karłowski
Uniwersytet im. Adama Mickiewicza w Poznaniu
Instytut Biologii Molekularnej i Biotechnologii
Zakład Biologii Obliczeniowej
ul. Uniwersytetu Poznańskiego 6
61-614 Poznań
e-mail: wkarlowski@amu.edu.pl

Oświadczenie określające wkład w powstanie artykułu

Niniejszym oświadczam, że mój wkład w powstanie poniższego artykułu:

Paweł Segal, Katarzyna Kruszk, Dawid Bielewicz, **Wojciech Karłowski**, Przemysław Nuc, Zofia Szwejkowska-Kulińska, Andrzej Pacak. 2021. Pi-starvation induced transcriptional changes in barley revealed by a comprehensive RNA-Seq and degradome analyses. BMC Genomics 22 (165), doi: 10.1186/s12864-021-07481-w

polegał na: opracowaniu i analizie danych degradomowych oraz recenzji manuskryptu.



Wojciech Karłowski

Poznań, 03.03.2021

Dr Przemysław Nuc
Uniwersytet im. Adama Mickiewicza w Poznaniu
Instytut Biologii Molekularnej i Biotechnologii
Zakład Ekspresji Genów
ul. Uniwersytetu Poznańskiego 6
61-614 Poznań
e-mail: przemyslaw.nuc@amu.edu.pl

Oświadczenie określające wkład w powstanie artykułu

Niniejszym oświadczam, że mój wkład w powstanie poniższego artykułu:

Paweł Segal, Katarzyna Kruszką, Dawid Bielewicz, Wojciech Karłowski, **Przemysław Nuc**, Zofia Szweykowska-Kulińska, Andrzej Pacak. 2021. Pi-starvation induced transcriptional changes in barley revealed by a comprehensive RNA-Seq and degradome analyses. BMC Genomics 22 (165), doi: 10.1186/s12864-021-07481-w

polegał na: przygotowaniu degradomowych bibliotek do głębokiego sekwencjonowania i pomocy w edycji manuskryptu



Przemysław Nuc

Poznań, 03.03.2021

Prof. dr hab. Zofia Szweykowska-Kulińska
Uniwersytet im. Adama Mickiewicza w Poznaniu
Instytut Biologii Molekularnej i Biotechnologii
Zakład Ekspresji Genów
ul. Uniwersytetu Poznańskiego 6
61-614 Poznań
e-mail: zofia.szweykowska-kulinska@amu.edu.pl

Oświadczenie określające wkład w powstanie artykułu

Niniejszym oświadczam, że mój wkład w powstanie poniższego artykułu:

Paweł Sega, Katarzyna Kruszka, Dawid Bielewicz, Wojciech Karłowski, Przemysław Nuc, **Zofia Szweykowska-Kulińska**, Andrzej Pacak. 2021. Pi-starvation induced transcriptional changes in barley revealed by a comprehensive RNA-Seq and degradome analyses. BMC Genomics 22 (165), doi: 10.1186/s12864-021-07481-w

polegał na: dyskusji uzyskanych wyników i korekty pisanego manuskryptu

Zofia Szweykowska-Kulińska

Poznań, 03.03.2021

Dr hab. Andrzej Pacak, prof. UAM
Uniwersytet im. Adama Mickiewicza w Poznaniu
Instytut Biologii Molekularnej i Biotechnologii
Zakład Ekspresji Genów
ul. Uniwersytetu Poznańskiego 6
61-614 Poznań
e-mail: wkarlowski@amu.edu.pl

Oświadczenie określające wkład w powstanie artykułu

Niniejszym oświadczam, że mój wkład w powstanie poniższego artykułu:

Paweł Segal, Katarzyna Kruska, Dawid Bielewicz, Wojciech Karłowski, Przemysław Nuc, Zofia Szweykowska-Kulińska, **Andrzej Pacak**. 2021. Pi-starvation induced transcriptional changes in barley revealed by a comprehensive RNA-Seq and degradome analyses. BMC Genomics 22 (165), doi: 10.1186/s12864-021-07481-w

polegał na: przygotowaniu koncepcji pracy, przygotowaniu bibliotek do głębokiego sekwencjonowania, przeprowadzeniu analizy danych pochodzących z głębokiego sekwencjonowania, analizie ekspresji wybranych genów metodą ddPCR oraz hybrydyzacji typu Northern, pomocy w pisaniu oraz edycji manuskryptu

Andrzej Pacak

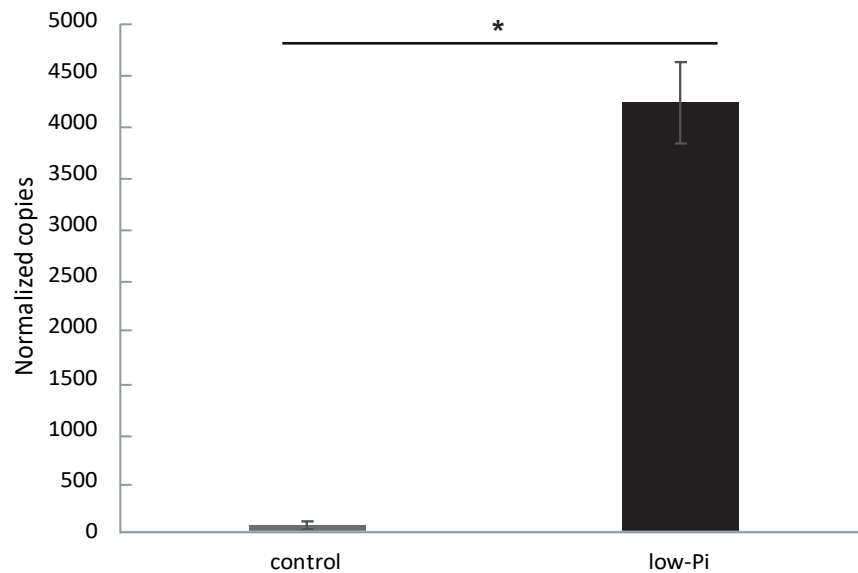


Z powodu wielkości arkuszy danych następujące suplementy dla publikacji „Pi-starvation induced transcriptional changes in barley revealed by a comprehensive RNA-Seq and degradome analyses” znajdują się na płycie:

Due to the size of the data sheets, the following files for the publication "Pi-starvation induced transcriptional changes in barley revealed by a comprehensive RNA-Seq and degradome analyses" can be found on the CD:

- **Additional file 3.** MicroRNAs and small RNAs (other) for which expression is significantly changed during Pi-starvation in barley roots and shoots. ID numbers 1–138: miRNAs identified in roots (p-value < 0.05); ID numbers 139–1934: other small RNAs identified in roots (Bonferroni p-value correction < 0.05); ID numbers 1935–2096: miRNAs identified in shoots (p-value < 0.05); ID numbers 2097–2295: other small RNAs identified in shoots (Bonferroni p-value correction < 0.05). Samples R4–R6 = low-Pi root; R16–R18 = control; S4–S6 = low-Pi shoot; S16–S18 = control shoot. NaN means “Not a Number”, describing molecules that were exclusively expressed in low-Pi or control samples. Yellow color marks DEMs with Bonferroni adjusted p-value < 0.05. Data created using CLC Genomics Workbench.
- **Additional file 5.** List of differentially expressed other small RNAs (ID 2097–2295) in barley shoots (low-Pi vs. control) identified in this study (Bonferroni corrected p-value < 0.05). Based on the available Ensembl Plants database, we classified each sequence into best-matching functional classes of cDNAs. DESs were also mapped to miRbase allowing 1, 2 or 3 mismatches.
- **Additional file 6.** List of differentially expressed other small RNAs (ID 139–1934) in barley roots (low-Pi vs. control) identified in this study (Bonferroni corrected p-value < 0.05). Based on the available Ensembl Plants database, we classified each sequence into best-matching functional classes of cDNAs. DESs were also mapped to miRbase allowing 1, 2 or 3 mismatches.
- **Additional file 11.** The extracted data from GO analysis for 98 DEGs used as a query.
- **Additional file 12.** Upstream sequences (2 kb) extracted from all 98 DEGs used for cis-regulatory motif prediction analysis.
- **Additional file 15.** Degradome profile (TargetSeek approach) demonstrates potential mRNA targets for differentially expressed miRNAs (DEMs) identified in barley shoots (low-Pi vs. control). The lower the alignment score, the more reliable the prediction.
- **Additional file 16.** Degradome profile (TargetSeek approach) demonstrates potential mRNA targets for differentially expressed other sRNAs (DESs) identified in barley shoots (low-Pi vs. control). The lower the alignment score, the more reliable the prediction.
- **Additional file 17.** Degradome profile (TargetSeek approach) demonstrates potential mRNA targets for differentially expressed miRNAs (DEMs) identified in barley roots (low-Pi vs. control). The lower the alignment score, the more reliable the prediction.

- **Additional file 18.** Degradome profile (TargetSeek approach) demonstrates potential mRNA targets for differentially expressed other sRNAs (DESSs) identified in barley roots (low-Pi vs. control). The lower the alignment score, the more reliable the prediction.
- **Additional file 19.** Degradome profile (PAREsnip2 approach) demonstrates potential mRNA targets for differentially expressed miRNAs (DEMs) identified in barley shoots (low-Pi vs. control). The lower the alignment score, the more reliable the prediction.
- **Additional file 20.** The t-plots generated by PAREsnip2 software showing the potential mRNA targets for differentially expressed miRNAs (DEMs) identified in barley shoots (low-Pi vs. control).
- **Additional file 21.** Degradome profile (PAREsnip2 approach) demonstrates potential mRNA targets for differentially expressed other sRNAs (DESSs) identified in barley shoots (low-Pi vs. control). The lower the alignment score, the more reliable the prediction.
- **Additional file 22.** The t-plots generated by PAREsnip2 software showing the potential mRNA targets for differentially expressed other sRNAs (DESSs) identified in barley shoots (low-Pi vs. control).
- **Additional file 23.** Degradome profile (PAREsnip2 approach) demonstrates potential mRNA targets for differentially expressed miRNAs (DEMs) identified in barley roots (low-Pi vs. control). The lower the alignment score, the more reliable the prediction.
- **Additional file 24.** The t-plots generated by PAREsnip2 software showing the potential mRNA targets for differentially expressed miRNAs (DEMs) identified in barley roots (low-Pi vs. control).
- **Additional file 25.** Degradome profile (PAREsnip2 approach) demonstrates potential mRNA targets for differentially expressed other sRNAs (DESSs) identified in barley roots (low-Pi vs. control). The lower the alignment score, the more reliable the prediction.
- **Additional file 26.** The t-plots generated by PAREsnip2 software showing the potential mRNA targets for differentially expressed other sRNAs (DESSs) identified in barley roots (low-Pi vs. control).
- **Additional file 28.** miRbase annotation report from CLC Workbench (QIAGEN) analysis of shoot small RNAs.
- **Additional file 29.** miRbase annotation report from CLC Workbench (QIAGEN) analysis of root small RNAs.



Additional file 1. Normalized copy numbers of barley *IPS1* gene in low-Pi treated root material.

DdPCR was performed to examine the absolute gene expression of the barley *IPS1* gene. Obtained copy numbers were normalized per 1000 copies of the *ARF1* reference gene. Asterisks indicate a significant differences (* $p < 0.05$) calculated using two-tailed Student's *t*-tests. Error bars = SD.

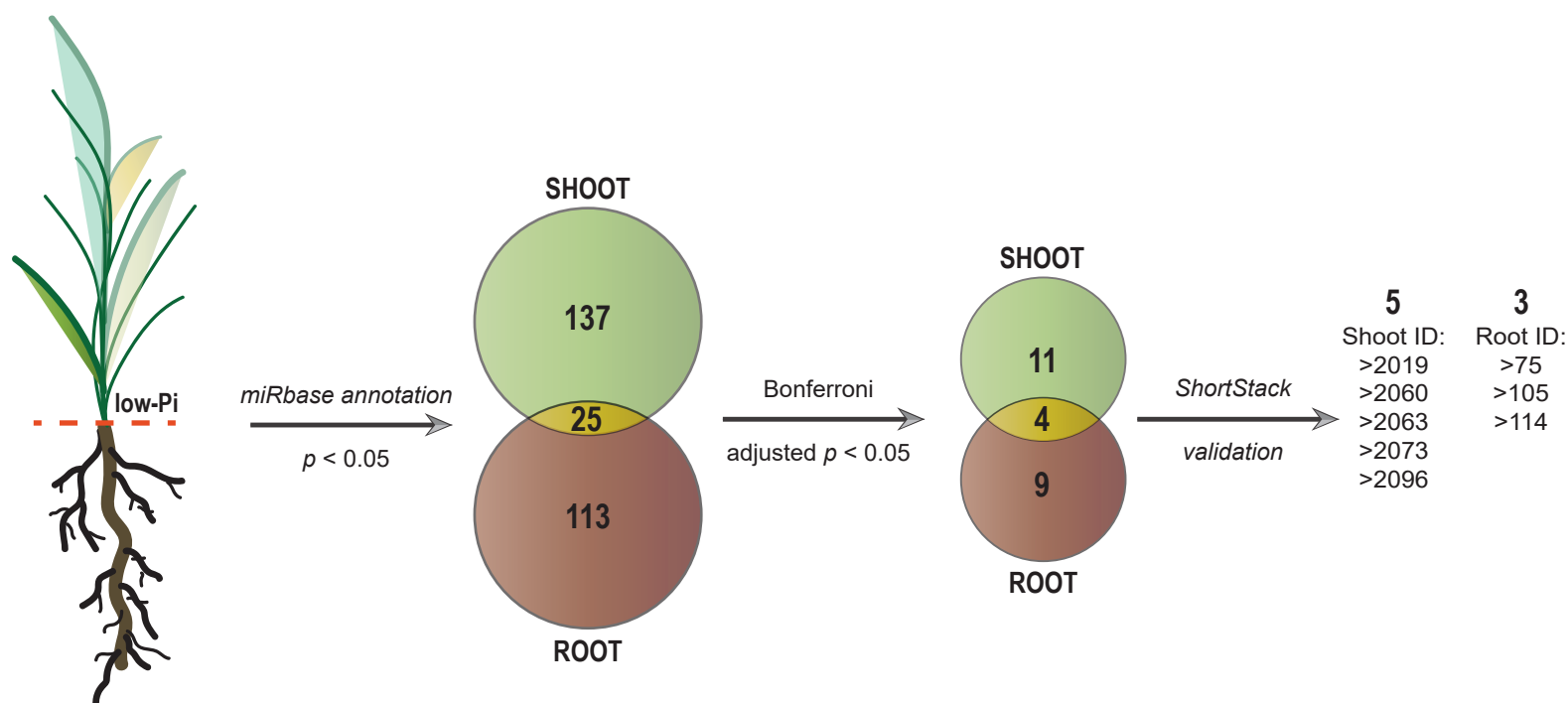
Additional file 2. Characteristic of reads obtained from small RNA deep sequencing

Sample^a	Imported reads	18-25 reads trimmed^b	Count^c	Unique small RNAs
IDG1-1 R4	34735164	15551099	14999744	1300624
IDG1-2 R5	35333413	18255470	17614581	1399307
IDG1-3 R6	33730981	15633917	15074481	1386357
IDG1-4 S4	25840628	15397986	14644436	2878110
IDG1-5 S5	22518257	12862872	12168277	2246671
IDG1-6 S6	33960212	11083898	10565625	2053332
IDG1-7 R16	29891715	11801770	11434616	1479725
IDG1-8 R17	26274498	8450311	8091106	1145909
IDG1-9 R18	22516020	7744130	7470998	1069374
IDG1-10 S16	24148668	13971695	13414482	2672149
IDG1-11 S17	21928170	12710312	12249247	2403672
IDG1-12 S18	22971234	11013610	10640396	1882556

^aNamed after R4-R6 – root low-Pi; S4-S6 – shoot low-Pi; R16-R18 – root control-Pi; S16-S18 – shoot control-Pi

^bNumber of reads counted after adapter removal and length selection (18 nt – 25 nt). Reads is the oligonucleotide that has been sequenced

^cCounts are the number of reads that overlap at a particular genomic position



	ID	Name	Sequence (5'-3')	Prediction	Locus	Length	Reads	Strand	Major RNA reads	Complexity	Dicer Call
ROOT	>75	miR399b†	GGGCGCTTCTCCTTTGGCACG	+	chr4H:491992339-491992480	142	535	+	389	0.043	21
	>105	miR399a†	TGCCAAAGGAGAGTTGCCCTG	+	chr2H:666055710-666055856	147	2030	+	1813	0.016	21
	>114	miR827†	TTAGATGACCATCAGCAAACA	+	chr2H:620316212-620316424	213	1090	+	693	0.039	21
SHOOT	>2019	miR399b†	GGGCGCTTCTCCTTTGGCACG	+	chr4H:491992339-491992480	142	535	+	389	0.043	21
	>2060	miR399b//miR399a	TGCCAAAGGAGAATTGCCCTG	+	chr7H:540840753-540840845	93	1626	-	1143	0.009	21
	>2063	miR399a†	TGCCAAAGGAGAGTTGCCCTG	+	chr2H:666055710-666055856	147	2030	+	1813	0.016	21
	>2073	miR827†	TTAGATGACCATCAGCAAACA	+	chr2H:620316212-620316424	213	1090	+	693	0.039	21
	>2096	miR827	TTTTGTTGGTTGTCATCTAACC	+	chr2H:620316273-620316498	226	5203	+	2678	0.007	22

† = miRNA expressed in both organs

Additional file 4. Identification of differentially expressed miRNAs (DEMs) in barley plants under low-Pi regime. The graph illustrates step-by-step annotation of unique small RNAs obtained in this study. The table summarizes the ShortStack output data.

Additional file 7. Length distribution of DESs identified in barley roots and shoots

Length [nt]	Root	Root [%]	Shoot	Shoot [%]
18	274	15.26	28	14.07
19	216	12.03	42	21.11
20	207	11.53	28	14.07
21	247	13.75	26	13.07
22	219	12.19	19	9.55
23	201	11.19	17	8.54
24	196	10.91	32	16.08
25	236	13.14	7	3.52
	Σ1796	=100%	Σ199	=100%

Additional file 8. Annotation distribution of DESs identified in barley roots and shoots

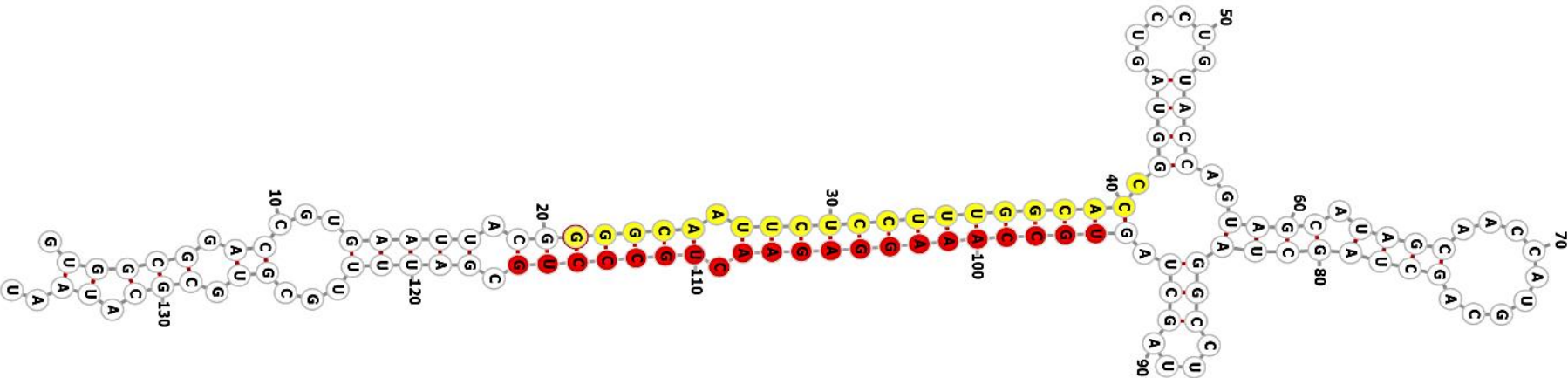
cDNA class	Root	Root %	Shoot	Shoot %
Protein coding	890	38.54	101	47.87
total rRNA	789	34.17	18	8.53
5S rRNA	3	0.13	-	-
5.8S rRNA	42	1.82	1	0.47
16S rRNA	-	-	4	1.90
18S rRNA	18	0.78		0.00
26S rRNA	113	4.89	1	0.47
SSU rRNA	320	13.86	4	1.90
LSU rRNA	293	12.69	8	3.79
Non-translating CDS	450	19.49	77	36.49
snoRNA	59	2.56	1	0.47
tRNA	57	2.47	14	6.64
SRP_RNA	27	1.17	0	0.00
snRNA	22	0.95	0	0.00
pseudogene	15	0.65	0	0.00
	Σ2309*	=100%	Σ211*	=100%

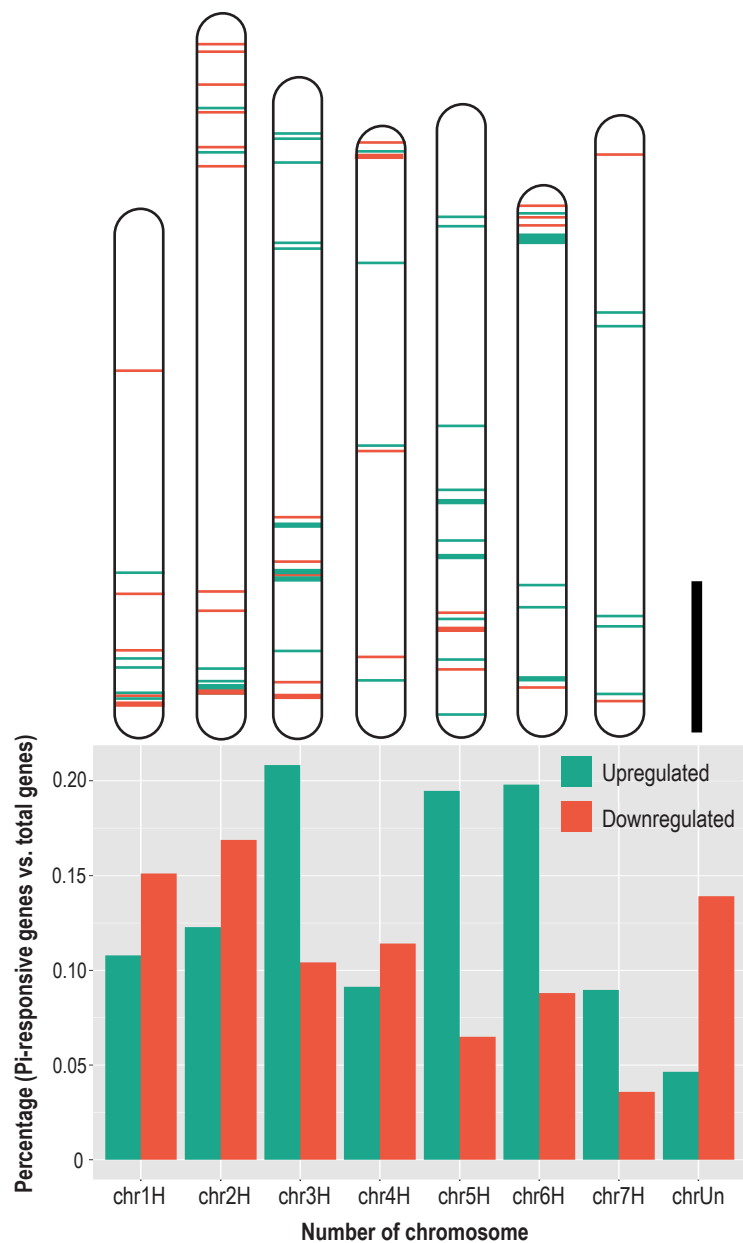
*Overall number of DESs is higher (we identified 1796 DESs in roots and 199 DESs in shoots), cause some sequences were matching to more than one barley genomic locus and may represent several cDNA's classes

SSU = small subunit ribosomal, LSU = large subunit ribosomal

Additional file 9. The output of DES ShortStack analysis (upper panel) and RNA secondary structure visualization of potential new miRNA generated by forna tool (lower panel). Red color marks miRNA; yellow color marks miRNA star.

		ID	Name	Sequence (5'-3')	Size	Log ₂ (FC)	Prediction	Locus	Length	Reads	Strand	Major RNA reads	Complexity	Dicer Call
DES	SHOOT	>1813	miR399b//miR399a	TGCCAAAGGAGAACTGCCCTG	21	4.64	+	chr3H:525872399-525872497	99	205	-	195	0.039	21
	ROOT	>2265	miR399b//miR399a			6.27								





Additional file 10. Chromosomal mapping of 98 DEGs identified in this study. Lower panel illustrates the percentage between quantitative distribution of either up-regulated or down-regulated genes under low-Pi conditions and total number of protein-coding genes in each barley chromosome. Scale bar for chromosomes = 160 Mbp.

Additional file 13. List of identified P1BS motifs within the DEGs' promoters

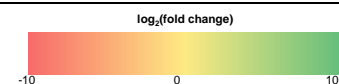
#	Gene ID	FC	log ₂ (FC)	Function	Motif consensus	Position	Strand	Hit sequence
1	HORVU4Hr1G079600	59,41	5,89	IPS1	GNATATNC	1562	+	GGATATCC
	HORVU4Hr1G079600		5,89		GNATATNC	1694	+	GCATATCC
2	HORVU3Hr1G017440	18,54	4,21	Sn1-specific diacylglycerol lipase alpha isoform X1	GNATATNC	1828	+	GAATATCC
	HORVU3Hr1G017440		4,21		GNATATNC	1872	+	GGATATGC
3	HORVU3Hr1G068380	16,16	4,01	Inorganic pyrophosphatase 1-like	GNATATNC	1904	+	GAATATTC
4	HORVU7Hr1G113020	14,84	3,89	Hydrophobic protein RCI2A-like	GNATATNC	849	+	GGATATCC
	HORVU7Hr1G113020		3,89		GNATATNC	1923	+	GAATATTC
5	HORVU3Hr1G010540	13,35	3,74	Sulfoquinovosyl transferase SQD2-like	GNATATNC	1098	+	GCATATCC
	HORVU3Hr1G010540		3,74		GNATATNC	1132	+	GAATATCC
	HORVU3Hr1G010540		3,74		GNATATNC	1352	+	GAATATAC
6	HORVU6Hr1G007360	13,22	3,72	Uncharacterized protein	GNATATNC	188	+	GAATATCC
7	HORVU3Hr1G068390	11,17	3,48	Inorganic pyrophosphatase 1-like	GNATATNC	1811	+	GAATATTC
	HORVU3Hr1G068390		3,48		GNATATNC	1917	+	GCATATGC
8	HORVU2Hr1G112830	8,66	3,11	Endonuclease, S1/P1 nuclease	GNATATNC	1624	+	GCATATGC
9	HORVU2Hr1G116250	7,64	2,93	Alpha/beta hydrolase superfamily	GNATATNC	1992	+	GTATATCC
10	HORVU5Hr1G055570	6,08	2,60	Purple acid phosphatase	GNATATNC	1970	+	GAATATCC
11	HORVU3Hr1G078360	5,62	2,49	Purple acid phosphatase	GNATATNC	1726	+	GGATATAC
	HORVU3Hr1G078360		2,49		GNATATNC	1758	+	GGATATAC
	HORVU3Hr1G078360		2,49		GNATATNC	1827	+	GCATATGC
12	HORVU5Hr1G066460	5,61	2,49	Uncharacterized protein	GNATATNC	1632	+	GCATATAC
13	HORVU1Hr1G075570	4,89	2,29	Profilin	GNATATNC	1891	+	GAATATTC
14	HORVU5Hr1G055740	4,88	2,29	Carotenoid 9,10(9',10')-cleavage dioxygenase	GNATATNC	1946	+	GGATATTC
15	HORVU3Hr1G076060	4,42	2,14	Purple acid phosphatase	GNATATNC	1669	+	GCATATAC
16	HORVU5Hr1G051160	4,34	2,12	Probable Tyrosine-protein phosphatase, DSP4	GNATATNC	657	+	GAATATCC
17	HORVU2Hr1G110540	3,85	1,95	Molybdate transporter 2	GNATATNC	585	+	GGATATTC
18	HORVU1Hr1G054430	3,85	1,95	Haloacid dehalogenase-like hydrolase domain-containing	GNATATNC	1861	+	GCATATAC
19	HORVU5Hr1G097130	3,84	1,94	Peroxidase 57-like	GNATATNC	642	+	GAATATAC
20	HORVU5Hr1G079600	3,58	1,84	Uncharacterized protein	GNATATNC	733	+	GGATATTC
	HORVU5Hr1G079600		1,84		GNATATNC	741	+	GCATATCC
	HORVU5Hr1G079600		1,84		GNATATNC	1859	+	GCATATGC
21	HORVU6Hr1G058780	3,45	1,79	Phosphoenolpyruvate carboxylase kinase 2	GNATATNC	293	+	GAATATGC
	HORVU6Hr1G058780		1,79		GNATATNC	329	+	GAATATGC
	HORVU6Hr1G058780		1,79		GNATATNC	1670	+	GAATATTC
22	HORVU7Hr1G089910	3,44	1,78	SPX domain-containing protein 1-like	GNATATNC	857	+	GCATATGC
	HORVU7Hr1G089910		1,78		GNATATNC	1765	+	GAATATTC
	HORVU7Hr1G089910		1,78		GNATATNC	1795	+	GCATATCC
23	HORVU1Hr1G088920	3,36	1,75	Chlorophyll a-b binding protein of LHCII type 1-like	GNATATNC	249	+	GGATATCC
	HORVU1Hr1G088920		1,75		GNATATNC	1132	+	GAATATAC
	HORVU1Hr1G088920		1,75		GNATATNC	1480	+	GCATATGC
24	HORVU6Hr1G016890	3,35	1,75	Chlorophyll a-b binding protein, chloroplastic	GNATATNC	887	+	GTATATAC
25	HORVU3Hr1G076320	3,31	1,73	Inositol hexakisphosphate and diphosphoinositol-	GNATATNC	503	+	GAATATTC
26	HORVU3Hr1G029200	3,31	1,73	Phosphoenolpyruvate carboxylase 1-like	GNATATNC	734	+	GCATATGC
	HORVU3Hr1G029200		1,73		GNATATNC	754	+	GTATATGC
	HORVU3Hr1G029200		1,73		GNATATNC	1704	+	GAATATTC
27	HORVU5Hr1G044460	3,09	1,63	Purple acid phosphatase 5	GNATATNC	1267	+	GAATATTC
	HORVU5Hr1G044460		1,63		GNATATNC	1982	+	GAATATCC
	HORVU5Hr1G106010		-1,40		GNATATNC	4	+	GTATATCC
28	HORVU5Hr1G106010	-2,63	-1,40	Pathogenesis-related protein 1-like	GNATATNC	25	+	GTATATGC
	HORVU5Hr1G106010		-1,40		GNATATNC	721	+	GAATATCC
	HORVU5Hr1G106010		-1,40		GNATATNC	721	+	GAATATCC
29	HORVU3Hr1G108100	-2,70	-1,43	Carotenoid 9,10(9',10')-cleavage dioxygenase 1	GNATATNC	1653	+	GTATATAC
30	HORVU5Hr1G077920	-2,82	-1,50	Beta-glucosidase 31-like	GNATATNC	383	+	GTATATTC
31	HORVU3Hr1G109350	-2,92	-1,54	Cysteine-rich receptor-like protein kinase 10	GNATATNC	400	+	GGATATTC
32	HORVU0Hr1G038320	-3,32	-1,73	Prolyl endopeptidase-like	GNATATNC	899	+	GTATATGC
33	HORVU2Hr1G012980	-3,92	-1,97	Prenaspirodiene oxygenase-like	GNATATNC	1849	+	GGATATGC
34	HORVU4Hr1G071300	-4,05	-2,02	Aminotransferase ALD1 homolog	GNATATNC	968	+	GTATATGC
35	HORVU4Hr1G001250	-4,14	-2,05	Caffeic acid-O-methyltransferase (COMT)	GNATATNC	1162	+	GGATATTC
36	HORVU4Hr1G044460	-4,24	-2,09	Potential Tubulin alpha-6 chain	GNATATNC	2	+	GAATATGC
	HORVU4Hr1G044460		-2,09		GNATATNC	1347	+	GTATATGC
37	HORVU1Hr1G081410	-5,24	-2,39	Chaperone protein dnaJ C76, chloroplastic isoform X1	GNATATNC	284	+	GCATATGC
38	HORVU7Hr1G116080	-5,70	-2,51	Endoplasmic reticulum metalloproteinase 1	GNATATNC	1316	+	GCATATTC
39	HORVU2Hr1G094690	-5,97	-2,58	OsSPX -MFS1 ortholog (targeted by miR827)	GNATATNC	1823	+	GTATATGC
40	HORVU6Hr1G005720	-6,05	-2,60	High-affinity nitrate transporter 2.1-like	GNATATNC	291	+	GCATATAC
	HORVU6Hr1G005720		-2,60		GNATATNC	345	+	GCATATAC
	HORVU6Hr1G005720		-2,60		GNATATNC	345	+	GCATATAC
41	HORVU1Hr1G070220	-6,09	-2,61	Pyridoxal phosphate-dependent transferase	GNATATNC	1458	+	GAATATAC
	HORVU1Hr1G070220		-2,61		GNATATNC	1506	+	GAATATAC
	HORVU1Hr1G070220		-2,61		GNATATNC	1763	+	GAATATTC
42	HORVU4Hr1G005440	-6,13	-2,62	Oxalate oxidase	GNATATNC	728	+	GTATATAC
43	HORVU2Hr1G006830	-6,15	-2,62	Cytochrome P450	GNATATNC	9	+	GAATATGC
44	HORVU2Hr1G031400	10,87	-3,44	SPX domain-containing protein 6-like	GNATATNC	599	+	GTATATTC
45	HORVU2Hr1G020140	13,90	-3,80	Transcription factor NIGT1	GNATATNC	1693	+	GGATATTC
46	HORVU4Hr1G005380	-21,29	-4,41	Oxalate oxidase 2	GNATATNC	1579	+	GAATATTC

log₂(fold change)



Additional file 14. List of identified P-responsive PHO motifs within the DEGs' promoters

#	Gene ID	FC	log ₂ (FC)	Function	Motif consensus	Position	Strand	Hit sequence
1	HORVU3Hr1G079900	54,85	5,78	Glycerophosphodiester phosphodiesterase GDPD1, chloroplastic-like	ATGCCAT	391	+	ATGCCAT
2	HORVU3Hr1G091170	19,72	4,30	Inactive protein kinase	ATGCCAT	1188	+	ATGCCAT
	HORVU3Hr1G091170		4,30		ATGCCAT	1783	+	ATGCCAT
3	HORVU3Hr1G010540	13,35	3,74	Sulfoquinovosyl transferase SQD2-like	ATGCCAT	220	+	ATGCCAT
4	HORVU2Hr1G031400	10,87	3,44	SPX domain-containing protein 6-like	ATGCCAT	644	+	ATGCCAT
5	HORVU6Hr1G065710	6,89	2,79	OsSPX-MFS2 ortholog	ATGCCAT	128	+	ATGCCAT
6	HORVU5Hr1G055740	4,88	2,29	Carotenoid 9,10(9',10')-cleavage dioxygenase	ATGCCAT	1466	+	ATGCCAT
7	HORVU7Hr1G091060	4,76	2,25	TLC domain-containing protein	ATGCCAT	1379	+	ATGCCAT
8	HORVU5Hr1G028140	4,24	2,08	Heptahelical transmembrane protein 4	ATGCCAT	1408	+	ATGCCAT
9	HORVU1Hr1G089620	3,36	1,75	Chlorophyll a-b binding protein of LHClI type 1-like	ATGCCAT	197	+	ATGCCAT
10	HORVU3Hr1G029200	3,31	1,73	Phosphoenolpyruvate carboxylase 1-like	ATGCCAT	18	+	ATGCCAT
	HORVU3Hr1G029200		1,73		ATGCCAT	1743	+	ATGCCAT
11	HORVU5Hr1G044460	3,09	1,63	Purple acid phosphatase 5	ATGCCAT	480	+	ATGCCAT
12	HORVU3Hr1G108100	-2,70	-1,43	Carotenoid 9,10(9',10')-cleavage dioxygenase 1	ATGCCAT	1870	+	ATGCCAT
13	HORVU3Hr1G109350	-2,92	-1,54	Cysteine-rich receptor-like protein kinase 10	ATGCCAT	1968	+	ATGCCAT
14	HORVU3Hr1G077950	-3,76	-1,91	Subtilisin-like protease SBT3.8	ATGCCAT	7	+	ATGCCAT
15	HORVU1Hr1G070220	-6,09	-2,61	Pyridoxal phosphate-dependent transferase	ATGCCAT	1208	+	ATGCCAT
16	HORVU1Hr1G089540	-8,29	-3,05	Chalcone synthase 2	ATGCCAT	120	+	ATGCCAT
	HORVU2Hr1G030090	-90,52	-6,50	Uncharacterized protein	ATGCCAT	1314	+	ATGCCAT
	HORVU2Hr1G030090		-6,50		ATGCCAT	1662	+	ATGCCAT
17	HORVU2Hr1G030090		-6,50		ATGCCAT	1700	+	ATGCCAT



Additional file 27. List of genes predicted in degradome analysis to be guided for cleavage by putative regulatory sRNAs (identified as DES) with best scoring matches.

	ID	Sequence	Size	DES annotation	log ₂ (FC)	Target	Cut	Score	MFE
SHOOT	>2279	TTAGATGACCATCAGCAAAC	21	*miR827	3.11	HORVU6Hr1G065710 ^{TS} SPX-MFS2	21 out of 30 isoforms are cleaved	3.5	-26
	>2118	AATCGTCTTTACATCGGATG	20	Protein-coding	3.24	HORVU2Hr1G094690 ^{PS} SPX-MFS1	17 out of 24 isoforms are cleaved	2.5	-27.5
	>2117	AATCGTCTTTACATCGGA	18	Protein-coding	3.24	HORVU7Hr1G003920 ^{TS} Glutaminyl-peptide cyclotransferase	7 out of 24 isoforms are cleaved	4.5	-20.7
						HORVU7Hr1G003920.11 ^{PS}	1961	2	-19.6
ROOT	>1016	CGCATTTATTAGATAAAAGGCT	22	rRNA	3.19	HORVU0Hr1G023930.1 ^{TS} Uncharacterized protein with unknown PTHR33047 domain	1741	0	-31.3
						HORVU5Hr1G015600 ^{TS} Potential E3 ubiquitin-protein ligase	3 out of 18 isoforms are cleaved	0	-31.3
						HORVU6Hr1G024220.1 ^{TS} Non-translating CDS	299	0	-31.3
	>1770	TCGGATCGCGGCGACGGGGGC	21	rRNA	-1.02	HORVU4Hr1G066070.1 ^{TS} RING-type E3 ubiquitin transferase containing U-box domain	1277	6.5	-39.3
	>1591	GTTCAGCCGGAGGTAGGGTCC	21	rRNA	-1.09	HORVU0Hr1G020230 ^{TS} Putative kinase-like protein TMKL1 (TRANSMEMBRANE KINASE-LIKE)	2 out of 2 isoforms are cleaved	4.5	-36.1
						HORVU1Hr1G027340.1 ^{PS}	284	0	-49.4
	>463	AGAGGAAACTCTGGTGGAGGCTCG	24	rRNA	-3.58	HORVU1Hr1G027340.2 ^{PS} Uncharacterized protein with unknown PTHR47188 domain	156	0	-49.4
						HORVU1Hr1G027340.3 ^{PS}	748	0.5	-48.5
	>1220	CTGCACTCCTTGCCGCT	18	sRP-RNA	4.17	HORVU2Hr1G092650 ^{PS} Trihelix transcription factor GTL1-like	4 out of 8 isoforms are cleaved	3	-28.6
	>718	CCAGTCTTAGGATCCGGCT	19	snoRNA	1.78	HORVU3Hr1G001430.1 ^{PS} PAF1 domain containing protein, PAF1	2410	3.5	-26.8
	>399	ACCTCCTGGGAAGTCCTCGTG	21	Unannotated	2.36	HORVU7Hr1G096650 ^{PS} Uncharacterized transmembrane protein with unknown PTHR37735 domain	5 out of 7 isoforms are cleaved	4	-31.5

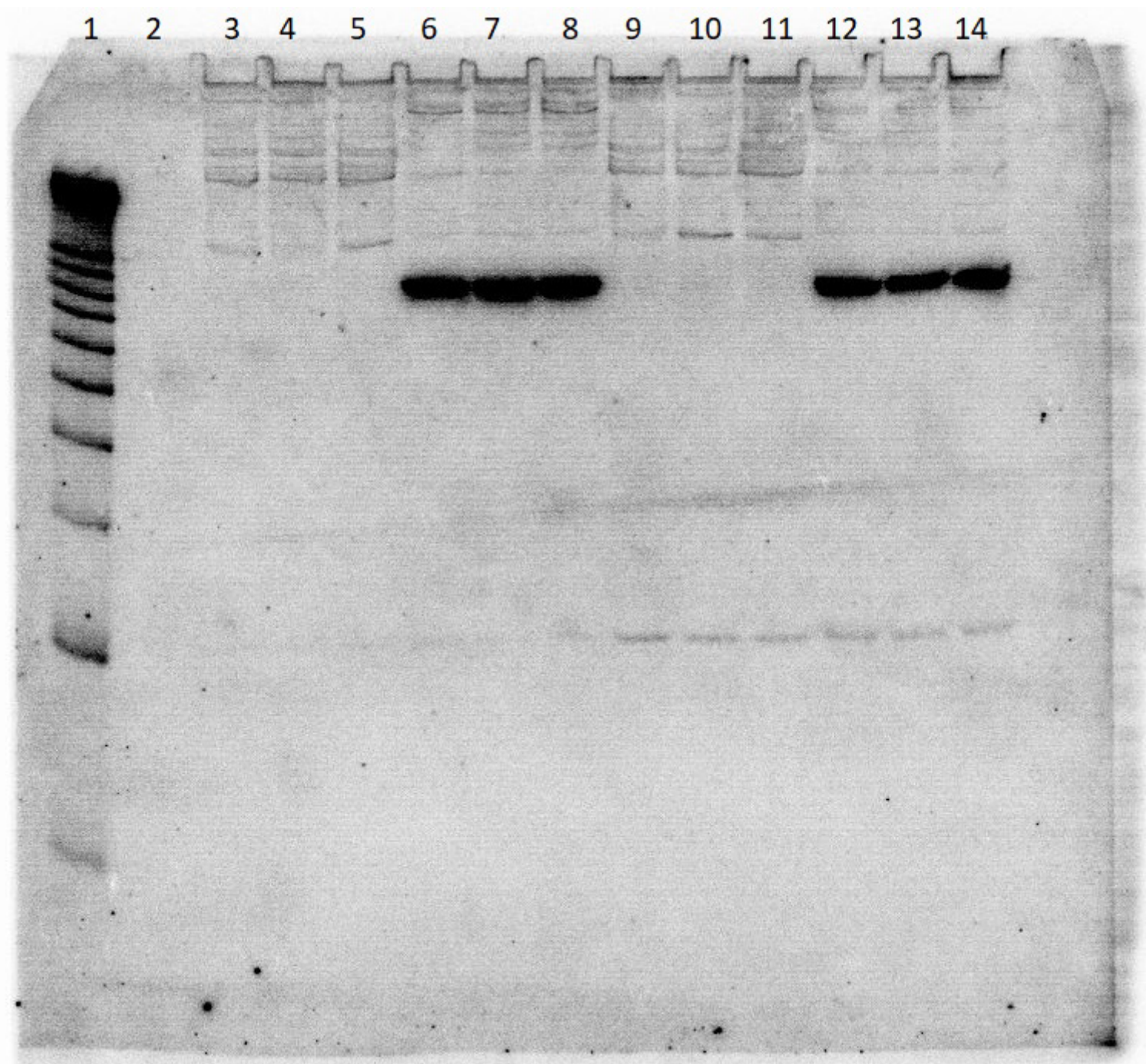
* = annotated to miRbase with at least one mismatch; TS = TargetSeek; PS = PAREsnip2

Additional file 30. Spike-in quality control of RNA-Seq samples from barley shoots (low-Pi vs. control). Correlation between known and measured spike-in concentrations.

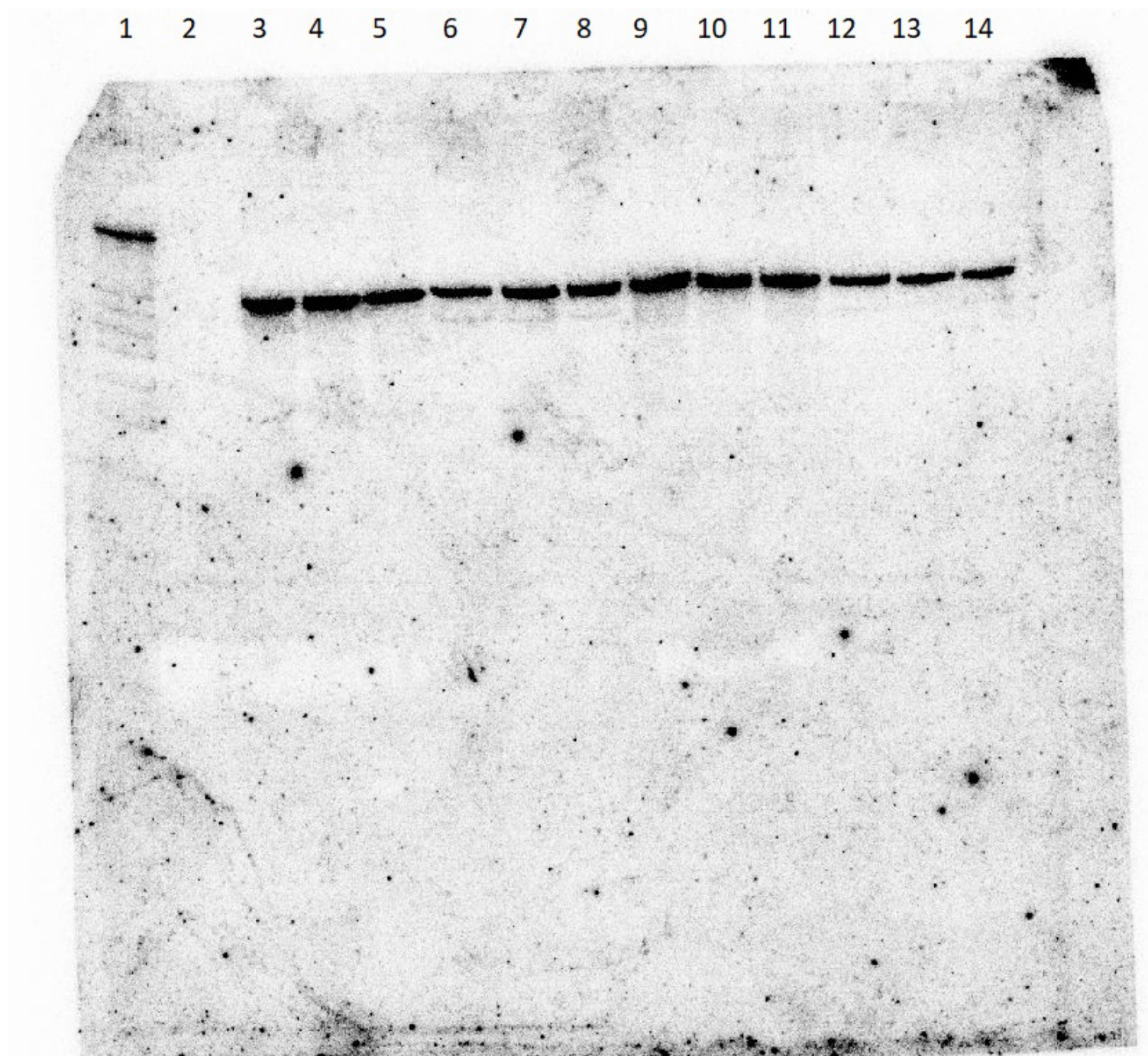
	Sample	Number of spike-ins detected	R²
	S4	51/92	0.77
-P	S5	63/92	0.86
	S6	66/92	0.84
	S16	60/92	0.84
+P	S17	65/92	0.84
	S18	61/92	0.84

Additional file 31. List of primers and probes used in this study.

	Name	Sequence (5' - '3)	Product size (bp)	Destiny
ddPCR analysis	APO387-F	CGTGACGCTGTGTTGCTTGT	61	Primers for ddPCR gene expression analysis of <i>HvARF1</i>
	APO388-R	CCGCATTCATCGCATTAGG		
	APO796-F	GGCGACTTCTCACCTCTAC	114	Primers for ddPCR gene expression analysis of <i>HvIPS1</i>
	APO797-R	CTGTGATCTTCACCGGTAGT		
	APO704-F	GTAGGCCTGACCTGCATCTG	163	Primers for ddPCR gene expression analysis of <i>HvSPX-MFS1</i>
	APO705-R	ACCAATGGCTGAGGAAACAG		
	PS579-F	ACAGGCTGAAGATGAGGCAC	127	Primers for ddPCR gene expression analysis of 3'5' - exonuclease
	PS580-R	TCAATCAAGGCAACTGCCATAC		
	PS581-F	CACGACACCAAGGGGAACAAG	123	Primers for ddPCR gene expression analysis of S1/P1 endonuclease
	PS582-R	GAAGTGCGCCAGGAACATCAG		
	PS583-F	GTCCTTCAACAGCCAGAACCC	130	Primers for ddPCR gene expression analysis of oxalate oxidase
	PS584-R	CTTGAGAAGTTCCACGACCCC		
	PS585-F	TCTCCTTCAACAGCCAAAACC	130	Primers for ddPCR gene expression analysis of oxalate oxidase 2
	PS586-R	TTGAGAAGTTCCACGACCCC		
Northern	APO697	TGTTTGCTGATGGTCATCTAA	-	Probe for mature hvu-miR827
	U6_Probe	TCATCCTTGCGCAGGGGCCA	-	Probe for U6 snRNA



Additional file 32. Original, full-length blot of mature hvu-miR827 analysis. Lane 1: Decade™ Marker System (Invitrogen, Thermo Fisher Scientific); Lane 2: empty space (no sample loaded); Lane 3-5: RNA samples from root (Pi sufficient); Lane 6-8: shoot (Pi sufficient); Lane 9-11: root (low-Pi); Lane: 12-14: shoot (low-Pi).



Additional file 33. Original, full-length blot of U6 snRNA analysis. Lane 1: Decade™ Marker System (Invitrogen, Thermo Fisher Scientific); Lane 2: empty space (no sample loaded); Lane 3-5: RNA samples from root (Pi sufficient); Lane 6-8: shoot (Pi sufficient); Lane 9-11: root (low-Pi); Lane: 12-14: shoot (low-Pi).

PODZIĘKOWANIA / ACKNOWLEDGMENTS

Powyższa praca nie posiadałaby takiego kształtu i ducha, bez nieocenionego wsparcia akademickiego, edukacyjnego oraz ludzkiego, jakiego doświadczyłem w trakcie lat pracy na Uniwersytecie im. Adama Mickiewicza w Poznaniu.

Chciałbym w pierwszej kolejności ogromnie podziękować mojemu *Promotorowi* - *dr hab. Andrzejowi Pacakowi*, za to że obdarzył mnie zaufaniem zatrudniając do swojego grantu badawczego i dając szansę na dalszy rozwój naukowy. Jak również za to, że zawsze znajdował dla mnie czas mimo natłoku obowiązków i dał mi pełną swobodę w realizacji moich pomysłów. Dziękuję za spokój, cierpliwość, wyjazdy na konferencje, jak i rozmowy o Skandynawii.

Z całego serca pragnę podziękować *Rodzinie oraz Przyjaciółom* za wsparcie. Kilka ostatnich lat, które poświęciłem nauce spowodowały, że często Was zaniedbywałem. Mimo to zawsze byliście przy mnie, szczególnie wtedy gdy przeżywałem momenty zwątpienia.

Dziękuję *Pani Profesor dr hab. Zofii Szwejkowskiej-Kulińskiej* oraz *Panu Profesorowi dr hab. Arturowi Jarmołowskiemu*, za to że zapewniłście mi świetne warunki do rozwoju naukowego i wykonywania badań na wysokim poziomie w Zakładzie Ekspresji Genów UAM. Pragnę również podziękować za wszystkie cenne wskazówki, które mi przekazywaliście podczas seminariów. Chciałbym ogromnie podziękować *Koleżankom i Kolegom z Zakładu*. Za wspólne lata pracy, dyskusje naukowe, niezapomniane wyjazdy na konferencje i życzliwość.

Dziękuję Dziekanowi Wydziału Biologii – *Panu Profesorowi dr hab. Przemysławowi Wojtaszkowi* za to, że nigdy nie odmówił mi pomocy w sfinansowaniu naukowych przedsięwzięć. Pragnę również podziękować za zaufanie i przyznanie mi Grantu Dziekana Wydziału Biologii UAM.

Dziękuję także wszystkim pracownikom administracyjnym Wydziału Biologii UAM. Szczególnie dziękuję *Pani dr Karolinie Cerbin*, *Pani mgr Iwonie Kanonik-Jędrzejak*, *Pani mgr Arlecie Kucz* oraz *Panu mgr Tomaszowi Bieleckiemu* za to, że zawsze byliście pomocni i rozwiązywaliście problemy, z którymi do Was przychodziłem.

Dziękuję wszystkim *Współautorom moich prac* za Wasze cenne uwagi, dzielenie się swoim doświadczeniem i wspólną przygodę.

Dziękuję wszystkim *Recenzentom* prac za konstruktywną krytykę, pomysły i komentarze, które bardzo mnie rozwinęły jako Naukowca. Z perspektywy czasu każde Wasze słowa były bezcenne.

Dziękuję także *lekarzom* oraz *pracownikom Wielkopolskiego Centrum Onkologii* w Poznaniu za to, że otoczyliście mnie wsparciem, w tym nieoczekiwanym i trudnym momencie mojego życia.

*Nauka to rachunek różniczkowy umysłu,
Sztuka to rachunek całkowity; osobno mogą być
Piękne, ale wielkie – tylko wtedy, gdy są razem.*
Sir Ronald Ross

FINANSOWANIE BADAŃ / FUNDINGS

Badania, których wyniki przedstawiono w niniejszej rozprawie zostały sfinansowane z następujących źródeł:

- Narodowe Centrum Nauki, grant OPUS 6, numer 2013/11/B/NZ9/01761, „*Badanie roli genu PHO2 oraz jego produktu, białka PHO2, w utrzymaniu homeostazy fosforanowej w jęczmieniu*”,
- Narodowe Centrum Nauki, grant OPUS 12, numer 2016/23/B/NZ9/00857, „*Badanie interakcji białek typu E2 (PHO2) i E3 (NLA) z białkami zaangażowanymi w utrzymanie homeostazy fosforanowej w jęczmieniu w warunkach wysokiej temperatury oraz niedoboru fosforu*”,
- Narodowe Centrum Nauki, grant PELUDIUM 10, numer 2015/19/N/NZ9/00218, „*Identyfikacja oraz charakterystyka jęczmiennych homologów czynnika transkrypcyjnego PSR1 związanych z regulacją ekspresji genów w odpowiedzi na niedobór fosforanów w jęczmieniu (Hordeum vulgare)*”,
- Grant Dziekana Wydziału Biologii Uniwersytetu im. Adama Mickiewicza, numer GDWB-06/2016, „*Identyfikacja potencjalnych partnerów białkowych dla enzymu PHOSPHATE 2 w jęczmieniu*”,
- Krajowy Naukowy Ośrodek Wiodący (KNOW), Poznańskie Konsorcjum RNA, stypendium numer 01/KNOW2/2014,
- Stypendium wyjazdowe w ramach międzynarodowego programu COST Action, numer CA15223.